Differential Roles of the Tissue Inhibitors of Matrix Metalloproteinases (TIMPs) in Heart Failure

by

Abhijit Ramchandra Takawale

A thesis submitted in partial fulfillment of the requirements for the degree of

Doctor of Philosophy

Department of Physiology
University of Alberta

Abstract

Considering the morbidity and mortality associated with heart failure, there is an increasing demand to develop new therapeutic alternatives for cardiac diseases. Advanced left ventricular remodeling following ischemic and pressure-overload cardiomyopathy causes changes in LV geometry, myocyte size, extracellular matrix and vascular compartments which altogether contribute to heart failure. Normal homeostasis of the myocardial extracellular matrix (ECM) is maintained by enzymes known as matrix metalloproteinases (MMPs), and their inhibitors, tissue inhibitors of metalloproteinases (TIMPs). Depending on the type of cardiac injury, an altered balance between MMP/TIMPs exacerbates heart disease and eventually leads to heart failure.

The research presented in this thesis identifies novel and differential roles of TIMP1, TIMP3 and TIMP4 in cardiac diseases. We observed that TIMP4 is required for recovery from myocardial ischemia-reperfusion injury through its MT1-MMP inhibitory function since its deficiency caused significantly higher MT1-MMP activity, exacerbation of heart dysfunction and LV remodeling post-I/R. On the other hand, TIMP1 promotes cardiac fibrosis in response to pressure-overload and Ang II infusion) in an MMP-independent manner, by mediating an interaction between CD63 and integrinβ1 in cardiac fibroblasts. Adenoviral delivery of TIMP3 but not TIMP4 improved cardiac function and ameliorated adverse remodeling post-MI. Interestingly, TIMP3 promoted endothelial proliferation and angiogenesis in the infarcted myocardium in a dose-dependent manner.

The research described in this thesis reveals the ECM-dependent and ECM-independent functions of TIMPs in heart disease. The differential functions of TIMP1, TIMP4 and TIMP3 in heart failure demonstrate that TIMPs do not always exert a beneficial effect in heart disease, and

that their function is not limited to their MMP-inhibitory function. Rather, each TIMP has unique functions depending on the type of cardiac injury and can play differential roles in heart failure.

Preface

Non-failing human hearts were procured through Human Organ Procurement and Exchange program (HOPE) program while failing hearts with ischemic cardiomyopathy and dilated cardiomyopathy were procured through the Human Explanted Heart Program (HELP) at the Mazankowski Alberta Heart Institute (Edmonton, AB). All experiments were performed in accordance with the institutional ethics committee. Informed consent was obtained from study subjects. The research projects in the current thesis were mainly performed in Dr. Zamaneh Kassiri's laboratory in Heritage Medical Research Center, 474, University of Alberta

Dedications

To all my family members, relatives who supported me throughout this journey

ACKNOWLEDGEMENTS

I would like to acknowledge my supervisor Dr. Zamaneh Kassiri for her continuous support throughout my PhD program. Dr. Kassiri has been very helpful towards me in developing scientific acumen, writing research proposals as well as writing scholarship applications. She has guided me through a variety of experiences and was there to provide a feedback to bring best out of me. Dr. Kassiri also helped to challenge established scientific concepts thereby improved my thinking ability thereby helped to build new theories during my research work.

A special thank you to my funding agencies such as Faculty of Graduate Studies and Research, Alberta Innovates Health Solution (AIHS) and Canadian Institutes of Health Research (CIHR) for their rewarding efforts and funding opportunities provided to me.

My sincere thanks to my committee members Drs. Alexander Clanachan and John Seubert for their valuable suggestions and comments during my PhD program. They were available, supportive and approachable through out my PhD program and I respect their accomplishments and valuable insights they shared with me. Their inputs throughout PhD helped me to improve presentation skills, scientific writing and advancing my research projects to next level. I would like to thank Dr. Gavin Oudit for collaborations and translational insights in my research projects.

My laboratory environment has been constant source of learning in last five years. It is an amazing feeling to work in such cooperative, helpful and motivating environment for PhD. My sincere thanks to Drs. Sue Wang and Dong Fan for their help in my research projects for MI surgery and culture experiments, respectively. I would like to appreciate my fellow lab member Mr. Mengcheng Shen for his constant help and working together during this program. We all have worked together and everyone has significant contribution to research work presented in this thesis.

Thank you to graduate co-ordinators of Department of Physiology, Faculty of Medicine and Dentistry for their support and direction towards completion of this program. I would like to appreciate the Cardiovascular Research Center (CVRC) for their technical assistance.

My family members have been constant source of motivation to me during this PhD. Their sacrifice back home always motivated me to work hard and to bring best out of me. The freedom and trust they put on me to fulfill my dreams makes me more responsible while staying away from family. I would like to share a joy of this journey with all my family members and relatives.

TABLE OF CONTENTS

List of Tables **Page number**

List of Figures

List of symbols

α- alpha
β- beta
μ- micro

Prefix

k- kilo
c- centi
m- mili
μ- micro
n- nano
U- units
Hz- hertz
L- litre
m- meter
g- gram
^{0}C- degree Celsius

List of Abbreviations

ACEi- Angiotensin converting enzyme inhibitor

ACUC- Animal Care and Use Committee

ADAM- A Disintegrin And Metalloproteinase

ADAMTS- A Disintegrin And Metalloproteinase With Thrombospondin Motif

AP- Activator Protein

Ang II-Angiotensin-II

ANP- Atrial Natriuretic Peptide

ARB- Angiotensin Receptor Blocker

BMP- Bone Morphogenetic Protein

BNP- Brain Natriuretic Peptide

BRILLIANT- Batimastat Anti-Restenosis Trial

BSA- Bovine Serum Albumin

β-MHC- β Myosin Heavy Chain

CVB3- Coxsackievirus

cFB- Cardiac Fibroblast

DAMP- Danger Associated Molecular Patterns

DAPI- 4',6-Diamidino-2-Phenylindole

DHE- Dihydroethidium

DTT- Dithiothreitol

ECM-Extracellular Matrix

ECL- Enhanced Chemiluminescence

EKV- Electrocardiography-based Kilohertz Visualization

ERK-Extracellular Signal-Regulated Kinases

EF-Ejection Fraction

ESPVR-End Systolic Pressure Volume Relationship

EDPVR- End Diastolic Pressure Volume Relationship

EDV- End Diastolic Volume

ESV- End Systolic Volume

GPI- Glycosylphosphatidylinositol

FS- Fractional Shortening

GMCSF- Granulocyte Macrophage Chemoattractant Protein

HELP- Human Explanted Heart Program

HOPE- Human Organ Procurement and Exchange

HUVEC- Human Umbilical Vein Endothelial Cell

HCAEC- Human Coronary Arterial Endothelial Cells

HFpEF- Heart Failure with Preserved Ejection Fraction

HFrEF- Heart Failure with Reduced Ejection Fraction

I/R- Ischemia-Reperfusion

IL1- Interlukin1

IL6- Interleukin-6

IVRT- Isovolumic Relaxation Time

IVCT- Isovolumic Contraction Time

LAD- Left Anterior Descending

LAP- Latency Associated Peptide

LLC- Large Latent TGFβ Complex

LTBP- Latent TGFβ Binding Protein

LVDP- Left Ventricular Developed Pressure

LVESD- Left Ventricular End Systolic Dimension

LVEDD- Left Ventricular End Diastolic Dimension

LV- Left Ventricle

LVP_{sys}- Left Ventricular Systolic Pressure

LVP_{dias}- Left Ventricular Diastolic Pressure

LA size- Left Atrial Size

LOX- Lysyl Oxidase

mRNA– Messenger RNA

MMP- Matrix Metalloproteinase

MT1- MMP-Membrane type-1 Matrix metalloproteinase

MI- Myocardial Infarction

M-mode- Motion Mode

MIDAS- Metalloproteinase Inhibition with Doxycycline to Prevent Acute Coronary Syndromes

MCP1- Macrophage Chemoattractant Protein-1

NFκB- Nuclear factor κB

PBS- Phosphate-Buffered Saline

PDEGF- Platelet Derived Endothelial Growth Factor

PFA- Paraformaldehyde

PCOLCE 1 and 2- Procollagen C-Endopeptidase Enhancer 1 And 2

PIIICP- Procollagen III C-terminal Propeptide

PIIINP- Procollagen III N-terminal Propeptide

PICP- Procollagen I C-terminal Propeptide

PINP- Procollagen I N-terminal Propeptide

PLOD1- Procollagen-Lysine, 2-Oxxoglutarate 5-Dioxygenase-1

PREMIER- Prevention of Myocardial Infarction Early Remodeling

PSR- Picrosirius Red

PV loop- Pressure-Volume Loop

PVDF- Polyvinyl Difluoride

RAS- Renin Angiotensin System

ROS- Reactive Oxygen Species

SDS- Sodium Dodecyl Sulfate

SPARC- Secreted Protein Acidic and Rich in Cysteine

SR- Sarcoplasmic Reticulum

SERCA- Sarco-/Endoplasmic Reticulum $Ca2^{+-}$ATPase

sFRP2- Secreted Frizzled Related Protein2

TAC- Transverse Aortic Constriction

TNFα- Tumor Necrosis Factor-α

TGFβ-1- Transforming Growth Factorβ1

TIMP- Tissue Inhibitor of Matrix Metalloproteinase

TIGM- Texas A&M Institute for Genomic Medicine

TGFα- Transforming Growth Factor-α

TGFRI/II- Transforming Growth Factor Receptor I/II

TUNEL- Terminal deoxynucleotidyl transferase dUTP Nick-End Labelling

WMSI- Wall Motion Score Index

CHAPTER 1

INTRODUCTION

1.1. Introduction

Cardiovascular diseases and the associated morbidities and mortalities remain major health risks, and the medical cost of cardiovascular disorders in North America has been projected to triple by 2030.[2,3] The function of a healthy heart is the result of a complex interaction between the cardiomyocytes and non-cardiomyocytes within the myocardium and this interaction is mediated by a network structure known as the extracellular matrix (ECM). Myocardial ECM occupies a major fraction of the extracellular space (interstitium), while the remaining fraction of the interstitium is occupied by a fluid phase containing water, electrolytes, nutrients and some plasma proteins. Different levels of organization exist within the ECM, the fibrillar component, the basement membrane and the proteoglycans. Heart failure and its progression result in changes in the structure, composition and geometry of the left ventricular myocardium. These changes are generically termed as adverse LV remodeling. Depending of pathological stimulus, such as ischemic cardiomyopathy or pressure-overload heart disease, the distinct patters of LV remodeling cause changes in the structure and function of the myocyte, vascular compartment and ECM components, thereby contributing to heart failure. Therefore, preserving the integrity of the extracellular matrix network for structural support of the myocardium is critically important and provides a target for therapeutic intervention to minimize the burden of heart disease.

1.2. Basic Anatomy and Physiology of the Heart

The human heart is a muscular organ located in the thoracic cavity and sits within fluid filled cavity called as pericardial cavity. Anatomically, its apex points to the left with its base attached to the aorta, pulmonary artery and the vena cava, while the tip of the heart known as the apex, rests just superior to the diaphragm. The heart acts as a circulatory pump, as the right side of the heart takes deoxygenated blood from the veins, delivers it to the lungs for oxygenation through the pulmonary artery, while the left side of the heart receives oxygenated blood from the lungs through the pulmonary veins that is then transported throughout the body tissues.

1.2.1. Structure of the heart wall

The heart wall consists of three muscular layers: Pericardium, Myocardium and Endocardium.

i) Pericardium: The lining of the pericardial cavity is known as the pericardium and consists of two layers called the serous layer and visceral layer. The serous pericardial layer produces serous fluid and lubricates the heart, thereby preventing friction, while the visceral layer prevents excess movement of the heart.

ii) Myocardium: This is a muscular middle layer of the heart wall and responsible for pumping blood. The thickness of the myocardium varies within parts of the heart. The atria of the heart have thin myocardium because the atria do not need to pump blood very far, while ventricles have a very thick myocardium (compared to atria) to pump blood to the lungs or throughout the entire body. The right side of the heart has less myocardium than the left side of heart because the left side has to pump blood through the entire body, whereas right side has to pump blood only to the lungs.

iii) Endocardium: This is a single layer of squamous endothelium that lines the inside of the heart and is responsible for keeping blood from sticking to the inside of the heart and thereby preventing potential blood clots.

1.2.1.1. Chambers of the heart

The heart contains four chambers: right atrium, left atrium, right ventricle and left ventricle. The atria are smaller in size, possess a less muscular layer than ventricles and act as receiving chambers for blood. On the other hand, the ventricles are larger in size, have a more muscular layer and carry blood away from heart. The right-sided chambers of the heart are smaller than those on the left side because the right side of the heart maintains pulmonary circulation to the nearby lungs, while the left side of the heart pumps all the way to the extremities of the body in the systemic circulation.

1.2.1.2. Valves of the heart

As the heart functions by pumping blood both to the lungs and to the systems of the body, the backflow of blood or regurgitation of blood is prevented by the presence of one-way valves. There are two different types of heart valves:

i) Atrioventricular valves (AV): These valves are located in the middle of the heart between the atria and ventricle, thereby allowing the flow of blood from the atria into the ventricle. The AV valves are attached to each other with chordae tendineae. The right side AV valve is called the tricuspid valve because it is made up of three cups (flaps), while the AV valve on the left side of the heart is called the mitral valve or bicuspid valve because it has two cups or flaps.

ii) Semilunar valves: These valves are located between the ventricles and the arteries that carry blood away from the heart. Semilunar valves on the right and left side of the heart are the pulmonary valves and aortic valves, respectively. These valves are smaller than AV valves and do not have chordae tendineae to hold them in place. Instead, the cups of the semilunar valves are cup shaped to catch regurgitating blood.

1.2.2. Different cell types in the mammalian heart

The four-chambered human heart consists of different cell types such as the cardiomyocyte and non-myocardial cells. The non-myocardial cells are fibroblasts, endothelial cells and smooth muscle cells. All these cells contribute to the structural, functional, biomechanical and electrical properties of a functional heart.

1.2.2.1. The cardiac myocyte

The adult cardiomyocyte is a terminally differentiated, contracting cell of the heart with highly specialized organelles. Individual myocytes are interconnected and form a syncytium by homogenous electrical activation myocytes contacts called gap junctions whose organization is critical for the propagation of action potential, excitation-contraction coupling and other biomechanical events. Cardiomyocyte organelles that are important for the excitation-contraction coupling are the following: **sarcolemmal layer** (cell membrane of myocytes)**, sarcoplasmic reticulum** and **sarcomere:**

(**A) The sarcolemmal layer:** This layer of cardiomyocytes contains transmembrane receptors, ion pumps and exchangers. There are three components of the sarcolemmal layer that are important for the inotropic state of myocytes: i) the L-type calcium channel that initiates excitation-contraction coupling, ii) the Na^+/Ca^{2+} exchanger that is responsible for transporting Na^+ and Ca^{2+} across the cell membrane and iii) the Ca^{2+}-ATPase system that pumps Ca^{2+} relatively slowly from myocytes into interstitial space.

(**B) The sarcoplasmic reticulum:** This is major storage site for calcium ions (Ca^{2+}) and acts as the primary storage site for Ca^{2+} in the contractile process. It consists of the following components: **a)** the ATP dependent Ca^{2+} pump called SERCA-2, which determines accumulation of Ca^{2+} within myocytes. This SERCA2A pump eliminates Ca^{2+} from the cytosol along with the Na^{+}/Ca^{2+} exchanger that helps for myocyte relaxation. **b)** the Ca^{2+} release channel that is called the ryanodine receptor. These receptors facilitate the translation of electrical events into chemo-mechanical events. Activation of ryanodine receptors cause Ca^{2+} entry through the voltage-gated L-type Ca^{2+} channels thereby stimulate a process called as Ca^{2+}-induced Ca^{2+} release. This entered Ca^{2+} through these channels causes release of Ca^{2+} from SR via Ca^{2+} release channels into cytosol. **c)** Phospholamban is a regulatory protein in SR that determines amount of Ca^{2+} is retained within SR for the next depolarization and contraction cycle. Phospholamban in its un-phosphorylated form inhibits SERCA2A to reduce the uptake of Ca^{2+} in the cytoplasm. This regulation of Ca^{2+} uptake by phospholamban and SERCA in cytosol is critical to control the inotropic state of myocardium as a defect in the SR-mediated uptake of Ca^{2+} contributes to the progression of various cardiomyopathies.[4-7]

(**C) Sarcomere:** The fundamental contractile unit of myocyte contains all components of the contractile apparatus. The major proteins involved in contractile apparatus are as follows: actin, myosin, tropomyosin and troponin complex. The specific interactions of these proteins cause ATP hydrolysis and physiochemical interaction, which results in the development of tension in the presence of Ca^{2+}.

1.2.2.2. Non-myocyte myocardial cells

Cardiac fibroblasts are flat, spindle-shaped cells of mesenchymal origin that produce various ECM proteins, mainly collagens, and provide a 3D network for myocytes and other cells of the heart to ensure proper cardiac form and function.[8, 9] Cardiac fibroblast responds to a wide range of different stimuli during cardiac diseases such as ischemia[10, 11], hypoxia[12] and biomechanical stress.[13] These various stimuli result in the activation of fibroblasts to myofibroblasts with more ability to increase ECM protein synthesis, thereby contributing to cardiac fibrosis.[14]

Coronary arteries passing through the myocardium contain smooth muscle and endothelial cells that regulate vascular tone and blood flow to the myocardium. The

endocardium contains a single layer of endothelial cells, while the medial layer of coronary arteries contains smooth muscle cells.

1.2.3. Cardiac physiology

The heart serves as pump to drive blood flow throughout the body by rhythmic contraction. A complete heart beat involving a systole and diastole which is called as the cardiac cycle and its frequency is described by heart rate. Each cardiac cycle involves five different phases. The first two phases of the cardiac cycle are called "ventricular filling," which is the movement of blood from the atria to the ventricles, while the next three phases involve "ventricular emptying," where movement of blood from the ventricles to the pulmonary arteries and aorta occurs. During the initial phases of the cardiac cycle, the conducting system of the heart generates an electrical signal in the "pacemaker cells" that are distributed through the heart. In response to electrical stimulation, the myocardium of atria and ventricles undergoes contraction, closing of aortic valve and pumping of blood out of LV, which is followed by sequential relaxation characterised by the opening of the mitral valve and inflow of blood in the ventricles through the atrium.

1.2.3.1. Functional measurements

The heart functions due to contraction and relaxation of cardiomyocytes, and this function of myocytes in the myocardium is governed be the geometry of ventricles (elliptical LV and crescent shaped RV), orientation of myocardial fibers and elasticity of muscle wall. This complex interplay is optimal for cardiac function during systole and diastole. In response to cardiac injury, such as during ischemic cardiomyopathy or pressure-overload with heart disease, cardiac remodeling causes alteration in the shape and size of the LV, as well as changes in the velocity of myocardial fibers, thereby resulting in systolic and diastolic dysfunction. Cardiac function may be measured by using ultrasound echocardiography and pressure-volume (PV) loops.

1.2.3.1.1. Echocardiography

Echocardiographic measurement of cardiac function is based on ultrasound techniques. The sound beams of high frequency penetrate the thoracic cavity and are reflected back to the

transducer (2-4 MHz) when beams reach to interface between tissues of different sound impedance. This signal is processed by software and produces a real time image of heart. The amplitude of the returning signal decides the brightness of the image as the myocardium appears more bright, white and hyperechoic because it reflects more ultrasound than blood which appears less bright and hypoechoic. There are four major echocardiographic imaging to measure cardiac function: Brightness mode (B-mode), Motion mode (M-mode) Doppler imaging (colour and pulse wave doppler) and 3-D imaging.

a) Brightness mode (B-mode): This displays a two-dimensional view of the heart and produces real time black and white images of the heart, thereby helping in visualizing cardiac structures, chamber dimensions, non-quantitative assessment of cardiac phenotype, chamber dimensions and heart function.[15]

***b) Motion mode (M*-mode):** These images are obtained by a rapid sequence of B-mode along a single line and the sequence provides a very high temporal resolution of tissue motion. The M-mode images are useful for calculating or assessing global LV functional parameters such as ejection fraction (EF), fractional shortening (FS), cardiac output, stroke volume and interventricular diameters when measured at the long or short axis view of the B-mode images.

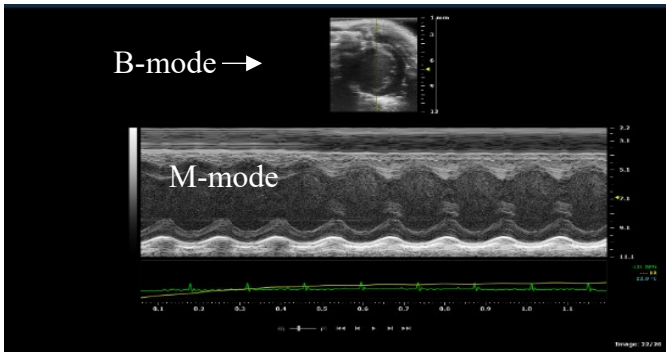

Figure 1.1: M-mode imaging of LV- M-mode image of LV displays movement of ventricular walls, LV cavities during systole and diastole. These images were obtained from B-mode view of LV. Image obtained from echocardiography analysis machine software (Vevo 3100).

c) Doppler mode: This mode of echocardiography uses the Doppler effect to examine the direction and velocity of blood flow in vessels and within the heart. Ultrasound waves are transmitted from transducer and reflected back towards transducer. The increase in the

ultrasound signal is positively correlated with the direction of blood flow. Echocardiographic data are analyzed using computer based software to measure hemodynamic parameters.

In the pulse wave doppler, the determination of the blood flow velocity profile from a precise location using a 2D imaging obtain from the transducer that transmits and receive sound waves. Using transvalvular and mitral Doppler useful for measurement of various diastolic function such as isovolumic relaxation and contraction times, ratio of early (E) to late (A) ventricular filling velocities, and to calculate peak velocities and ejection time.

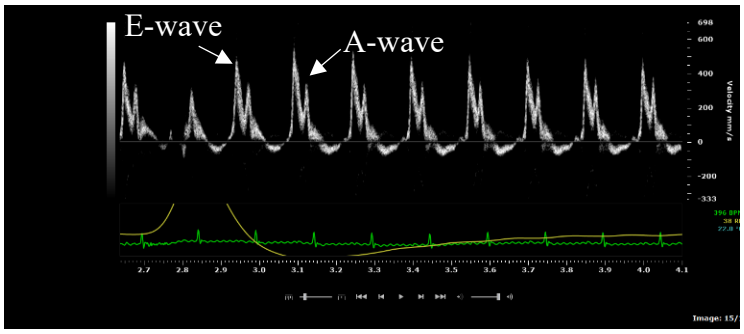

Figure 1.2: Transmitral Doppler for LV filling velocities with early filling (E-wave) and late filling (A-wave). Image was obtained from echocardiography analysis machine software (Vevo 3100).

Colour Doppler is used to measure the direction of blood flow and it is a valuable tool to measure aortic as well as mitral regurgitation and stenosis of valves. Blood flowing towards the transducer shows an increase in the echo frequency, which is identified by the red colour, while blood flowing away from the transducer has decreased in echo frequency, which is identified by the colour blue.

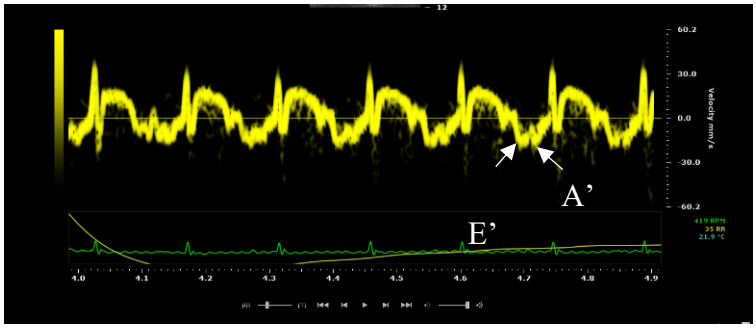

Figure 1.3: Tissue doppler measurement for LV at mitral annulus showing LV filling velocities with early filling (E'-wave) and late filling (A'-wave). Image was obtained from echocardiography analysis machine software (Vevo 3100).

d) Measurement of cardiac function with echocardiography:

Echocardiography is a widely used and reliable technique for assessment of human cardiac structure and function. The main advantages of this technology are its portability, non-invasiveness and real time imaging. Although technological advances made it possible to use this technique in small animals, murine heart characteristics require more spatial and temporal resolution considering the physiology of rodents, such as animal size, orientation of the heart and heart rates.[16,17]

Measurement of systolic function: Altered LV systolic function the cause of heart failure in patients. LV systolic function is assessed using M-mode, 2-D and Doppler techniques. LV ejection fraction is measured using the M-mode measurement at the papillary muscles with a long axis or short axis view. The LV internal dimensions at the end systole (LVESD) and end diastole (LVEDD) measured the LV papillary leaflets using a parasternal long axis view. Fractional shortening is calculated using these measurements and it is a percentage change in LV internal dimension between systole and diastole.[15]

$$\text{Fractional shortening} = (\text{LVEDD-LVESD/LVEDD}) \text{ X } 100$$

If we assume LV is an elliptical shape using the Teichholz method, then the LV cavity volumes are derived from the cubed equation of volume, $V=D^3$.Therefore, percentage change in these blood volumes at systole and diastole is volume of blood pumped out of LV during each contraction/heart beat called as ejection fraction.

$$EF= (LVEDD)^3\text{-}(LVESD)^3/(LVEDD)^3 \text{ X}100.$$

The measurement of LV contractility during ischemic cardiomyopathy where LV adopts complex geometric shapes due to regional wall abnormalities is performed using Simpson's method. Therefore, Simpson's method divides the LV chamber into multiple known thicknesses and diameter by taking various short axis views and then calculates the volume of each slice (area $(A = \pi D/2^2)^2$) X thickness). The accurate measurement depends on thickness of slices, where thinner slices will give a more accurate measurement.

LV movement is classified into five different classes as per *American Society of Echocardiography,* as follows:[15,18,19]

1- Normal; 2-Hypokinetic; 3-Akinetic; 4-Dyskinetic; 5-Aneurysmal.

Measurement of diastolic function: Diastole is a phase of the cardiac cycle where myocardium becomes unstressed and loses its ability to generate force in order to fill the blood in the heart. Due to abnormalities such as a decrease in ventricular relaxation and/or increase in LV stiffness, the ventricular chamber is unable to achieve an adequate volume of blood during diastole, at normal diastolic pressure and volume to maintain normal stroke volume, thereby resulting in diastolic dysfunction. Diastolic dysfunction can occur with preserved ejection fraction (HFpEF) or occur along with systolic heart failure (HFrEF).[20] Diastolic function using echocardiography is traditionally measured using transmitral flow velocities, including early (E) and late (A), E/A ratio and deceleration time from an apical four chamber view using pulse wave Doppler. The transmitral E wave is related to the time course of active LV relaxation, while the A wave is related to passive LV relaxation. The normal LV myocardium relaxes without an increase in the LV volume during the interval between the closure of the aortic valve and opening of the mitral valve, which is called isovolumic relaxation time (IVRT). IVRT increases with diastolic dysfunction and impaired relaxation, but decreased compliance and elevated LV filling result in decreased IVRT. Therefore, the IVRT measurement is useful in determining the severity of diastolic dysfunction. Severity of heart disease or heart failure is defined based on four basic transmitral inflow patterns with respect to E/A ratio. Using the echocardiography technique, the diastolic dysfunction can be classified in four different ways:[21,22]

A. Normal (E>A) **B**. Abnormal (E<A) **C.** Pseudonormal (E>A) D> **D.** Restrictive filling (E>>>A).

Abnormal relaxation pattern of transmitral (E>A, prolonged IVRT and DT) is commonly associated with ischemic cardiomyopathy, hypertension, LV hypertrophy and aging. Further delayed relaxation affects the early filling phase and the resulting increased left atrial pressure that causes the filling pattern appears to be normal as E>A. This transition phase/zone of abnormal relaxation and restrictive filling is termed as pseudonormalization which shows normal diastolic values. This pseudonormalization is evaluated using the Valsalva maneuver or agent that will reduce preload, such as nitroglycerin. Advanced diastolic dysfunction are characterised by reduction in LV compliance with impaired myocardial relaxation with increase in left atrial pressure or LVEDP. This causes an increase in pressure gradient between LV and LA thereby significantly higher E wave velocities while reduction of DT due to noncompliant

ventricle. This is called a restrictive filling pattern, which is characterised by E>>>A, decreased IVRT and DT. This is often observed in restrictive cardiomyopathies with LVEF>40 and dilated cardiomyopathies with poor systolic function. The mitral echocardiography has limitations of preload dependency, atrial fibrillation, tachycardia, and resurgent valve stenosis, as well as commonly observed pseudo-normalization patterns. Therefore, tissue Doppler echocardiography is used for transthoracic echocardiographic assessment of diastolic function.

1.2.3.1.2. Pressure-volume (PV) loop

The hemodynamic events of the cardiac cycle can be displayed by instantaneous pressure-volume graphs under constant steady state condition as these graphs are repeated with each contraction. During each cardiac cycle, there is a single pressure-volume point that coincides with end diastole (lower right corner of loop) and other single pressure-volume points that coincide with end systole (upper left corner of loop). A series of pressure-volume loops can be obtained for each cardiac cycle by acute change in loading conditions with transient inferior vena cava occlusion to reduce preload or with administration of agent that will increase afterload (e.g. phenylephrine) without affecting myocardial contractility. The end systolic (ESPVR) and end diastolic (EDPVR) boundaries of these loops are obtained by connecting the end systolic and end diastolic pressure volume points for each loop. The EDPVR represents the passive physical properties of a chamber with myocytes mostly in relaxed states and shows a non-linear relationship, while the ESPVR represents mostly properties of myocytes in a state of maximum activation and shows a linear relationship.[23]

This PV loop technique was initially developed and demonstrated by Sagawa and colleagues [24] around 35 years ago using a canine model. Technically, in PV loop analysis, a pressure-volume catheter with conductance is inserted along the axis of a ventricle and provides real-time volume signal as well as a micro-manometer pressure signal. (Non-invasive methods such as echo and MRI are limited by reliance on motion parameters that are influenced by loading conditions, though offer an advantage in that they can be repeated in the same animal and provide direct quantification of absolute volume). [25] Bann et al [26] developed a modified technique and it became possible to correlate the change in LV volume with the change in electrical resistance of blood pool. The conductance catheter used in this technique has multiple ring electrodes placed along its length and a high-frequency low-amplitude current passed

through an outer pair of electrodes to generate electric fields between these electrodes that then pass through the blood and muscle walls. The strength of this field is directly proportional to the distance from the electrodes.

1.3. Heart Disease

1.3.1. Ischemic cardiomyopathy

Ischemic cardiomyopathy results from weakening of the heart muscle due to the narrowing of the coronary arteries that causes reduced blood supply, nutrients and oxygen to the myocardium. This ischemic insult causes the LV to dilate, enlarge, and therefore reduces the pumping ability of the heart. Permanent blockage of a coronary artery causes a heart attack, which is also called a myocardial infarction. Myocardial ischemia triggers many cellular and molecular events such as cell death, apoptosis, inflammation, reduced angiogenesis, cardiomyocyte growth, adverse remodeling of LV and myocardial fibrosis. These events gradually combine and develop LV dilation, wall thinning, infarct formation and expansion, thereby affecting overall heart geometry and pumping function of LV and can result in heart failure.

1.3.1.1. Ischemic cardiomyopathy and oxidative stress

Ischemic cardiomyopathy causes an increase in the production of reactive oxygen species (ROS) and activating mechanisms. ROS that contribute to ischemic preconditioning are cardioprotective; [27,28] however, oxidative stress has deleterious effects and contributes to the progression of ischemic cardiomyopathy with an altered balance of natural antioxidant systems. ROS, when generated, activates immune cells in the infarcted hearts and promotes leucocyte chemotaxis by activating the complement system, by stimulating expression of P-selectin and cytokine and chemokine synthesis through NFkB activation. [29, 30] Oxidative stress has been reported in the remodeling process post-MI. As ROS contribute to the remodeling process with the activation of the MMPs, which participate in reconfiguration of ECM[31, 32], ROS acts to signal molecules in the development of compensatory hypertrophy.[33] Increased NADPH oxidase linked ROS activity in ischemic cardiomyopathy patients with increased rac-1 GTPase activity suggested that ROS plays a role in clinical heart failure patients and contributes to heart failure progression. [34,35]

1.3.1.2. Ischemic cardiomyopathy and necrosis and apoptosis

Myocyte loss during ischemic cardiomyopathy involves apoptosis, and during the acute stage of post-MI, apoptotic myocytes are localized in the border zone between the central infarct area, while the peri-infarct region was shown to upregulate the apoptotic regulatory proteins Bax and Blc2. Ischemic cardiomyopathy post-MI apoptosis occurs during the first 2-4 hours of occlusion of the coronary artery, while necrosis becomes prominent between 6-24 hours. Cell death in the infarct zone is large in magnitude but of shorter duration because it is then followed by LV remodeling, with infarct formation and expansion.[36] Studies using genetic and pharmacological approaches show that inhibiting myocyte apoptosis can decrease infarct size and LV dilation and improve LV pumping function. Some studies also indicate a reduced mortality in the rodent model of ischemia reperfusion. The rate of apoptosis has been correlated strongly with thinning of infarct and LV dilation in patients with heart failure and with a traumatic cause within 10-62 days of post-MI.[37]

1.3.1.3. Ischemic cardiomyopathy and inflammation and remodeling

Post-MI repair is the result of a complex series of events initiated by inflammation and immune cell infiltration. These events help to digest and clear the damaged cells and ECM degradation. This is followed by reparative phase with resolution of inflammation, proliferation of fibroblasts and scar formation. Inflammation activation is a critical determinant for the transition to late reparative and proliferative phases because the proper and timely resolution of inflammation determines further if the healing and remodeling process is disproportionately prolonged or if insufficient suppression of inflammation can further lead to sustained tissue damage, improper healing and defective scar formation.[38] Various molecules are involved in the inflammatory phases of post-MI repair, as hypoxia during ischemia has been reported to impair vascular cell integrity, while restoration of blood flow with reperfusion further causes ROS generation.[39,40] Inflammation post-MI affects all myocardial cell types such as cardiomyocytes, endothelial cells and fibroblasts. Immune cells have also been implicated as cellular effectors of post-MI inflammation.[38] Danger associated molecular patterns (DAMPs) released from necrotic myocytes provide stimulus for post-MI inflammation,[41] while surviving myocytes also contribute to post-MI inflammation by production and secreting cytokines.[42] Endothelial activation leads to extravasation of leukocytes in the infarcted area. Activation of endothelial cell specific transcription factor forehead box O4 post-MI has been demonstrated to promote neutrophil infiltration in the infarct area.[43] DAMPs from necrotic myocytes induce expression of adhesion molecules, trigger

adhesive interaction and help infiltration of the inflammatory cells while activated. Endothelial cells in the infarct areas also serve as an important source of cytokines and chemokines. [44, 45] The neutrophils captured by activated endothelium sense chemokines bound to glycosaminoglycan on endothelial surface. These chemokines promote neutrophil transmigration, as these cells actively crawl towards endothelial junctions, then neutrophil extravasation. These infiltrated neutrophils then release proteolytic enzymes, secreting MMP8 and MMP9 to cause further damage. Therefore, various approaches to inhibit or limit inflammation post-MI have been tried such as reducing the generation of chemokines by compliment activation[46] and reducing the neutrophil number through anti-neutrophil antibodies.[47] Neutrophil depleting antibodies[48] were successful to some extent in reducing ischemic injury.

The adult mammalian myocardium contains a small population of resident macrophages, which are inconspicuous in the healthy heart but take central stage after post-MI injury. Post-MI, monocyte adherence to the ECM basement membrane stimulates conversion to a macrophage, by inducing expression of cytokines such as GMCSF, TNFα, PDEGF, TGFα and THGβ and IL1. Among these cytokines, MCSF is required for macrophage survival, while PDEGF acts as an endothelial chemoattractant and mitogen for fibroblasts. TGFβ-1 released from the macrophages contributes to cardiac fibrosis and further scar formation. Due to the heterogeneity of macrophage activation, there are different types of macrophage classes with diverse immunological properties that are activated post-MI. Classical (M1) macrophages promote inflammation and ECM degradation and are activated by TH1 related cytokines, while M2 (alternative) macrophages activation is induced by Th2 cytokines, and M2 macrophages promotes ECM deposition, and angiogenesis. Therefore, transition as well as dynamic balance between the two activation processes, determines the LV dilation and post-MI remodeling.

1.3.2. Pressure-overload cardiomyopathy

Pressure-overload cardiomyopathy occurs during aortic stenosis and systemic hypertension, as the LV is unable to pump blood due to an increased afterload. The LV develops a compensatory response and bears an extra load by augmentation of muscle mass, thereby increasing in myocyte size and developing compensatory concentric hypertrophy.[49] These compensatory mechanisms become out shaded with a persistent increase in the afterload and a concomitant increase in LVEDP. These cause dilation of the LV chamber, creating a mismatch between contractility and affect speed of shortening of LV chamber. [50] At the cellular level, it has been reported that increased myosin heavy chain synthesis (~35%) within hours of pressure-overload [51] and further LV dilation causes alteration of Ca^{2+}

homeostasis[52,53], ionic currents[54,55] and fibrosis.[56,57] These changes result in the expression of fetal genes [58 59] as follows: **(i)** genes that modify motor unit composition and regulation, **(ii)** genes that modify energy metabolism, **(iii)** genes which are components of hormonal pathways such as ANAP and Ang II, and **(iv)** extracellular matrix regulatory genes, mainly collagen-I and collagen-III.

A decompensated pressure-overload state is often characterised by an increase in the deposition of ECM proteins, mainly collagens, and causes myocardial fibrosis. This myocardial fibrosis following pressure-overload is a reactive process where interstitial and perivascular fibrosis occurs in the absence of myocyte loss. It has been shown in animal models and hypertensive, aortic stenosis patients that deposition of collagens occurs in the interstitium and perivascular areas.[60,61] This cardiac fibrosis impairs myocardial compliance, creates diastolic dysfunction, reduces LV filling, and can alter structure and function of LV, thereby causing LV dilation.

1.4. Extracellular Matrix Structure

Cardiac ECM is a highly organized structure that provides architectural integrity to adjoining myocytes and the neighbouring blood vessels and capillaries. An intact ECM translates single myocyte contractility into ventricular syncytium, prevents myocyte slippage and overstretching during the cardiac cycle, and contributes to cardiac recoil during diastole. Myocardial ECM can be broadly divided into three components, the fibrillar structure that is comprised of structural proteins (primarily collagen type I and III); the basement membrane that forms an interface between the cardiomyocytes and the interstitial space; and the non-structural proteins such as proteoglycans.

1.4.1 Fibrillar network structure

The network structure of the ECM is primarily comprised of fibrillar collagens (type I and type III). These collagens are produced as pro-collagens and undergo a number of processing steps before collagen fibrils and collagen fibers are deposited in the interstitium. A defect in any of these steps can lead to adverse ECM remodeling.

Collagens are present in the majority of tissues and organs and make up 2-4% of a healthy human body.[62] Based on their structure, collagen molecules are divided into two main classes: fibril forming collagens, which include collagen type I, type II, type III, type V and type XI; and non-fibril forming collagens, including collagen type IV and type VI that are

expressed in the heart.[63,64] The fibril forming collagens have long continuous triple helix structures, whereas non-fibril forming collagens are more heterogeneous and further classified based on molecular and supramolecular structures [65,66]. Fibrillar collagen type I and type III are the predominant components of the fibrillar network structure of myocardial ECM. Collagen type I provides the myocardium with tensile strength, while collagen type III accounts for distensibility of the myocardium.[67]

Collagens are produced as triple helix pro-collagens consisting of three α-chains with the characteristic Gly-X-Y repeat sequence[68]. Pro-collagens are secreted to the extracellular compartment for post-translational modifications. Multiple intracellular and extracellular steps are required from mRNA synthesis of collagen α-chains until the deposition of collagen fibres in the interstitium. Pro-collagen-α is produced in the ribosome of cFB and is imported to the endoplasmic reticulum (ER) where it undergoes hydroxylation of proline and lysine residues, N- and O-linked glycosylation, trimerization, disulphide bonding, isomerization and finally folding of the triple helix structure.[66] In the ER, stability of the triple helix collagen molecule is maintained by a chaperone molecular, Hsp47.[69] The soluble pro-collagen triple helix is then transported to the Golgi apparatus and packed inside secretory COPII vesicles, and then secreted into the interstitial space.[70] Recently, the ubiquitin ligases CUL3-KLHL12 have been reported to regulate large COPII coat formation that is essential to accommodate the large size of the collagen triple helix prior to its secretion from the cFB .[70] In the extracellular space, the N- and C-propeptides are enzymatically removed from the pro-collagen molecule. The N-propeptide can be cleaved by a disintegrin and metalloproteinase with a thrombospondin motif (ADAMTS)-2, -3, -14, while removal of the C-propeptide can be mediated by bone morphogenic protein-1 (BMP1)[63,65] whose activity is enhanced by procollagen C-endopeptidase enhancer (PCOLCE 1 and 2) and the secreted frizzled-related protein (sFRP2).[71-74] PCOLCE 1 and 2 show the highest expression levels in the myocardium and can increase the efficiency of C-propeptidases by up to 20-fold. [73,75] Metalloproteases meprin α and meprin β can function as both C- and N-propeptide proteinases.[76] The C-terminal and N-terminal propeptides of type I procollagen (PICP, PINP), and those of type III procollagen (PIIICP and PIIINP) are released during biosynthesis of these collagen fibrils in a stoichiometric manner, and have been considered biomarkers of collagen synthesis.[9] Following the removal of the C- and N-propeptides, lysyl hydroxylase (PLOD1) and lysyl oxidase (LOX) mediate hydroxylation and

oxidative deamination of collagens, leading to cross-linking and stabilization of collagen fibres.[77,78]

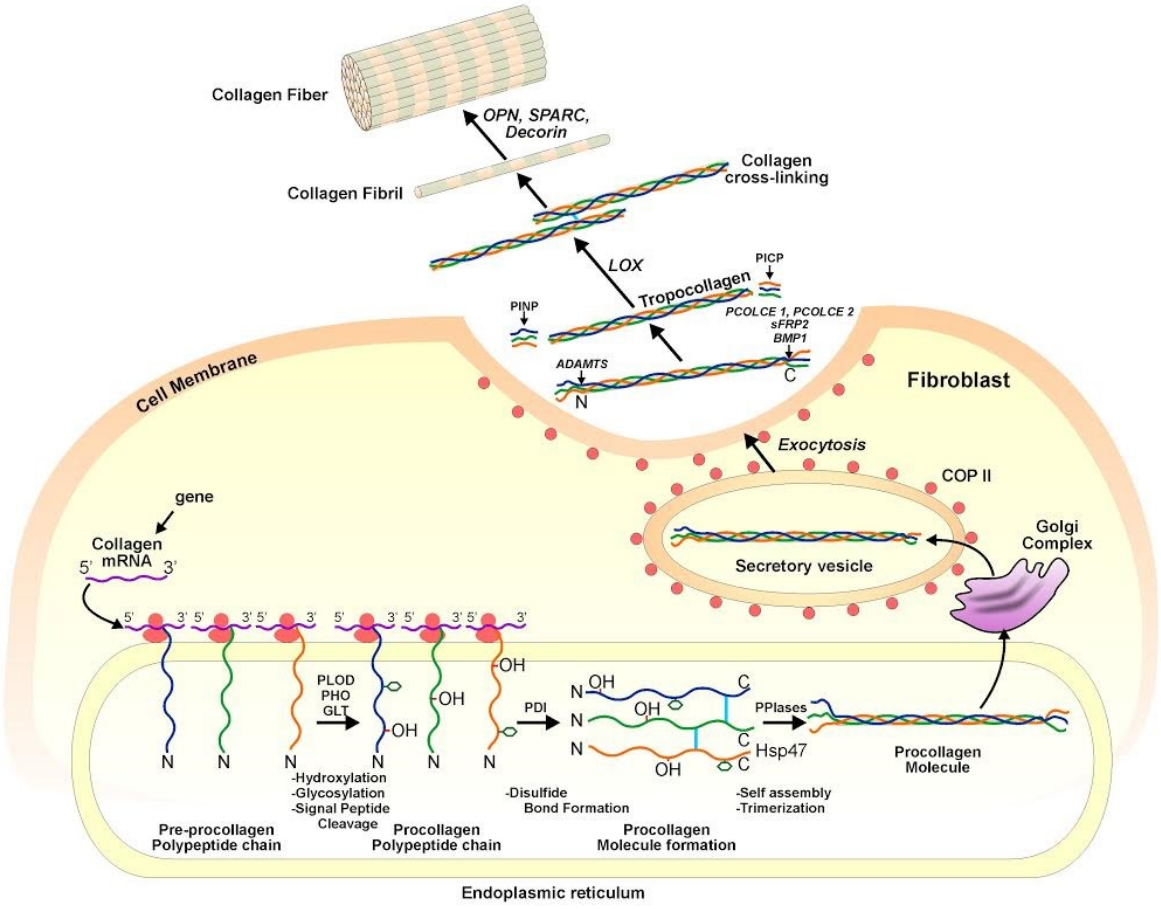

Figure 1.4: Collagen biosynthesis pathway: The steps involved in collagen transcription, translation and post-translational modification, hence the formation of collagen fibers that are then deposited in the extracellular space and contribute to cardiac fibrosis in heart diseases. Extracted from Takawale et al[79]

Further post-translational regulations of collagen fibres are mediated by matricellular proteins, the non-structural ECM molecules that can mediate collagen stabilization and accumulation in the interstitium.[80]

Among the matricellular proteins, SPARC (secreted protein acidic cysteine-rich) and osteopontin (OPN) have been linked to cardiac fibrosis.[60] In normal physiology, SPARC regulates the processing of pro-collagen-α and its interaction with the fibroblast cell surface,

and can alter collagen formation and deposition in cardiac interstitium without altering the baseline cardiac systolic function or the blood pressure. [60,81] OPN similarly stabilizes collagen fibres; however, OPN could be involved in additional aspects of cardiovascular function since OPN-null mice have increased heart rate, lower blood pressure and enhanced arterial compliance.[82] The deletion of SPARC or OPN increased the rate of LV rupture following myocardial infarction (MI),[83-85] indicating the critical role of these matricellular proteins in assembly and deposition of collagen fibres in generating a supportive matrix within the post-MI scar.

1.4.2 Basement membrane

An intact connection between the cardiomyocytes and the ECM is critical in the function of a healthy heart. The basement membrane provides an interface between the ECM and the cardiomyocytes wherein molecules such as integrins mediate the cell-ECM connection. [86-87] Myocardial basement membrane contributes to structure, protection, and polarization of cells, and it is important for embryonic development, tissue homeostasis. The ECM maintains the alignment of myofibrils within the myocytes through a collagen-integrin-cytoskeleton-myofibril link. The basement membrane consists of a number of proteins, such as laminin, fibrillin, fibronectin, and collagen type IV, which serve distinct function in the myocardium.

1.4.2.1. Laminin: Laminins are heterotrimeric, multidomain extracellular proteins consisting of 5-α, 3-β, and 3-γ chains that recombine to form at least 14 distinct laminin isoforms .[88] In the heart, laminin 8 and laminin 9 are the major constituents of the basement membranes of the cardiomyocytes, and deficiency of laminin α4, a component of laminin-8 and -9, resulted in an impaired cardiovascular ECM structure and defective microcirculation leading to cardiomyopathy.[89]

1.4.2.2. Fibrillin: Fibrillins are a group of glycoproteins containing 40-80 amino acid residues and Ca^{2+} binding epidermal growth factor domains. Fibrillin has three isoforms, fibrillin-1, -2, and -3, among which fibrillin-1 and fibrillin 2 are well studied, whereas fibrillin-3 has been less explored.[90] In normal physiology, fibrillin-1 and fibrillin-2 function as supporting structures that provide tissue integrity, as well as temporal and hierarchical assembly of micro fibrils and elastic fibers. These proteins also serve as regulators of signalling events by sequestering TGFβ and bone morphogenic protein complexes in the ECM.[91] Mutations in

fibrillin-1 and fibrillin-2 resulted in fibrillinopathies such as Marfan syndrome and congenital contractual arachnodactyly, respectively.[92]

1.4.2.3. Fibronectin: Fibronectin is a large ECM glycoprotein (230-271kD) that is ubiquitously expressed and is present in the ECM as well as in plasma.[93-95] The cellular fibronectin is expressed by fibroblasts and is deposited locally at ECM, while plasma fibronectin is expressed at high levels by hepatocytes and later secreted in soluble form into the plasma where it has a half-life of two days in the circulation.[96] Various cardiac cell types such as fibroblasts, endothelial cells, and vascular smooth muscle cells have the ability to secrete, bind and assemble fibronectin into fibrils in the ECM. The assembly of fibronectin and the ECM is a stepwise process. First, fibronectin binds to cell surface receptors such as integrins via its 70kDa N-terminal domain. Next, fibronectin needs to be unfolded from its compact structure into an extended structure that exposes binding sites buried in the soluble structure to promote the interaction of fibronectin with other fibronectin molecules and ECM components. [94]

1.4.2.4. Collagen type IV: Collagen IV is a non-fibrillar collagen present in the basement membrane.[97] Six isoforms for collagen IV have been described, α-I to α-VI, while collagen IVα-5 isoform is highly expressed in the heart. [97, 98] Collagen IV can act as a substrate for a number of MMPs such as gelatinase, stromelysins, and matrylysins. It has been reported that collagen IV mRNA is expressed in fibroblasts and in myocytes and its expression increases transiently following cardiac pressure-overload, returning to baseline levels by day-7.[99] In the patients with hypertrophic cardiomyopathy, collagen IV was significantly increased, which correlated with the observed systolic and diastolic dysfunction.[100]

1.4.3. Proteoglycans within the ECM

Proteoglycans are non-structural proteins of the ECM. They can bind to and sequester soluble growth factors and cytokines within the interstitial space, which can be released in response to cellular or signaling cues. In this fashion, the activity of these growth factors and cytokines is tightly regulated beyond their mRNA and protein synthesis.[101] Based on their extracellular localization, size and structural properties, proteoglycans are divided into four groups: **cell surface proteoglycans** (syndecans, glycan), **hyalectans** (Versican, Aggrecan, Neurocan, Brevican), **basement membrane proteoglycans** (Perlecan, Collagen type XVIII, Agrin), and **small leucine rich proteoglycans** (Biglycans, Decorin, Lumican). Below is a

description of proteoglycans that are well-characterized and involved in cardiac physiology and/or pathology.

1.5. ECM Turnover and Homeostasis

During physiological turnover, ECM proteins are degraded by the proteolytic function of matrix metalloproteinases (MMPs) and are replaced by newly synthesized proteins. The function of MMPs is kept under check by their inhibitors, predominantly the tissue inhibitors of metalloproteinases (TIMPs). A tightly controlled balance in the function of these two groups of proteins is essential in maintaining the integrity of ECM structure.

1.5.1. Matrix metalloproteinases

MMPs are a family of zinc-dependent proteolytic enzymes that were first identified in the tadpole fin skin undergoing metamorphosis by Gross and Lapiere in 1962.[102] MMPs are believed to be the predominant proteases responsible for degradation of the ECM proteins, the first step in ECM turnover, but also perform additional function such as regulating inflammation, inducing oxidative stress in multiple tissues.[103] As such, MMPs play critical roles in physiological remodeling and during development. Different MMPs share a great degree of structural homology, generally consisting of a prodomain, a catalytic domain, a hinge and a hemopexin domain. To date, 24 MMPs have been identified in vertebrates, 23 of which are found in humans. MMPs have been divided into 6 groups based on their structure and target substrates.

Collagenases include MMP1, MMP8, MMP13 and MMP18 (Xinopus), which can cleave interstitial collagen type I, type II and type III at a specific site three-fourths from the N-terminus [104-105], as well as a number of other ECM and non-ECM molecules. MMP1 degrades collagen types I, II, III and the basement membrane proteins, MMP8 and MMP13 can process collagen types I, II and III. Rodents lack the MMP1 gene but express MMP1a (mColA) and MMP1b (mColB) genes primarily in the reproductive organs but not in the heart in baseline conditions.[106] **Gelatinases** include only two MMPs, MMP2 (gelatinase A) and MMP9 (gelatinase B), which digest gelatins. In addition, MMP2 cleaves collagens type I, II and III [107-109], while MMP9 can digest elastin.[110] **Stromelysins** include MMP3 (stromelysin 1) and MMP10 (stromelysin 2), which have similar substrate specificities, although MMP3 has a

higher efficiency. In addition to digesting ECM components, MMP3 can activate pro-MMPs such as pro-MMP1.[111] MMP11 is often included in this group as stromelysin 3, although its sequence and substrate specificity (gelatin, laminin, fibronectin, collagen type IV)[112] are different from MMP3. **Metrilysins** lack the hemopexin domain. MMP7 (metrilysin 1) and MMP26 (metrilysin 2) belong to this group, which process a number of ECM proteins and cell surface molecules. **Membrane type MMPs** (MT-MMPs) are a group of MMPs that, unlike the soluble MMPs, are connected to the cell membrane. This group includes 6 members: four are type I transmembrane proteins, MMP14 (MT1-MMP), MMP15 (MT2-MMP), MMP16 (MT3-MMP) and MMP24 (MT5-MMP); and two are glycosylphosphatidylinositol (GPI)-anchored proteins, MMP17 (MT4-MMP) and MMP25 (MT6-MMP). With the exception of MT4-MMP, all MT-MMPs can activate pro-MMP through interacting with TIMP2 such as MT1-MMP [113] or independently as with MT2-MMP.[114] Among the MT-MMPs, the role of MT1-MMP, which can cleave a number of ECM proteins including fibronectin, laminin-1 and fibrillar collagen type I, has been best characterized in heart disease.[87, 115-117]

The MMPs that do not fit in the above groups have been grouped as **other MMPs**, and these include 5 members. MMP12 (metalloelastase) is mainly expressed in macrophages [118] and is essential for macrophage migration.[119] MMP19 was identified as a T-cell-derived auto-antigen from patients with rheumatoid arthritis.[120] MMP20 or enamelysin digests amelogenin and is primarily located within newly formed tooth enamel. MMP22 was first cloned from chicken fibroblasts [121], and later a human homologue was identified, but the function of this MMP is unknown. MMP23 lacks the hemopexin domain, and instead has a cysteine-rich domain followed by an immunoglobulin-like domain. It is cleaved in the Golgi and is released into the interstitial space as an active enzyme.[122] MMP23 is mainly expressed in the reproductive tissues.[123] A list of genetically modified mouse models with deficiency or overexpression of MMPs or TIMPs, as well as their response to different experimental heart disease models is presented in **Table 1**.

1.5.2. Activation of MMPs:

MMPs are primarily synthesized as inactive zymogens (pro-MMPs), and can be activated by the removal of the amino-terminal propeptide domain either by auto proteolysis or via processing by another MMP or serine protease. Proteolytic activation of MMPs can occur

in a stepwise fashion, involving an initial proteolytic cleavage at an exposed loop region between the first and the second helices of the propeptide. This proteolytic cleavage destabilizes the rest of the propeptide, including the cysteine switch–zinc interaction, and allows the intermolecular processing by partially activated MMP intermediates or other active MMPs.[124] The stepwise activation system could be nature's way of a finer regulation of MMP activities to control these destructive enzymes. For instance, it is possible that TIMPs could interact with the intermediate MMP forms and prevent their full activation.

A number of treatments *in vitro* can activate pro-MMPs, most likely through disruption of the cysteine-zinc interaction of the cysteine switch.[125] These include chemical agents such as thiol-modifying agents, oxidized glutathione, SDS, chaotropic agents, ROS, as well as low pH and heat treatment.[105] An activation pathway relevant to *in vivo* events is plasmin-mediated MMP activation. Plasmin is a serine protease that is produced as a zymogen, plasminogen, and converted to its active form by either a tissue plasminogen activator that is bound to fibrin or a urokinase plasminogen activator that is bound to a specific cell surface receptor. The membrane-associated localization of the plasminogen and urokinase plasminogen activator can create localized proMMP activation and subsequent ECM turnover. Plasmin has been reported to activate proMMP1, proMMP3, proMMP7, proMMP9, proMMP10, and proMMP13.[126] Activated MMPs can participate in processing other MMPs in the stepwise activation system described above.

Pro-MMP2 is not readily activated by general proteinases. While intracellular activation of pro-MMP2 has been reported in the cardiomyocytes[127], the main activation of proMMP2 occurs on the cell surface by the action of MT-MMPs. MT1-MMP, MT2-MMP[114], MT3-MMP [128], MT5-MMP [129] and MT6-MMP[130], but not MT4-MMP [131], can activate pro-MMP2. MT1-MMP- mediated activation of pro-MMP2 is unique as it requires the involvement of TIMP2 through the formation of the MT1-MMP/TIMP2/pro-MMP2 complex. This complex can be formed in two ways. TIMP2 and pro-MMP2 form a complex through their C-terminal domains, leaving the N-terminal domain (the inhibitory domain) of TIMP2 to form a complex with MT1-MMP anchored to the cell-surface. Alternatively, TIMP2 forms a complex with a MT1-MMP on the cell membrane which then acts as a receptor to recruit pro-MMP2 to form a complex with the free C-terminal domain of TIMP2. Proteolytic activation of pro-MMP2 will take place in two steps by an adjacent MT1-MMP that is free of TIMP2. [113, 132] A similar mechanism has

been proposed for MT3-MMP-mediated activation of pro-MMP2.[133] Such mechanism of activation has not been described for any other pro-MMP. Activation of pro-MMP2 by MT2-MMP [114], MT5-MMP and MT6-MMP [134] occurs independently of TIMP2.

1.5.3. Physiological inhibitors of matrix metalloproteinase

TIMPs are specific inhibitors of MMPs, which can reversibly bind to activated MMPs in a 1:1 stoichiometry. TIMPs are small proteins (21-30 kDa) that have two major domains, the N-terminal and the C-terminal domains, each containing 3 loops that are maintained by 12 conserved cysteine residues folding the protein into a 6-loop structure.[135] There is a great degree of structural homology among the four TIMPs. In general, a TIMP molecule looks like a wedge that slots into the active side-cleft of an MMP in the same manner as a substrate [105], and inhibition of MMPs occurs through an interaction between the TIMP N-terminal cysteine residues, particularly the cys1–cys70 disulfide bonds, with the TIMP and Zn^{2+} of the MMP active site. TIMPs inhibit all MMPs, except TIMP1 that does not inhibit MT1-MMP [136], and perhaps other MT-MMPs. The inhibitory profile of TIMP3 is more diverse than other TIMPs, as it can inhibit a number of disintegrin and metalloproteinases [137], including ADAM 10 [138], ADAM12 [139], ADAM17 [140], and aggrecanase 1 (ADAMTS4) and aggrecanase 2 (ADAMTS5) [141], while TIMP1 can inhibit ADAM 10.[138] It has also been reported that TIMP3 is a high-affinity inhibitor for MT3-MMP, whereas TIMP2 is a more potent inhibitor for MT1-MMP. [12, 133]

While interaction of TIMPs with specific MMPs and the resulting inhibition or activation of the MMPs is well recognized, increasing evidence suggests that TIMPs possess MMP-independent function, such as regulating cell growth and function by directly interacting with cellsurface receptors and activating intracellular pathways.[142-145] Studies in fibroblasts have shown that TIMP1 can bind to membrane receptor CD63 and activate extracellular signal-regulated kinase (ERK) [146] [144], and can activate the protein kinase B (Akt) and the related intracellular pathways in an MMP-independent fashion [145], while TIMP2 has been shown to reduce fibroblast proliferation by reducing MAPK-mediated signaling [147], and to bind to α3/β1-integrin dimer.[143]

These findings offer a new angle to the MMP-TIMP interaction, since MMPs, by binding to TIMPs, can serve as inhibitors of the TIMPs and such TIMP-mediated signaling

pathways. It has been proposed that different function of TIMPs (MMP-dependent or independent) could be distinctly regulated by their and N- and C-terminus.[142,148-150] For instance, the C-terminal domain of TIMP2 is essential for anchoring to the proMMP2 and initiating its activation but is not required for the MMP inhibitory function of TIMP2.[105,151] A single point mutation in the N-terminal domain of TIMP3 significantly impaired its MMP inhibitory function, but did not alter its inhibitory capacity against ADAM17 inhibition.[150] TIMPs are inducible proteins and their expression is altered during development and in pathological remodeling. A number of factors have been identified to induce the expression of TIMP1, such as growth factors (b-FGF, PDGF, EGF), phorbol esters, serum, cytokines (IL-6, IL-1 and IL-1β) [152], and erythropoietin [153]; TIMP2 by cAMP [154]; TIMP3 by TGFβ [155], IL-1β [156], TNFα [157] and ROS [155]; and TIMP4 by hypoxia [158] and cytokines [12,159]. However, it is important to note that induction of each TIMP can vary based on the cell type, organ and the pathology. The promoter structure of each TIMP is distinct, which could explain their different expression and induction patterns. The promoters of TIMP1, TIMP2 and TIMP3, but not TIMP4, contain the activator protein 1 (AP-1) motif that is involved in baseline and inducible expression of these genes.[160] The TIMP1 promoter lacks the TATA-box, but contains multiple transcription start points and GC boxes that give rise to its highly inducible nature [157, 161] The promoter for TIMP2 has a TATA box as well as multiple transcription start points, several Sp sequences, one AP-1 and two AP-2 sites.[162] The TIMP3 promoter has a TATA-box, six AP-1 sites, one transcription start point, two NFκB sites and two p53 sites.[163] The TIMP4 promoter also lacks the TATA-box sequence, similarly to TIMP1, but contains consensus motifs for Sp1 and an inverted CCAAT box upstream of an initiator-like element that is in close proximity to a transcription start site and essential in basal expression of TIMP4.[164] Recent studies indicate that TIMPs can also be regulated by microRNAs (miRNAs), the small non-coding RNAs (19-25 nucleotides) that bind to mRNA, inhibiting its transcription and leading to reduced translation and/or degradation of the target mRNA molecule.[165, 166] Recently, two functionally related miRNAs, miRNA20a and miRNA106a, have been shown to target TIMP2 in human glioma stem cells [167] and miRNA 200b in HEC-1A cells.[168] miRNA 17 has been reported to target TIMP1 and TIMP2 in the myocardium post-MI.[169] MiRNA221/222 suppressed expression of TIMP3 and its tumor-suppressing effects in aggressive cell lung cancer and

hepatocarcinoma cells [170], miRNA21 in breast cancer cells [171], miRNA206 in skeletal muscle [172], and miR17 in prostate tumor cells.[173]

MMPs can also be inhibited by other proteins in addition to TIMPs. Plasma α-macroglobulins are endopeptidase inhibitors that inhibit most proteinases, including MMPs. α2-macroglobulin is a large (170 kDa) plasma protein that is produced mainly by the liver in response to inflammatory cytokines. It irreversibly inhibits MMPs by trapping them within the macroglobulin, forming a complex that is subsequently removed by the scavenger receptor-mediated endocytosis. [174] MMP1 has been shown to interact with α2-macroglobulin more readily than with TIMP1.[175] The supplementation of α2-macroglobulin was effective in hindering cartilage degradation and progression of osteoarthritis.[176] While expression of α2-macroglobulin has been reported in the endothelial cells within the cardiovascular tissue [177], information on the functional significance of this proteinase inhibitor in physiology or pathophysiology of the cardiovascular system remains lacking. RECK (reversion-inducing-cysteine-rich protein with Kazal motifs) is a GPI-anchored glycoprotein with MMP inhibitory capacity.[178] RECK can also suppress endothelial cell migration and angiogenic sprouting, [179] and therefore it is essential during development as its deficiency leads to embryonic lethality around gestational day 10 (E10.5).[178] The baseline expression of RECK in the heart is minimal [106], but it has been shown to be elevated in the right atrium free wall for patients with atrial fibrillation [180], and recent studies have reported a role for RECK in cardiac fibroblast migration.[181, 182] Several other proteins have also been reported to inhibit MMPs, including a C-terminal fragment of the procollagen C-terminal proteinase enhancer [183] and the C-terminal glycosylated region of the secretory form of the membrane-bound β-amyloid precursor protein, [184] which has been reported to possess MMP2 inhibitory properties.

Table 1.1: Genetic manipulation of MMPs and TIMPs in cardiovascular diseases

Gene	Disease model	Disease model, Cardiac phenotype	References
MMP2$^{-/-}$	• Myocardial infarction	• Improved LV rupture rate and late remodeling but no significant change in cardiac function post-MI.	185, 186
	• LV pressure-overload	• Improved cardiac function, LV mass and fibrosis following pressure-overload.	187
MMP2 overexpression	• Cardiac-restricted overexpression	• Myocyte hypertrophy, myofilament lysis, sarcomere and mitochondrial disruption, fibroblast proliferation at 4 month's age.	188 189
	• N-terminal overexpression	• Impaired contractility. • Cardiomyocyte hypertrophy, inflammation, systolic dysfunction.	190
MMP3$^{-/-}$	• Radiofrequency induced myocardial injury	• Improved inflammation and hypertrophy.	191
MMP7$^{-/-}$	• Myocardial infarction	• Improved survival rate, conduction velocity and connexin-43 but similar dilatation and post-MI	192
MMP8$^{-/-}$	• Viral myocarditis	• Decreased T-cell infiltration and myocardial fibrosis, with reduced viral load post-myocarditis	193
MMP9$^{-/-}$	• Myocardial infarction	• Reduced LV dilation, decreased collagen accumulation	194
	• Viral myocarditis	• Increase in viral infection, exacerbation of heart function, increase in LV thickness, fibrosis, T-cell infiltration post viral myocarditis	195
MMP12$^{-/-}$	Viral myocarditis	• Early post-infection, higher rate of mortality.	195, 196

MT1-MMP $^{+/-}$	• Myocardial infarction	• Heterozygous MT1-MMP deletion improved survival and ejection fraction, reduced collagen content and pro-fibrotic signalling.	[197]
MT1-MMP Overexpression	• Myocardial infarction	• Cardiac overexpression of human MT1-MMP reduced survival, worsened systolic dysfunction, increased collagen content and pro-fibrotic signalling.	[198,199]
MMP28$^{-/-}$	• Myocardial infarction	Increased LV volume, pulmonary edema, reduced ejection fraction, worsened remodeling index, impaired M2 macrophage activation and fewer myofibroblasts	[200]
TIMP1$^{-/-}$	• Aged mice • Myocardial infarction. • Viral myocarditis	• Preserved systolic function but LV dilation at 4 months of age • Accelerated LV remodeling, increased dilation following myocardial infarction. • Improved survival, attenuation of viral myocarditis.	[201] [202, 203]
TIMP2$^{-/-}$	• LV pressure-overload	• Increased myocardial cross sectional area, suppressed systolic function, increased left atrial size, LV dilation, disturbed integrinβ1D and ECM interaction with excessive fibrosis following pressure-overload	[61]
	• Myocardial infarction	• Increased infarct size, increased LV dilation and reduced EF, no change in LV rupture rates.	[204]
	• Ang II infusion	• Enhanced myocardial hypertrophy, lack of fibrosis, impaired active relaxation.	[60]

TIMP3$^{-/-}$	• Aging	• At 21 months of age, dilated cardiomyopathy, myocyte hypertrophy and contractile dysfunction.	205-207
	• Myocardial infarction	• Decreased survival rate due to LV rupture, increased infarct size, exacerbation of systolic and diastolic dysfunction.	206
	• Cardiac pressure-overload	• Myocyte hypertrophy, severe LV dilation and dysfunction • Perivascular and interstitial fibrosis.	208
	• Ang II infusion	• Excessive cardiac fibrosis, lack of myocyte hypertrophy, LV diastolic dysfunction, increased LV passive stiffness.	60
TIMP4$^{-/-}$	• Myocardial infarction	• Increased rupture, reduced collagen synthesis and collagen content. • Increased LV dilation and dysfunction	209 210
	• Cardiac pressure-overload	• No change in LV dilation and dysfunction. • Increased LV dilation • No change in LV dysfunction.	209 211
	• *In vivo* ischemia-reperfusion injury	• Enhanced myocardial oxidative stress, inflammation, followed by increased cardiomyocyte hypertrophy, fibrosis, LV systolic and diastolic dysfunction.	12

1.5. ECM Microenvironment as a Reservoir

Subsequent to their production, growth factors are often localized to the ECM basement membrane by binding to heparin sulphate proteoglycans (HSPGs) rather than being freely diffused in the interstitial space. Among growth factors, transportation of fibroblast growth factors (FGFs) through the interstitial space has been most extensively studied. FGF encompasses a large family of proteins that are critical in cell proliferation, survival, migration and differentiation during development, growth and in disease.[212-216] In the cardiovascular system, FGFs are essential in embryonic development of the cardiovascular system[217-218], and can be protective in cardiomyopathies.[219-222] Therefore, optimal transportation of these growth factors to the target cells is essential. Movement of a number of growth factors (IGFs, FGFs, and TGFs) [223] in the interstitial space is controlled by HSPGs, which also orchestrate the binding of these growth factors to their receptors on the target cells. [212,213,224,225] The interaction between the growth factors and HSPGs offers a number of additional advantages, such as preventing proteolytic degradation [226] and hindering passive diffusion [227] of the growth factors, as well as further serving as a storage site to allow their rapid release of growth factors upon demand. Disruption of this association, due to compromised ECM integrity, can enhance diffusion and transport of growth factors through the interstitial space [228], resulting in excess downstream signaling and adverse outcomes. For instance, shedding of syndecan-4, an HSPG and a basement membrane protein, from the myocardial ECM correlated with the inflammatory response in the failing human heart and in an experimental model of heart disease .[229] Further, as discussed earlier, a number of proteoglycans are essential in cardiac development, growth and pathology. Therefore, the HSPG-mediated transportation of growth factors in the interstitial space is essential in cardiac remodeling.

In addition to the HSPG-FGF interactions, other components of the ECM can bind to and retain cytokines and growth factors in the interstitial space, where they remain inactive until released in response to a trigger. For instance, transforming growth factor-β (TGFβ) is secreted and sequestered within the ECM by binding to latent TGFβ-binding peptide (LTBP), an ECM protein [230], and is released in response to proteolytic [231-232] or mechanical triggers [233]. TGFβ is a multifunctional cytokine and a potent mediator of myofibroblasts transformation and collagen production; therefore, its activity needs to be tightly regulated. All three isoforms of TGFβ (TGFβ1, TGFβ2, and TGFβ3) are transcribed with the latency-associated pro-protein (LAP). LAP

is cleaved intracellularly but stays associated with TGFβ through a non-covalent bond, forming the small latent complex (SLC), and secreted as the large latent complex (LLC) bound to LTBP (Latent TGFβ-Binding Protein) via a disulphide bond. After secretion, LLC is sequestered in the ECM through covalent binding to fibrillin, a basement membrane protein and a central component of the micro fibrils in elastin fibres. Activation of TGFβ requires a sequence of proteolytic activities that eventually result in the release of the active TGFβ homodimer (25 kDa) and its interaction with the TGFβ receptors. Proteolytic cleavage of LTBP results in release of the TGFβ homodimer and its subsequent dissociation from LAP or through integrin-mediated processes. [233] The MMPs that have been identified so far to mediate this process are MMP2, MMP9 and MT1-MMP. [208, 231] Other proteases such as plasmin and bone morphogenic protein-1 (BMP-1) have also been shown to cleave the LTBP-ECM bond, but only inhibition of MMPs prevented the release of the TGFβ homodimer from LAP. [234] This highlights an important notion that MMPs can contribute to synthesis and production of the ECM proteins, through activation of the TGFβ pathway, therefore defying the traditional dogma that recognizes MMPs only as matrix-degrading enzymes.

Once the TGFβ homodimer is released from the latent complex, it the homodimer binds to its receptors (TGFRI/II) and initiates the activation of the downstream pathways **(Figure 1.4)**. TGFβ binds to TGFβRII, which then dimerizes with and phosphorylates TGFβRI, inducing intracellular signaling pathways, the canonical Smad pathway, and the non-canonical MAPK pathways (ERK, JNK and p38) [235-236]. In canonical TGFβ signaling, the TGFβRI/II complex phosphorylates Smad2/3 on the serine residue, which then forms a heterotrimeric complex with Smad4. Smad4 translocates into the nucleus and induces transcription of the target genes including collagen, elastin and MMPs. [237]

TGFβ also induces the expression of inhibitory Shads, Smad6 and Smad7, which prevent activation of Smad2/3 and their interaction with Smad4, thereby acting as an autoinhibitory feedback mechanism. [238] In non-canonical TGFβ signaling, TGFβ binds to TGFβRI, resulting in tyrosine phosphorylation of this receptor, allowing it to recruit and directly phosphorylate SchcA proteins.

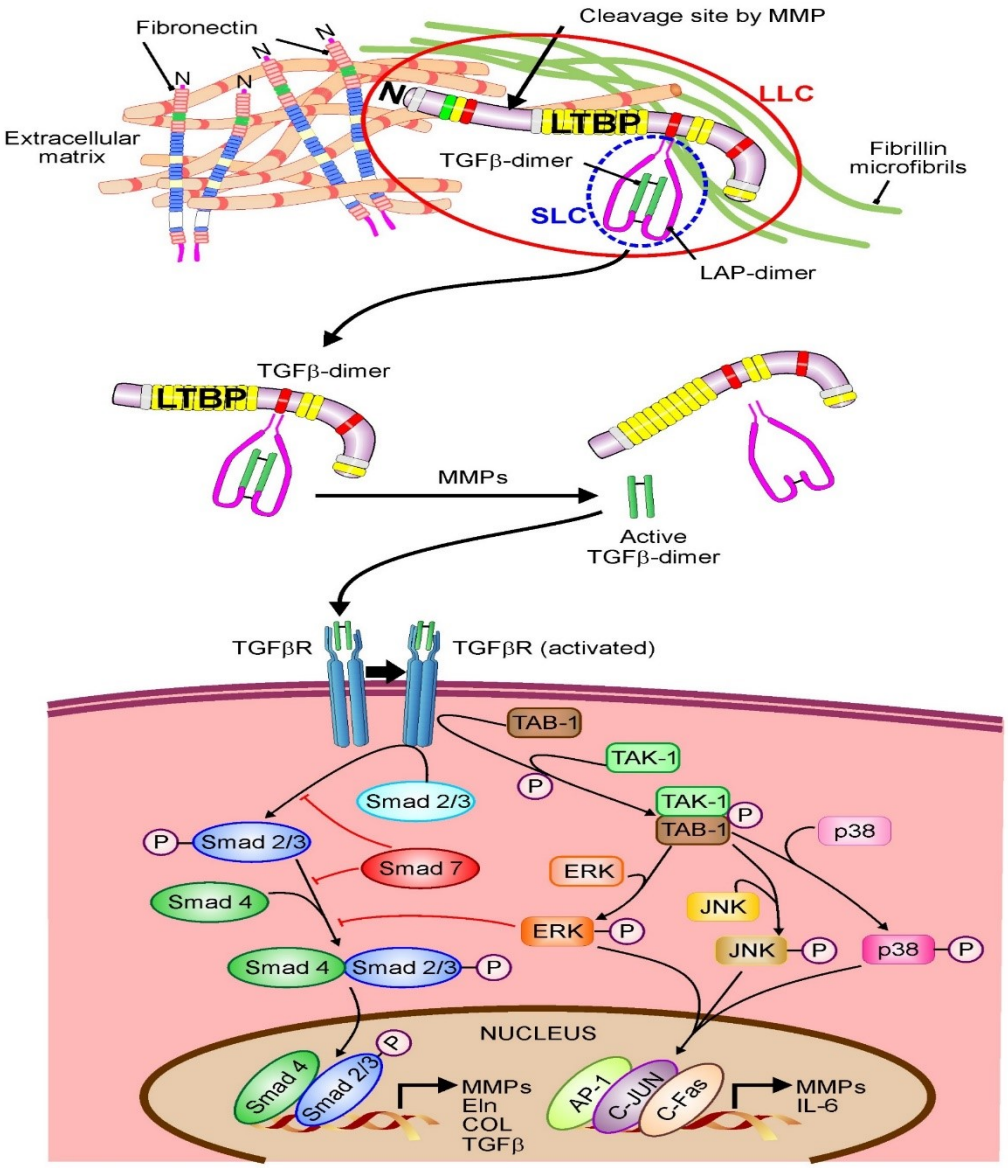

Figure 1.5: TGFβ pathway- Activation of TGFβ and its downstream signaling pathway leads to synthesis of ECM regulatory genes and thereby contributes to cardiac fibrosis. Extracted from Takawale et al [79]

1.7. Adverse ECM Remodeling

A common feature of heart failure is a disrupted structure or compromised integrity of the ECM. Excess accumulation of ECM proteins, or fibrosis, has been clearly linked to myocardial stiffness, and diastolic and systolic dysfunction.[239] On the other hand, excess degradation of the ECM can also negatively impacts myocardial compliance, structure and function with adverse

outcomes [67,75,135,198,240,241] As ECM provides structural support as well as regulating bioavailability of a number of growth factors and cytokines, intact ECM integrity is critical for optimal cardiac function.

In heart disease, depending on the initiating cause(s), adverse ECM remodeling could involve excess deposition of ECM proteins leading to fibrosis, or aberrant degradation and disruption of the ECM network structure. In general terms, myocardial fibrosis often occurs in response to an increased afterload and increased myocardial stiffness, which can lead to diastolic dysfunction, with or without systolic dysfunction. Inversely, volume overload leads to disruption of the ECM network, ventricular dilation and systolic dysfunction mainly due to cardiomyocyte slippage and loss of cell-ECM connections. Moreover, it is not uncommon for both types of adverse ECM remodeling to take place within the same heart, resulting in a complex systolic and diastolic dysfunction. [61]. Cardiac fibroblasts (cFBs) are the primary source of ECM proteins. [9, 242] In response to appropriate stimuli, cFBs can differentiate into the more mobile and contractile myofibroblasts (myoFBs) with enhanced ability to produce ECM proteins. [9, 243] In addition, other cell types such as inflammatory cells and endothelial cells can transform into myofibroblasts. [9]

1.7.1. Different types of myocardial fibrosis and impact on cardiac function

Heart failure is a complex progressive syndrome that can be initiated by a number of factors such as hypertension, valvular disorders, viral myocarditis, ischemic or dilated cardiomyopathies. [244, 245] A common characteristic among different types of heart diseases is fibrosis.[9, 246] Myocardial fibrosis impairs myocardial compliance, and can alter cardiac structure and function. It can lead to diastolic dysfunction, abnormal left ventricular (LV) filling, reduced LV compliance, and increased diastolic pressure. These series of effects may occur in patients with normal LV ejection fraction (EF) and can eventually lead to heart failure with preserved EF (HFpEF).[247] Patients with HFpEF have similar hospital re-admission rates as patients with HF and reduced EF (HFrEF), while worsening of diastolic dysfunction has been shown to be an independent predictor of mortality.[248] However, different therapeutic approaches are required for each type of HF. Therefore, an understanding the molecular mechanisms underlying different types of myocardial fibrosis in a disease-dependent fashion is critical in developing effective therapies. A thorough

assessment of collagen turnover and factors that disturb this balance in HF, using animal models, can translate into significant contributions to the advancement of clinical care of HF patients.

The underlying molecular mechanism and the functional consequences of fibrosis can be different in different types of heart disease. For instance, after acute MI, necrotic cardiomyocyte loss sets off a cascade of events leading to recruitment of inflammatory cells, MMP release and ECM degradation, fibroblast transdifferentiation and proliferation, leading to production of new ECM proteins to replace the lost cardiomyocytes with fibrotic scar tissue, also known as 'reparative fibrosis'. The degradation products of the original ECM in the infarcted myocardium serve as chemoattractants that trigger infiltration of inflammatory cells into the site of injury. [249] These inflammatory cells release a number of factors including cytokines and MMPs, while a subpopulation of the infiltrated cells transforms into myofibroblasts.[137] These cells produce collagen and other ECM proteins, thereby playing a critical role in formation of the scar (infarction) tissue that replaces the necrotic myocardium.[250] The ECM in the myocardium remote to the infarct zone also undergoes remodeling mainly in response to mechanical strain due to altered compliance of the infarcted myocardium and neurohormonal stimuli triggered by the ischemic injury. [251] After the scar is formed at the injured sites, myofibroblasts return to a quiescent phenotype. However, unlike the wound healing response in static tissue such as skin, prolonged collagen production by the expanded population of myofibroblasts in infarcted myocardium results in infarct expansion, LV dilation and eventually suppression of systolic function and eventually HF. Therefore, the initial fibrotic response following myocardial infarction is a healing process and its interruption can lead to cardiac rupture with devastating outcomes.

Myocardial ECM remodeling following cardiac pressure-overload, secondary to aortic stenosis or hypertension, is often a reactive process where interstitial and perivascular fibrosis occur in the absence of myocyte necrosis or loss. This process is driven predominantly by neurohormonal stimuli. The impacts of Ang II, aldosterone, salt loading and nephrectomy have been extensively investigated on collagen deposition in hypertensive and pressure-overload-induced cardiomyopathy.[252-255] All major components of the renin-angiotensin-system (RAS) exhibit profibrotic activities, and angiotensin converting enzyme inhibitors (ACEi) [256] and angiotensin receptor blockers (ARBs) [257] have had beneficial effects in heart disease patients. In the RAS system, Ang II is a major contributor to myocardial hypertrophy, fibrosis and remodeling.[146] In severe cases of hypertensive cardiomyopathy, myocyte necrosis can occur due

to catecholamine or Ang II-mediated toxicity and damage to coronary arteries resulting in a combination of reparative and reactive fibrosis in the myocardium. [146, 258]

Table 1.2: Types of fibrosis in cardiovascular pathologies

Cardiac pathology	Type of fibrosis	Cardiac events and altered functions
Myocardial infarction	Reparative fibrosis	i. Death of myocytes induces inflammatory cell infiltration. ii. Secreted pro-inflammatory cytokines induce fibroblast-myofibroblasts differentiation. iii. Newly synthesized and secreted ECM by myofibroblasts forms a scar which replaces the lost myocytes. iv. Persistent activation of myofibroblasts in the scar further expands in the infarct, leading to mechanical strain, LV dilation and systolic dysfunction and heart failure.
Cardiac pressure-overload (Aortic stenosis or hypertension)	Reactive fibrosis	i. Mediated by neurohormonal stimuli such as angiotensin-II, or aldosterone. ii. Stimuli trigger myofibroblast differentiation and collagen synthesis leading to deposition of collagen initially in perivascular spaces and later in interstitial spaces leading to altered myocardial stiffness and dysfunction.
Severe hypertensive cardiomyopathy	Reactive and reparative fibrosis	In severe hypertension, coronary damage leads to myocyte necrosis, triggering reparative fibrosis (similar to MI) while neurohormonal stimuli trigger reactive fibrosis.
Myocarditis	Reparative fibrosis	Myocyte loss due to chronic myocardial inflammation initiates reparative fibrosis similar to that post-MI which eventually leads to LV dilation and heart failure.

Inflammatory dilated cardiomyopathy, or myocarditis, accounts for about one-tenth of HF cases [259]. Myocarditis usually results from infection with viruses, most commonly coxackievirus B (CVB), and is often associated with autoimmune responses against heart tissue. Chronic myocardial inflammation leads to fibrosis LV dilation, and impaired contractility. Similar to MI,

myocardial fibrosis associated with myocarditis is reparative fibrosis that replaces the lost cardiomyocytes due to inflammation and apoptosis, to maintain cardiac structure and function. Myocardial fibrosis following myocarditis is mediated by the action of infiltrating immune cells that can either transform to pathogenic myofibroblasts or produce cytokines and other inflammatory mediators that activate the resident cardiac fibroblasts to myofibroblasts. [195, 260] In such cases, the pathological remodeling of the myocardial matrix and tissue continues after inflammation is resolved. TGFβ and IL-1 have been identified as cytokines that promote myocardial fibrosis in inflammatory cardiomyopathy by converting fibroblasts or inflammatory cells to myofibroblasts[260, 261], stimulating cardiac fibroblast migration, collagen synthesis and expression of MMPs and TIMPs.[217, 262, 263] Studies on an experimental model of myocarditis induced by coxsackievirus B3 (CVB3) have shown suppressed cardiac function and hemodynamics, elevated cytokine levels, increased MMP2, -3, -8 and TIMP1 levels[264], elevated MMP2, MMP9 and MMP12 and reduced TIMP3 and TIMP4 levels[265], or elevated MMP2, -3, 8, 9, 13, TIMP1 and TIMP2 levels.[266] Interestingly, despite elevated MMP levels in myocarditis, deletion of MMP2[267], MMP8, MMP9-[268] or MMP12[196] led to exacerbation of inflammation and adverse outcomes following CVB3 infection. Therefore, the elevated MMP levels in response to myocardial inflammation are perhaps a protective mechanism in resolving the inflammation within the myocardium. Overexpression of TIMP1 was protective against cardiac inflammation, fibrosis and dilation mainly by preventing cleavage of MMP zymogens.[266] Matricellular proteins are also important contributors to ECM remodeling in myocarditis.[269] Mice lacking thrombospondin-2, a glycoprotein that mediates cell-matrix interactions, exhibited enhanced cardiac inflammation, dilation and dysfunction following CVB3 infection, mainly due to suppressed activation of anti-inflammatory T-regulatory cells.[270] On the other hand, ablation of osteopontin, a matricellular protein that mediates stabilization of collagen fibres, hindered macrophage infiltration and suppressed myocardial fibrosis. [271]

Studies on genetically-modified mice have provided valuable information on functional impact of reparative versus active fibrosis in different types of heart disease. Interruption of myocardial fibrosis in mice lacking SPARC or OPN, mediators of post-translational regulation and stabilization of collagen fibres, led to an increased rate of LV rupture and adverse outcomes post-MI.[83-85] However, following cardiac pressure-overload, lack of OPN or SPARC attenuated myocardial fibrosis with beneficial outcomes such as lack of myocardial hypertrophy and reduced

diastolic stiffness. [272-273] These studies demonstrate the differential impact of replacement fibrosis post-MI versus reactive fibrosis following mechanical stress in the heart and the important role of post-translational modification of collagen in these processes.

1.8. Targetting MMPS OR TIMPS as Therapy for Heart Disease

A considerable amount of knowledge has been gained in that past couple of decades on the function and contribution of MMPs and TIMPs to development and progression of heart disease. While the initial intention in manipulating these molecules was to alter ECM composition and integrity, novel ECM-independent function of these molecules have also been revealed. The MMPs that have been studied and identified so far to be involved in pathological myocardial remodeling or other aspects of heart disease include MMP1, MMP2, MMP3, MMP7, MMP8, MMP9, MMP12, MMP13, MMP28 and MT1-MMP.[142, 199-200, 274] Moreover, unlike the initial belief that all TIMPs serve a similar function, each TIMP has been shown to play distinct functions in cardiovascular pathologies. To date, at least 56 MMP inhibitors have been recognized as clinical candidates, among which 10 have been found to be potentially suitable for cardiovascular diseases [275], while clinical data has been published on only 3 of these compounds, plaque destabilization (MIDAS)[276], stent restenosis (BRILLIANT)[277], and post-ischemic myocardial remodeling (PREMIER)[278], all of which reported a lack of or marginal beneficial effects of MMP inhibition. The major reason for failure of clinical trials of MMP inhibitors has been inadequate assessment of therapeutic index due to attempt to avoid musculoskeletal side effects.[275] Due to the side effects of systemic MMP inhibition, and the associated complications in reaching the effective dose, and as animal studies on MMP-deficient mice have revealed that complete inhibition of MMPs is not a suitable intervention **(Table 1)**, the complete inhibition of MMPs is not a suitable treatment strategy for heart disease. In addition, based on the negative outcomes of the few clinical trials using MMP inhibitors, despite the experimental design limitations, it is highly unlikely that pharmaceutical companies will invest in an MMP inhibitor as a therapeutic approach for heart disease.

Another group of ECM-regulatory proteins that are also altered in heart disease are TIMPs, and while TIMP levels are altered in heart disease, TIMP-deficiency adversely impacts the outcomes in heart disease. Therefore, replenishment of TIMPs in the diseased myocardium could

provide an alternative therapeutic approach for limiting myocardial injury, e.g. infarct expansion in ischemic cardiomyopathy. Moreover, to avoid systemic side-effects such as those associated with MMPi treatments, targeted therapy could be a more effective alternative. Injectable acellular hydrogels, consisting of both synthetic and natural materials, have been proposed as suitable medium for delivering therapeutic agents into the myocardium.[279] In fact, intramyocardial injection of hydrogels containing collagen post-MI improves scar thickening and function[280], prevents LV dilation[281] and induces angiogenesis[282] in mice. Therefore, replenishment of reduced levels of TIMPs using a gene delivery or hydrogel approach could provide alternative therapeutic approach for treating ischemic cardiomyopathy.

1.9. Hypothesis

Recent studies have shown that TIMPs have a number of additional functions apart from their traditional MMP inhibitory properties.[60, 121] It has been shown that TIMP2 and TIMP3 have divergent roles in heart disease.[60, 283] TIMP3 and TIMP4 levels are reduced shortly after post-MI [284] and therefore replenishing these TIMPs after MI could offer a therapeutic alternative for patients with heart attack. Also, TIMP4 shows higher expression in the heart and has been reported to have unique intracellular localization,[285] as well as reported to inhibit intracellular MMP2, thereby preventing myocardial I/R injury in a rat model.[285] Meanwhile, TIMP1 is the only TIMP used as a biomarker for tissue fibrosis and its elevated levels have been correlated with diastolic dysfunction as well as various organ fibrosis.[286, 287] Hence, considering these divergent roles of TIMP1, TIMP4 and TIMP3 in heart diseases, we hypothesized that these TIMPs could have different roles in heart failure depending on the type of cardiac injury.

1.10. Rationale

Project 1: TIMP4 exhibits a tissue-specific expression pattern with higher expression in heart and brain compared with all other tissues. It has been reported to be present intracellularly in rat cardiomyocyte.[285] In an *ex vivo* rat model of I/R, TIMP4 was found to be released from the myocardium along with loss of contractile proteins.[21] TIMP4$^{-/-}$ mice have been reported to have more LV rupture without deteriorating LV function as compared with WT mice in a mouse model

of myocardial infraction.[209] Therefore, tissue-specific expression and unique intracellular localization indicate a potential role of TIMP4 in myocardial I/R.

Project 2: In a mouse model of myocardial infarction, TIMP3 deficiency causes exacerbation of systolic as well as diastolic dysfunction[206], while TIMP4 deficiency results in increased LV rupture rate.[209] Similarly, TIMP3 and TIMP4 levels are reduced shortly after post-MI. Therefore, restoring these reduced levels of TIMPs post-MI using adenoviral- mediated gene delivery may provide a new therapeutic alternative for LV remodeling.

Project 3: In heart failure patients, TIMP1 has been shown to be a useful marker for tissue fibrosis. TIMP1 levels increase in response to hypertrophy[288] and fibrosis.[286] In patients with hypertension and normal ejection fraction[289] and with aortic stenosis, elevated TIMP1 levels have been proposed to prevent collagen degradation, thereby promoting myocardial fibrosis.[290] Various heart disease animal models and patient studies show that myocardial fibrosis is associated with a rise in mRNA expression as well as protein levels of TIMP1. But the exact role of TIMP1 as a disease marker, whether only a bystander in cardiac remodeling or a key player in promoting cardiac fibrosis, has not been determined. Therefore, it is necessary to elucidate the exact role of TIMP1 in cardiac fibrosis.

1.11 Objectives

The aim of the research in this thesis was to identify the novel roles of TIMP1, TIMP3 and TIMP4 in common heart diseases, specifically I/R, MI and pressure-overload cardiomyopathies. The following chapters will present details of the investigation of the role and therapeutic potential of TIMPs, using TIMP4$^{-/-}$ and TIMP1$^{-/-}$ mice, and adenovirus-mediated TIMP4 and TIMP3 delivery approach post-MI, and utilization of end stage failing heart specimens from patients with ischemic or dilated cardiomyopathy. We investigated the proteolytic regulation of the ECM, MMP-independent functions of TIMPs and the ways TIMPs could provide a novel therapeutic alternative. The underlying mechanical and structural basis for development of heart failure is diverse and therefore understanding of mechanisms responsible for progression of heart diseases is important for developing preventive and therapeutic strategies. Depending on stimulus, heart failure progression results in changes in the structure and composition of the LV myocardium resulting in adverse LV remodeling.[291-293] These changes cause alterations in the structure and function of cardiomyocyte, the vascular compartment as well as extracellular matrix composition.

It has been proven that fundamental defects in myocyte structure and function play a major role in development and progression of heart failure[293-294] with growing evidence suggesting that ECM mediates both biological and mechanical signals. [199,295-296] The adverse LV remodeling is associated with poor patient outcomes in ischemic heart diseases, cardiac hypertrophy and fibrosis. Therefore, understanding the detailed role of ECM regulatory proteins in adverse LV remodeling and during progression of heart failure is necessary.

CHAPTER 2

MATERIALS AND METHODS

2.1. Animal Care

Wild type (WT) and TIMP1-deficient ($TIMP1^{-/-}$) male mice, in C57BL/6 background, were purchased from Jackson Laboratories and bred in house in the animal facility of the University of Alberta. $TIMP4^{-/-}$ mice were obtained from Texas A&M Institute for Genomic Medicine (TIGM) and backcrossed into C57BL/6 background as reported previously.[297] All animal experiments were carried out in accordance with Canadian Council on Animal Care Guidelines and regulations of Animal Care and Use Committee (ACUC) at University of Alberta.

2.2. Experimental Animal Disease Models

2.2.1. *In vivo* myocardial ischemia-reperfusion (I/R) injury

In vivo ischemia-reperfusion (I/R) was induced in 10-11 week-old male mice of either genotype by temporary ligation of the left anterior descending artery as before. [298]-[299] In anesthetized, intubated and ventilated mice, the left anterior descending artery [298] was ligated with a 7-0 silk suture for 20 minutes or 30 minutes to induce ischemia,[300] and reperfusion was initiated by releasing the ligation. The chest was closed and mice were allowed to recover on heating pad.

2.2.2. Isolated heart ischemia-reperfusion (*Ex vivo*)

Male WT and $TIMP4^{-/-}$ mice, at 10-11 weeks of age, were heparinized (1000 IU/kg, IP) and anesthetized with 2% isoflurane. Hearts were quickly excised, mounted on a Langendorff apparatus and perfused at a constant pressure of 80 mmHg with modified Krebs-Henseleit (K-H) solution (in mM: 116 NaCl, 3.2 KCl, 1.2 $MgSO_4$, 1.2 KH_2PO_4, 25 $NaHCO_3$, 11 glucose, 1.5 $CaCl_2$, 2 pyruvate), continuously oxygenated with 95% O_2 and 5% CO_2 to maintain a final pH of 7.4, at 37^{o}C.[299] EDTA was not included in the perfusion solution since its MMP-inhibitory properties would interfere with the objective of our study to decipher the role of TIMP4 in I/R. A water-filled balloon was inserted into the LV chamber, and connected to a pressure transducer, to record the changes in LV pressure using the Power Lab system (AD Instruments, Australia). After 15 minutes of baseline recording, hearts were subjected to 20 minutes (or 30 minutes) of global ischemia (while submerged in warm 37^{0}C K-H solution), followed by 45 minutes of reperfusion. The coronary effluent was collected from each heart prior to ischemia, and at different times after

reperfusion, and stored at -80^{o} C and later used to determine creatine kinase levels, as a measure of myocyte death, using a commercial kit (BioAssay).

2.2.3. Transverse aortic constriction (TAC)-induced pressure-overload

Cardiac pressure-overload was induced in male WT and TIMP1$^{-/-}$ mice (8-10 weeks age) by transverse aortic constriction (TAC) as described previously.[61, 301-302] Anesthetized and intubated mice underwent partial thoracotomy at the second rib, a blunt 27-gauge needle was placed next to the aortic arch between the left carotid artery and the brachiocephalic trunk, and a suture was then tied around the needle and aorta. The needle was quickly removed to resume blood flow through the aorta. This constriction consistently generates a pressure gradient of 55-60 mmHg. The thorax was then sutured in layers and Buprenorphine (1.3 μg/25g mouse, 100μL) was administered as post-surgery analgesic. The mouse was allowed to recover on a heating pad.

At the indicated time-points, hearts were excised, either froze in OCT medium, or formalin-fixed and processed for immunohistochemical analyses. Alternatively, hearts were excised and flash-frozen for molecular analyses **(Figure 2.4.D).**

2.2.4. Angiotensin II (Ang II) induced cardiac fibrosis

Male 8-9 weeks old mice of either genotype received angiotensin II (Ang II, 1.5 mg/kg/day) or saline by Alzet micro osmotic pumps (Model 1002, Durect Co.) implanted dorsally and subcutaneously (under 2% isoflurane anesthesia).[60,299] MMP inhibitor, PD166793 (30 mg/kg/day) was administered by daily gavage in parallel groups of WT and TIMP1$^{-/-}$ throughout the 2 weeks of Ang II/saline infusion.[206-207]

At the indicated time-points, hearts were excised, either frozen in OCT medium, or formalin-fixed and processed for immunohistochemical analyses. Alternatively, hearts were excised and flash-frozen for molecular analyses **(Figure 2.4.D)**.

2.2.5 *In vivo* animal model for myocardial infarction and intramyocardial injections of adenovirus encoding human TIMP3 (Ad-hTIMP3), TIMP4 (Ad-hTIMP4) and null (Ad-null)

Male wild type mice of 8-10 weeks of age were subjected to myocardial infarction by left anterior descending artery ligation as before. [298,204, 303] Immediately after LAD ligation, adenovirus

expressing human TIMP3 (Ad-hTIMP3) and human TIMP4 (Ad-hTIMP4) was injected in peri infarct regions at five different spots (5.54×10^7, 5µl/spot). A control group received only adenovirus (Ad-null). A separate set of mice received 10-times higher dose of Ad-null and Ad-hTIMP3 (5.54×10^8, 5µl/spot) to study dose-dependent effect of Ad-null and Ad-hTIMP3 post-MI. At 1 week post-MI, heart function were assessed using echocardiography.[303, 304] Ad-hTIMP3, Ad-hTIMP4 and Ad-Null were kind gifts from Dr. Douglas L. Mann (Washington University School of Medicine at St. Louis).[305]

2.3. Human Explanted Heart Tissue

Cardiac tissues from patients with post-MI and dilated cardiomyopathy heart failure were collected from the explanted hearts at the time of cardiac transplantation as part of the Human Explanted Heart Program (HELP) at the Mazankowski Alberta Heart Institute (Edmonton, AB). Non-failing control hearts were obtained through the Human Organ Procurement and Exchange (HOPE) program (Edmonton, AB). All experiments were performed in accordance with the institutional guidelines and were approved by Institutional Ethics Committee. Informed consent was obtained from all subjects.

2.4. *In vivo* Cardiac Structure and Function Assessment

2.4.1 Echocardiographic imaging

Systolic and diastolic cardiac function were measured by non-invasive echocardiographic technique, equipped with a 30-MHz transducer (RMV-707B, Visual Sonics, Toronto, ON Canada) as described previously.[206, 303] For WT and TIMP4$^{-/-}$ mice, echocardiography was performed using Vevo 770 imaging system at 1 week and 4 weeks post-I/R while for Ad-hTIMPs injected mice or WT and TIMP1$^{-/-}$ mice Vevo 2100 or Vevo 3100 imaging systems were used at 1 week post-MI, 2,5 and 9 weeks post-TAC or 2 weeks post-Ang II. Mice were placed on heating pad under 0.75-1% isoflurane anesthesia, temperature maintained at 36-37^0 C and ultrasound gel was placed on the chest. An ultrasound probe was placed in contact with ultrasound gel and scanning was performed over 30 minutes. Body temperature, heart rate was constantly monitored during ultrasound imaging.

LV wall thickness and chamber sizes such as LV end-diastolic diameter (LVEDD) and LV end systolic diameter (LVESD) were obtained from M-mode images. Qualitative and quantitative measurements were made using analytical software offline and LV ejection fraction was calculated from M-mode images for Ang II, TAC and corresponding sham mice. [61]

For post-MI and post-I/R, the wall motion score index was used to calculate LV EF and Simpson's method was used for calculation of LV systolic and diastolic volume according to *American Society of Echocardiography* which recommended 17 segment LV model where 1= normal wall motion, 2= hypokinetic segment, 3= akinetic segment, 4= dyskinetic segment and 5= aneurysmal segment. This 17-segments model is validated in mice model of MI. An increase in wall motion score index (WMSI) (>1) indicates suppressed LV systolic wall. [206,303]

FIGURE 2.1: *IN VIVO* MODEL OF MYOCARDIAL ISCHEMIA-REPERFUSION

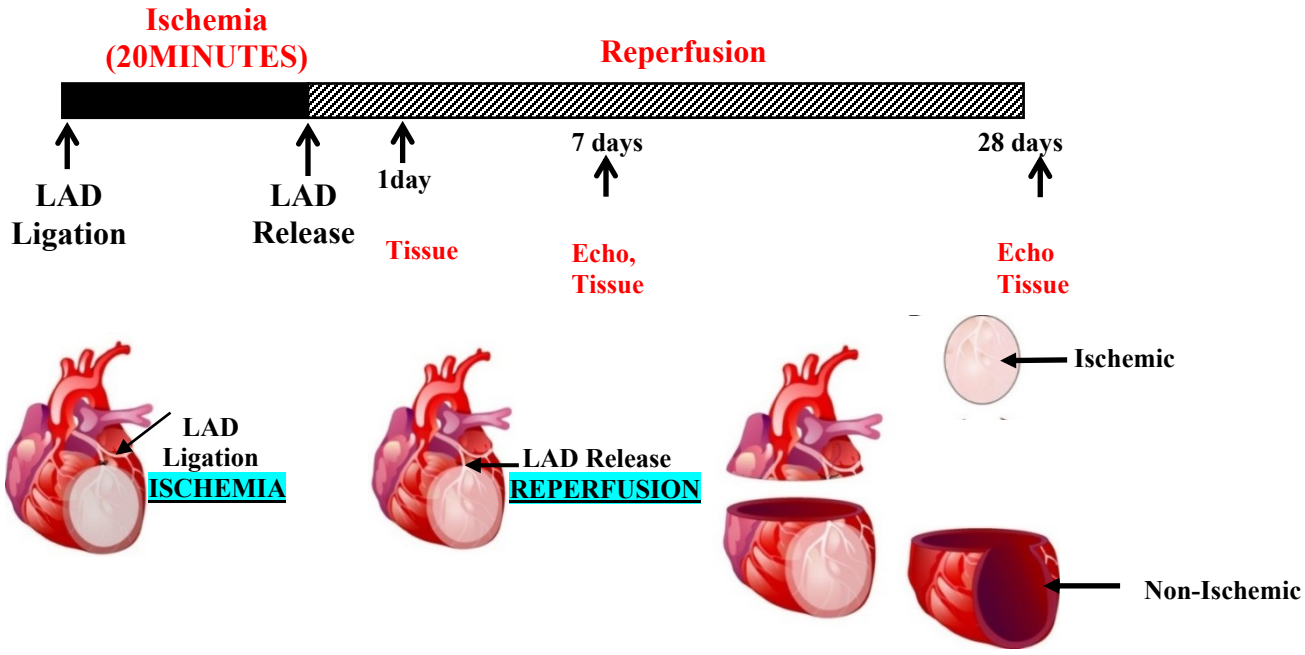

FIGURE 2.2: *EX VIVO* MODEL OF MYOCARDIAL ISCHEMIA-REPERFUSION INJURY

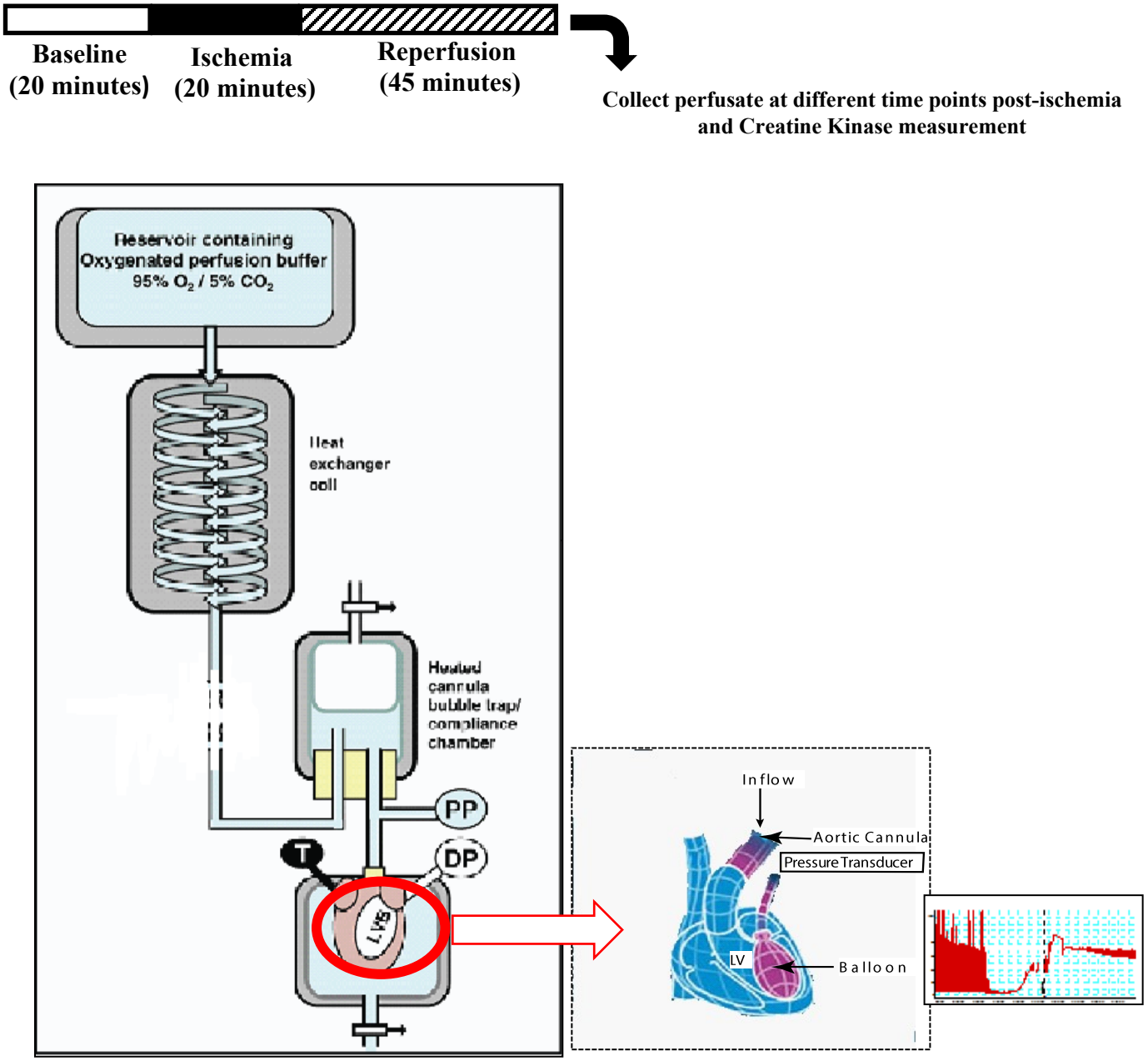

FIGURE 2.3: INTRAMYOCARDIAL INJECTION OF hTIMP3 AND hTIMP4 IN MOUSE MODEL OF MYOCARDIAL INFARCTION

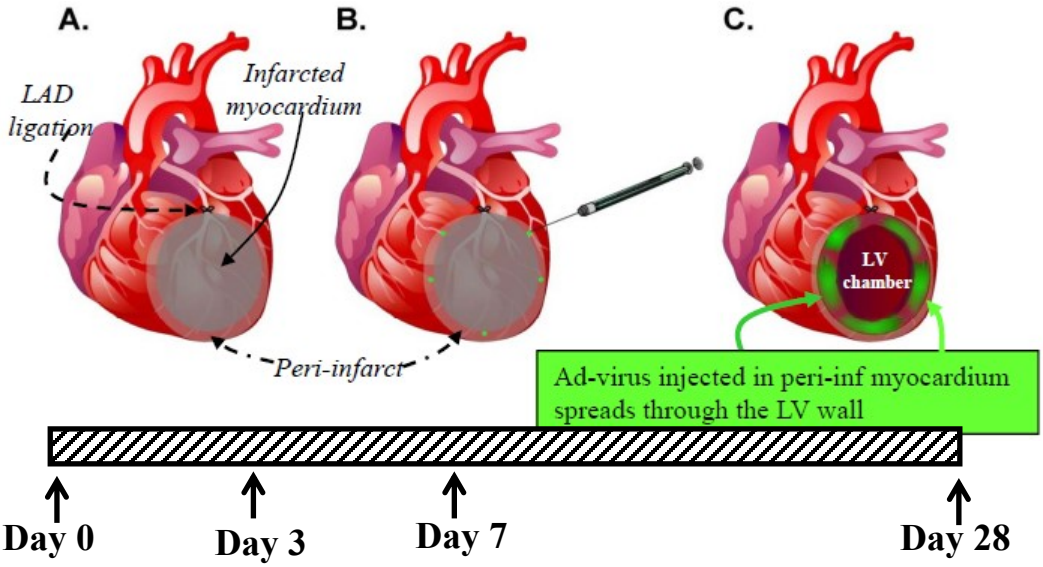

Day 0- MI + Ad-Null/Ad-hTIMP3/Ad-hTIMP4

Day 3- Cell proliferation, Inflammation

Day 7- Echocardiography, Angiogenesis
Structural changes- PSR, WGA+ Phalloidin staining

Day 28- Echocardiography, Angiogenesis
Structural changes- PSR, WGA+ Phalloidin staining

Day 0 — **MI+ Ad-hTIMP3/ Ad-null/Ad-hTIMP4**

Day 7 — **Echocardiography**

Day 28 — **Echocardiography**

Structural changes-PSR & WGA+ Phalloidin

hTIMP3 } **5.54×10^7, 5µl/spot (5 spots)**
hTIMP4

Higher dose of hTIMP3- 5.54×10^8, 5µl/spot

FIGURE 2.4: TIMP1 IN CARDIAC HYPERTROPHY AND FIBROSIS

A)

Ang II-induced myocardial remodeling

WT &TIMP1$^{-/-}$

- **Functional changes** – Echocardiography
- Hypertrophy- WGA staining, HW/TL
  Fibrosis- Trichrome and PSR staining
- **Molecular analyses-**
  a. fluorescent activity assays for MMPs
  b. mRNA expression profiles for MMPs

B

WT &TIMP1$^{-/-}$

Transverse aortic constriction induced pressure-overload

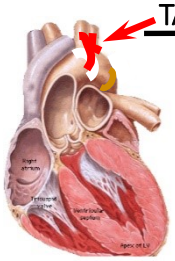

- **Functional changes** – Echocardiography, PV loop
- **Structural alterations-**
  Hypertrophy- WGA staining, HW/TL
  Fibrosis- Trichrome and PSR staining
- **Molecular analyses-**
  a. fluorescent activity assays for MMPs
  b. mRNA expression profile for MMPs
  c. MMP-independent role: Integrinβ1 & CD63 pathway

Human Samples

Non-failing control and dilated cardiomyopathy samples

FIGURE 2.5: CARDIAC FIBROBLAST ISOLATION EXPERIMENTAL SET UP AND PROTOCOL

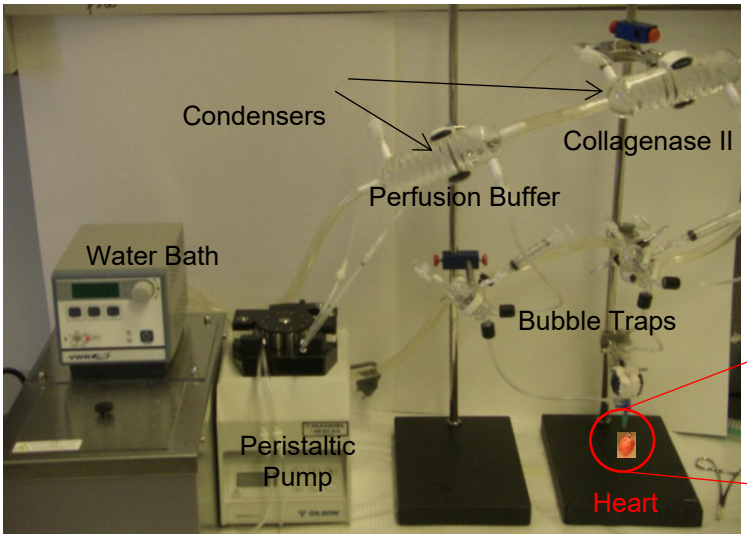

1) 3 min Kreb-Henseleit solution
2) 7-8 min digestion solution (+collagenase 2)

The ventricles are cut off and transferred to a beaker

Tissue is dissociated using forceps and transfer pipettes
Myocytes are allowed to settle (by gravity),
while fibroblasts remain in suspension.

Fibroblast
Centrifuged
(1,500 rpm, 5 minutes)

Pellet washed in DMEM+10%FBS

Centrifuged
(1,500 rpm, 5min)

Plated in DMEM +10%FBS

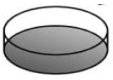

Incubate in
5% CO_2 / 95% O_2

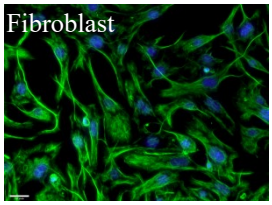

Vimentin Staining

Diastolic function were assessed using transmitral Doppler filling pattern with early transmitral filing wave (E wave) followed by late filling wave (A wave) due to atrial contraction. Isovolumic relaxation time (IVRT) was calculated as time from closure of aortic valve to initiation of E wave.

2.4.2 Pressure-volume (PV) loop analysis

WT and TIMP1$^{-/-}$ mice were anesthetized with 2% isoflurane and hemodynamic pressure-volume (PV) measurements post-TAC/sham were measured using 1.2F Scisense catheter connected to an amplifier (TCP-500 Scisense Inc.).[299] After baseline PV loop measurements, end-diastolic (EDPVR) and end-systolic (ESPVR) PV relationships were derived during transient occlusion of inferior vena cava and infra renal occlusion respectively.[306]

2.5. Isolation and Culture of Mouse Adult Cardiac Fibroblasts (cFB)

Adult cFB were isolated from WT and TIMP1$^{-/-}$ mice as described previously.[12,60] Briefly, 10-11 week-old mice were heparinized (0.05 mL i.p. injection of 1000 USP/L heparin) and anesthetized with 2% isoflurane. The heart was quickly excised and perfused with perfusion buffer at a constant flow (4 mL/minute), after 10 minutes, perfusion buffer was replaced with digestion buffer (containing collagenase type 2, Worthington). Subsequently, LV was separated, and gently dissociated into small pieces in stopping buffer (perfusion buffer containing 10% FBS). Cardiac myocytes and fibroblasts were separated using differential centrifugation. Fibroblasts were cultured in DMEM media containing 10% FBS. Fibroblasts were used at second passage, and serum-deprived for 24 hours prior to experiments. Fibroblasts from WT and TIMP1$^{-/-}$ mice were treated with TGFβ (10 ng/mL) or Ang II (1 μM/mL) for 24 hours. Cells were then harvested and flash-frozen for co-IP experiments, or fixed in 4% paraformaldehyde (PFA) for immunostaining and proximity ligation assay.[12, 60]

2.6. Isolation and Culture of Adult Cardiac Fibroblasts (cFB) and Myocytes (cMYO) and Hypoxia Treatment

cFB and cMyo were isolated from adult WT and TIMP4$^{-/-}$ mice as previously described.[60, 307,308, 309] Briefly, 10-11 week- old mice were injected with 0.05 mL of 1000 USP/mL heparin 15 minutes prior to being anesthetized with 2% isoflurane. Once the animal was deeply anesthetized,

the heart was quickly excised and perfused at a constant flow (4 mL/min) with perfusion buffer followed by digestion solution containing collagenase type 2 (Worthington). After digestion, the LV was separated and dissociated into small pieces using forceps and a transfer pipette in stopping buffer (perfusion buffer containing 10% fetal bovine serum (FBS). cMyo and cFB were separated by differential centrifugation. cFB were centrifuged (1,500 rpm) and plated in culture dishes with DMEM + 10% FBS in a humidified incubator (37°C, 5% CO_2). All cFB were used at second passage. Fibroblasts were cultured under serum deprived for 24 hours. Cardiomyocytes were subjected to an increasing concentration of Ca^{2+} ions prior to culture in plating media (DMEM with 10% FBS, Gibco) and cultured in laminin-coated plates in plating media (37°C, 2% CO_2) for 90 minutes. The medium was then replaced with culture medium (DMEM with 0.1% BSA) overnight.

For hypoxia treatment, the cells were cultured in DMEM (cFBs) or culture medium (cMyo) and put in hypoxic incubator (1% O_2) for 24 hours. For ischemia, cells were cultured in Kreb's modified buffer (120.4 mM NaCl, 14.7 mM KCl, 0.6 mM KH_2PO_4, 0.6 mM Na_2HPO_4, 1.2 mM $MgSO_4$-$7H_2O$, 10 mM Na-HEPES, 4.6 mM $NaHCO_3$ and 1 mM $CaCl_2$) for 5 hours in hypoxic incubator. During I/R protocol, cells were subjected to 5 hours of ischemia in hypoxic incubator followed by 24 hours reperfusion using DMEM (cFBs) or culture medium (cMyo) in normoxic incubator. During cytokine treatment, cFBs and cMyos were treated with IL6 (10 ng/ml), MCP1 (10 ng/ml) or both for 24 hours.[310-311] At the end of all protocols, cells were harvested and RNA was extracted using Trizol as described previously.

2.7. *In vitro* Angiogenesis Assay

In vitro angiogenic function of recombinant TIMP3 (rTIMP3) was determined using human umbilical vein (HUVEC) [312-314] and human coronary artery endothelial cells (HCAEC, purchased from ATCC). Cytodex 3 microcarrier beads were coated with endothelial cells by incubation at 37° C in 5% CO_2 for 4 hours. The coated beads were then transferred to tissue culture flasks, incubated for 2 hours, then washed with PBS and mixed with fibrinogen solution (2 mg/mL) containing 0.15 U/mL aprotinin. In 24-wells plates, 500 µL of EC-coated beads and fibrinogen solution were mixed with 0.625 U/mL of thrombin for polymerization and incubated for 15 minutes. 3D culture was maintained in M199 culture medium with 50 ng/mL VEGF. After 24

hours, cells were observed under microscope, z-stack images were captured, and sprout length and sprout number were measured per bead.

2.8. Morphological Analysis

2.8.1 Trichrome staining

Freshly excised hearts were arrested in diastole with 1 M KCl, fixed in formalin, paraffin embedded and stained for Masson Trichrome at Alberta Diabetes Institute, Histology Core, University of Alberta, Edmonton, AB, Canada. All images were captured with a Leica DM4000B microscope using Infinity Capture Software (Lumenera, Ottawa, ON, Canada).

2.8.2 Picrosirius red staining

Picrosirius red staining for myocardial collagen deposition was performed on 5µm paraffin embedded heart sections.[60, 306] Briefly, the sections were dewaxed in xylene and brought down to water through graded alcohols and incubated with celestin blue + ferric ammonium sulphate solution and washed with acid alcohol. The sections were then incubated in 0.1% phosphomolybdic acid [99] solution in dark for 45-60 minutes and then again incubated for 90 minutes in Sirius red and picric acid solution. Later, the sections were dehydrated using alcohol and cleared in xylene and mounted with histomount (National Diagnostics; 1330-20-7). The sections were imaged using Metamorph Basic software (version 7.7.0.0) and myocardial collagen content was quantified using same software.

2.8.3 Wheat glut agglutinin staining

Wheat glut agglutinin (WGA) staining to assess myocardial hypertrophy was performed on 5µm paraffin embedded heart sections from WT, TIMP4$^{-/-}$ sham and post-I/R (1week and 4 weeks) as well as from WT and TIMP1$^{-/-}$ sham and post-TAC (5 and 9 weeks) by measuring myocardial cross sectional area.[304,300] Briefly, the sections were dewaxed in xylene and brought down to water, washed with PBS and incubated with 4% bovine serum albumin for 1-1.5 hours at room temperature. The WGA (Thermofisher, W7024) then diluted in 2% bovine serum albumin and then sections incubated with WGA for 30 minutes at room temperature, washed with PBS and mounted with Prolong Gold antifade mounting medium containing DAPI (Life Technologies). The

sections were imaged using Metamorph Basic software (version 7.7.0.0) and myocardial cross sectional area was measured using same software.

The infarct area and viable myocytes post-MI from Ad-hTIMP3 and Ad-null groups were assessed by co-staining of WGA (stains myocyte membrane) and Phalloidin (stains for actin). The sections were dewaxed in xylene and brought down to water through graded alcohols, washed with PBS and incubated with 4% bovine serum albumin for 1-1.5 hours at room temperature. The sections were incubated with Phalloidin (Thermofisher, A12379) at 1:40 dilution at room temperature for 30 minutes. After that, these sections were washed with PBS (3× 5 minutes) and incubated with WGA for 30 minutes and again washed with PBS which were mounted usin Prolong Gold antifade mounting medium containing DAPI (Life Technologies). The sections were imaged using Metamorph Basic software (Version 7.7.0.0).

2.9. Immunostaining

2.9.1 Neutrophil and macrophage immunostaining

The neutrophil staining was performed from WT and TIMP4$^{-/-}$ sham and post-I/R (1 day) as well as Ad-hTIMP3 injected and Ad-null control group at 3 days post-MI while macrophage staining was performed on Ad-hTIMP3 injected and Ad-null control group at 3 days post-Ml.[60, 303, 315]

Five-µm thick paraffin (for WT and TIMP4$^{-/-}$ post-I/R) sections were dewaxed in xylene and brought down to water through graded alcohol. Sections were then pretreated with 1% pepsin in 0.01N HCl at pH 2.0 for 15 minutes at 37°C. For Ad-hTIMP3 and Ad-null, 5 µm thick OCT sections were used. The sections were fixed in 4% paraformaldehyde, washed with PBS, permeabilized with 0.1% Triton X-100 and then incubated with 4% BSA for non-specific blocking. Both OCT and paraffin sections were incubated with anti-mouse neutrophil (Serotec: MCA771GA) and macrophage CD68 antibody (Serotac 1957A) overnight. On day 2, after washing with PBS (3 × 5 minutes) sections were incubated with fluorescent secondary Cy3 antibody at 37^0 C for 1 hour. Sections were washed again and mounted with Prolong Gold antifade mounting medium containing DAPI (Life Technologies). The sections were imaged using Metamorph Basic software (version 7.7.0.0) and total number of neutrophils were measured using same software.

2.9.2 CD63, integrinβ1 immunostaining and co-immunostaining

Immunostaining for CD63 and integrinβ1 was performed in OCT-embedded hearts (sham and TAC) and cardiac fibroblasts (saline, Ang II and TGFβ1) from WT and TIMP1$^{-/-}$. Briefly, the 5 μm thick sections cryosections were fixed with 4% paraformaldehyde, permeabilized with 0.1% Triton X100, and blocked with 4% bovine serum albumin at room temperature.[303, 304] Sections were then incubated with primary antibodies for CD63 (R&D Mab5417; Novus NBP2-32829) and integrinβ1 (Millipore Mab 1900) overnight (4°C in a humidified chamber), then washed and incubated with respective secondary antibodies for 1 hour at 37° C and washed with PBS. Sections were mounted in Prolong Gold antifade mounting medium containing DAPI (Life Technologies). The sections were imaged using Metamorph Basic software (Version 7.7.0.0).

Co-immunostaining for CD63 and integrinβ1 in WT and TIMP1$^{-/-}$ post-TAC hearts and cardiofibroblats treated with Ang II and TGFβ1 was performed as described above. The primary antibodies for CD63 and integrinβ1 were mixed and sections were incubated overnight followed by respective secondary antibodies, and mounted with Prolong Gold antifade mounting medium containing DAPI (Life Technologies). The sections were imaged using Metamorph Basic software (Version 7.7.0.0).

2.9.3 Immunostaining for scleraxis

Immunostaining for scleraxis was performed on 5 μm OCT hearts from WT and TIMP1$^{-/-}$ mice at 2 weeks post-TAC. Five micrometer thick sections cryosections were fixed with 4% paraformaldehyde, permeabilized with 0.1% Triton X100, and blocked with 4% bovine serum albumin at room temperature.[303-304] Sections were then incubated with primary antibody for scleraxis (Ab58655). On day 2, after washing with PBS (3 × 5 minutes) sections were incubated with fluorescent secondary antibody at 37^0 C for 1 hour and washed again. The sections were mounted with Prolong Gold antifade mounting medium containing DAPI (Life Technologies).

2.9.4 CD31 staining and Ki67 staining

At 1 week post-MI, OCT-embeded hearts from Ad-Null, Ad-hTIMP3 group were stained for vascular endothelial cells by immunofluorescence using rat anti-CD31 primary antibody (BD Pharmingen) and Cy3 conjugated goat anti-rat secondary antibody (Life Technologies) as before.

[299, 303-304] Briefly, 5-µm thick OCT-embedded cryosections were fixed with 4% paraformaldehyde, permeabilized with 0.1% Triton X100, and blocked with 4% bovine serum albumin. Sections were then incubated with primary antibody overnight (4°C in a humidified chamber), then washed and incubated with secondary antibody for 1 hour at 37°C. Sections were then visualized and images captured using a fluorescence microscope, and CD31-positive vessels were quantified (Metamorph software) and reported as percent per field. A similar protcol was used to study endothelial proliferation at 3 days post-MI using Ki67 staining (AF7649).

2.9.5 Lectin staining

Lectin immunofluorescence assay was perfomed to assess microvascular density in Ad-null, Ad-hTIMP3 post-MI at 1week using fluorescein conjugated Ricinus communis agglutinin I (RCA; lectin; Vectorlabs).[299, 303] Briefly, heparinized mice were anesthetized and 0.2 mg of lectin in 100 µL saline was injected into the jugular vein. After 18 minutes of lectin circulation, 0.2 mg of papaverine HCl (Vasodilator, Sigma Aldrich) in 50 µL saline was injected to promote maximal dilation of microvessels and circulated for 2 minutes. The hearts were then excised, and frozen in OCT mounting medium. Five-µm thick cryosections were cut, fixed with 4% paraformaldehyde for 20 minutes followed by rehydration (PBS, 30 minutes). Sections were mounted in Prolong Gold antifade mounting medium containing DAPI (Life Technologies). Images were captured using a fluorescence microscope (Olympus IX81). Images were analyzed using Metamorph software (Version 7.7.0.0) and vascular density reported as percentage of lectin-positive vessels per field.

2.9.6. Dihydroethidium (DHE) staining and TUNEL Assay

In WT and TIMP4$^{-/-}$ hearts at 1-day post-I/R, superoxide anion (O_2^-) levels were measured using an oxidative fluorescent dye as described previously.[316] Twenty-µm fresh OCT samples were washed with Hanks balanced salt solution (HBSS) followed by incubation at 37^{0}C with minutes with DHE (20 µM) in HBSS. Sections were washed with PBS and mounted with mounting medium containing DAPI.

In WT and TIMP4$^{-/-}$ hearts at 1-day post-I/R, myocardial injury was determined by assessing apoptosis in the ischemic and remote regions through *in situ* detection of DNA fragmentation using TUNEL (Terminal deoxynucleotidyl transferase mediated dUTP nick end

labeling) assay kit (Invitrogen) according to manufacturer's instructions as before.[299] Briefly, 5µm-thick LV cryosections were fixed with 4% paraformaldehyde and washed in Dulbecco's PBS. The sections were then permeabilized with 0.1% Triton X-100 in 0.1% sodium citrate. After one-hour of incubation with DNA labeling solution (terminal deoxynucleotidyl transferase and BrdUTP), the sections were treated with Alexa Fluor 488-conjugated mouse anti-BrdU and counterstained with propidium iodide. The sections were mounted using Prolong Gold antifade mounting medium and visualized under a fluorescence microscope (Olympus IX81). TUNEL-positive cells were counted per field using the MetaMorph software (Basic version 7.7.0.0) and expressed as percentage of total number of cells per field.

2.10. Co-Immunoprecipitation

2.10.1 Immunoprecipitation of integrinβ1 and CD63 from post-TAC and cardiac fibroblasts.

Protein extracts were prepared by homogenizing LV tissue (or 1×10^6 fibroblasts) in 300 µL of IP lysis buffer (Thermo Scientific). Lysates were centrifuged at 16,000 ×*g* for 15 minutes at 4°C. Pellet was discarded and the supernatant was precleared with Dynabeads protein G (Thermo Scientific). Anti-CD63 (Novus) or IgG isotype control (Santa Cruz) was cross-linked to Dynabeads protein G in Bissulfosuccinimidyl substrate (*BS3*) according to the manufacturer's directions. Precleared lysates were incubated with anti-p120 preabsorbed with Dynabeads protein G-antibody over night at 4°C under a continuous mixing. Pellets were collected after 4 washes with lysis buffer and mixed with 2×SDS buffer (0.2% bromophenol blue, 4% SDS, 100 mM Tris [pH 6.8], 200 mM DTT, 20% glycerol) in 1:1 ratio. Samples were boiled for 3 min and 30 µL was loaded onto a SDS-PAGE gel and proteins were transferred to a PVDF membrane by electroblotting. Primary antibodies, anti-CD63 (Abcam) and anti-integrinβ1 (Novus), were used to detect respective antigens. The labeled proteins were visualized using Amersham ECL prime Western Blotting Detection Reagent (GE Healthcare Lifer Sciences).

2.10.2 Immunoprecipitation of VEGFR2 and TIMP3 in endothelial cells.

Co-immunoprecipitation of VEGFR2 and TIMP3 was assessed in endothelial cells as before. [301] Briefly, cell lysates were centrifuged at 16,000 ×*g* and supernatant was precleared with

Dynabeads protein G (Thermo Scientific). Anti-TIMP3 or IgG isotype control were cross-linked to Dynabeads protein G in Bissulfosuccinimidyl substrate (*BS3*) according to the manufacturer's instructions. The precleared lysates were incubated with anti-p120 pre-absorbed with Dynabeads protein G-antibody overnight at 4º C and pellets were collected under 4 washes with lysis buffer and mixed with SDS running buffer with a 1:1 ratio. Samples were loaded onto a SDS-PAGE gel after boiling for 3-4 minutes and transferred to a nitrocellulose membrane by electroblotting. Primary antibodies were used to detect respective antigens and labelled proteins were visualized by chemiluminescence (Invitrogen).

2.11 RNA Expression Analysis

2.11.1. RNA extraction and purification

RNA was extracted using Trizol reagent (Invitrogen, Burlington, ON, Canada) followed reverse transcriptase to cDNA for TaqMan real-time polymerase chain reaction.[61, 204, 304] The tissue samples were homogenized in 500 µL of Trizol reagent in RNAase free centrifuge tube in a tissue lyser (Qiagen; Germany; Catalogue 85300), followed by centrifugation at 12,000 × *g* at 4 °C for 10 minutes. The supernatant was then transferred in another RNAase free centrifuge tube and pellet was resuspended in another 500 µL of Trizol which was then centrifuged again, two supernatants were combined and 200 µL of chloroform was added. The tubes were shaken vigorously for 10-15 seconds, incubated at room temperature for 3-5 minutes and centrifuged at 12,000× *g* at 4ºC for 15 minutes. The upper colorless aqueous phase containing RNA was carefully transferred to a new RNAase free centrifuge tube, with interphase and pink organic phenol phase discarded. Isopropanol (500 µL /tube) was added to each tube and gently inverted several times, and tubes were incubated overnight at -20 °C. Next day, the samples were centrifuged at 12,000 × *g* at 4 °C for 10 minutes and supernatant was discarded. The pellet was washed with 1 mL of 75% ethanol and pellet was dislodged by gently pipetting and samples were centrifuged at 7,500 × *g* at 4 °C for 5 minutes. The supernatant was removed, the pellet was air-dried for 10 minutes and then dissolved in 20 µL of RNAase free water for quantification using the Nanodrop 1000 spectrophotometer (Nanodrop; Wilmington, DE, USA).

2.11.2. TaqMan RT-PCR

The reverse transcription was performed for RNA samples to generate complementary DNA (cDNA). For each gene, mouse brain cDNA samples were used to generate standard curve of known concentrations as a function of cycle threshold (Ct). The standard curve of $[cDNA]_{brain}$ as a function of Ct is fit to a linear regression: Y=aX+b, where Y=cycle threshold, a=slope of the standard curve, X=[cDNA] experimental sample. The SDS2.2 software fits the Ct values for the experimental samples in this formula and generates values for cDNA levels. 18S (Ribosomal RNA) and HPRT (hypoxanthine-guanine phosphoriboslytransferase-1) were used as internal control for human and mouse samples respectively and values were normalized using these two genes. All values were expressed as relative expression (R.E) and samples were run in triplicate in 384 -well plates.

Table 2.1 TaqMan Primer probes

***TIMP* 1**	Forward Primer Reverse Primer Probe	**5'-CATGGAAAGCCTCTGTGGATATG-3'** 5'-AAGCTGCAGGCACTGATGTG-3' 5'-FAM-CTCATCACGGGCCGCCTAAGGAAC-TAMRA-3'
***TIMP* 2**	Forward Primer Reverse Primer Probe	5'-CCAGAAGAAGAGCCTGAACCA-3' 5'-GTCCATCCAGAGGCACTCATC-3' 5'-FAM-ACTCGCTGTCCCATGATCCCTTGC-TAMRA-3'
***TIMP* 3**	Forward Primer Reverse Primer Probe	5'-GGCCTCAATTACCGCTACCA-3' 5'-CTGATAGCCAGGGTACCCAAAA-3' 5'-FAM-TGCTACTACTTGCCTTGTTTTGTGACCTCCA-TAMRA-3'
***TIMP* 4**	Forward Primer Reverse Primer Probe	5'-TGCAGAGGGAGAGCCTGAA-3' 5'-GGTACATGGCACTGCATAGCA-3' 5'-FAM-CCACCAGAACTGTGGCTGCCAAATC-TAMRA-3'
MMP-1	Forward Primer Reverse Primer Probe	5'- GTCTTTGAGGAGGAAGGCGATATT -3' 5' - AGTTAGGTCCATCAAATGGGTTGTT -3' 5'-FAM-CTCTCCTTCCACAGAGGAGACCATGGTGA-TAMRA -3'
MMP-2	Forward Primer Reverse Primer Probe	5'-AACTACGATGATGACCGGAAGTG -3' 5'-TGGCATGGCCGAACTCA -3' 5'TCTGTCCTGACCAAGGATATAGCCTATTCCTCG -3'

MMP-3	Forward Primer: Reverse Primer: Probe	5'-GGAAATCAGTTCTGGGCTATACGA -3' 5'-TAGAAATGGCAGCATCGATCTTC -3' 5'AGGTTATCCTAAAAGCATTCACACCCTGGGTCT-3'
MMP-7	Forward Primer Reverse Primer Probe	5'- GCAGAATACTCACTAATGCCAAACA -3' 5'- CCGAGGTAAGTCTGAAGTATAGGATACA -3' 5'- CCAAAATGGCATTCCAGAATTGTCACCTAC -3'
MMP-8	Forward Primer Reverse Primer Probe	5'- GATTCAGAAGAAACGTGGACTCAA -3' 5'- CATCAAGGCACCAGGATCAGT -3' 5'CATGAATTTGGACATTCTTTGGGACTCTCTCAC-3'
MMP-9	Forward Primer Reverse Primer Probe	5'-CGAACTTCGACACTGACAAGAAGT -3' 5'- GCACGCTGGAATGATCTAAGC-3' 5'-TCTGTCCAGACCAAGGGTACAGCCTGTTC -3'
MMP-10	Forward Primer Reverse Primer Probe	5'- CCTGATGTTGGTGGCTTCAGT -3' 5'- CTGGTGTATAATTCACAATCCTGTAGGT -3' 5'- CCTTCCCAGGTTCGCCAAAATGGA -3'
MMP-11	Forward Primer Reverse Primer Probe	5'- ATTGATGCTGCCTTCCAGGAT -3' 5'- GGGCGAGGAAAGCCTTCTAG -3' 5'- TCCTTCGTGGCCATCTCTACTGGAAGTTTG -3'
MMP-12	Forward Primer Reverse Primer Probe	5'- GAAACCCCCATCCTTGACAA -3' 5'- TTCCACCAGAAGAACCAGTCTTTAA -3' 5'-AGTCCACCATCAACTTTCTGTCACCAAAGC -3'
MMP-13	Forward Primer: Reverse Primer: Probe:	5'-GGGCTCTGAATGGTTATGACATTC -3' 5'-AGCGCTCAGTCTCTTCACCTCTT -3' 5'AAGGTTATCCCAGAAAAATATCTGACCTGGGATTC -3'
MMP-14 **MT1-MMP**	Forward Primer: Reverse Primer: Probe:	5'- AGGAGACAGAGGTGATCATCATTG -3' 5'- GTCCCATGGCGTCTGAAGA -3' 5'-FAM-CCTGCCGGTACTACTGCTGCTCCTG-TAMRA -3'
MCP-1	Forward Primer: Reverse Primer: Probe	5'- GTTGGCTCAGCCAGATGCA-3' 5'-AGCCTACTCATTGGGATCATCTTG-3' 5'-FAM-TTAACGCCCCACTCACCTGCTGCTACT-TAMRA3'
IL-6	Forward Primer: Reverse Primer: Probe	5'-ACAACCACGGCCTTCCCTACTT-3' 5'-CACGATTTCCCAGAGAACATGTG-3' 5'-FAM-TTCACAGAGGATACCACTCCCAACAGACCT-TAMRA-3'

TNFα	Forward Primer Reverse Primer Probe	5'- ACAAGGCTGCCCCGACTAC-3' 5'- TTTCTCCTGGTATGAGATAGCAAATC-3' 5'-FAM-TGCTCCTCACCCACACCGTCAGC-TAMRA-3'
Pro-col I-α1	Forward Primer Reverse Primer Probe	5'-CTTCACCTACAGCACCCTTGTG-3' 5'-TGACTGTCTTGCCCCAAGTTC-3' 5'-FAM-CTGCACGAGTCACACC-TAMRA-3'
Pro-col III-α1	Forward Primer Reverse Primer Probe	5'- TGTCCTTTGCGATGACATAATCTG-3' 5'- AATGGGATCTCTGGGTTGGG-3' 5'-FAM- ATGAGGAGCCACTAGACT-TAMRA-3'
α-skeletal muscle actin	Forward Primer Reverse Primer Probe	5'-CAGCCGGCGCCTGTT-3' 5'-CCACAGGGCTTTGTTTGAAAA-3' 5'FAMTTGACGTGTACATAGATTGACTCGTTTTACCTCATTTTG- TAMRA-3'
ANP	Forward Primer Reverse Primer Probe	5'-GGA GGA GAA GAT GCC GGT AGA-3' 5'-GCT TCC TCA GTC TGC TCA CTC A-3' 5'-TGA GGT CAT GCC CCC GCA GG-3'
β-MHC	Forward Primer: Reverse Primer: Probe:	5'-CAGCCGGCGCCTGTT-3' 5'-CCACAGGGCTTTGTTTGAAAA-3' 5'-FAM-TTGACGTGTACATAGATTGACTCGTTTTACCTCATTTTG- TAMRA-3'
α-skeletal muscle actin	Forward Primer Reverse Primer Probe	5'-CAGCCGGCGCCTGTT-3' 5'-CCACAGGGCTTTGTTTGAAAA-3' 5'-FAM-TTGACGTGTACATAGATTGACTCGTTTTACCTCATTTTG- TAMRA-3'

2.12. Proximity Ligation Assay

Proximity ligation assay was performed as per manufacturer's instructions and protocol (Sigma Aldrich, DUO92102) to study interaction between integrinβ1 and CD63. Ang II and TGFβ1 treated cardiac fibroblasts or sham/post-TAC OCT frozen sections from WT and TIMP1$^{-/-}$ mice were fixed in 4% PFA for 20-25 minutes and washed with PBS for 3 × 5 minutes. The sections and cells were permeabilized with 0.1% Triton X-100 for 10 minutes and blocked with Duolink blocking solution followed by incubation at 37^{0}C for 30 minutes. The primary antibodies for integrinβ1 and CD63 were added on sections or cells and again incubated for 1 hour in humidified chamber at 37^{0}C followed by wash with Duolink II wash buffer A (2 × 5minutes). The

PLA probes against primary antibodies (Duolink II Anti-rabbit PLUS +Duolink II anti-mouse MINUS) were diluted as per manufacturer's instructions and sections were incubated at 37^0 C with PLA probes. Sections/cells were washed with Wash Buffer A (2 × 5 minutes) and incubated with ligase-ligation solution for 30 minutes at 37^0 C. The ligation-ligase solution was prepared by mixing ligation stock and ligase solution. Next, the reaction was amplified by adding amplification solution to polymerase and addition of this mixture to sections/fibroblasts later incubation at 37^0 C for 100 minutes. The sections/fibroblasts were washed with Duolink wash Buffer B for 10 minutes and mounted using Duolink II mounting medium and DAPI.

2.13. Protein Analysis

2.13.1. Tissue protein extraction

Total protein was extracted from frozen tissues using EDTA-free RIPA buffer **(Table number 2.1)** or Sigma Extraction buffer (Cell Lytic Catalogue number C2978) with tissue lyser (Qiagen; Germany; Catalogue 85300) including protease inhibitor (Table number 2.2 539134, 524628; Calbiochem, San Diego, CA, USA) and phosphatase inhibitor cocktails (Table number 2.1 P5726, Sigma-Aldrich, Oakville, ON, Canada). The recommended concentration for phosphatase inhibitor and protease inhibitors from manufacturer's instructions are 1 mL/100 mL of extraction buffer.

Table 2.2: Phosphatase inhibitor cocktail 2

Phosphatase inhibitor cocktail 2-Ty, Acidic and Alkaline (Sigma; product #5726)				
	Chemical name	M.W. (g/mol)	Concentration Stock	Concentration Final
1	Na-orthovandate	183.91	100×	1×
2	Na-molybdate	241.95	100×	1×
3	Na-tartarate	230.08	100×	1×
4	Imidazole	68.08	100×	1×

Table 2.3: Phosphatase inhibitor cocktail-Ser/Thr and alkaline phosphatases

Phosphatase inhibitor cocktail IV-Ser/The and Alkaline (Calbiochem; product #527628)				
	Chemical name	M.W. (g/mol)	Concentration $_{Stock}$	Concentration $_{Final}$
1	(-)-p-Bromotetramisole oxalate	373.22	100 ×	1×
2	Cantharidin	196.20	100×	1×
3	Calyculin A	1009.20	100×	1×

The samples were centrifuged at 14,000 ×g for 12 minutes and total protein-containing supernatant was then transferred into a new tube. Total protein concentration was determined using Bio-Rad DC protein assay (Bio-Rad; Mississauga, ON, Canada) using a clear flat bottom 96-wellplate and spectrophotometric plate reader at 750 nm.

Table 2.4: RIPA protein extraction buffer pH7.4 in ddH_2O- Western Blot

	Chemical name	M.W. (g/mol)	Concentration	Concentration $_{Final}$
1	Tris-HCl	121.14	N/A	50mM
2	Sodium chloride (NaCl)	58.44	N/A	120mM
3	EDTA	372.24	N/A	1mM
4	Triton X-100 (Detergent)	624	N/A	1%

2.13.2. Membrane and cytosolic protein extraction

Membrane fraction was extracted from sham, ischemic and remote tissue from WT and TIMP4$^{-/-}$ hearts as before[61, 204] with some modifications. Frozen tissue was homogenized in RIPA buffer (50 mM Tris-HCl pH 7.4,150 mM NaCl, 1 mM EDTA) with DTT (1 mM), PMSF (1 mM), protease inhibitor (Calbiochem, San Diego, USA) and phosphatase inhibitor cocktails (Sigma-Aldrich, Oakville, Canada), centrifugation at 2,900 ×*g* for 20 minutes. The supernatant containing cytosolic and membrane proteins was transferred to a new tube. The pellet containing the nuclear protein was discarded. The supernatant containing the cytosolic and membrane proteins was centrifuged at 100,000 ×*g* for 45 minutes. This high speed centrifugation separated the cytosolic protein (supernatant) from the membrane protein (pellet). The pellet was resuspended in 50 µL RIPA buffer (containing DTT, PMSF, protease and phosphatase inhibitors, with 0.25% sodium deoxycholate and 1% NP40) centrifuged at 15,000 ×*g* for 20 minutes. This supernatant was stored at -80 ºC as the membrane fraction. The western blot analysis performed on 8% acrylamide gel,

transferred on the PVDF membrane and blocked with 5% BSA and blotted for MT1-MMP mAb rabbit MT1-MMP antibody (1:1000 dilution; Cell Signaling).

2.13.3. Nuclear and cytosolic protein extraction

Nuclear and cytosolic protein fractionation was performed from WT and TIMP1$^{-/-}$ hearts in sham and post-TAC groups using hypotonic lysis buffer (10 mM potassium-HEPES, 1.5 mM $MgCl_2$, 10 mM KCl, 1 mM dithiothreitol (DTT) and 0.2 mM Na_3VO_4) containing protease and phosphatase inhibitors. After centrifugation (100 ×*g*, 5 min), supernatant was collected and centrifuged again (10 min, 2,000 ×*g*) to separate the nuclear protein (pellet) from the non-nuclear protein (supernatant). The pellet was suspended in 200 µL hypotonic lysis buffer with 2.4 M sucrose and centrifuged using ultra-centrifuge 1000,000 ×*g* for 90 minutes to obtain the nuclear protein. Purities of the nuclear and the cytosolic protein were assessed by blotting for a nuclear-specific protein (Histone), and cytosol-specific protein (caspase 3), respectively.

2.14. Western Blot

SDS based electrophoresis was used to run protein samples and for transfer of loaded protein from gel to polyvinylidene fluoride (PVDF) membrane. The SDS page electrophoresis gel was prepared depending on molecular weight of protein. The appropriate amount of protein concentration was prepared by combining calculated volume of protein extract, phosphate - buffered saline **(Table 2.3)** and loading dye buffer **(Table 2.2)** and boiling for 5 minutes (at 35 mA; Bio-Rad; Mississauga, ON, Canada) in the presence of running buffer solution (Table 2.4). The SDS gel then transferred using transfer buffer solution **(Table 2.5)** (200mA; BioRad) onto a polyvinylidene fluoride (PVDF) membrane. After transfer of protein, the PVDF membrane was blocked with 5% BSA for two hours at room temperature and later incubated with primary antibodies overnight at 4^0 C at specific dilution recommended from manufacturer, usually ranging from 1:100 to 1:5000 in 5 % BSA. The membrane was then washed with TBS (Table 2.6) with 0.1% Tween, followed by the incubation with appropriate species-based horse radish peroxidase (HRP) linked secondary antibody at room temperature. After, another 3× 15 minutes of washing of membrane with TBST, Enhanced Chemiluminescence (ECL Prime; GE Amersham; Baie d'Urfe, QC, Canada) was applied to the PVDF membrane for minutes which binds specifically to

the HRP segment of secondary antibody. The PVDF membrane was then imaged a luminescent image analyzer with a chemiluminescence-sensitive camera (GE Image Quant 4000; GE). The PVDF membrane was then stripped using stripping buffer for 20 minutes at 37° C for subsequent immunoblotting of the membrane. Gels and membrane were stained for Coomassie blue or membrane stain (Thermofisher, 24580) respectively and used as loading control. The Coomassie blue staining solution has 2% Coommassie blue, 25% methanol. 10% Acetic acid.

Western blot analyses were performed by using the following antibodies: CD63 (Abcam, Ab193349), integrinβ1 (Novus, NBP110-57123), p-Smad2/3 S465/467 & S423/425 (CST8828S), totalSMAD2/3 (CST3102S), p-β-catenin Tyr654 (SC57333), total-β-catenin (Ab79089), histone (CST44995), caspase3 (CST9665S) and SCX (ab58655).

Table number 2.5: Sample loading buffer pH6.8 in ddH_2O for western blot

Sample loading buffer pH6.8 in ddH_2O for Western blot				
	Chemical name	M.W. (g/mol)	Concentration	Concentration $_{Final}$
1	Tris-HCl	121.14	130mM	65mM
2	SDS	288.38	4.6%	2.3%
3	Bromophenol Blue	669.96	0.2%	0.1%
4	Glycerol	92.09	20%	10%
5	Dithiothreitol (DTT)	154.25	2%	1%

Table 2.6: Phosphate-Buffered Saline (PBS) pH 7.4 in double-distilled water (ddH_2O)

Phosphate-Buffered Saline (PBS) pH 7.4				
	Chemical name	M.W. (g/mol)	Concentration	Concentration $_{Final}$
1	NaCl	58.44	1370mM	137mM
2	KCl	74.55	27mM	2.7mM
3	Na_2HPO_4	141.96	100mM	10mM
4	KH_2PO_4	136.09	18mM	1.8mM

Table 2.7: Running Buffer pH 8.3 in ddH_2O

Running buffer pH8.3				
	Chemical name	M.W. (g/mol)	Concentration	Concentration Final
1	Tris HCl	121.14	250mM	25mM
2	Glycine	75.04	1920mM	192mM
3	SDS	288.38	10%	1%

Table 2.8: Transfer Buffer pH 8.3 in ddH_2O

Transfer buffer pH8.3				
	Chemical name	M.W. (g/mol)	Concentration	Concentration Final
1	Tris HCl	121.14	200mM	20mM
2	Glycine	75.04	1500mM	150mM
3	Methanol	32.04	N/A	20%

Table 2.9: Tris-Buffered Saline (TBS) pH 8.0 in ddH_2O

Tris-Buffered Saline (TBS) pH 8.0				
	Chemical name	M.W. (g/mol)	Concentration	Concentration Final
1	Sodium chloride (NaCl)	58.44	1250mM	125mM
2	Tris HCl	121.14	250mM	25mM

2.15. Gelatin Zymography

Table 2.10: RIPA protein extraction buffer pH7.4 in ddH_2O

RIPA protein extraction buffer pH7.4 in ddH_2O for Zymography				
	Chemical name	M.W. (g/mol)	Concentration	Concentration Final
1	Tris-HCl	121.14	N/A	50mM
2	Sodium chloride (NaCl)	58.44	N/A	120mM
3	Triton X-100 (Detergent)	624	N/A	1%

Gelatin zymography was used to measure cleaved MMP2, active MMP2 and MMP9 activation following sham, post-I/R in WT and TIMP4$^{-/-}$ and post-TAC and Ang II in WT and TIMP1$^{-/-}$ mice. Proteins were extracted from frozen LV tissues using RIPA extraction buffer as mentioned above **(Table 2.10)**.[60, 206] Gelatin was included in polyacrylamide gel to make final concentration of 2 mg/mL. Each sample to be loaded was prepared by combining volume of loading dye with non-desaturating loading dye for 40µg of protein as mentioned above **(Table 2.8)**.

Table 2.11: Sample loading buffer for Zymography (pH-6.8)

Sample loading buffer for Zymography (pH-6.8)				
	Chemical Name	M.W. (g/mol)	Conc $_{stock}$	Conc $_{final}$
1	Tris HCl	121.14	125mM	62.5mM
2	Glycerol	92.09	20%	10%
3	SDS	288.38	4%	2%
4	Bromophenol Blue	669.96	0.02%	0.01%

Table 2.12: Incubation buffer for Zymography

Incubation buffer for Zymography				
	Chemical Name	M.W. (g/mol)	Conc $_{stock}$	Conc $_{final}$
1	Tris HCl	121.14	2000 mM	50 mM
2	Calcium chloride ($CaCl_2$)	147.02	2000 mM	5 mM
3	Sodium chloride (NaCl)	58.44	N/A	150 mM
4	Sodium azide (NaN_3)	65.01	5%	0.05%

Table 2.13: Polyacrylamide Gel staining solution

Polyacrylamide Gel staining solution				
	Chemical Name	M.W. (g/mol)	Conc $_{stock}$	Conc $_{final}$
1	Coomassie blue	854.0	2000 mM	2%
2	Methanol	32.04	2000 mM	25%
3	Acetic acid	60.05	N/A	10%

After electrophoresis, the gelatin-based polyacrylamide gel was washed with Triton X-100 3 times for 20 minutes each and then with incubation buffer **(Table number 2.9)**. The zymography gel was then incubated at 37^0 C for 48 hours with change of incubation buffer after 24 hour of interval. After 48 hours of incubation, the gel was stained with Coomassie Blue (2%) overnight for visualization of white and clear bands for MMPs and then washed with destaining buffer **(Table 2.10)**. On a separate 10% polyacrylamide gel, remaining 10µg of protein was run and stained with coomassie blue solution as a loading control.

2.16. MMP *In vitro* Activity Assay

2.16.1 *In vitro* inhibitory function of TIMPs against MT1-MMP, MMP2 and MMP9

Recombinant MT1-MMP (Calbiochem), MMP2, MMP9, and TIMPs (-1, -2, -3, -4) were purchased (R&D Systems).[61, 204] Fluorescent-tagged substrates specific to MT1-MMP, or MMP2/9 were purchased (Calbiochem, San Diego, CA, USA). For all three assays, the same concentrations of the fluorescence-tagged substrate (30 μM) and the recombinant MMP enzymes (100 ng/mL) were used. TCNB assay buffer was used for MMP2 and MMP9 activity assays (in mM: 50 Tris, 150 NaCl, 10 $CaCl_2$, and 0.05% Brij). Modified TCNB buffer was used for MT1-MMP activity assay as before (containing 200 mM NaCl and 0.05mM $ZnCl_2$).[61] In parallel experiments, increasing amounts of recombinant TIMPs (rTIMP, 0, 0.1, 1, 5, 10, 20, 40, 80 ng) were used to compare the inhibitory function of each TIMP against rMMP2, rMMP9 or rMT1-MMP. Activity of MT1-MMP was detected at 328 nm excitation and 400 nm emission wavelengths, and for MMP2 and MMP9 at 280 nm Excitation, 360 nm Emission, using Spectra max M5 microplate reader (Molecular Devices).

2.16.2 MMP activity assay

Total gelatinase and collagenase activities were measured using EnzChek fluorescent based substrate.[61, 204, 317] The proteins were extracted using cytobuster protein extraction buffer and the fluorescein isothicynate (FTIC) conjugate substrate was added to each well. 100 μg of protein samples were added to each well and the assay was incubated at room temperature and fluorescent intensity of degraded substrate was measured for six hours on fluorescent microplate at 280 nm Ex, 360 nm Em. The slope of the curve indicates rate of fluorescence of collagen or gelatin and as an indication of the amount of MMP (gelatinase or collagenase) available.

2.16.3 MT1-MMP activity assay

MT1-MMP activity from WT and $TIMP4^{-/-}$ sham and post-I/R groups measured using MT1-MMP specific flurogenic substrate (Catalogue number 44258, Calbiochem, San Diego, CA, USA), LV myocardial protein from sham, ischemic, non-ischemic from WT and $TIMP4^{-/-}$ mice was extracted using a Cacodylic acid-base extraction buffer[61,204,318]. LV myocardial protein extracts of 100 μg were incubated with fluorescent MT1-MMP substrate at 37^0 C, and excitation and emission (328/400nm, Spectramax M5 microplate reader) were recorded for six hours. A parallel set of negative controls with extraction buffer and with substrate were used. Concentrations of MT1-MMP catalytic domain for standard curve included 12.5, 25, 50, 100, 200,

400 ng/mL. The optical density reading indicating fluorescence magnitude to the conversion of MT1-MMP present in test sample was derived from the standard curve linear relationship between fluorescence and the known concentrations of MT1-MMP catalytic domain construct standards.

Table 2.14: Protein extraction buffer for MT1-MMP activity assay.

Protein Extraction buffer pH5 for MT1-MMP activity assay				
	Chemical Name	M.W. (g/mol)	Conc $_{stock}$	Conc $_{final}$
1	Cacodylic acid	138.01	N/A	10 mM
2	Sodium chloride (NaCl)	58.44	N/A	150mM
3	Zinc chloride ($ZnCl_2$)	136.29	N/A	0.1mM
4	Sodium azide (NaN_3)	65.01	N/A	2mM
5	Triton X-100	624	N/A	0.1%

2.17. Quantitative Analysis of Protein Levels

Quantitation of protein bands from Western blot and zymography was performed using ImageJ Densitometry software. Image J software allows measurement of band density by producing histograms with respect to the band density relative to the background for a set of selected bands. The areas of histograms obtained individually indicated density of band which is an arbitrary value. Hence this arbitrary value was normalized first to density obtained from the relevant band on the loading control. For phosphor and total proteins (p-SMAD2/3, p-β-catenin), phospho to total ratio was used to represent the phosphorylation of protein in particular samples.

2.18. Statistical Analyses

All statistical analyses were performed using IBM SPSS Statistics 19 Software. Shapiro-Wilk test for normality and homogeneity of variance was performed for all data. Comparison of groups from different genotypes was done by two-way ANOVA. Multiple comparisons among groups within the same genotype was performed using 1-way ANOVA followed by Bonferroni test. Averaged values represent Mean ± SEM. Statistical significance determined at $p<0.05$.

CHAPTER 3

ROLE OF TIMP4 IN MYOCARDIAL ISCHEMIA-REPERFUSION INJURY

MYOCARDIAL RECOVERY FROM ISCHEMIA-REPERFUSION IS COMPROMISED IN THE ABSENCE OF TISSUE INHIBITOR OF METALLOPROTEINASE 4

Abhijit Takawale, MSc[1,3], Dong Fan, PhD[1,3], Ratnadeep Basu, MD, PhD[1,3], Mengcheng Shen, MSc[1,3], Nirmal Parajuli, PhD[2,3], Wang Wang, MSc[2,3], Xiuhua Wang, PhD[1,3], Gavin Y. Oudit, MD, PhD[1,2,3], Zamaneh Kassiri, PhD[1,3]

[1]Department of Physiology, [2]Department of Medicine/Division of Cardiology, University of Alberta, Edmonton, AB, Canada,[3] Mazankowski Alberta Heart Institute, Edmonton, AB, Canada.

Contributions:

AT: Generated hypothesis, experimental design, and performed Langendorff *ex vivo* perfusion, neutrophil immunostaining, DHE staining, TUNNEL assay for apoptosis, WGA staining, PSR staining, gelatin zymography, and *in vitro* protease activity assay, planned surgeries, cared for and monitored animals, collected tissues post-surgeries at different time points, extracted proteins for WBs and activity assays. AT had critical role in interpreting results, writing manuscript and preparing figures.
DF: Myocyte and fibroblast co-culture, *in vitro* hypoxia treatment experiment.
RB: Analysis of all acquired raw echocardiography data.
MS: WB for mouse TIMP4 at 1 week post-I/R.
NP: Collected human heart samples.
WW: Helped for setting Langendorff *ex vivo* animal model.
XW: Performed I/R surgeries, activity assays for MMPs, MT-1 MMP, TaqMan for various genes.
GYO: Provided ischemic and healthy control human samples.
ZK: Supervisor of AT, overall project planning and corresponding author.

A version of this chapter has been published. Circulation: Heart failure. Takawale et al. 2014 July 7(4):652-62. This chapter has been modified from above mentioned article.

3.1. Introduction

Post-ischemic myocardial reperfusion (I/R) is an effective therapeutic approach in salvaging the ischemic myocardium, however it can also trigger a number of unfavourable events.[319] Adverse remodeling of the myocardial extracellular matrix (ECM) is one of the key aspects of the post- (I/R) injury. ECM turnover and remodeling is mediated through the function of ECM-degrading enzymes, matrix metalloproteinases (MMPs), and their physiological inhibitors, TIMPs.[135, 298, 320] ECM is the structural scaffold for the myocardial tissue, and also provides a micro-environment for a number of growth factors and cytokines. As such, abnormal ECM turnover in heart disease can result in activation of a number of cellular and molecular events in addition to structural instability. Among the four TIMPs, TIMP4 exhibits a tissue-specific expression pattern primarily in the heart and brain,[106] Also, TIMP4-deficient mice exhibited increased rate of left ventricular (LV) rupture following myocardial infarction (MI).[209]

3.2. Objective and Rationale

TIMP4 exhibits tissue specific expression pattern with higher expression in heart and brain and it has been reported to be present intracellularly in rat cardiomyocyte.[21] In an *ex vivo* rat model of I/R, TIMP4 has been found to be released from myocardium with loss of contractile proteins.[21] TIMP4$^{-/-}$ mice have been reported to have more LV rupture without deteriorating LV function as compared with WT mice in a mouse model of MI.[209] Tissue-specific expression and unique intracellular localization suggest a potential role of TIMP4 in myocardial I/R.

3.3. Methods

3.3.1. Myocardial Ischemia-Reperfusion *in vivo*

In vivo I/R was induced in 10-11week-old male WT and TIMP4$^{-/-}$ mice by temporary ligation of the left anterior descending artery (LAD ligation) according to protocol in described in section 2.2.1

3.3.2. Isolated Heart Ischemia-Reperfusion (*Ex vivo*)

Male mice of either genotype, at 10-11 weeks of age, were subjected to *ex vivo* ischemia-reperfusion on a Langendorff apparatus according to protocol mentioned in 2.2.2.

3.3.3. Human Explanted Heart Tissue

Cardiac tissues from patients with post-MI heart failure were collected from the explanted hearts at the time of cardiac transplantation as part of the Human Explanted Heart Program (HELP) at the Mazankowski Alberta Heart Institute (Edmonton, AB). Non-failing control hearts were obtained through the Human Organ Procurement and Exchange (HOPE) program (Edmonton, AB).

3.3.4. Cardiac Function Analysis by Echocardiography

Systolic and diastolic cardiac function were determined by non-invasive transthoracic echocardiography using a Vevo 770 high-resolution imaging system equipped with a 30-MHz transducer (RMV-707B; Visual Sonics, Toronto, ON, Canada) as before.[61,204,206,299] The detail protocol is described in section 2.4.1.

3.3.5. Protein Analysis, Western Blotting, Gelatin Zymography, Gelatinase and MT1-MMP Activity Assays

Protein extraction, Western blots, gelatin zymography and total gelatinase activity (EnzCheck fluorescent-based activity assays, Molecular Probes) were measured as described before.[204,206] MT1-MMP activity was measured using a specific MT1-MMP flurogenic substrate (Calbiochem) as described.[61,321] The detailed protocol is mentioned in sections 2.13, 2.14, 2.15, 2.16.2. and 2.16.3.

3.3.6. *In vitro* Inhibitory Function of TIMPs against MT1-MMP, MMP2 and MMP9

In vitro MMP inhibitory potential of TIMPs against MMP2, MMP9 and MT1-MMP was measured using fluorescence-based activity assay. Detail protocol is mentioned in 2.16.1.

3.3.7. Protein Levels for MT1-MMP in the Membrane Fraction

Membrane fraction was extracted from sham, ischemic and remote tissue from WT and TIMP4$^{-/-}$ hearts as before.[204,206] The detail protocol for MT1-MMP extraction is described in section 2.16.3.

3.3.8. RNA Expression Analysis

Total RNA was extracted using Trizol Reagent (Invitrogen) and mRNA expression analysis was performed by TaqMan RT-PCR as before.[204,322] HPRT (hypoxanthine-guanine phosphoribosyltransferase-1) was used as the internal control for mouse samples, and 18S for human samples. TaqMan primers and probes were used to measure the expression of IL-6, MCP1, TIMPs, MMPs, MT1-MMP, pro-col I-α1 and pro-col III-α1 as before.[204,315] The detailed protocol for RNA extraction and TaqMan is described in section 2.11.

3.3.9. Dihydroethidium, Neutrophil and TUNEL staining

At 1 day post-I/R, DHE staining was performed on 20-µm thick myocardial cryosections as before,[301] as mentioned in detail protocol sections 2.9.6.

Myocardial injury was determined at 1 day post-I/R by assessing apoptosis in the ischemic and remote regions through in situ detection of DNA fragmentation using TUNEL (Terminal deoxynucleotidyl transferase mediated dUTP nick end labeling) assay kit (Invitrogen) according to manufacturer's instructions as before.[299] The detailed protocol is described in 2.9.6. Neutrophil infiltration at 1 day post-I/R was assessed by immunostaining for neutrophils as described in sections 2.9.1.

3.3.10. Histological Analysis

Freshly-excised hearts were arrested in diastole in 1 M KCl, fixed in 10% buffered formalin, paraffin-embedded and processed for trichrome, picrosirius red (PSR) and wheat germ agglutinin (WGA) staining as before.[299] Myocyte cross sectional areas and collagen content for WGA and PSR staining were quantified using Metamorph Basic software (version 7.7.0.0). The detailed protocol is described in 2.8

3.3.11. Isolation and Culture of Adult Cardiac Fibroblasts (cFB) and Myocytes (cMyo)

cFB and cMyo were isolated from adult WT and TIMP4$^{-/-}$ mice as previously described.[60, 309-308] The detailed protocol is mentioned in sections 2.6 .

3.4. RESULTS

3.4.1 TIMP4 is Critical in Myocardial Recovery from I/R Injury *In vivo*

In WT mice, TIMP4 protein and mRNA levels decreased in the ischemic myocardium at 1 week post-I/R (**Figure 3.4.1Ai-ii**). Interestingly, myocardial tissue from patients with post-MI heart failure showed a similar decrease in TIMP4 protein and mRNA levels (**Figure 3.4.1Bi-ii**). To determine if this reduction in TIMP4 promotes the post-I/R pathology or if it is simply a by-stander, we subjected TIMP4-deficient mice to *in vivo* myocardial I/R. At 1 week post-I/R, TIMP4$^{-/-}$ mice, but not WT mice, exhibited systolic dysfunction as determined by reduced ejection fraction (**Figure 3.4.1 Di**) and elevated wall motion score index (**Figure 3.4.1Dii**). Diastolic dysfunction was more severe in TIMP4$^{-/-}$ mice as determined by a significantly greater increase in isovolumic relaxation time, deceleration time, E'-to-A' ratio, and left atrial size (**Figure 3.4.1 Diii-vi**) compared with WT-I/R group. Sham-operated TIMP4$^{-/-}$ and WT mice showed similar cardiac systolic and diastolic function (**Table 3.1**).

Parameters	WT-Sham	WT-I/R	TIMP4$^{-/-}$-sham	TIMP4$^{-/-}$-I/R
n	5	8	5	8
HR (bpm)	442 ± 19	426 ± 24	453 ± 39	409 ± 16
E-wave (mm/s)	755.7 ± 40.3	739.7 ± 35.0	735.9 ± 37.1	572.2 ± 35.6*$^{\#}$
A-wave (mm/s)	573.3 ± 31.1	440.6 ± 45.3*	527.2 ± 36.3	378.5 ± 36.5*$^{\#}$
E/A Ratio	1.38 ± 0.03	1.76 ± 0.10*	1.4 ± 0.03	1.5 ± 0.11
E'(mm/s)	34.5 ± 2.1	32.6 ± 2.9	30.9 ± 2.7	21.5 ± 1.6*$^{\#}$
A' (mm/s)	27.5 ± 3.1	28.2 ± 2.3	23.3 ± 2.2	27.5 ± 2.5
E'/A' Ratio	1.28 ± 0.10	1.16 ± 0.10	1.28 ± 0.03	0.80 ± 0.02*$^{\#}$
IVRT [323]	11.6 ± 0.9	13.1 ± 1.1	11.6 ± 0.8	20.5 ± 2.6*$^{\#}$
DT [323]	24.6 ± 0.4	23.8 ± 1.2	25.1 ± 0.9	30.0 ± 1.4*$^{\#}$
LA Size/BW	1.5 ± 0.1	1.7 ± 0.01	1.6 ± 0.1	2.1 ± 0.1*$^{\#}$
WMSI	1.00 ± 0.00	1.00 ± 0.00	1.00 ± 0.00	1.10 ± 0.1
LVEF (%)	65.2 ± 3.8	60.8 ± 1.9	65.6 ± 2.4	54.1 ± 3.6*$^{\#}$
Systolic vol (µL)	16.9 ± 2.5	22.2 ± 2.3	15.3 ± 2.4	43.0 ± 3.9*$^{\#}$
Diastolic vol (µL)	55.7 ± 4.5	61.8 ± 4.5	45.1 ± 2.3	98.9 ± 6.3*$^{\#}$
LVID-D	3.9 ± 0.1	4.0 ± 0.1	3.6 ± 0.2	4.3 ± 0.1*
LVID-S	2.3 ± 0.2	2.7 ± 0.1	2.2 ± 0.2	2.9 ± 0.1*
LVPW-S	1.01 ± 0.04	1.09 ± 0.03	0.99 ± 0.03	1.22 ± 0.11*
LVPW-D	0.72 ± 0.01	0.8 ± 0.02	0.6 ± 0.02	0.9 ± 0.1*$^{\#}$

Table 3.1: Echocardiographic assessment of systolic and diastolic function in WT and TIMP4$^{-/-}$ mice and corresponding shams at 4 weeks post-I/R. HR=Heart rate; E-wave=early transmitral peak velocity; A-wave=transmitral inflow velocity due to atrial contraction; E'=Early tissue Doppler velocity; A'=Tissue Doppler velocity due to atrial contraction. IVRT=Isovolumic relaxation time of LV; DT=Deceleration Time of E wave, LA=Left atrium; WMSI=Wall motion score index; LVEF=LV ejection fraction; LVID=LV internal diameter at the end of diastole (LVID-D) or systole (LVID-S); LVPW=LV posterior wall thickness at the end of systole (LVPW-S) or diastole (LVPW-D). *$p<0.05$ compared with corresponding sham; #$p<0.05$ compared with WT-I/R.

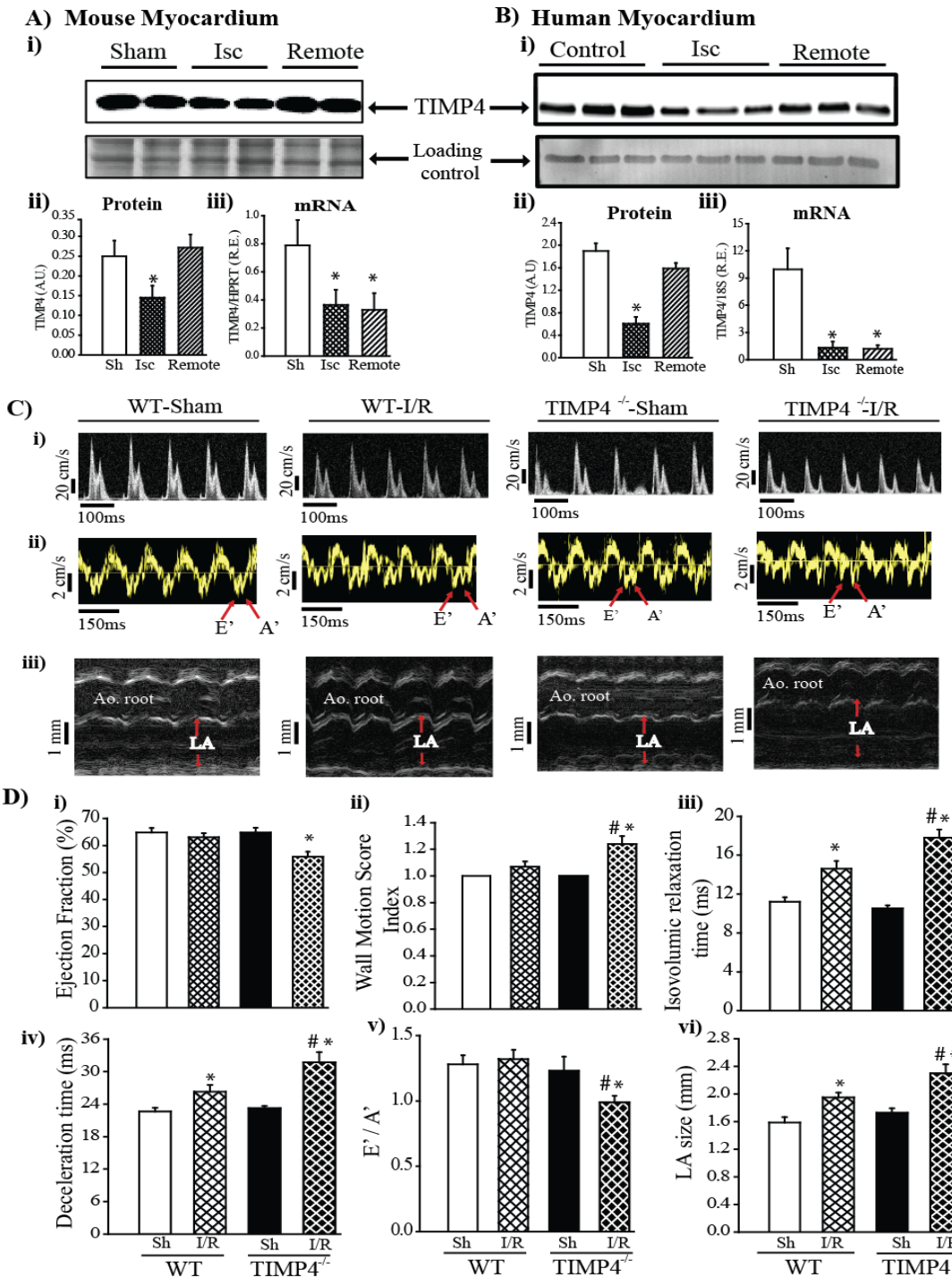

Figure 3.4.1: TIMP4-deficiency suppresses cardiac function following ischemia-reperfusion *in vivo*. **(A)**TIMP4 protein **(i, ii)** and mRNA **(iii)** levels are reduced in ischemic myocardium of WT mice at 1 week post-I/R and in patients with ischemic cardiomyopathy **(B)** Representative

echocardiographic images **(C)** (transmitral Doppler) **(i)**, tissue Doppler **(ii)** and M-mode recording **(iii)** from WT and TIMP4$^{-/-}$ mice at 1week post-sham or I/R. Averaged parameters of systolic function **(D) (i-ii)** and diastolic function **(iii-vi)** in WT and TIMP4$^{-/-}$ mice. n=6/sham and 10/I/R per genotype. *p<0.05 compared with corresponding sham; #p<0.05 compared with WT-I/R.

3.4.2 Enhanced Myocardial Fibrosis and Hypertrophy in TIMP4$^{-/-}$ Mice Post-I/R

We assessed the impact of TIMP4-deficiency on myocardial hypertrophy and fibrosis which are often associated with diastolic and systolic dysfunction. PSR-staining and fluorescence microscopy showed enhanced collagen content in the ischemic region of TIMP4$^{-/-}$ compared with WT hearts at 1 week post-I/R (**Figure 3.4.2Ai-ii**). In addition, mRNA expression of collagen type-I was increased to a greater extent in TIMP4$^{-/-}$-I/R hearts (**Figure 3.4.2Bi**) while the elevation in collagen type III mRNA was similar between genotypes (**Figure 3.4.2Bii**). In addition, TIMP1 levels were significantly increased in TIMP4$^{-/-}$-I/R hearts (**Figure 3.4.2Biii**), which has been strongly linked to myocardial fibrosis in patients as well as in animal models.[208, 287]

Assessment of myocardial hypertrophy by cardiomyocyte cross-sectional area in WGA-stained sections (**Figure 3.4.2Ci-ii**), and heart weight-to-tibial length ratio (**Figure 3.4.2D**) indicate greater myocardial hypertrophy in TIMP4$^{-/-}$ compared with WT mice at 1 week post-I/R, primarily in the ischemic myocardium (**Figure 3.4.2Ci-ii**). Therefore, the more severe diastolic dysfunction in TIMP4$^{-/-}$I/R mice is associated with enhanced fibrosis and hypertrophy.

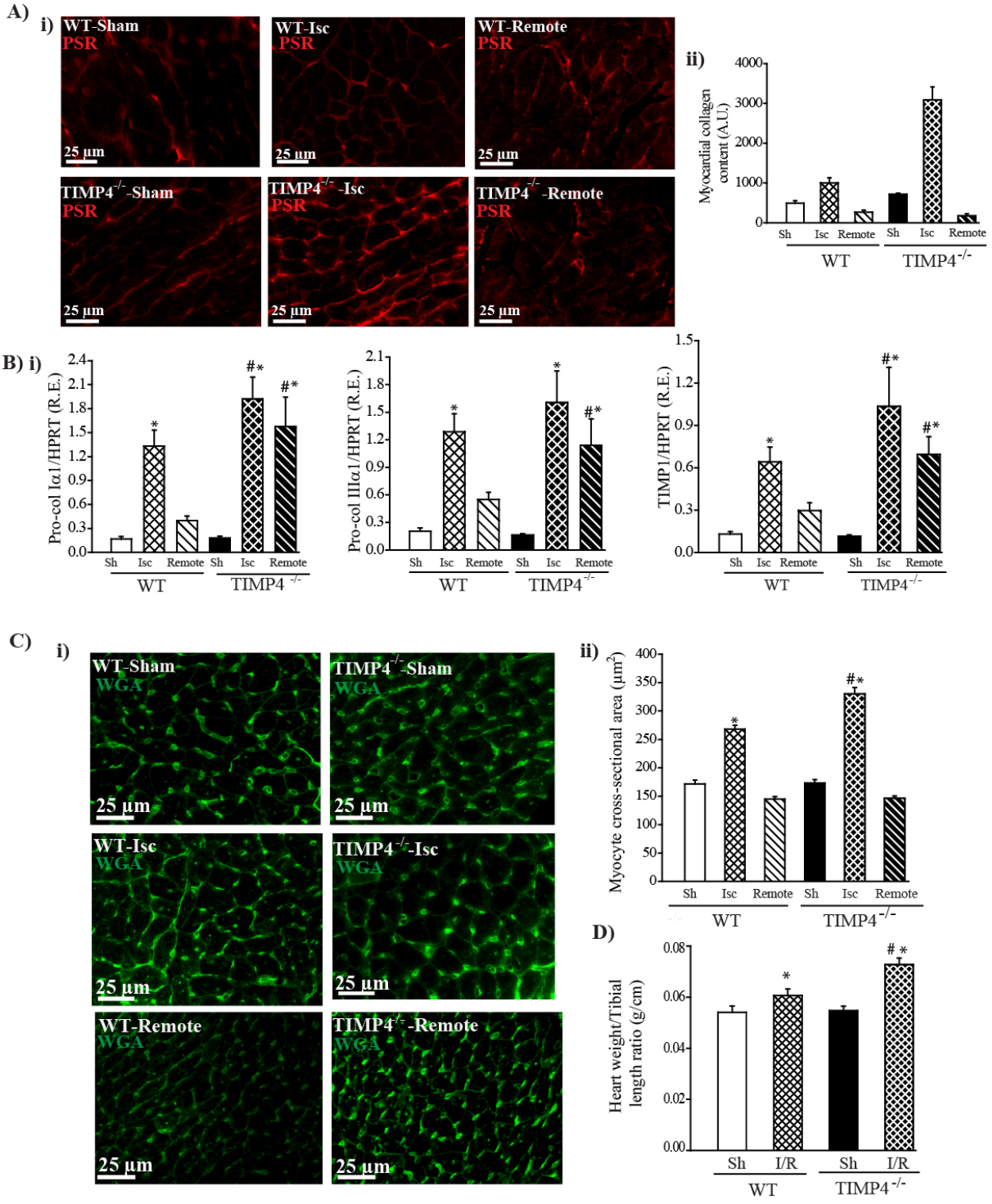

Figure 3.4.2: Enhanced myocardial fibrosis and hypertrophy in TIMP4$^{-/-}$ mice at 1week post-I/R. (A) Representative Picrosirius red (PSR)-stained images **(i)** and averaged myocardial collagen

content **(ii)** in indicated groups at 1 week post-I/R (n=4 hearts/group/genotype; 4 sections/region/heart). (**B)** mRNA expression levels of collagen type I (pro-Col Iα1) **(i)**, collagen type III (pro-Col IIIα1) **(ii)**, and TIMP1 **(iii)** (n=6-8/group/genotype). (**C) i)** representative images from Wheat Germ Agglutinin (WGA)-stained myocardial sections at 1-week post-sham or I/R. **ii)** Averaged cardiomyocyte cross-sectional area measured from WGA-stained sections (n=100 cells/ group/genotype). Heart weight-to-tibial length ratio in WT and TIMP4$^{-/-}$ mice (n=10/group/genotype). A.U.= arbitrary units; R.E.=relative expression. *$p<0.05$ compared with corresponding sham; $^{\#}p<0.05$ compared with corresponding region in WT-I/R.

3.4.3 Excess Oxidative Stress and Inflammation in TIMP4$^{-/-}$ Hearts at 1 Day Post-I/R

In identifying the early molecular and cellular events that lead to the observed diastolic dysfunction in TIMP4$^{-/-}$-I/R hearts, we found that at 1 day post-I/R, superoxide levels were markedly elevated in the ischemic region of TIMP4$^{-/-}$-I/R hearts, as determined by increased number of cells positively stained for dihydroethidium (**Figure 3.4.3Ai-ii**). Further, elevated neutrophil infiltration (**Figure 3.4.3Bi-ii**) and enhanced expression of inflammatory markers, interleukin-6 (IL-6) and monocyte chemoattractant protein-1 (MCP1) (**Figure 3.4.3Ci-ii**) were detected in the ischemic myocardium of TIMP4$^{-/-}$ compared with WT mice. Concomitantly, enhanced myocardial injury, determined by a larger number of apoptotic cells, was observed in TIMP4$^{-/-}$ ischemic myocardium (**Figure 3.4.3Di-ii**). The oxidative stress and inflammation subsided by 1 week post-I/R which is consistent with the transient nature of these events following injury.

We investigated how these early events impact TIMP4 levels in myocardial cells using cultured adult cardiomyocyte (cMyo) and cardiofibroblast (cFB) under different conditions, hypoxia, ischemia, I/R and cytokine that were elevated *in vivo* (IL6, MCP1, MCP1+IL6) (**Figures 3.4.1 and 3.4.2A**). Following hypoxia and I/R, TIMP4 mRNA increased in the cMYO (but not cFB), while exposure to IL6 or IL6+MCP1 increased TIMP4 mRNA in cFB**.** While ischemia triggered an increase in TIMP2 and TIMP3 levels in cMYO, it did not alter TIMP4 levels. Next, we asked how these findings correlate with early *in vivo* changes in TIMP4 levels post-I/R. Interestingly, we found that after 24 hours of I/R, TIMP4 mRNA levels are in fact elevated in the ischemic and non-ischemic myocardium (**Figure 3.4.2B**).

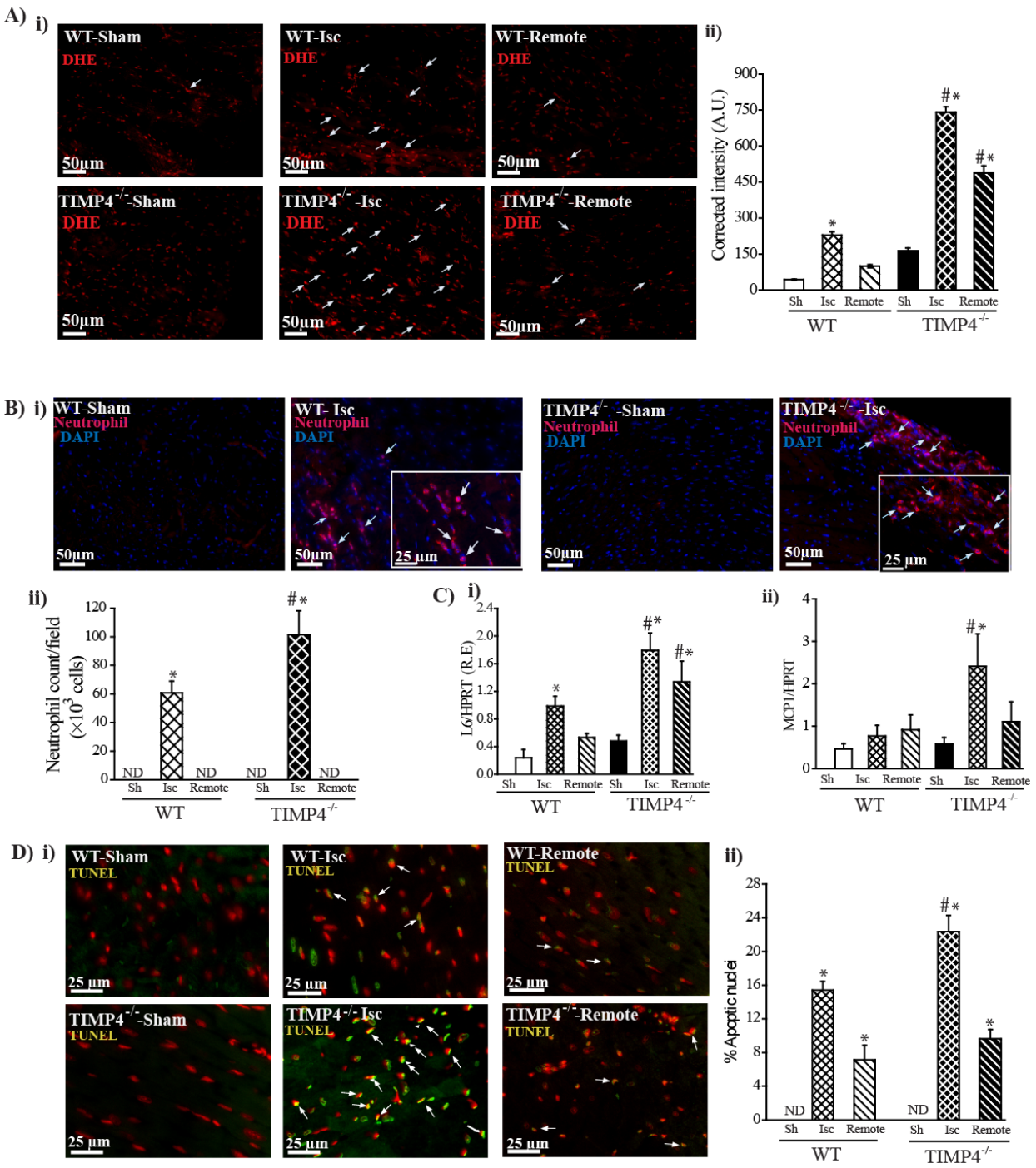

Figure 3.4.3: Excess oxidative stress and inflammation in TIMP4$^{-/-}$ hearts at 1-day post-I/R. **(A)** Representative images of dihydroethidium (DHE)-stained **(i)**, and averaged quantification of DHE-positive cells **(ii)** in indicated groups in WT and TIMP4$^{-/-}$ mice (n=4 hearts/group/genotype). **(B)** representative images of neutrophil-stained sections **(i)**, and averaged neutrophil count per

field in indicated groups (n=4 hearts/group/genotype) **(ii) (C)** mRNA expression of pro-inflammatory markers, IL-6 **(i)** and MCP1 **(ii)** normalized to HPRT levels in WT and TIMP4$^{-/-}$ mice (n=4-6/group/genotype). **(D)** Representative images of TUNEL-stained hearts **(i)** and averaged quantification of TUNEL-positive cells **(ii)** in indicated groups. (n=4 hearts/group/genotype; 4 sections/region/heart), Isc=ischemic, ND=not detected. * $p<0.05$ compared with corresponding sham; $^{\#}p<0.05$ compared with corresponding region in WT-I/R. R.E.=Relative Expression; A.U.=Arbitrary Units.

3.4.4 Absence of TIMP4 Inhibitory Function Elevates MT1-MMP Activity

Since tissue proteolysis is one of the major contributors to overall cardiac remodeling, fibrosis and diastolic dysfunction, we measured the levels and the activity of a number of key matrix metalloproteinases (MMPs) and their inhibitors, TIMPs that could contribute to these events. At 1 week post-I/R, *in vitro* gelatine zymography showed elevated MMP2 (pro- and cleaved) levels in the ischemic myocardium of TIMP4$^{-/-}$-I/R mice (**Figure 3.4.4Ai-iii**), while the changes in MMP9 levels did not reach statistical significance (**Figure 3.4.4Ai, iv**). This was accompanied by increased mRNA expression for MMP2 but not MMP9, while MMPs -7, -8, -9, or -13 were not elevated in either group post-I/R (**Figure 3.4.10Ai-iv**). At 1 week post-I/R, mRNA expression and protein levels of MT1-MMP (**Figure 3.4.10Av and 3.4.10 Bi**), a membrane-bound MMP was markedly elevated in the ischemic and remote regions of TIMP4$^{-/-}$-I/R hearts. TIMP2 and TIMP3 levels remained unaltered in both genotypes post-I/R (**Figure 3.4.10Ci-ii**). *In vitro* fluorescent-based activity assays were used to measure total gelatinase activity (reflective of MMP2 and MMP9 activities), and MT1-MMP activity in WT and TIMP4$^{-/-}$ myocardial tissue post-I/R. While total gelatinase activity was not altered in either genotype post-I/R (**Figure 3.4.4B**), MT1-MMP activity was markedly elevated in the ischemic region of TIMP4$^{-/-}$-I/R compared with the parallel WT group **(Figure 3.4.4C**). This was consistent with the elevated MT1-MMP activity in the ischemic myocardium from patients (**Figure 3.4.4D**).

Next, we compared the inhibitory function of TIMP4, compared with other TIMPs, against MT1-MMP, MMP2 and MMP9, the MMPs that were elevated in TIMP4$^{-/-}$-I/R hearts. *In vitro* assessment of the inhibitory function of the four TIMPs against MT1-MMP, MMP2 and MMP9 showed that TIMP4 is as potent as TIMP3, and second to the inhibitory effects of TIMP2 against

MT1-MMP, whereas TIMP1 lacks inhibitory function against rMT1-MMP (**Figure 3.4.4Di**). All TIMPs inhibited rMMP2 and rMMP9 with similar potency. The rTIMPs used here are not glycosylated, and glycosylation could impact their MMP-inhibitory function, while full length MT1-MMP could interact differently with TIMPs compared with its catalytic domain used in this experiment. Based on our findings, it is plausible that the elevated TIMP1 levels in TIMP4$^{-/-}$-I/R hearts suppressed the activity of MMP2 and MMP9 (leading to unaltered total gelatinase activity), while MT1-MMP activity remained elevated.

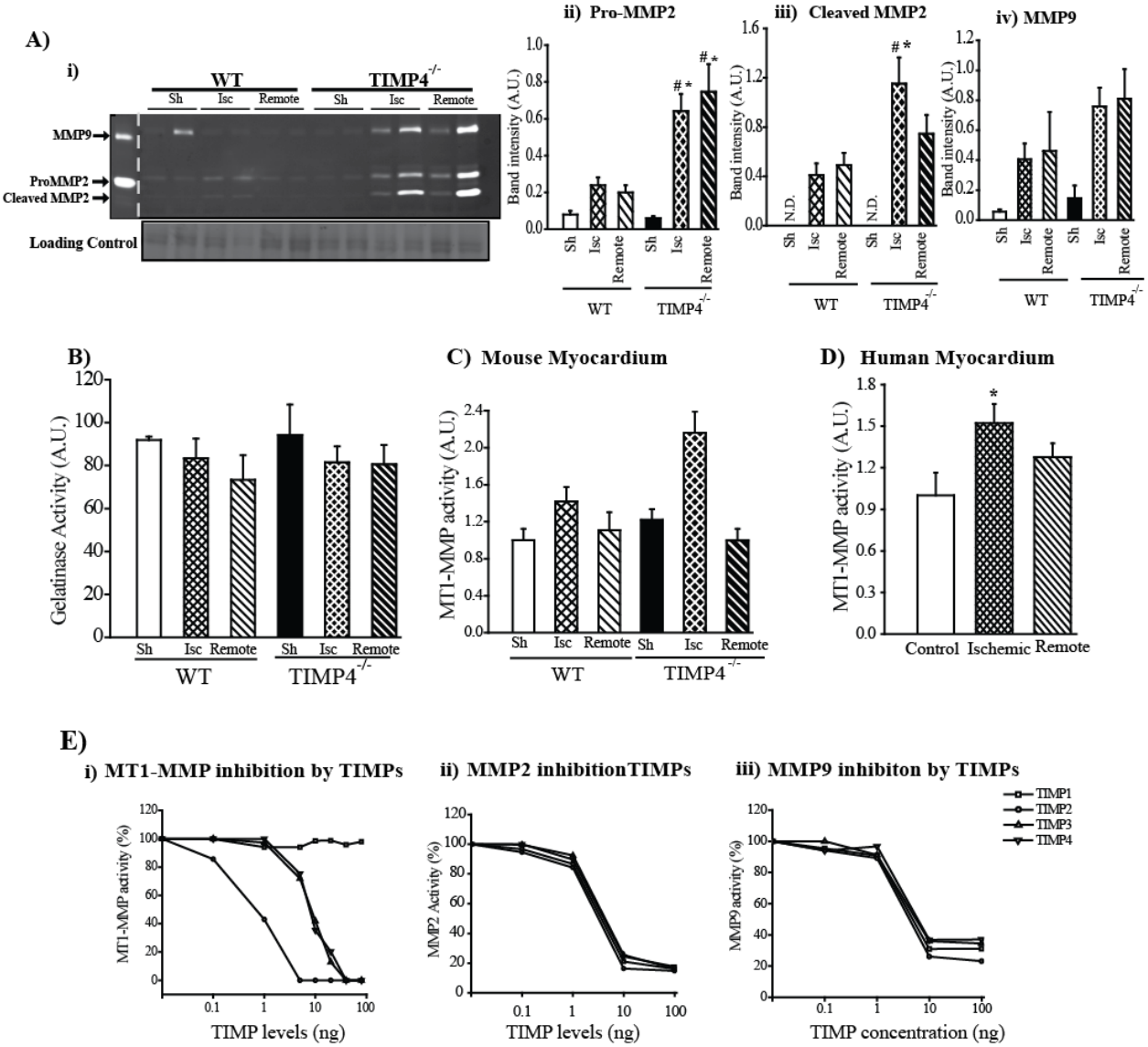

Figure 3.4.4: Elevated MT1-MMP activity in the ischemic myocardium of TIMP4-deficient mice at 1-week post-I/R. (A) (i) Representative gelatin zymography **(i)** and averaged band

intensity for pro-MMP2 **(ii)**, cleaved MMP2 **(iii)** and MMP9 **(iv)** in indicated groups (n=4/group/genotype). Coomassie blue-stained gel was used as loading control. **(B-D)** Total gelatinase and MT1-MMP activity in indicated groups (n=7-8/group) MT1-MMP activity in human ischemic myocardium compared with control (n=5/control, 8/ischemic heart). **(E)** Inhibitory potential of recombinant TIMPs (rTIMP1, rTIMP2, rTIMP3 and rTIMP4) against MT1-MMP **(i)** MMP2 **(ii)** and MMP9 **(iii)** Isc=ischemic; A.U.=Arbitrary Units; *$p<0.05$ compared with corresponding sham; $^{\#}p<0.05$ compared with corresponding region in WT-I/R.

3.4.5. TIMP4 is Essential for Chronic Recovery from I/R Injury

To investigate how TIMP4-deficiency influences the long term myocardial recovery from I/R injury, we followed up cardiac remodeling and function in WT and TIMP4$^{-/-}$ mice until 4 weeks post-I/R. Assessment of the hearts after 4 weeks of I/R showed a gross enlargement of TIMP4$^{-/-}$ hearts compared with WT hearts (**Figure 3.4.5A**), consistent with markedly increased heart weight-to-tibial length ratio (**Figure 3.4.5B**) in this group. Interestingly, by 4 weeks post-I/R, while the increase in myocyte cross-sectional area (**Figure 3.4.5Ci-ii**) and myocardial fibrosis (**Figure 3.4.5D**) became more pronounced in TIMP4$^{-/-}$-I/R hearts, the parallel WT-I/R group showed complete recovery from the I/R injury such that no hypertrophy or fibrosis were detected in these mice. Consistently, cardiac function in WT mice was comparable to the sham group at 4 weeks post-I/R (**Figure 3.4.6A, and Table 3.1**). TIMP4$^{-/-}$ mice, on the other hand, exhibited suppressed systolic function and adverse remodeling evident by increased wall thickness and LV dilation (**Figure 3.4.6Ai-iii**); as well as exacerbated LV diastolic dysfunction as evident by a marked increase in IVRT, deceleration time (DT), LA size, and a decrease in E'-to-A' ratio (**Figure 3.4.6Aiv-vii**). Intriguingly, the full recovery of the WT mice at 4 weeks post-I/R was associated with an increase in TIMP4 protein, to levels comparable to the sham group (**Figure 3.4.6Bi-ii**), and a concomitant normalization of MT1-MMP activity in these WT hearts (**Figure 3.4.6C**). MT1-MMP activity remained elevated in TIMP4$^{-/-}$-ischemic myocardium despite normalization of its protein levels (**Figure 3.4.10 Bii**), indicating the critical importance of TIMP4 in regulating the activity of MT1-MMP. These data collectively highlight the critical role of TIMP4 in recovery from myocardial I/R injury.

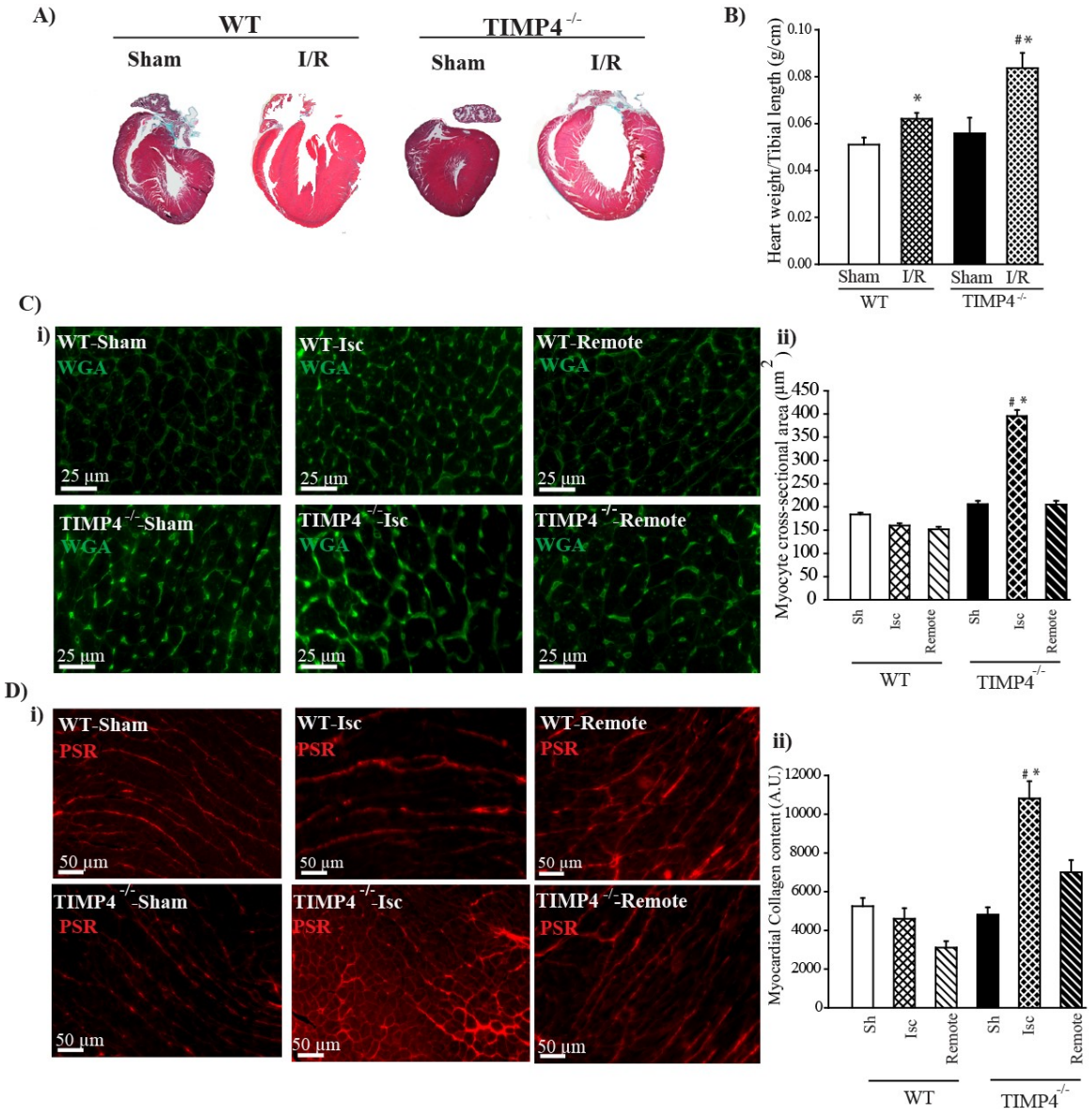

Figure 3.4.5: **Advanced myocardial hypertrophy, fibrosis and adverse remodeling in TIMP4$^{-/-}$ mice by 4 weeks post-I/R**. **(A)** Representative macroscopic images of trichrome stained hearts, (n= 4 hearts/group/genotype) **(B)** averaged heart weight-to-tibial length ratio in WT and TIMP4$^{-/-}$ mice at 4 weeks post-sham or I/R, **(C)** representative WGA-stained sections **(i)** and averaged myocyte cross-sectional area (CSA) from each genotype **(ii)**, **(D)** representative PSR-stained sections **(i)** and averaged collagen content in indicated groups **(ii)** (n=4 hearts/group, 4 sections/region/heart). Sh-Sham; Isc=ischemic; *p<0.05 compared with corresponding sham; $^{\#}$p<0.05 compared with corresponding regions in WT-I/R.

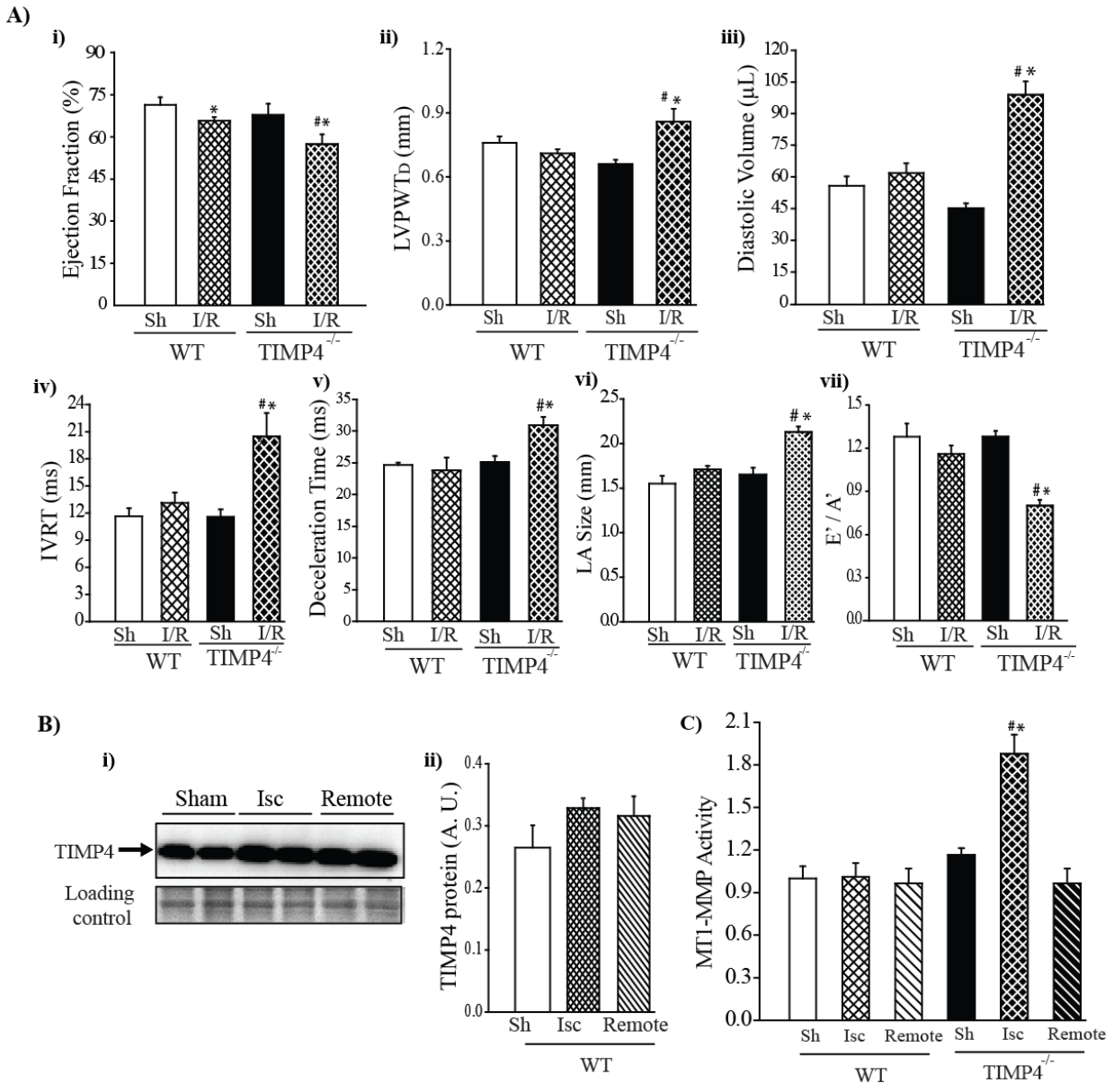

Figure 3.4.6: **At 4 weeks post-I/R, TIMP4-deficient mice show exacerbated diastolic dysfunction and systolic dysfunction. (A)** Averaged echocardiographic parameters for ejection fraction **(i)**, LV posterior wall thickness **(ii)**, LV diastolic volume **(iii)**, isovolumic relaxation time (IVRT) **(iv)**, deceleration time (DT) **(v)**, left atrial size **(vi)**, and E'-to-A' ratio **(vii)** in WT and TIMP4$^{-/-}$ mice (n=5/sham/genotype; 8/IR/genotype). **(B)** Representative Western blot **(i)** and averaged TIMP4 protein levels **(ii)** in ischemic and remote myocardium from WT hearts at 4 weeks post-I/R (n=4/group). **(C)** MT1-MMP activity in indicated groups at 4 weeks post-I/R. *$p<0.05$ compared with corresponding sham; $^{\#}p<0.05$ compared with WT-I/R.

3.4.6. *Ex vivo* ischemia-reperfusion resulted in similar post-ischemia recovery in TIMP4$^{-/-}$ and WT hearts.

Using the isolated heart Langendorff perfusion system, WT and TIMP4$^{-/-}$ hearts were subjected to 20 minutes of global ischemia (after 15 minutes of stabilization), followed by 45 minutes of reperfusion. The perfusion buffer did not contain EDTA to avoid the complications resulting from MMP-inhibitory function of this reagent. At baseline, WT and TIMP4$^{-/-}$ hearts showed comparable LV function, as assessed by LV developed pressure (LVDP), systolic pressure (LVP_{sys}), LV diastolic pressures (LVP_{dias}) and the rates of contraction and relaxation (±dP/dt) (**Figures 3.4.7A-D**). Following I/R, LVDP (**Figure 3.4.7A**) and the rates of contraction and relaxation (±dP/dt, **Figure 3.4.7D**) were suppressed similarly in both genotypes. This experiment was also performed with a longer ischemic period (30 min) and similar results were observed (**Figure 3.4.11**). Heart rate was sustained and comparable in WT and TIMP4$^{-/-}$ hearts throughout the protocol (**Figure 3.4.7E**). Flow rate before ischemia (2.72±.0.27 vs. 2.24 ±.0.20 mL/min) and during reperfusion (2.38±0.28 vs. 2.16±0.22 mL/min) were similar in WT and TIMP4$^{-/-}$ hearts, respectively. Consistent with similar LV function, myocyte damage post-I/R, as determined by creatine kinase levels in the coronary effluent, was not different between TIMP4$^{-/-}$ and WT hearts (**Figure 3.4.7F**). Therefore, TIMP4-deficient cardiomyocytes are not inherently more susceptible to acute ischemic injury.

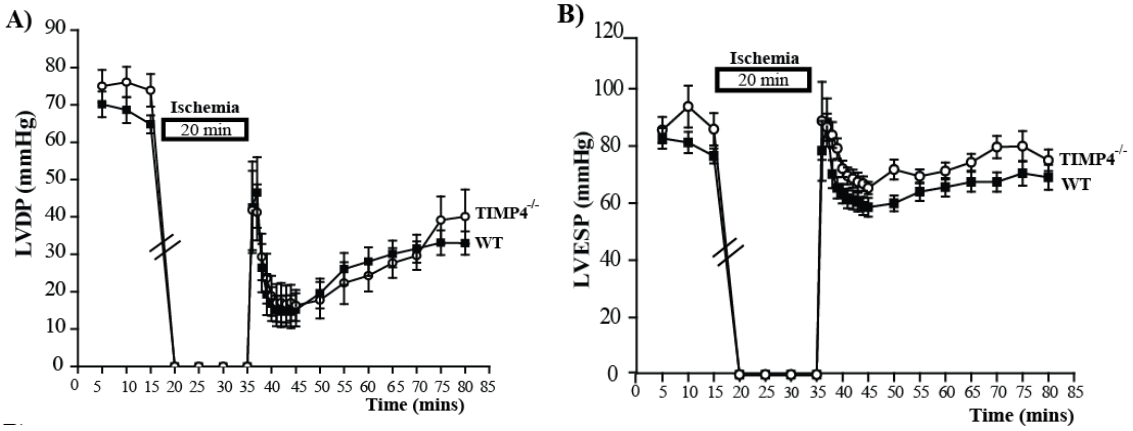

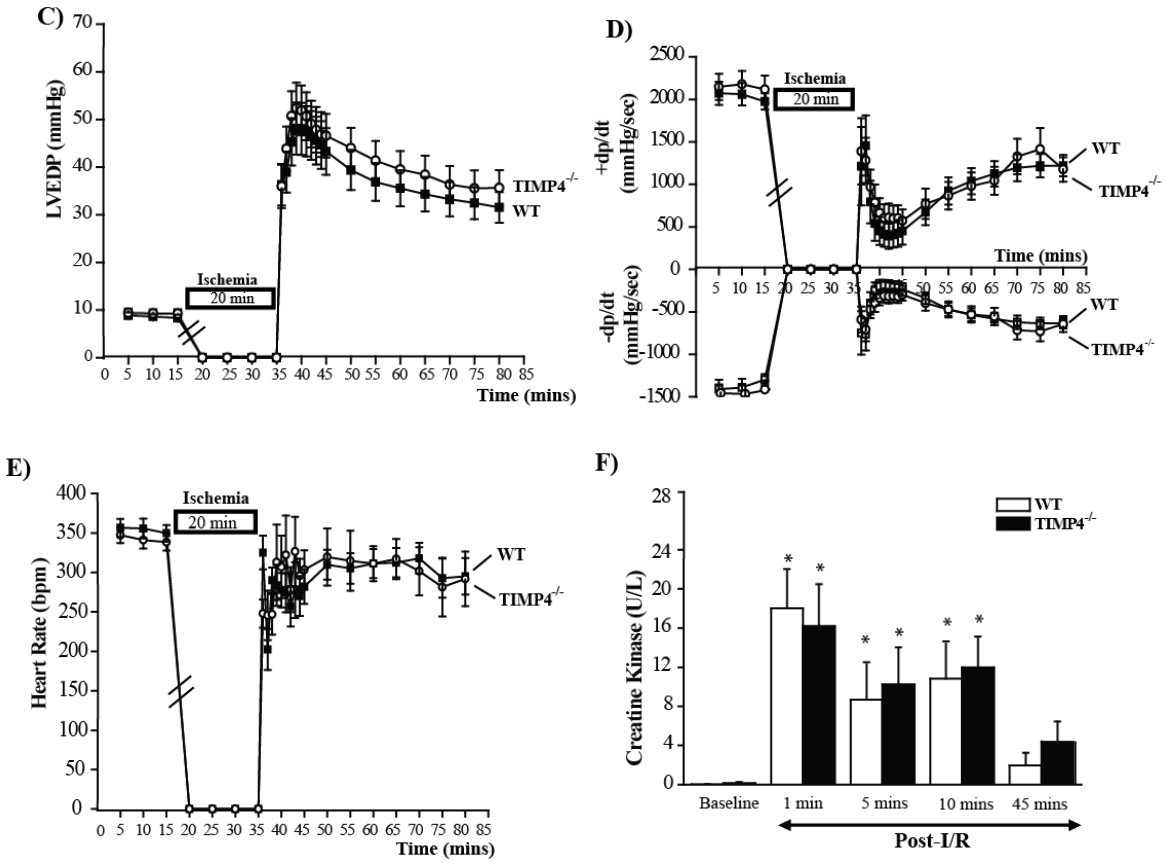

Figure 3.4.7: **TIMP4-deficiency does not impair cardiac recovery following acute ischemia-reperfusion injury *ex vivo***. (**A-D)** Parameters of cardiac function after 20 minutes of ischemia and 45 minutes of reperfusion, **(A)**left ventricular developed pressure (LVDP), **(B)** LV end-systolic pressure (LVESP), **(C)** LV end-diastolic pressure (LVEDP), **(D)** the rate of contraction and relaxation (±dP/dt), and **(E)** heart rate in WT and TIMP4$^{-/-}$ hearts (n=12/genotype). **(F)** Creatine kinase levels in the heart perfusate before ischemia (baseline) and at different times during reperfusion, n=7/genotype. *p<0.05 compared with corresponding baseline.

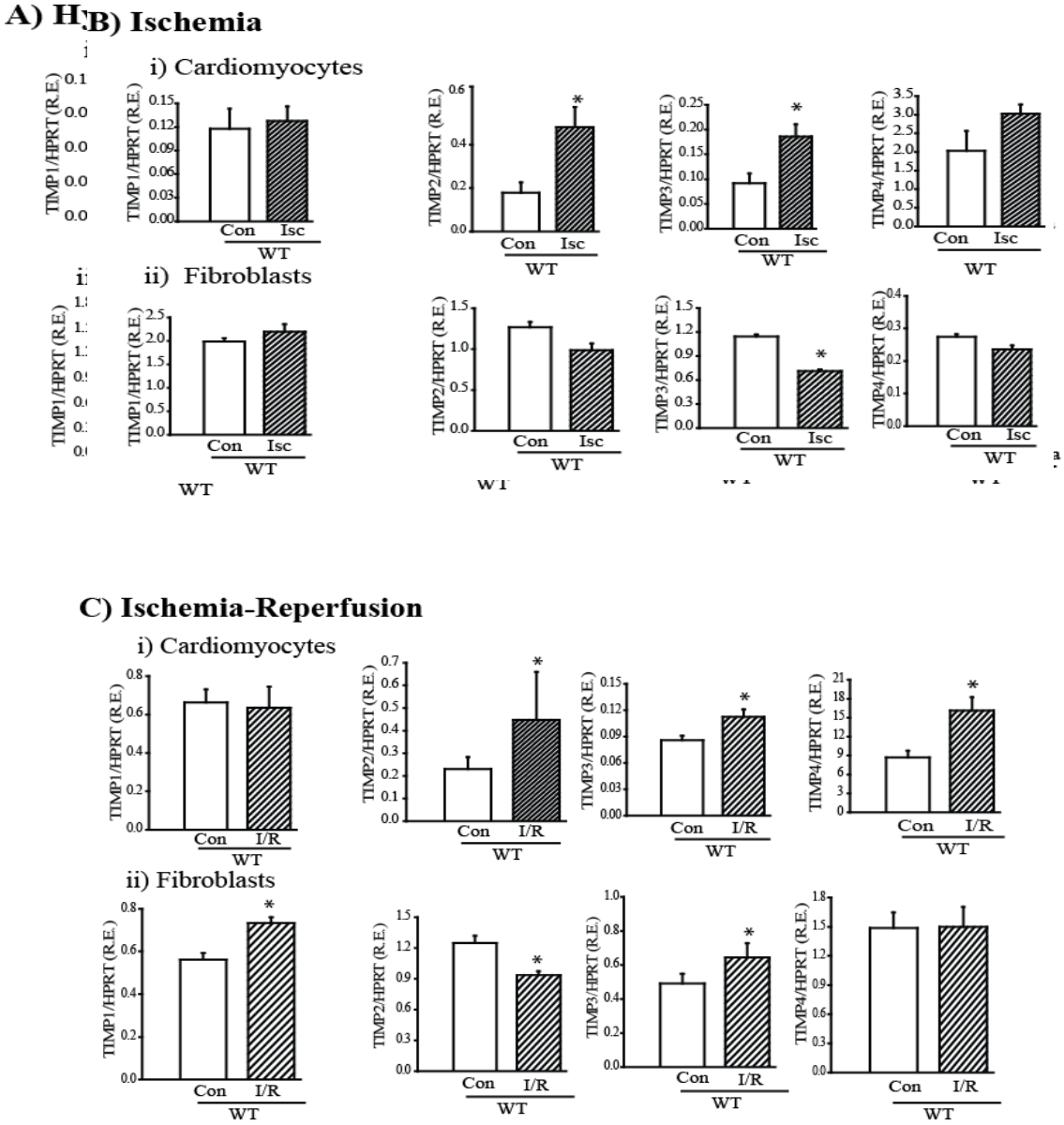

Figure 3.4.8: Expression of TIMPs in the cultured (wildtype) adult cardiomyocytes and fibroblasts *in vitro* under different conditions. **(A)** Hypoxia (24hours) **(B)** Ischemia (24hours) **(C)** Ischemia-Reperfusion (6hours/24 hours). *p<0.05 compared with control. n=2 independent cultures, 3 plates/group/experiments.

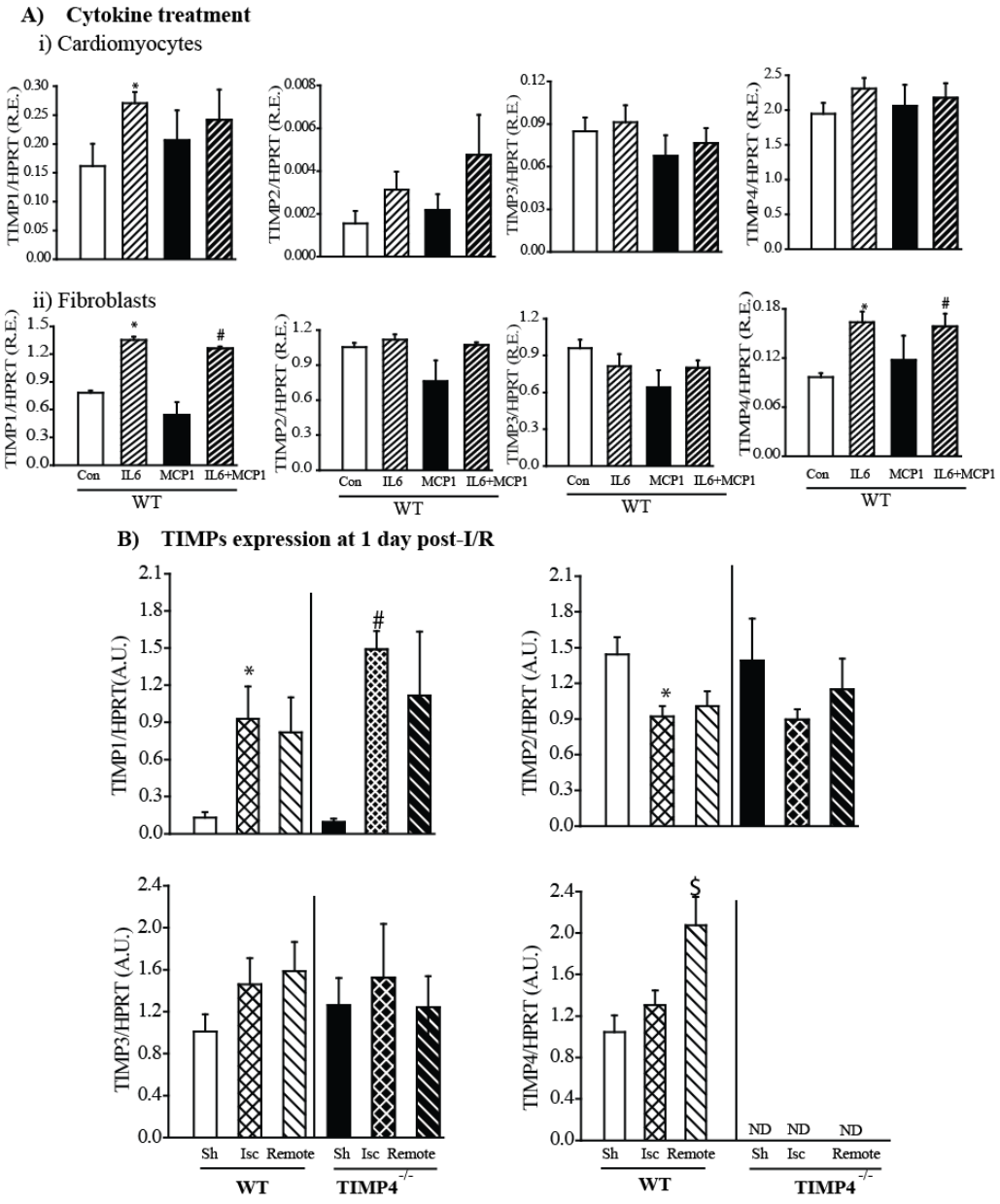

Figure 3.4.9: Expression of TIMPs with different treatments: (A) mRNA expression of TIMPs in cultured wildtype cardiomyocytes and fibroblasts treated with cytokines, interleukin-6, monocyte chemotactic protein-1 or both for 24 hours. *p<0.05 compared with saline- treated control group. **(B)** mRNA expression of TIMPs at 1day after I/R *in vivo* in sham, ischemic and remote myocardium. *p<0.05 compared with corresponding sham, #p<0.05 compared with corresponding WT group.

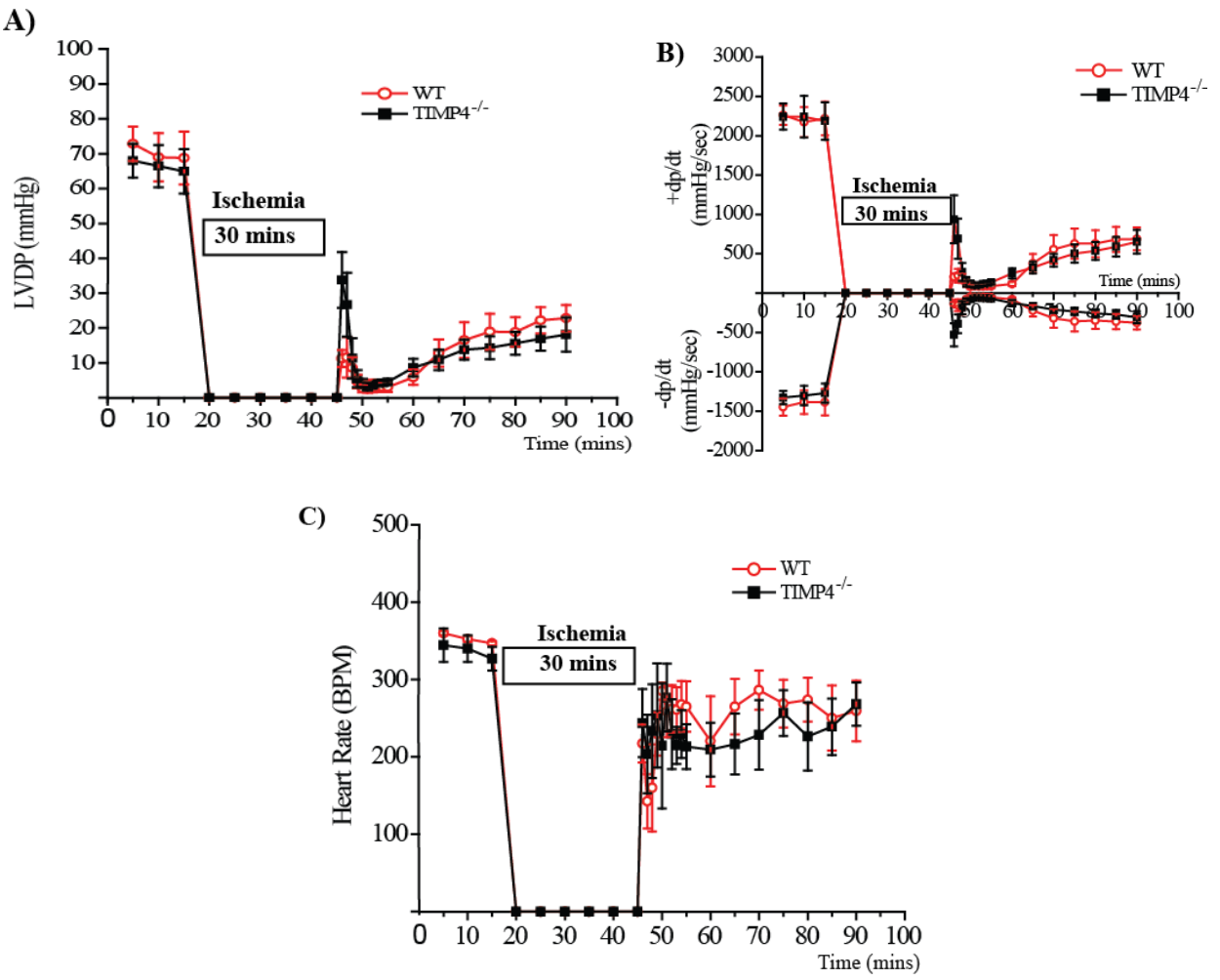

Figure 3.4.10: Recovery of WT and TIMP4$^{-/-}$ hearts from 30 minutes ischemia *ex vivo*: (A) Left ventricular developed pressure (LVDP mmHg). **(B)** Rate of contraction and relaxation (±dp/dt). **(C)** Heart rates were altered similarly in WT and TIMP4 deficient hearts after 30 minutes of ischemia, n=7-8/genotype.

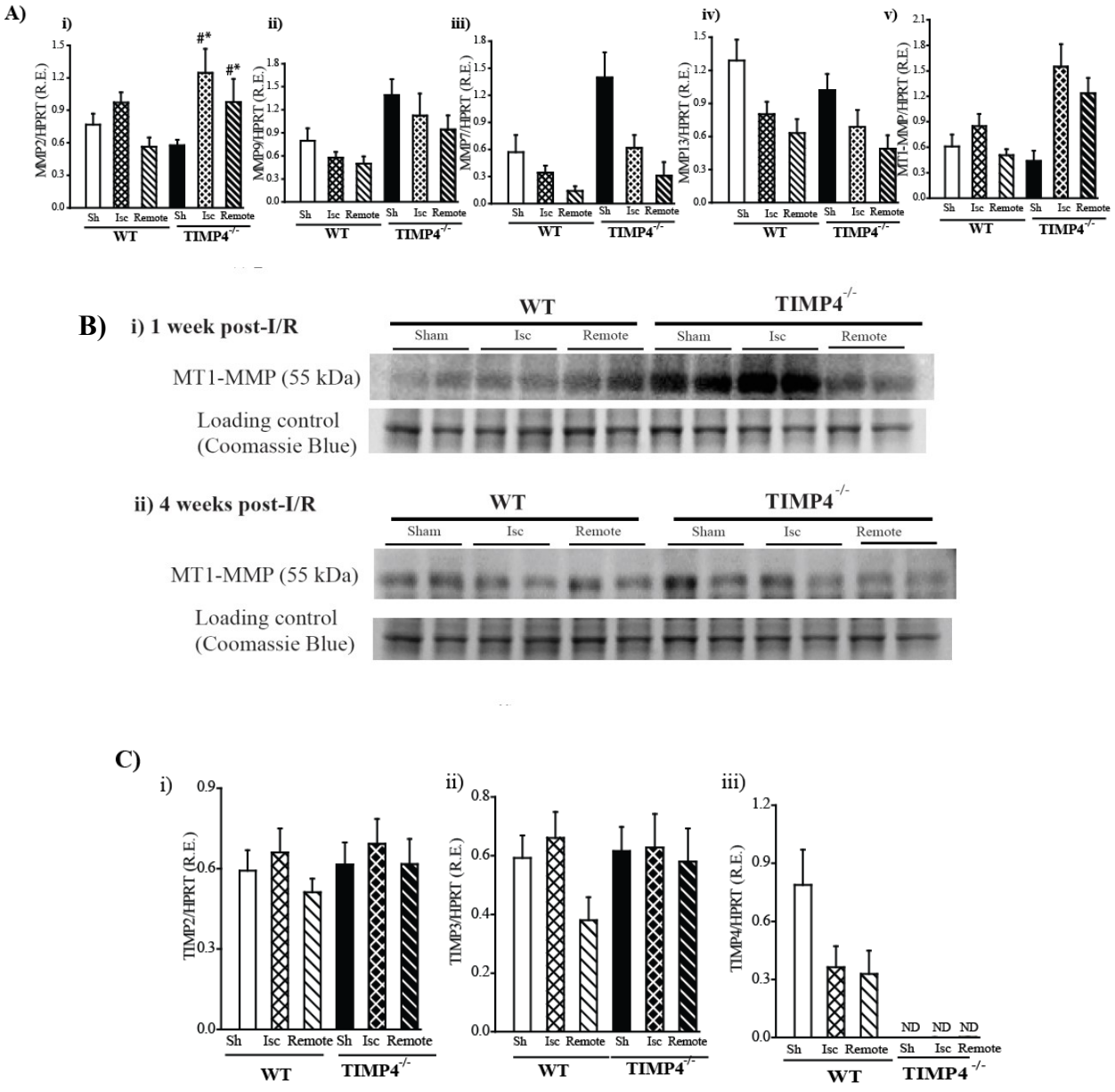

Figure 3.4.11: **TaqMan mRNA expression profile at 1-week post-I/R.** (A) Averaged mRNA levels of MMP2 **(i),** MMP9 **(ii),** MMP7 **(iii),** MMP13 **(iv),** MT1-MMP **(v**) in indicated region after 1 week of sham or I/R procedure. **(B)** MT1-MMP protein levels in membrane fraction of indicated groups at 1 week **(i)** and 4 weeks **(ii)** post-sham or I/R **(C)** Averaged mRNA expression for TIMP2 **(i)**, TIMP3 **(ii)** and TIMP4 **(iii)** at 1-week post-sham or I/R in indicated groups. *$p<0.05$ compared with corresponding sham; #$p<0.05$ compared with corresponding region in WT-I/R n=6/group/genotype.

3.5. Discussion

Adverse remodeling of the myocardial ECM post-I/R can impact cardiac function. Excess degradation of the ECM by MMPs is kept under control by their inhibitors, TIMPs. In patients, MMP/TIMP balance is altered in different cardiomyopathies.[135,320,324] Lack of TIMPs has been shown to impair cardiac response to pressure-overload[207,209] and myocardial infarction in murine models.[203,204,206,209] Among TIMPs, TIMP4 shows a tissue-specific expression pattern predominantly in the heart and brain,[106] and is an effective biomarker for LV diastolic dysfunction in patients.[325]

We found that while TIMP4 mRNA was elevated at 1 day post-I/R in WT myocardium, by 1 week post-I/R its protein and mRNA levels were reduced in the ischemic myocardium which corresponded to diastolic dysfunction and adverse remodeling. Similarly, ischemic (non-infarct) myocardium from MI patients showed decreased TIMP4 levels. Since lack of TIMP4 in our model led to a far more severe diastolic dysfunction and adverse structural remodeling post-I/R, we propose that the initial increase in TIMP4 levels early post-I/R is a compensatory attempt by the myocardium to overcome the I/R-induced injury, while a combination of acute and chronic events lead to the subsequent decline in TIMP4 levels, and structural and functional impairments by 1 week post-I/R. Intriguingly, in WT mice, TIMP4 levels recovered by 4 weeks post-I/R which corresponded with normalization of MT1-MMP activity and amelioration of the cardiac dysfunction in these mice. While factors such as hypoxia[158] and cytokines[159] have been reported to regulate TIMP4 expression, our findings reveal that a combination of factors could underlie this process which will require further investigation to be unravelled.

With longer ischemic periods (30 min) *in vivo*, WT mice additionally developed systolic dysfunction although less severe than that in TIMP4$^{-/-}$ mice. However, in order to investigate the adverse outcomes of diastolic dysfunction in the absence of systolic dysfunction, and to explore the underlying cellular and molecular mechanism of I/R injury in the absence of myocardial infarction which would ensue with longer ischemic periods, we performed the *in vivo* experiments with 20 minutes ischemia followed by reperfusion.

The inhibitory function of TIMP4 against MT1-MMP underlies the adverse myocardial remodeling and LV dysfunction in these mice. Consistent with our findings, reduced TIMP4 levels in the ischemic porcine myocardium correlated with elevated MT1-MMP levels and activity.[321,

[326] MT1-MMP is anchored to the cell membrane, unlike other MMPs that are secreted to the extracellular space, therefore capable of coordinating the extracellular signals with cellular responses. In addition to its proteolytic function, the cytosolic tail of MT1-MMP has been reported to induce signaling pathways such as ERK.[327] which can contribute to myocardial I/R injury.[300] MT1-MMP over-expression triggered myocardial fibrosis and adverse myocardial remodeling with poor outcomes post-MI,[328] Moreover, MT1-MMP can activate the latent TGFβ and trigger tissue fibrosis,[232,328-329] can activate a number of pro-MMPs, such as MMP2[113] and MMP13,[330] and has been associated with oxidative stress in the myocardium[331] and ROS production.[332]

In TIMP4-deficient mice TIMP1, but not TIMP2 or TIMP3, was markedly elevated post-I/R. TIMP1 has been strongly linked to fibrosis in multiple organs,[287,333-334] as well as to myocardial diastolic dysfunction in different cardiomyopathies.[335-336] As such, the elevated TIMP1 in TIMP4$^{-/-}$-I/R hearts is consistent with enhanced myocardial fibrosis and the diastolic dysfunction in these mice. In addition, TIMP1 is the only TIMP that does not inhibit the membrane-type MMPs (MT-MMPs) as shown in this study and by others,[337] and therefore unable to compensate for the lack of TIMP4 in inhibiting MT1-MMP post-I/R. TIMP4-deficiency did not impact the myocardial recovery following acute I/R *ex vivo*, indicating that TIMP4-deficiency does not increase the susceptibility of cardiomyocyte to acute I/R injury. Therefore, the observed dysfunction and remodeling in TIMP4$^{-/-}$-I/R mice *in vivo* is primarily through the cellular and molecular events, and the subsequent chronic myocardial and ECM remodeling.

The findings from this study demonstrate that TIMP4 is a critical factor in myocardial recovery from I/R injury and variations in myocardial TIMP4 is likely a critical determinant of disease progression. The post-I/R reduction in TIMP4 levels indeed mediates the subsequent diastolic dysfunction which over time culminates in a more severe diastolic dysfunction with systolic dysfunction.

3.6. Conclusion

TIMP4 is one of the four TIMPs that regulates the extracellular matrix. TIMP4 is unique among TIMPs shows highest expression in the heart than other organs. Myocardial ischemic injury is either unpredictable (during heart attack) or inevitable (in the operating room) and can cause perturbations of the myocardial extracellular matrix. Also, it is now understood that patients with

ischemic cardiomyopathy have normal preserved ejection fraction but diastolic function are compromised.[338, 339] Therefore, in order to improve diastolic properties of myocardium and improve extracellular matrix functions, TIMP4 delivery during ischemic cardiomyopathy could serve as a potential therapy.

CHAPTER 4

THERAPEUTIC POTENTIAL OF TIMPs IN MYOCARDIAL INFARCTION

MYOCARDIAL REPLENISHMENT OF TIMP3 FOLLOWING MYOCARDIAL INFARCTION EXERTS BENEFICIAL EFFECTS THROUGH PROMOTING ANGIOGENESIS AND SUPPRESSING EARLY PROTEOLYSIS

Abhijit Takawale[1,3], Pu Zhang[1,3], Abul Azad[2], Wang Wang[1,3], Xiuhua Wang[1,3], Allan G. Murray[2], Zamaneh Kassiri[1,3]

[1]Department of Physiology, [2]Department of Medicine, Faculty of Medicine and Dentistry, [3]Mazankowski Alberta Heart Institute, University of Alberta, Edmonton, AB, Canada.

Contributions:

AT: Generated hypothesis, experimental design, analyzed functional data using echocardiography, performed all immunostaining experiments for inflammatory cells, CD31, Lectin staining, WGA + Phalloidin co-staining, Picrosirius red staining, planned surgeries, cared for and monitored animals, collected tissues post-surgeries at different time points, extracted proteins for WBs and activity assays. AT had primary role in interpreting results, writing manuscript, and preparing figures.

PZ: Performed the angiogenesis experiments (3D spherical sprouting assay) using human umbilical vein (HUVEC) and coronary (HCEAC) cell lines, captured images at different time points for angiogenesis, Performed immunoprecipitation experiment for TIMP3 and VEGFR2.

AA: Helped with setting up *in vitro* angiogenesis assay.

WW: Helped in lectin injection for *in vivo* angiogenesis experiments.

XW: Performed LAD ligation surgeries and intramyocardial adenovirus injections, performed WB for hTIMP3, and the gelatinase activity assay.

AGM: Provided HUVEC cell line and input for *in vitro* angiogenesis studies.

ZK: Supervisor of AT, Overall project planning and corresponding author.

A version of this manuscript has been submitted to American Journal of Physiology-Heart and Circulatory Physiology. This chapter has been modified from manuscript submitted to AJP Heart Circ. Physiology.

4.1. Introduction

Coronary artery disease and ischemic cardiomyopathy are the major cause of systolic heart failure, and among the leading causes of morbidity and mortality worldwide. [3, 340-341] Myocardial infarction occurs secondary to interruption of coronary blood flow, resulting in loss of a significant number of cardiomyocytes which subsequently triggers a series of adverse events such as degradation of the existing myocardial extracellular matrix (ECM), inflammation, scar formation and expansion, left ventricular (LV) dilation, dysfunction and eventually heart failure. Due to advances in medical and surgical technology and the increased access to medical care, an increasing number of patients survive the heart attack, but later develop heart failure due to the subsequent adverse remodeling of the heart. Therefore, novel therapies to prevent adverse remodeling of the heart post-MI are necessary to prevent occurrence of heart failure.

While numerous factors contribute to post-MI remodeling, infarct expansion appears to be central to this process, and it is associated with continuous adverse turnover of the ECM in the myocardium surrounding the initial infarct site (peri-infarct region), resulting in LV wall thinning, loss of structural support and LV dilation. A family of enzymes that mediate ECM turnover are matrix metalloproteinases (MMPs) whose activity is kept in check by their physiological inhibitors, tissue inhibitor of metalloproteinases (TIMPs). [135] An imbalance in the MMP-TIMP axis can disrupt ECM integrity in disease. [79, 274] A correlation between plasma MMP and TIMP profiles and LV remodeling has been reported in patients post-MI.[342] Activation of MMPs early post-MI has been shown to be a critical contributor to post-MI LV remodeling in animal models [203, 204, 206] and in post-MI rupture in patients.[343] However, a clinical trial of MMP inhibitor treatment in MI patients did not show beneficial effects [278] although that clinical trial was not without limitations.[344] Therefore, new therapeutic approaches needed to control post-MI remodeling in heart failure patients.

4.2. Objective and Rationale

In the mouse model of myocardial infarction, TIMP3 deficiency causes exacerbation of systolic as well as diastolic dysfunction[206] while TIMP4 deficiency results in increased LV rupture rate.[209] Among the four TIMPs, TIMP3 is highly expressed in the heart. Its levels decrease markedly shortly post-MI in animal models [206] and in heart failure patients with ischemic

cardiomyopathy.[284] TIMP3 deficiency results in dilated cardiomyopathy with aging [205], exacerbates LV dilation and dysfunction, and increases rate of LV rupture post-MI. [206,345]. TIMP4 is highly expressed in the heart than other organs[106] and it is beneficial for myocardial post-I/R recovery. Post-MI remodeling of the LV is spatiotemporal, hence local delivery or targeting of potential players in this process could prove to be beneficial.[346-347] Therefore, we studied therapeutic potential of TIMP3 and TIMP4 in post-MI remodeling using a adenovirus-mediated gene delivery approach.

4.3. Methods

4.3.1. Experimental animals and *in vivo* model of myocardial infarction

WT male mice of 8-10 weeks of age were subjected to myocardial infarction by permanent left anterior descending artery (LAD) ligation as before.[204,303] Following LAD ligation, adenovirus containing human TIMP3 (Ad-hTIMP3) and human TIMP4 (Ad-hTIMP4) and control adenovirus (Ad-null) were injected in peri-infarct regions at five different spots (5.54×10^7, 5µl/spot) as described in sections 2.2.5 above.

At 3 days, 1 week and 4 weeks post-MI, hearts were excised and flash frozen in OCT medium or were fixed in 10% formalin and processed for immunohistochemical analyses or separated into infarct, peri-infarct and non-infarct regions and flash frozen for molecular work.

4.3.2 Cardiac function assessment

Cardiac systolic, and diastolic function and structure were assessed by noninvasive transthoracic echocardiography as described using Vevo 3100.[303-304] Modified parasternal long axis EKV analyses using Simpson's method were used to measure EF, FS, systolic and diastolic volume. Detailed methods are described in section 2.4.1.

4.3.3 Histochemical and immunostaining analysis

Hearts were arrested in diastole using 1M KCl, and fixed in 10% formalin, paraffin embedded and processed for trichrome and PSR staining as mentioned before.[204, 206, 304] For infarct size assessment, 5 µm sections were stained with WGA and phalloidin as described in section 2.8.2. At 3 days post-MI, hearts were collected in OCT medium and stained for neutrophil and

macrophages to assess inflammation using Ly6 (Serotac, MCA771GA) and CD68 (Serotac, MCA1957GA) as markers, respectively as described in sections 2.9.1.

4.3.4 Lectin immunofluorescence assay, CD31 and Ki67 staining

Microvascular density was assessed in Ad-null, and Ad-hTIMP3, groups using lectin immunofluorescence assay (FL1081, Vector labs) and CD31 staining (BD bioscience, BD550274) [299, 303] as described in sections above 2.10.5. CD31 and Ki67staining were performed to assess coronary endothelial cells and endothelial proliferation on OCT sections as described above sections 2.9.4., 2.9.5.

4.3.5 *In vitro* angiogenesis assay

Concentration-response relationship for recombinant TIMP3 (rTIMP3) was studied using human umbilical (HUVEC) and human coronary artery endothelial cells (HCAEC). The detailed methods are described in sections 2.7 above.

4.3.6 Immunoprecipitation for VEGFR2 and TIMP3

The immunoprecipitation of VEGFR2 and different concentrations of TIMP3 from endothelial cells was performed as described in sections 2.10.2.

4.3. Results

4.4.1 Adenoviral delivery of hTIMP3 but not hTIMP4 improved heart function at 1 week post-MI

We first examined how TIMP levels are altered early post-MI. Western blotting for the four TIMPs showed that within 24 hours of LAD ligation, TIMP1 and TIMP2 protein levels increased, whereas TIMP3 levels decreased markedly in the infarct and peri-infarct myocardium, while TIMP4 levels decreased primarily in the infarct area **(Figure 4.4.1)**. Given the drastic reduction of TIMP3 within 24 hours of MI, we investigated if preventing this early reduction could improve post-MI remodeling and cardiac function. TIMP3 was replenished in the peri-infarct myocardium by intramyocardial injection of replication-deficient adenovirus that express human TIMP3 (hTIMP3), while a blank adenovirus construct (Ad-Null) was used as parallel control. This

increased the TIMP3 protein levels in the infarct and peri-infarct regions **(Figure 4.4.1**B; antibody recognizes both human and mouse TIMP3), and mRNA for human TIMP3 was detected in the infarct, peri and non-infarcted myocardium **(Figure 4.4.1C)**.

After 1 week of MI, Ad-hTIMP3-injected group showed a smaller infarct expansion compared with the Ad-Null hearts **(Figure 4.4.2A.)**. In Ad-Null group, myocardial infarction resulted in LV systolic dysfunction (reduced ejection fraction, fractional shortening, increased WMSI), LV dilation (increased LV systolic and diastolic volume and diameter), and enlarged left atrial size **(Figure. 4.4.2C, Table 4.1)**. Ad-hTIMP3 injections (5.5 x10^7 pfu/heart) partially preserved LV function and contractility (EF, WMSI), ameliorated LV dilation (LV volume and diameter), reduced LA enlargement, and improved some parameters of diastolic function (E- and E'-waves) **(Figure. 4.4.2 C, Table 1)**. Consistent with these findings, mRNA expression of cardiac disease markers, β-myosin heavy chain (β-MHC), brain natriuretic peptide (BNP) and α-skeletal actin (α-SKA) were markedly elevated in Ad-Null-MI compared with the sham group, whereas this rise was hampered in Ad-hTIMP3-MI hearts particularly in the peri-infarct myocardium **(Figure 4.4.2D)**.

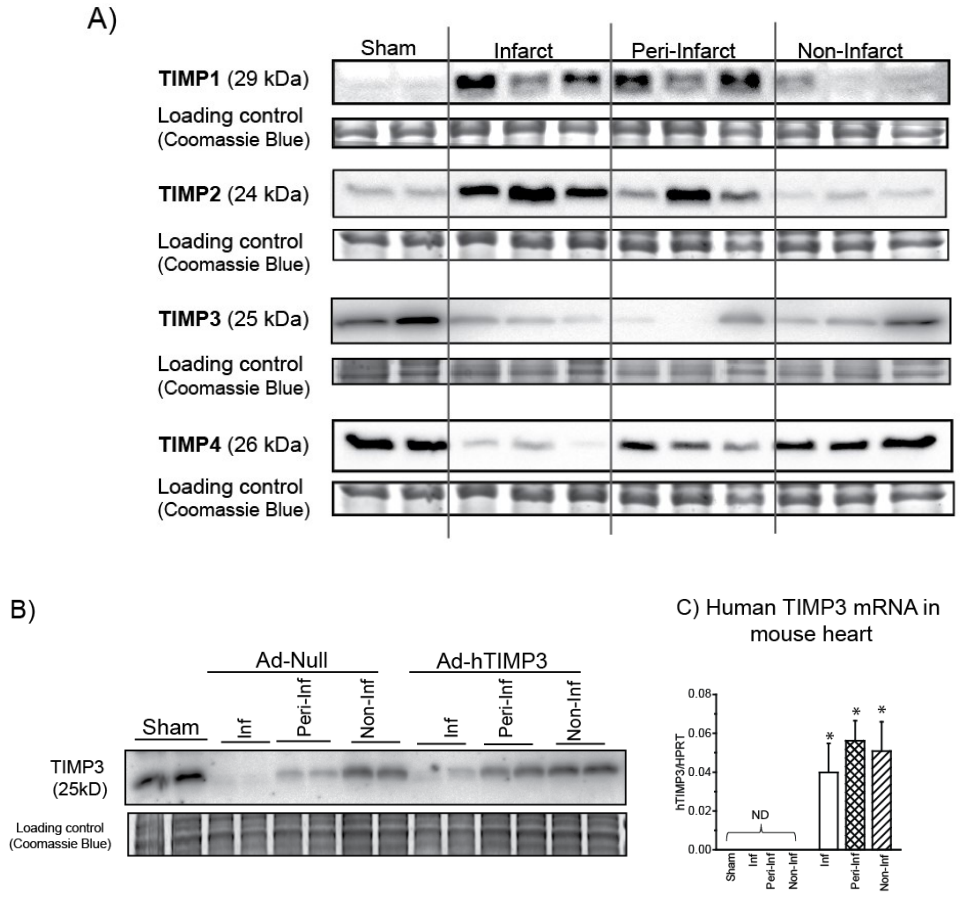

Figure 4.4.1: Protein levels for tissue inhibitors of matrix metalloproteinases (TIMPs) post-MI. (A) Protein levels of TIMPs 1-day following myocardial infarction (infarct, peri-infarct and non-infarct regions) or sham operation. Coomassie blue-stained gel visualizes total protein as loading control. **(B)** Representative Western blots showing TIMP3 protein levels in the infarct, peri- and non-infarct regions in Ad-null and Ad-hTIMP3-injected hearts compared with sham (2days post-MI). The TIMP3 antibody recognizes mouse and human proteins. **(C)** mRNA levels for human TIMP3 in the indicated groups (n=5/group). ND=not detectable. Averaged data represent mean± SEM. *p<0.05 compared with the corresponding region in Ad-Null group.

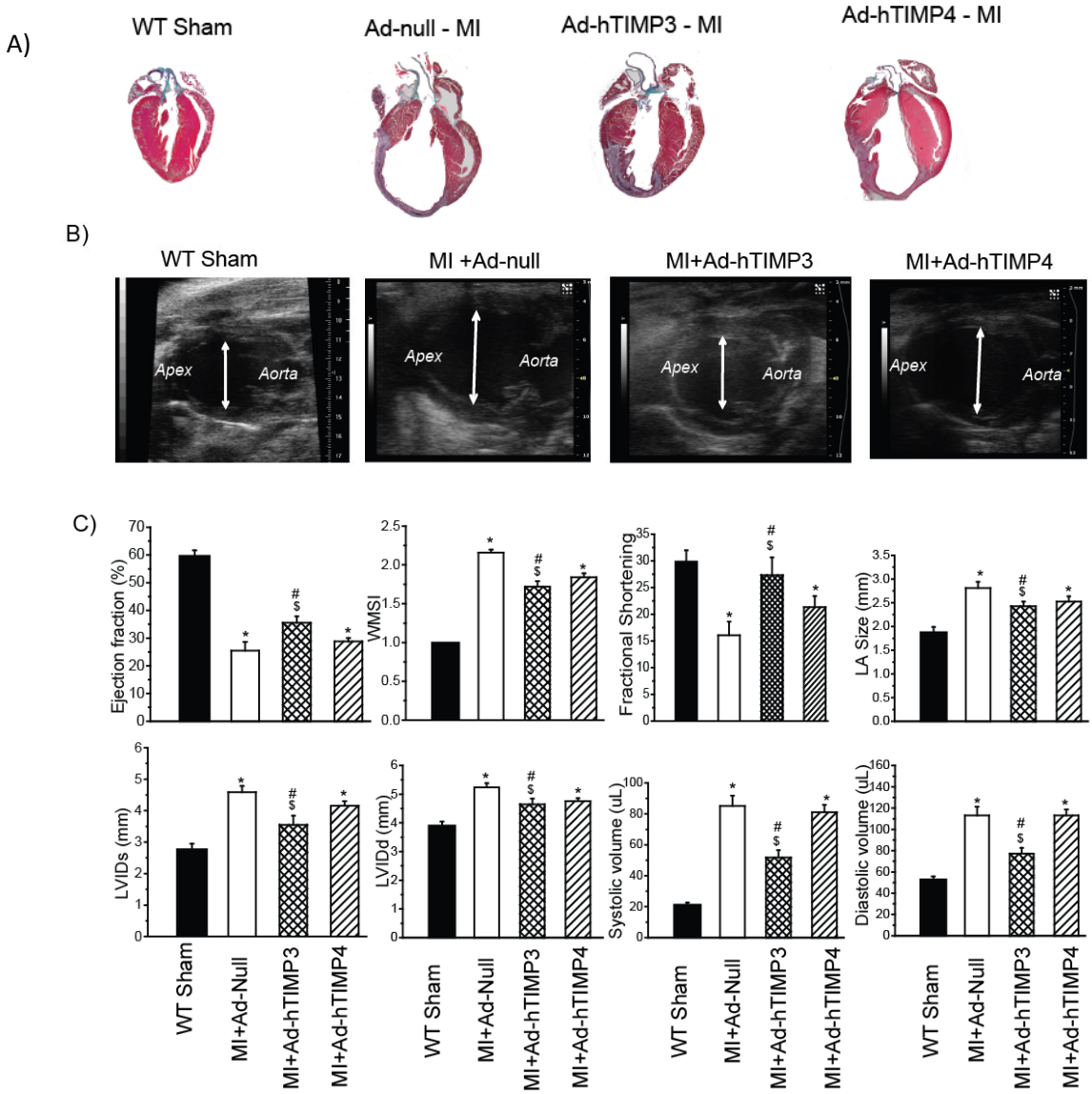

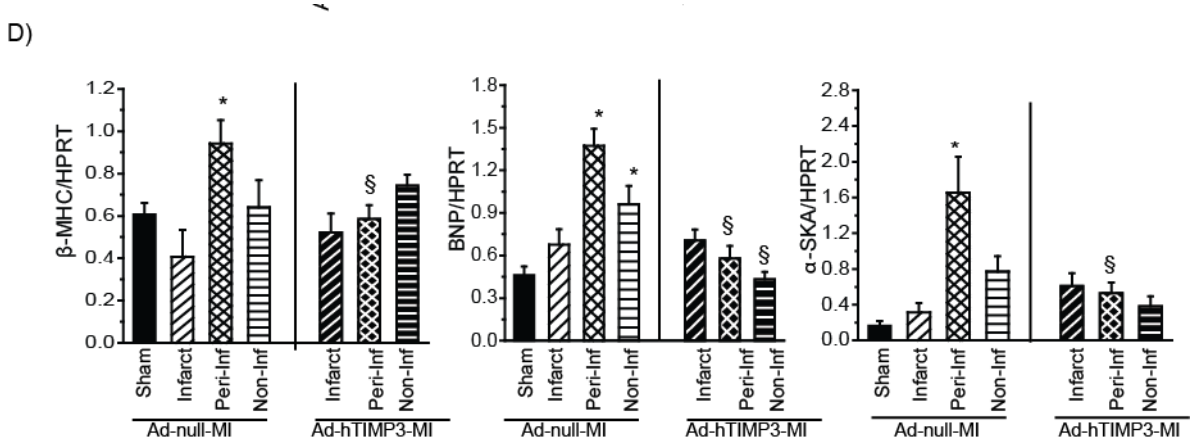

Figure 4.4.2:TIMP3 but not TIMP4 replenishment improves LV structure and function at 1-week post-MI. **(A)** Representative trichrome stained cross sections of hearts from sham, Ad-Null-MI, Ad-hTIMP3-MI, Ad-hTIMP4-MI groups. **(B)** Representative B-mode images from sham, Ad-null-MI, Ad-hTIMP3-MI and Ad-hTIMP4-MI group at 1-week post-sham/MI. **(C)** Averaged parameters for cardiac function, ejection fraction **(i)**, Wall Motion Score Index (WMSI, **(ii)**, and cardiac structure, LV systolic volume **(iii)**, LV internal diameter during diastole (LVIDd, **(iv)** and left atrial size **(v)** assessed using echocardiography (n=8/sham, 15/Ad-Null-MI, 18/Ad-hTIMP3-MI/ Ad-hTIMP4-MI). **(D)** Disease markers β-myosin heavy chain (β-MHC), brain natriuretic peptide (BNP) and α-skeletal actin (α-SKA) in indicated groups and regions (n=6/sham; 8-10/Ad-Null-MI and Ad-TIMP3-MI). Averaged data represents mean ±SEM. *$p<0.05$ compared with sham, § $p<0.05$ compared with the corresponding region in the Ad-null-MI group.

Parameters	Sham	Ad-null-MI	Ad-hTIMP3MI	Ad-null -MI	Ad-hTIMP3-MI
		Low dose		High dose	
n	7	15	18	8	8
HR (bpm)	450 ± 21	426 ± 24	453 ± 39	497± 13	445±21
E-wave (mm/s)	658.6± 58.2	451.8±29.2	587.1±16.2 *	310.6±19.8	397.3±44.1*
E'(mm/s)	33.3± 5.2	14.3±1.1	20.0±2.1 *	12.4±2.2	12.5±2.9
E/E'	28.0±1.6	33.3±2.8	34.5±3.1	29.9±5.3	38.5±7.9*
A' (mm/s)	25.7±4.5	19.6± 1.8	20.93±1.3	19.1±1.0	17.4±2.4
IVRT (ms)	11.8± 0.7	23.5 ±1.4	20.4±0.9	18.9±2.1	18.1±1.9
DT (ms)	12.2± 3.6	25.4±2.1	24.01±2.4	16.6±0.9	17.5±1.2 §
LVEF (%)	59.7± 2.0	25.4± 2.2	35.4± 2.5 *	21.4±4.7	26.3±4.4 §
LA size	1.8±0.10	2.8±0.10	1.7±0.08 *	2.61±0.13	2.16±0.14 §
WMSI	1.00±0.00	2.1±0.06	1.7±0.08 *	2.23±0.07	2.21±0.11§
LV Systolic Vol (µL)	21.5± 1.3	85.1±6.7	51.7± 5.4 *	98.9±13.7	88.2±11.6 §
LV Diastolic Vol. (µL)	52.8± 2.9	112.9±7.0	77.0± 6.2 *	117.3±13.5	117.9±9.9 §
LVID-D (mm)	3.9± 0.1	5.2±0.1	4.64±0.2 *	5.44±0.2	5.33±0.4
LVID-S (mm)	2.77± 0.2	4.5±0.1	3.55±0.3*	5.17±0.3	4.9±0.4 §
LVPW-S (mm)	1.05± 0.01	0.84±0.01	1.10± 0.06 *	0.76±0.08	0.89±0.18
LVPW-D (mm)	0.67±0.06	0.71±0.03	0.82±0.03	0.66±0.05	0.70±0.11

Table 4.1: Echocardiographic parameters of cardiac function and structure in mice. 1 week following sham-operation or following myocardial infarction, receiving Ad-Null or Ad-hTIMP3 at a low dose ($5.5x10^7$ pfu/heart) or a high dose ($5.5x10^8$ pfu/mL)

HR-Heart rate; E-wave= early transmitral inflow velocity; E'= Early tissue Doppler velocity; A'= Tissue Doppler velocity due to atrial contraction. E/E'=Ratio of early transmitral inflow velocity to early tissue Doppler velocity, LVEF= Left ventricular ejection fraction; IVRT=Isovolumic relaxation time; DT=deceleration time; WMSI= wall motion score index; LVID-D= LV internal diameter at the end of diastole; LVID-S= LV internal diameter at the end of systole; LVPW-S= LV posterior wall thickness at the end of systole; LVPW-D= LV posterior wall thickness at the end of diastole. *$p<0.05$ compared with corresponding Ad-Null group. § $p<0.05$ compared with corresponding low dose group.

4.4.2 Ad-hTIMP3 delivery partially preserves the infarcted myocardium

Next, we assessed how TIMP3 replenishment affected the infarct tissue remodeling at 1-week post-MI. We used picrosirius red (PSR) staining to visualize the fibrotic scar and fibrillar collagen deposition, Wheat Germ Agglutinin (WGA) and phalloidin co-staining to identify viable cardiomyocytes **(Figure 4.4.3)**. Compared with the Ad-Null-injected hearts, thinning of the infarcted myocardium was less in Ad-hTIMP3-injected hearts **(Figure 4.4.3. A, low magnification)**, exhibiting less collagen deposition and more preserved peri-cellular collagen arrangements **(Figure 4.4.3A)**. Similarly, less collagen deposition was observed in the peri-infarct region in hTIMP3-injected hearts **(Figure 4.4.3A)**. To determine if this reduced ECM remodeling was associated with preserved myocyte viability, we used WGA and phalloidin co-staining to visualize cell membrane and contractile proteins in viable cardiomyocytes, respectively. We found a higher density of viable cardiomyocytes in the infarct and peri-infarct regions in Ad-hTIMP3-injected hearts at 1-week post-MI **(Figure 4.4.3B)**. These results indicate that TIMP3 replenishment partially preserves the ECM and myocardial remodeling post-MI.

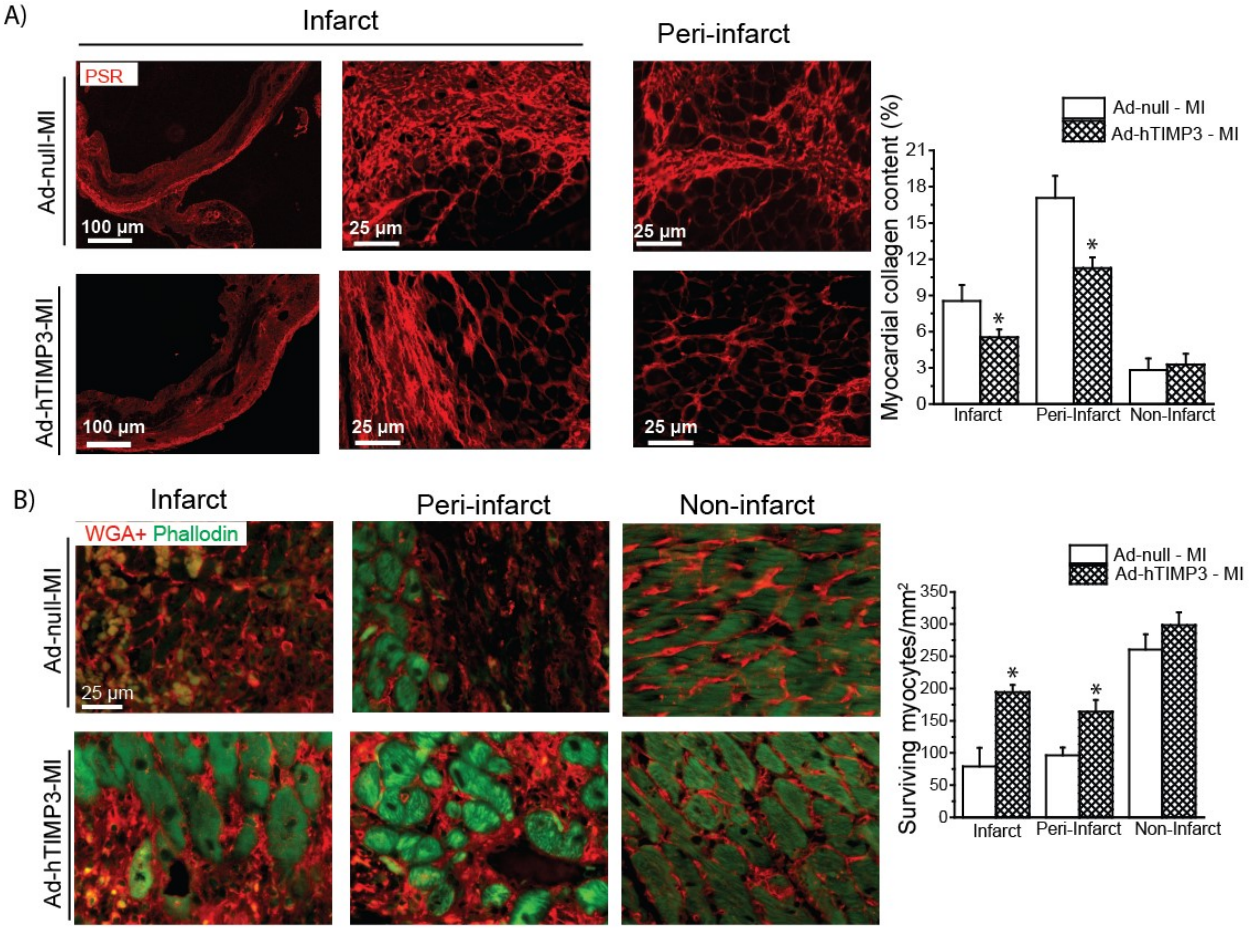

Figure 4.4.3: Ad-hTIMP3 delivery improves post-MI remodeling at 1-week post-MI. (A) PSR-stained images of the infarct (at two different magnifications) and peri-infarct regions in Ad-Null- or Ad-hTIMP3-injected hearts at 1-week post-MI. **(B)** Cardiomyocyte membrane and actin visualized by wheat Germ Agglutinin (WGA, red) and FITC-labeled phalloidin (green), respectively, in infarct, peri-infarct and non-infarct regions of Ad-Null or Ad-TIMP3-injected hearts at 1-week post-MI.

4.4.3. Injection of hTIMP3 at physiological level suppresses early proteinase activity, and promotes angiogenesis but did not alter inflammation post-MI

TIMP3 is best known as a broad-spectrum MMP inhibitor [135]. We found that TIMP3 levels are markedly reduced in the infarct and peri-infarcted myocardium early post-MI (Fig. 1A) which coincides with a significant rise in total proteinase (gelatinase and collagenase) activities early post-MI **(Figure. 4.3.4A)**. Replenishment of TIMP3 suppressed this early rise in total gelatinase and collagenase activities in Ad-TIMP3-MI compared with Ad-Null-MI group **(Figure 4.3.4B)**.

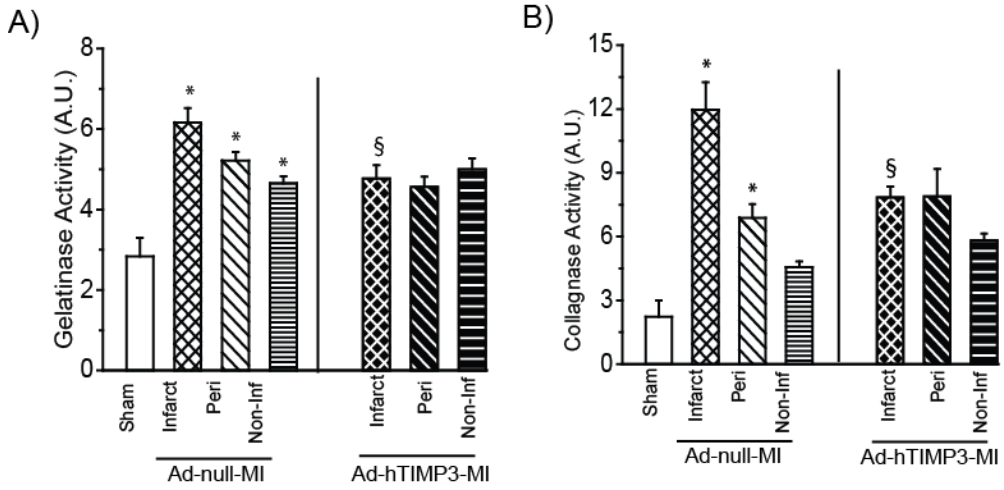

Figure 4.4.4: **Ad-hTIMP3 delivery significantly reduced proteolytic activities early post-MI.** Total **(A)**gelatinase (n=5-6/group) and **(B)** collagenase activities (n=5-6/group) (Enzcheck fluorescent-based assay) in sham, Ad-null (inf, peri and non-infarct) and Ad-hTIMP3 (inf, peri-infarct and non-infarct) groups at 2 days post-MI. *$p<0.05$ compared with sham, § $p<0.05$ compared with the corresponding region in the Ad-null-MI group.

Angiogenesis and inflammation are critical in post-MI repair and remodeling. Reduced angiogenesis due to decreased coronary density and impaired collateral network can impair LV function and promote structural deterioration. [348-349] Since we observed a greater number of viable myocytes in the infarct region of Ad-hTIMP3-MI compared with Ad-Null-MI group **(Figure 4.4.5)**, we investigated if this could be associated with preserved cardiac micro vessel density or formation of new collateral coronaries. *In vivo* injection of FITC-labeled lectin **(Figure 4.4.5)** and CD31 staining of fixed hearts to visualize endothelial cells **(Figure 4.4.3.B)** showed a higher density of coronaries in the infarct and peri-infarct regions of Ad-hTIMP3 compared with Ad-Null hearts at 1 week post-MI **(Figure 4.4.5.B)**. At 3 days post-MI, during the early stages of angiogenesis and neovascularization, co-staining for Ki67 (marker of cell proliferation) and CD31 (endothelial cells) revealed a higher number of replicating endothelial cells in the infarct and peri-infarct regions of Ad-hTIMP3-injected compared with Ad-Null-injected hearts at 3 days post-MI **(Figure 4.4.5.B)** while by 1 week post-MI endothelial proliferation in the infarct regions was quiescent in both groups (data not shown). These data collectively suggest that TIMP3 replenishment can promote angiogenesis and preserve the cardiac microvasculature early post-MI.

Inflammation is another early response and a determinant of tissue repair and remodeling post-MI. Staining for neutrophils (Ly6; **Figure 4.4.5C**) and macrophages (CD68; **Figure 4.4.5.C**) at 3 days post-MI, the peak of inflammatory response, showed that TIMP3injection to physiological level did not alter the severity of the inflammatory response and similar abundance of neutrophils and macrophages were detected in the infarct and peri-infarct regions of both groups **(Figure 4.4.6)**

A) 1 week post-MI

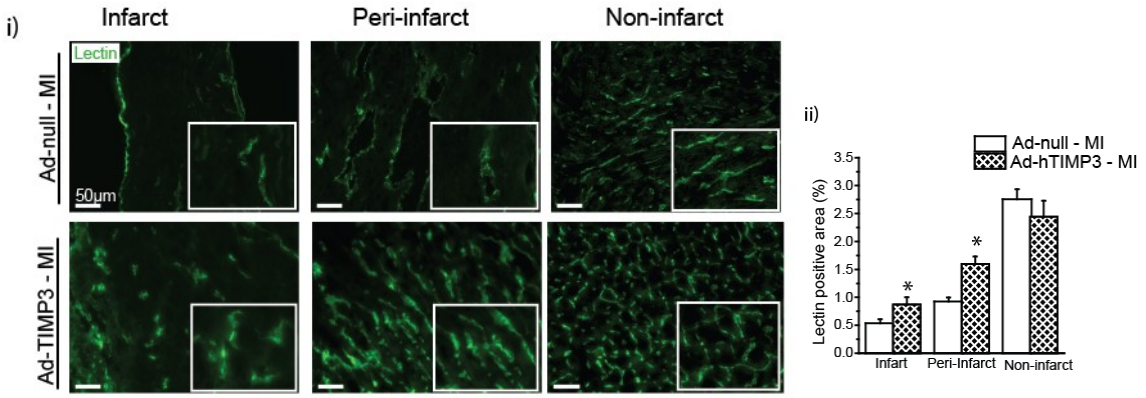

B) 1 week post-MI

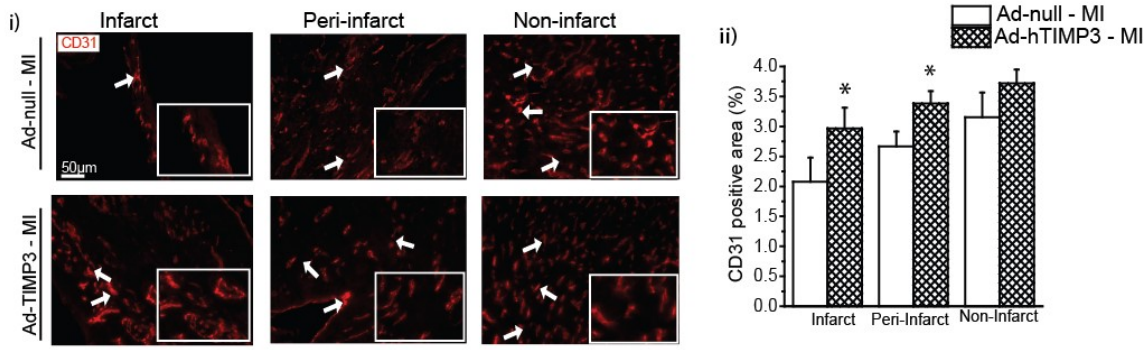

C) 3 days post-MI

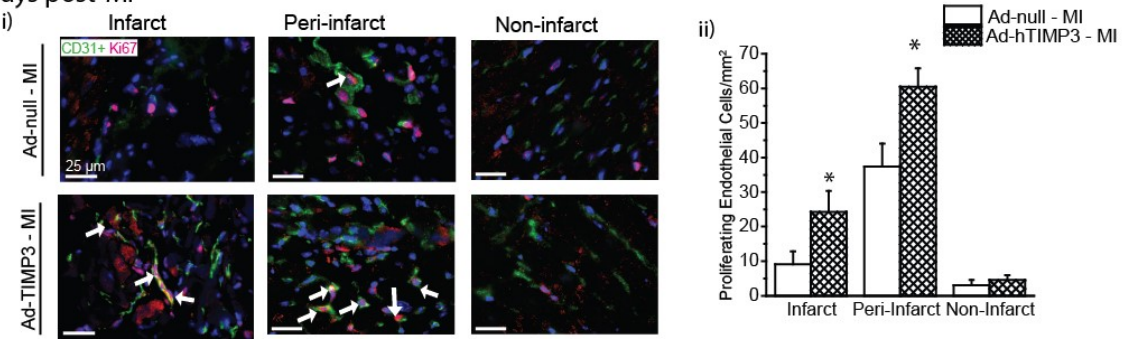

Figure 4.4.5: Ad-hTIMP3 promoted angiogenesis and endothelial proliferation post-MI.
(A) Representative images **(i)** and averaged quantification **(ii)** of *in situ* assessment of vascular density in indicated regions of Ad-Null- and Ad-hTIMP3-injected hearts at 1 week post-MI. **(B)** Coronary microvasculature density further confirmed by immuno-staining for CD31 and fluorescence microscopy in the indicated myocardial region of Ad-null- and Ad-hTIMP3-injected hearts at 1 week post-MI. **(C)** Representative images **(i)** and averaged quantification **(ii)** of co-staining for CD31 (endothelial cells) and Ki67 (marker of proliferation) at 3 days post-MI in indicated groups and myocardial regions. Averaged data represents Mean±SEM. n=4-5 hearts/group, 12-20 images/heart. *p<0.05 compared with the corresponding region Ad-Null-MI group.

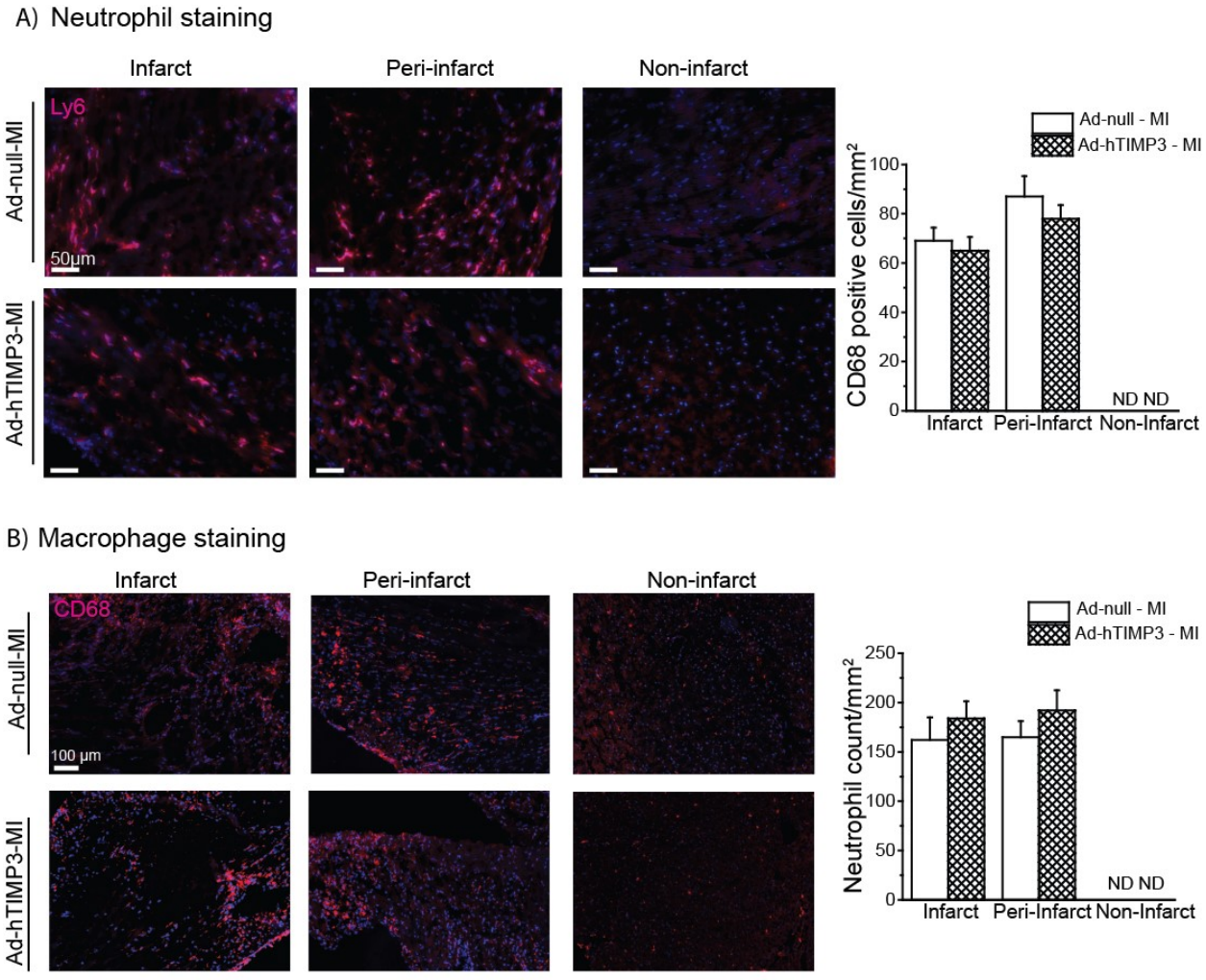

Figure 4.4.6: **Adenoviral delivery of hTIMP3 did not alter inflammation post-MI infarction.** Immunofluorescent staining for neutrophils (Ly6 antibody) **(A)**, and macrophages (CD68 antibody) **(B)** at 3 days post-MI in the indicated regions for each group.

4.4.4. TIMP3 promotes angiogenesis *in vitro* in a biphasic and concentration-dependent manner

To examine the pro-angiogenic effects of TIMP3 directly, we used an established *in vitro* model of angiogenesis using human endothelial cells and the 3-dimentional spheroid assay to investigate how TIMP3 affects endothelial sprout formation as before [312]. Treatment of human coronary artery endothelial cells (HCAEC; **Figure. 4.4.7.A**) and human umbilical vein endothelial cells (HUVEC; **Figure 4.4.7 B**) showed a bi-phasic angiogenic response to an increasing concentration of recombinant TIMP3 (rTIMP3). At lower concentrations, rTIMP3 enhanced the number **(Figure 4.4.7Aii)** and the length of endothelial sprouts **(Figure 4.4.7Aiii)** peaking at 100 ng/mL rTIMP3. However, a higher concentration of rTIMP3 showed a negative impact on sprout formation at 1000 ng/mL in HCAEC **(Figure 4.4.7.A)** and HUVEC **(Figure 4.4.7.B)**.

It has been reported that TIMP3 exerts anti-angiogenic effects by binding to and blocking VEGFR2 [350]. Hence, we examined if rTIMP3 binds to VEGFR2 at any of the concentrations that we used in our *in vitro* study. Co-immunoprecipitation experiments revealed a concentration-dependent interaction between TIMP3 and VEGFR2, with a marked interaction at the highest rTIMP3 concentration (1000 ng/mL) which corresponded to the anti-angiogenic (reduced length and number of sprouts) in endothelial cells **(Figure 4.4.7C)**. Therefore, TIMP3 promotes endothelial sprouting at lower concentrations, but can have anti-angiogenic effects when present in excess.

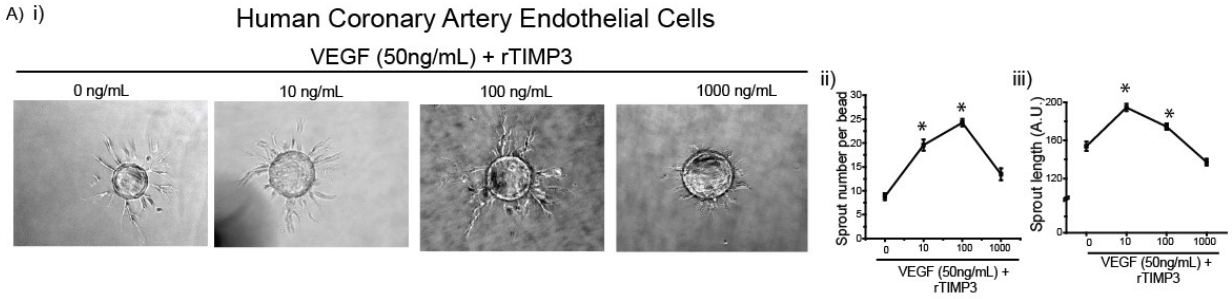

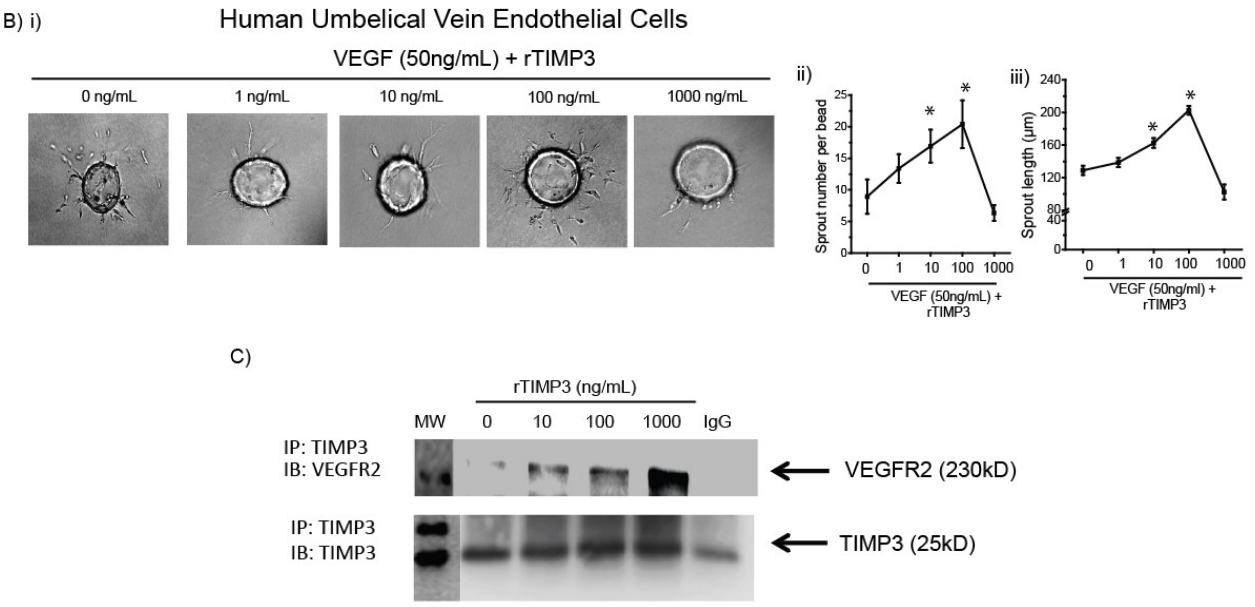

Figure 4.4.7: TIMP3 promotes angiogensis in a concentration dependent manner. (A) i) Representative images of 3D endothelial sprouting spheroid assay in human coronary artery endothelial cells (HCEAC) or human umbilical vein endothelial cells (HUVEC) **(Bi)** in response to increasing concentrations of recombinant TIMP3. **(A-B)** Averaged number of sprouts (ii) and sprout length **(iii)**, n=15-20 spheroid/group. **(C)** Co-immunoprecipitation for TIMP3 and VEGFR2 from HUVEC for different concentrations of rTIMP3 and the immunoblot for TIMP3 showing even loading in all groups. Averaged data represents Mean ±SEM. *p<0.05 compared with baseline.

4.4.5: Intramyocardial injection of a higher dose of Ad-hTIMP3 exacerbated post-MI LV remodeling and dysfunction

Since we observed that the impact of TIMP3 on angiogenesis is biphasic in a concentration-dependent manner with anti-angiogenic effects at excess levels, we investigated if this observation would apply to post-MI remodeling *in vivo*. A 10-fold higher dose of Ad-hTIMP3 (5.54×10^8 pfu/heart) was injected in the peri-infarct myocardium post-MI, and LV structure and function was assessed after 1 week. We found that this higher dose of Ad-hTIMP3 resulted in no improvement in cardiac function (ejection fraction, WMSI), structure (LV systolic or diastolic volume and diameters) or LA size at 1 week post-MI compared with the parallel high dose Ad-Null injected hearts. compared with the parallel high dose Ad-Null injected hearts **(Figure 4.4.8.A)**. PSR staining revealed similar thinning of the infarct area and collagen deposition in high dose Ad-

hTIMP3 and Ad-Null injected groups indicating no beneficial impact following overexpression of TIMP3 at a higher dose **(Figure 4.4.8.B)**.

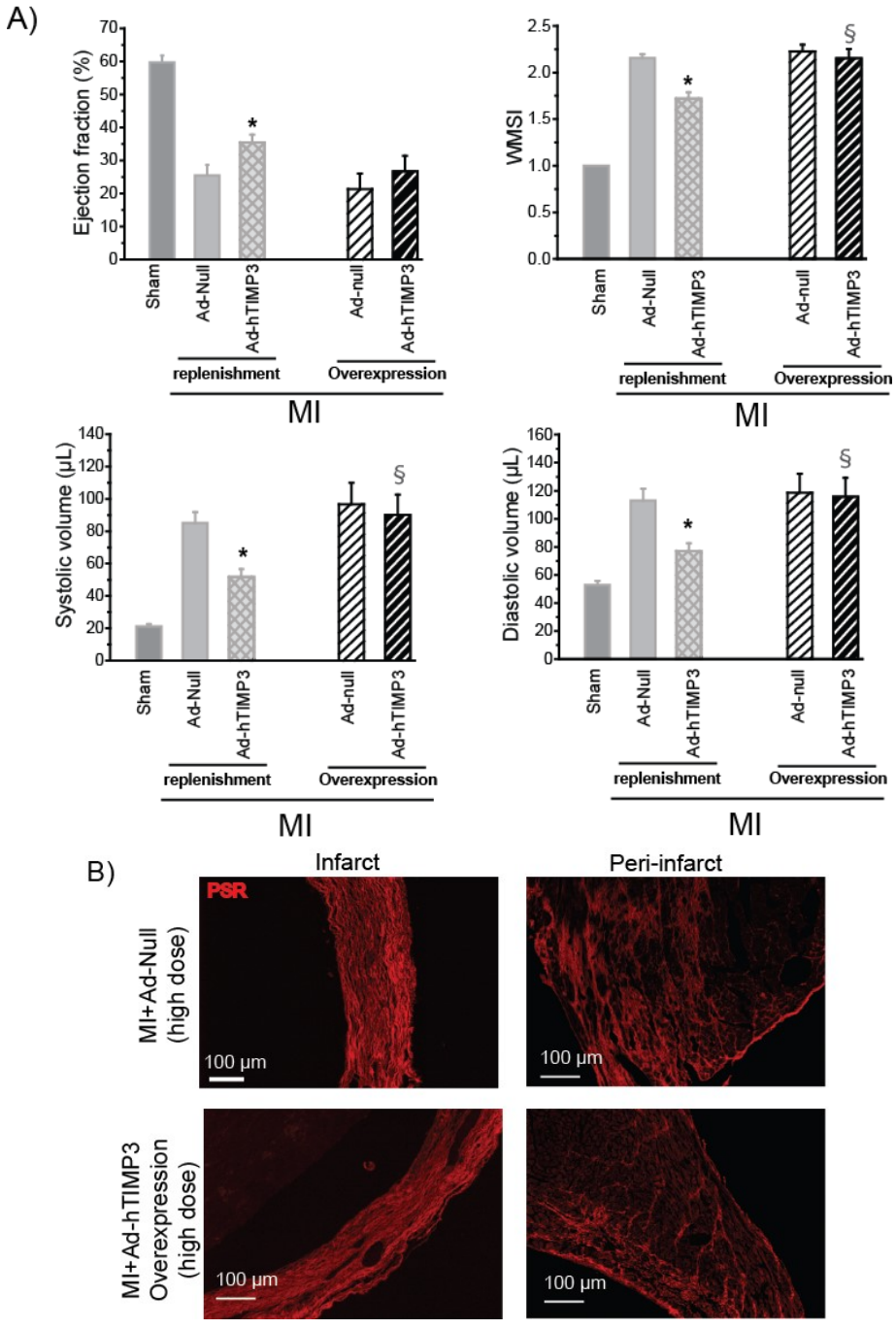

Figure 4.4.8: **Overexpression of hTIMP3 adversely affects post-MI recovery**. (**A)** Averaged cardiac function parameters in mice receiving a high dose of Ad-hTIMP3/Null (overexpression) compared with sham, and lower dose of Ad-hTIMP3/Null (replenishment) assessed by

echocardiography at 1 week post-MI: Ejection fraction, wall motion score index (WMSI), systolic LV volume, and diastolic LV. n= 8/group. **(B)** PSR-staining showing the remodeling in the infarct and peri-infarct regions after 1 week of TIMP3 overexpression (at high dose). Averaged data represents mean ± SEM. *p<0.05 compared with corresponding Ad-Null, § p<0.05 compared with the corresponding low dose Ad-hTIMP3/Null (replenishment). The data from sham and replenishment group are also shown in Figure 2, and therefore are presented here faded grey.

4.5. Discussion

Myocardial remodeling following MI is a complex process. It involves a number of cellular and extracellular events that collectively lead to altered LV architecture and impaired function. Infarct expansion results from continuous adverse ECM remodeling and myocyte loss leading to weakened structural support, LV wall thinning and dilation. The MMP-TIMP balance is essential in regulating ECM turnover and overall integrity, while MMPs and TIMPs can also have ECM-independent functions.[60,283,351-352] MMP levels and activities peak shortly (1day) after the onset of MI and are an important contributor to initial ECM degradation, infarct formation and expansion [206, 274]. Collateral coronary neovascularization or angiogenesis is another factor that can promote cardiomyocyte survival and limit infarct expansion.[353-354] In this study, we observed that between hTIMP3 and hTIMP4, intramyocardial delivery of hTIMP4 did not exert significant beneficial effect while hTIMP3 improved cardiac function at 1-week post-MI. We found that TIMP3 replenishment suppresses the early rise in proteinase activities and promotes angiogenesis post-MI thereby improving heart function and structure.

Traditionally, TIMPs are believed to be anti-angiogenic through inhibiting MMPs and preventing ECM degradation to accommodate neovascularization. In addition, a study by Qi *et al*[350]. reported that TIMP3 is anti-angiogenic through binding to VEGFR2 and preventing its interaction with its ligand, VEGF (vascular endothelial growth factor).[350] However, we found that the impact of TIMP3 on angiogenesis is biphasic in a dose-dependent manner. TIMP3 promotes endothelial cell sprouting at lower concentrations, but not at higher concentrations (>100 ng/mL). In the study by Qi *et al.* [350] TIMP3 was used at very high concentrations (>1000 ng/mL) which are well beyond the physiological levels of TIMP3. We similarly observed that very high levels of TIMP3 have adverse effects on angiogenesis *in vitro*, and in post-MI recovery *in vivo*. This

highlights the importance of achieving a physiological balance in TIMP3 levels as a therapeutic approach rather than an uncontrolled overexpression of this protein.

4.6. Conclusion

Injection of hTIMP3 to physiological level post-MI could provide beneficial effects by preventing early proteolysis and promoting angiogenesis post-MI while overexpression of TIMP3 beyond physiological concentration will exacerbate post-MI remodeling by inhibiting angiogenesis.

CHAPTER 5

ROLE OF TIMP1 IN CARDIAC FIBROSIS

TISSUE INHIBITOR OF MATRIX METALLOPROTEINASE-1 (TIMP1) PROMOTES MYOCARDIAL FIBROSIS BY MEDIATING CD63-INTEGRINβ1 INTERACTION

Abhijit Takawale, MSc[1,3]; Pu Zhang, Msc[1,3]; Vaibhav B. Patel, PhD[2,3]; Xiuhua Wang, PhD[1,3]; Gavin Oudit MD, PhD[1,2,3]; Zamaneh Kassiri, PhD*[1,3]

[1]Department of Physiology, [2]Department of Medicine/Division of Cardiology, [3]Cardiovascular Research Center, Mazankowski Alberta Heart Institute, University of Alberta, Edmonton, Alberta, Canada

Contributions:

AT: Generated hypothesis, experimental design, and performed TAC surgery, analyzed functional data using echocardiography, performed all immunostaining experiments such as integrinβ1, CD63, WGA staining, PSR staining on mouse as well as human heart samples, proximity ligation assay, analysed PV loop data, planned surgeries, cared for and monitored animals, collected tissues post-surgeries at different time-points, extracted proteins for western blots and activity assays. AT had primary role in interpreting results, writing manuscript, and preparing figures.

PZ: Performed all fibroblast culture experiments, immunostaining for fibroblast CD63 and integrinβ1, immunoprecipitation for integrinβ1 and CD63 in fibroblast and post-TAC, dilated cardiomyopathy samples, Scratch assay for fibroblasts, proximity ligation assay for integrinβ1 and CD63 interaction in fibroblasts.

VB: Performed PV loop experiments post-TAC

XW: Extracted protein for activity assay, WBs and performed all WBs, gelatinase activity assays, TaqMan for various genes.

GYO: Provided dilated cardiomyopathy patient samples, collaboration for PV loop experiments.

ZK: Supervisor of AT, overall project planning and corresponding author.

A version of this chapter is under revision for Hypertension. This chapter has been modified from manuscript submitted to Hypertension.

5.1. Introduction

Heart disease continues to be a major cause of morbidity and mortality worldwide. According to a recent report from American Heart Association, death due to cardiovascular diseases accounts for 1 in every 3 deaths in North America.[340] Fibrosis is a common feature of various cardiomyopathies including dilated and hypertrophic cardiomyopathy, and myocardial infarction, although the type of fibrosis differs in these diseases. Myocardial fibrosis in hypertrophic and dilated cardiomyopathy is 'reactive fibrosis', whereas fibrosis in myocardial infarction is 'reparative fibrosis' as it replaces the lost cardiomyocytes secondary to ischemia[79]. Reparative fibrosis in the infarcted myocardium is mediated by inflammatory cell influx[355], and transformation of fibroblasts to myofibroblasts[251,356] that rapidly populate the affected area, produce and deposit extracellular matrix (ECM), and form a fibrotic scar. The mechanism underlying reactive fibrosis is less explored as it occurs in the absence of cell (cardiomyocyte) loss. Fibrosis, regardless of its initiating cause, unfavourably alters cardiac structure and function, and can lead to heart failure.[101,357] Understanding the molecular mechanism underlying fibrosis is essential in developing effective therapies for heart failure patients.[198,358]

Fibrosis is the result of adverse remodeling and excess deposition of the ECM, primarily the fibrillar collagens type I and type III. Tissue inhibitors of metalloproteinases (TIMPs) maintain the homeostatic balance of myocardial ECM by inhibiting the activated matrix metalloproteinases (MMPs). Among the four TIMPs, TIMP2, TIMP3 and TIMP4 have been shown to contribute to myocardial fibrosis through different mechanisms[12,61,208,209,359], however the role of TIMP1 in this process has been less explored.

5.2. Objective and Rationale

TIMP1 is a well-known MMP inhibitor that can inhibit a number of MMPs except the membrane-bound MMPs (MT-MMPs).[79] Elevated tissue and plasma TIMP1 levels have been correlated with myocardial fibrosis and diastolic dysfunction[286,288,360], and TIMP1 has been used as a biomarker for fibrosis in patients and in animal models of heart disease.[361-362] Despite the consistent link between TIMP1 and fibrosis, it remains unknown whether TIMP1 directly promotes tissue fibrosis or if its rise is simply a by-stander alteration in this process. We investigated the role of TIMP1 in myocardial fibrosis in hypertrophic and dilated

cardiomyopathies, and whether its function is mediated through an MMP-dependent or MMP-independent mechanism.

5.3. Methods

5.3.1 Experimental animals and surgical procedures:

WT and TIMP1-deficient male mice ($TIMP1^{-/-}$) in C57BL/6 background, were subjected to pressure-overload by transverse aortic constriction or Ang II infusion as described in above sections 2.2.4 and 2.2.3 respectively.

At the indicated time-points in section 2.4, Figure D, hearts were excised, frozen in OCT medium, or formalin-fixed and processed for immunohistochemical analyses. Alternatively, hearts were excised and flash-frozen for molecular analyses.

5.3.2. Cardiac function assessment

Heart structure and function were assessed in sham and post- /TAC hearts non-invasively by transthoracic echocardiography using Vevo 3100 high resolution imaging system equipped with a 30-MHz transducer (Visual Sonics) as described in section 2.4.1. and cardiac function were assessed by PV loop as described in section 2.4.2.

5.3.3. Human explanted heart tissue

Heart tissues from heart failure patients were procured at the time of cardiac transplantation as described in detail above in section 2.3.

5.3.4. Histological and immunohistochemical staining and imaging

Freshly excised hearts were arrested in diastole (1M KCl) and fixed in 10% formalin, paraffin embedded and processed for trichrome, picrosirius red (PSR) as described above in section 2.8.1 and 2.8.2. and wheat glutamine staining (WGA) 2.8.3.[12, 60] OCT-frozen 5µm sections were used for immunostaining for CD63, integrinβ1. scleraxis and co-immunostaining of CD63 and integrinβ1 as described in above sections 2.9.2 and 2.9.3

5.3.5. Proximity ligation assay

Proximity ligation assay [296] detects a proximity of 40 nm or less between two molecules. PLA was performed on formalin-fixed heart sections, or on cultured adult cardiac fibroblasts, to detect physical proximity of integrinβ1 and CD63 using Duo link *in situ* fluorescence Sigma kit and PLA probes for mouse (DUO92004) and secondary, rabbit (DUO92002) as described detail in section 2.12.

5.3.6. RNA extraction and expression analysis

Total RNA was extracted from frozen heart tissues using Trizol reagent (Invitrogen) and mRNA expression analysis was performed by TaqMan RT-PCR as described in section 2.11.

5.3.7. Protein extraction, activity assay, Western blot, gelatin zymography and co-immunoprecipitation

Total protein was extracted and nuclear and cytosolic fractions were extracted as described in detail in sections 2.13.1 and 2.13.2. Fluorescent-based activity assays were performed using fluorescent-tagged gelatin (Enzcheck, Molecular Probes) to measure total gelatinase activity as described in sections 2.16.2. Protein quantification was performed as described in section 2.13 and then Western blots were performed as described in details above sections 2.14. For gelatin zymography, the detailed protocol described in sections 2.15 was used.

For co-immunoprecipitation (co-IP) experiments, protein extracts were prepared by homogenizing LV tissue (or $1X10^6$ fibroblasts) in 300 µL of IP lysis buffer (Thermo Scientific) and co-immunoprecipitation was performed as described in detail in section 2.10. 1.

5.3.8. Adult cardiac fibroblast (cFB) isolation and culture

Adult cFB were isolated from WT and TIMP1$^{-/-}$ mice as described in sections details above 2.6. Cells were then harvested for co-IP experiments, or fixed in 4% paraformaldehyde (PFA) for immunostaining and PLA assay[12,60]. These experiments were performed using protocol described in sections 2.5, 2.9.2, 2.10.1 and 2.12.

5.4. Results

5.4.1. Angiotensin II-mediated fibrosis is suppressed in TIMP1-deficient mice and not reversed by MMPi treatment

Ang II infusion triggered a significant increase in interstitial and perivascular fibrosis in WT mice, however, this fibrotic response was markedly suppressed in mice lacking TIMP1 **(Figure 5.1Ai-ii)**. A broad-spectrum MMP inhibitor (PD166793) did not increase myocardial fibrosis in TIMP1$^{-/-}$ mice, indicating that the reduced fibrosis in this group is not due too elevated MMP activities in the absence of TIMP1 **(Figure. 5.4.1Ai-ii)**.

Measurement of mRNA expression for collagen type I and collagen type III, the two main fibrillar collagens in the heart, showed a significant Ang II-induced rise in WT but not in TIMP1$^{-/-}$ mice **(Figure. 5.4.1B)**. Total gelatinase activity increased significantly but similarly in both genotypes following Ang II infusion **(Figure 5.4.1C)**. Gelatin zymography showed comparable levels of MMP2 and MMP9 in both genotypes **(Figure 5.4.1D)**. In addition, Ang II-induced myocardial hypertrophy assessed by heart weight-to-tibial length ratio, expression of molecular markers, atrial natriuretic peptide (ANP), brain natriuretic peptide (BNP), and α-skeletal actin, were comparable between the two genotypes **(Figure 5.4.8 Bi-iii)**. Ang II infusion also induced a marked increase in TIMP1 mRNA in WT mice, while mRNA expression of other TIMPs was comparable between the two genotypes **(Figure 5.4.8Ci-iv).** These data indicate that TIMP1-deficiency suppress the Ang II-mediated myocardial fibrosis but not hypertrophy, and this occurred independent of MMP mediated ECM degradation.

5.4.2. TIMP1-deficiency suppresses myocardial fibrosis following biomechanical stress by reducing collagen mRNA expression

We examined if the impact of TIMP1-deficiency on myocardial fibrosis applies to other models of heart disease. After 2 weeks of cardiac pressure-overload (TAC), significant interstitial and peri-vascular fibrosis was detected in WT mice, whereas this response was markedly suppressed in TIMP1$^{-/-}$ mice **(Figure 5.4.2Ai-ii)**. Similar to the Ang II model, mRNA expression of collagen type I and type III were markedly elevated in WT mice post-TAC but not in TIMP1-deficient mice **(Figure 5.4.2B)**, while the rise in total gelatinase activity was similar in both genotypes **(Figure 5.4.2C)**. Post-TAC myocardial hypertrophy was comparable between

genotypes **(Figure 5.4.8)**. mRNA expression of TIMP1 increased in WT mice post-TAC, while mRNA expression of other TIMPs remained comparable between the two genotypes **(Figure.5.4.9)**.

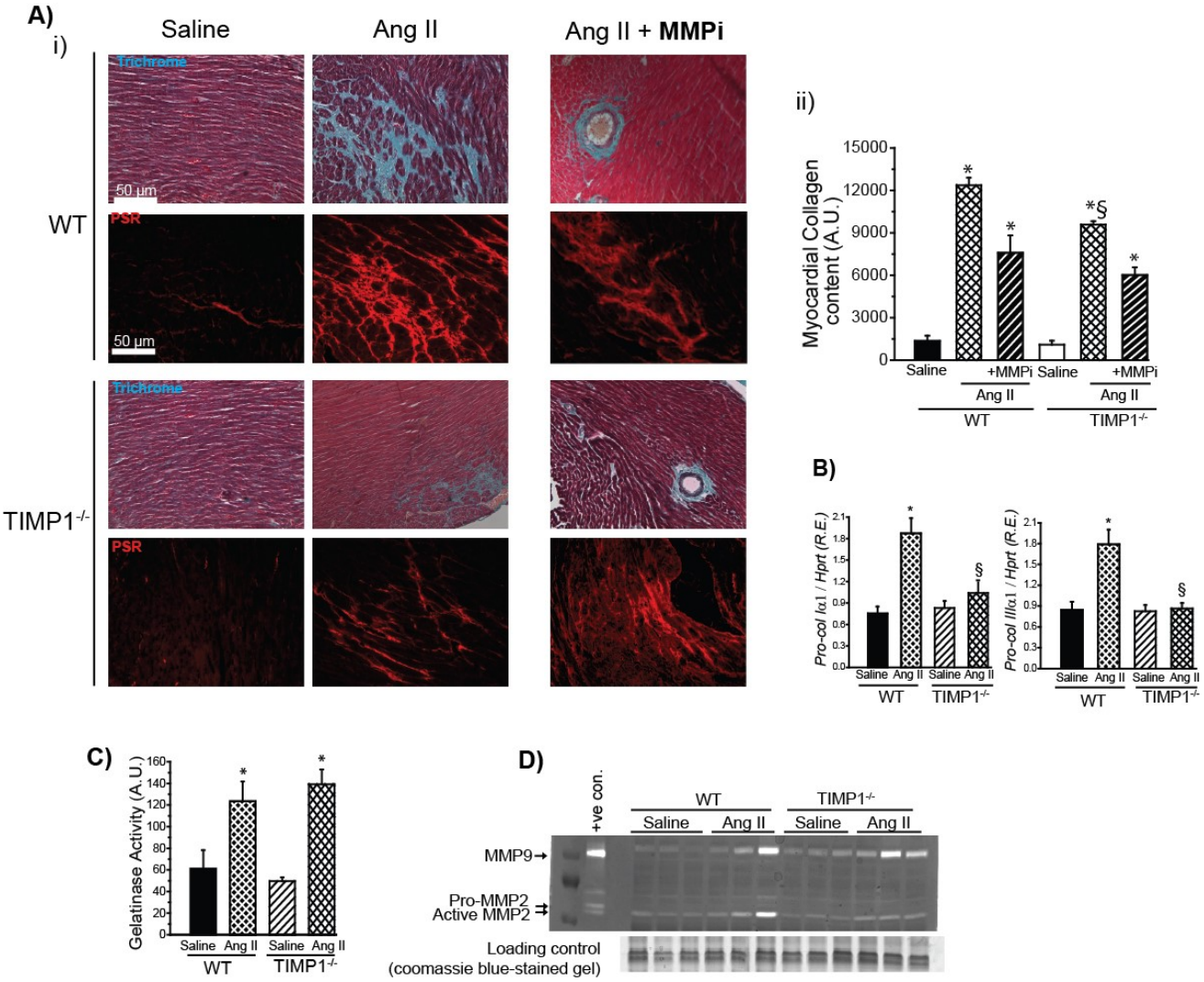

Figure 5.4.1: Angiotensin II-induced fibrosis is suppressed in TIMP1-deficient mice and not reversed by MMPi treatment. **(A) (i)** Representative Trichrome and PSR-stained images from WT and TIMP1$^{-/-}$ mice after 2 weeks of receiving saline, Ang II or AngII+MMP inhibitor (MMPi, PD166793) (4-5 hearts/group/genotype) **(ii)** Myocardial collagen content in indicated groups (n=10-15 images/heart; 4-5 hearts/group). **(B)** mRNA expression of pro-collagen Ia1 and pro-collagen IIIa1 in indicated groups (n=5-7/group). Total gelatinase activity (n=4-5/group) **(C)**, and gelatin zymography **(D)** in indicated groups. Averaged data represent Mean±SEM. A.U.=Arbitrary

Units; R.E.=Relative Expression. *p<0.05 compared with corresponding saline group, §p<0.05 compared with corresponding WT group.

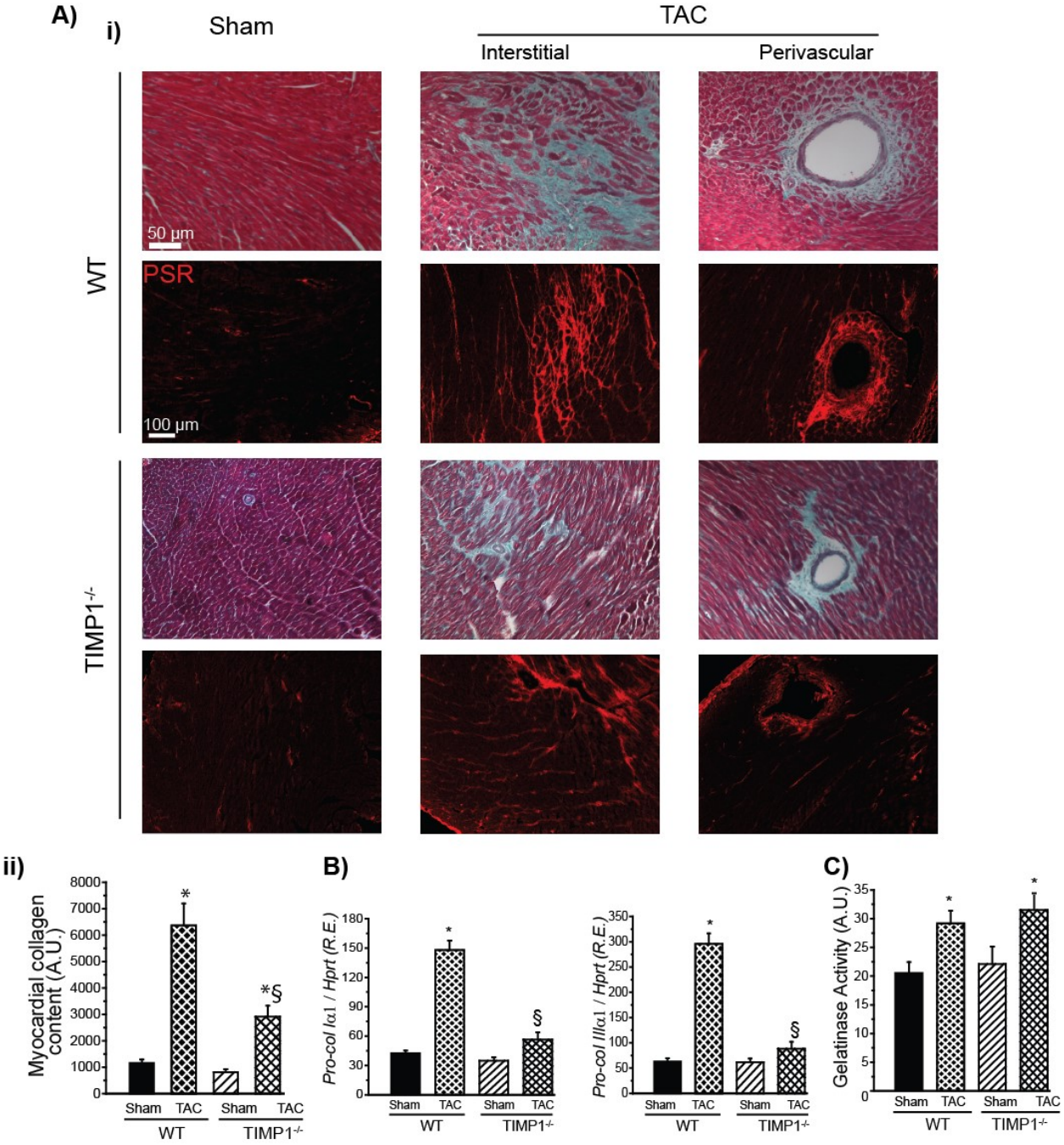

Figure 5.4.2: TIMP1-deficiency suppresses cardiac fibrosis following cardiac pressure-overload. (A) Representative Trichrome and PSR stained images (5 hearts/group/genotype) **(i)**, and myocardial collagen content **(ii)** in WT and TIMP1$^{-/-}$ mice after 2 weeks of cardiac pressure-overload induced by TAC. **(B)** mRNA expression of pro-collagen Ia1 and pro-collagen IIIa1 in indicated groups. **(C)** Total gelatinase activity (n=5-6/group/genotype) in indicated groups. A. U.=Arbitrary Units; R.E.=Relative Expression. *$p<0.05$ compared with corresponding sham group, §$p<0.05$ compared with corresponding WT group.

5.4.3. TIMP1 mediates the association between CD63 and integrinβ1 in mouse myocardium following pressure-overload and in adult cardiac fibroblasts.

CD63 is the only known cell surface receptor for TIMP1.[363] TIMP1 has been reported to mediate CD63 interaction with integrin in regulating chemotaxis in neural crest cells.[364] We investigated if TIMP1 could use a similar mechanism to modulate collagen expression in the heart. Co-immunoprecipitation experiments revealed a strong interaction between CD63 and integrinβ1 in the WT myocardium post-TAC, however, this interaction was significantly suppressed in TIMP1$^{-/-}$-TAC hearts **(Figure 5.4.3Ai-ii)**. Consistently, proximity ligation assay **(Figure 5.4.3B)** and co-immunostaining **(Figure 5.4.3C)** further confirmed a significantly greater increase in co-localization of CD63 and integrinβ1 following pressure-overload in WT compared with TIMP1-deficient mice.

Fibroblasts (FBs) are key players in ECM remodeling as they are the main cell source for production of fibrillary collagens and other ECM proteins. Therefore, we investigated if the observed TIMP1-mediated CD63-integrinβ1 interaction occurs in cardiac fibroblasts. In cultured adult cardiac fibroblasts from WT and TIMP1$^{-/-}$mice, treatment with profibrotic agents Ang II or TGFβ1 increased the interaction between CD63 and integrinβ1 in WT, but not in TIMP1$^{-/-}$ fibroblasts as determined by co-immunoprecipitation **(Figure 5.4.4 A)**, proximity ligation assay **(Figure 5.4.4 B)**, and co-immunostaining for these two molecules **(Figure 5.4.4C)**. These data collectively support the notion that TIMP1 is required for the CD63-integrinβ1 interaction.

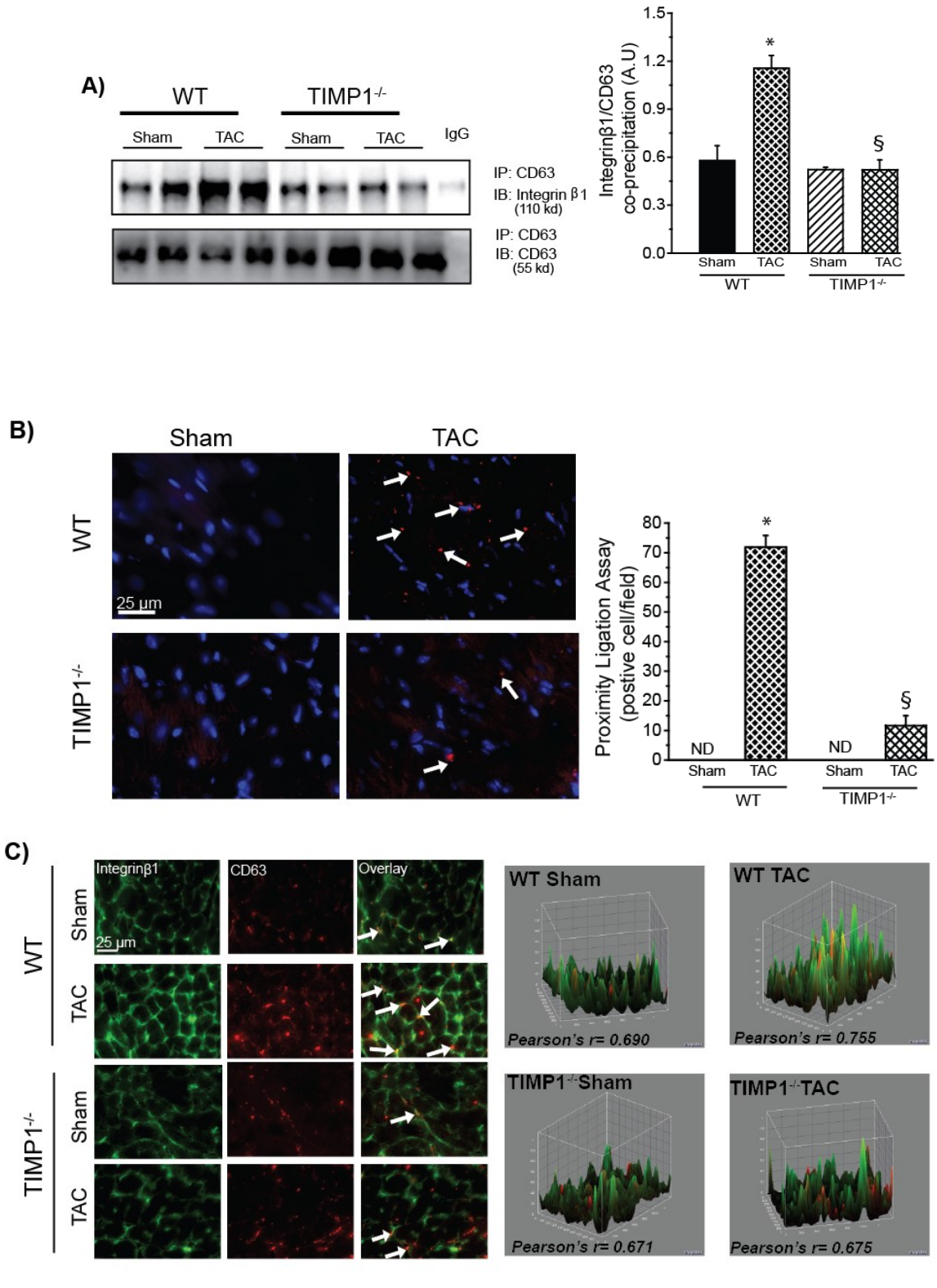

Figure 5.4.3: TIMP1 is required for CD63-integrinβ1 interaction following pressure-overload. **(A)** Co-immunoprecipitation of integrinβ1 and CD63 in WT and TIMP1$^{-/-}$ hearts after

sham or TAC. (n= 4-5 /group/genotype) **(B)** Proximity ligation assay shows increased interaction between integrinβ1 and CD63 following TAC in WT but to a lesser extent in TIMP1$^{-/-}$ hearts (n=3 hearts/group/genotype). **(C)** representative co-immunostaining images for integrinβ1 and CD63 and surface plot showing pixel intensity for immunofluorescent staining and colocalization of CD63 and integrinβ1 (yellow) in WT and TIMP1$^{-/-}$ hearts post-sham/TAC. A.U.=Arbitrary Units; N.D.=not detected; IP=immunoprecipitation; IB=immunoblot. *p<0.05 compared with corresponding sham group, § p<0.05 compared with corresponding WT group.

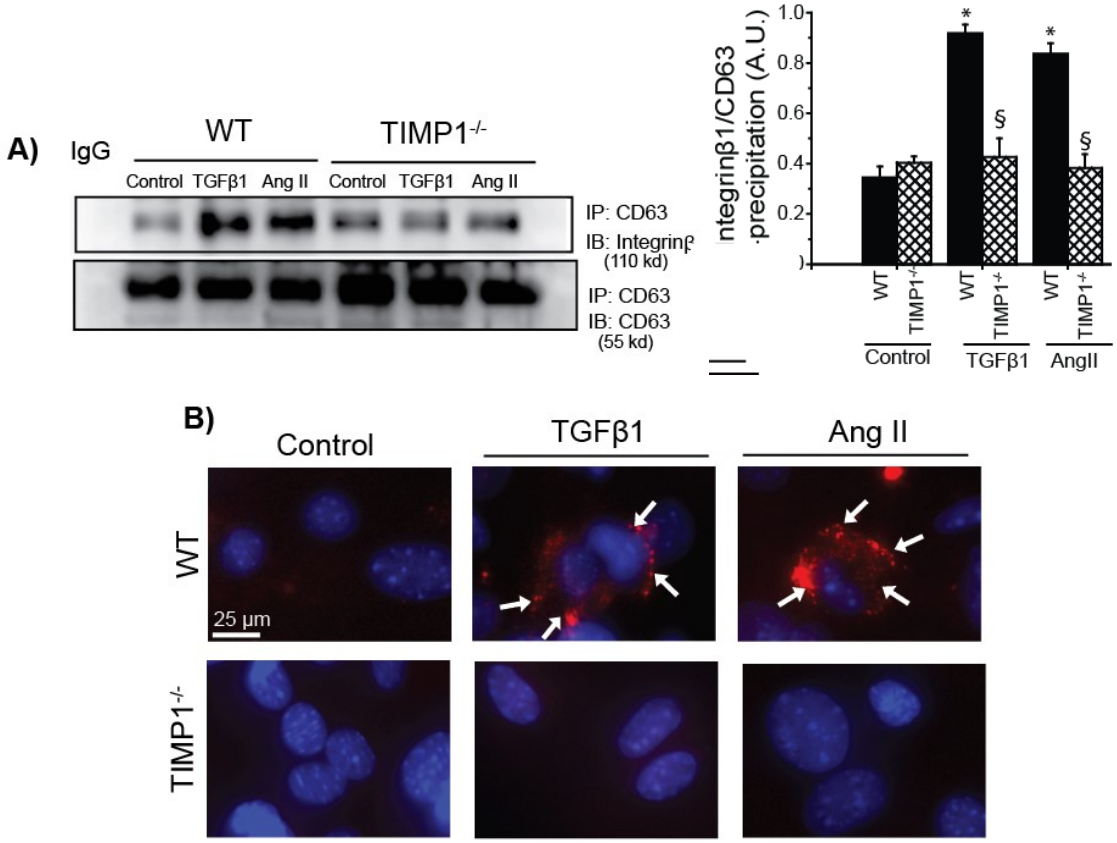

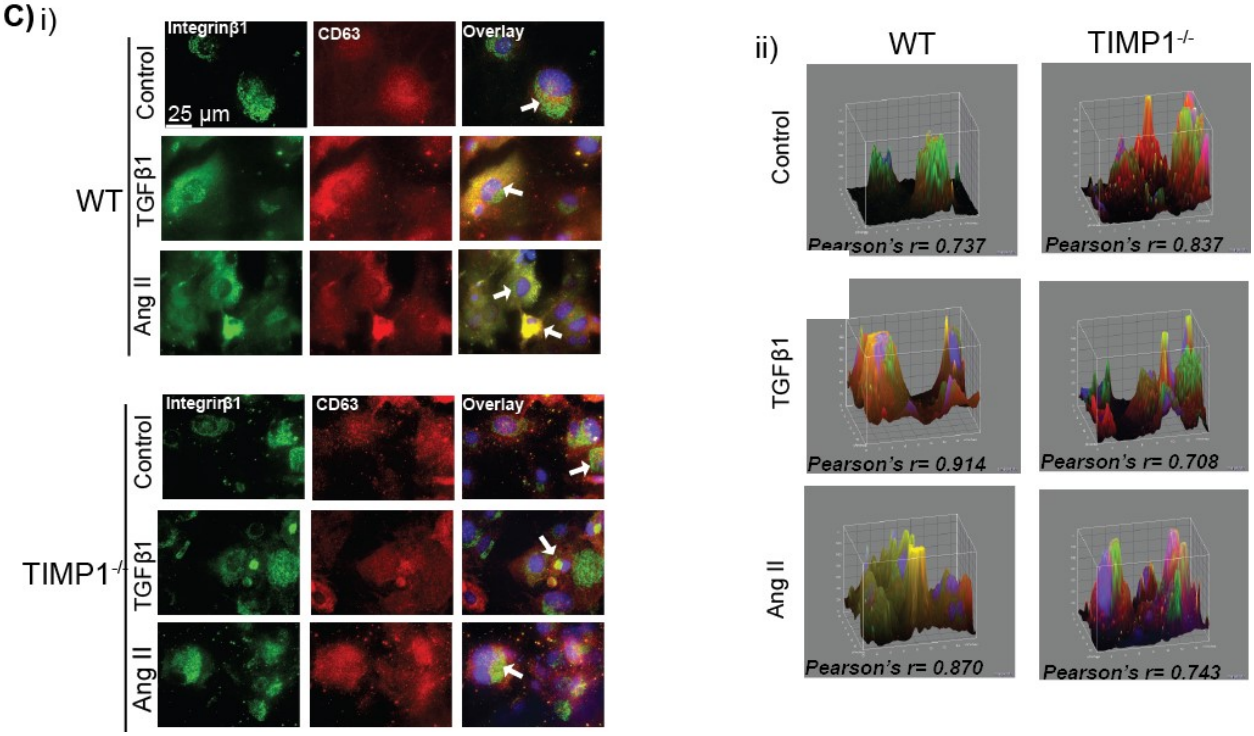

Figure 5.4.4: TIMP1 mediates the association between integrinβ1 and CD63 in adult cardiac fibroblast in response to pro-fibrotic stimuli (A) Representative immunoblots and quantification for co-immunoprecipitation of CD63 and integrinβ1 in cFBs from WT and TIMP1$^{-/-}$ hearts treated with Ang II or TGFβ1. (n=4-5/group/genotype) **(B)** Proximity ligation assay shows physical proximity (<40 nm) of integrinβ1 and CD63 in WT but not in TIMP1$^{-/-}$ cFBs. **(C)** Co-staining for integrinβ1 and CD63 in cFBs from WT and TIMP1$^{-/-}$ hearts (3-4 heats/group/genotype) **(i),** and surface plots of the overlay immunofluorescent images representing the intensity profile of individual pixels, and colocalization of CD63 and integrinβ1 (yellow) **(ii).** Pierson correlation coefficient is indicated in surface plots. Averaged data represent Mean ± SEM. A. U=Arbitrary Units. IP=immunoprecipitation; IB=immunoblot. *p<0.05 vs. corresponding saline group, §p<0.05 vs. corresponding WT group.

5.4.4. TIMP1-mediated CD63-integrinβ1 interaction correlates with myocardial fibrosis in patients with dilated cardiomyopathy.

Since TIMP1 has been consistently linked to myocardial fibrosis in patients with dilated cardiomyopathy (DCM)[286, 360], we investigated if TIMP1-mediated CD63-integrinβ1 interaction is also present in the human myocardium from DCM patients. As anticipated, DCM hearts exhibited marked fibrosis compared with non-failing control hearts as evident by PSR and trichrome-stained sections **(Figure 5.4.5 Ai-ii)**.

We performed co-IP on the membrane and the cytosolic protein fractions of the human myocardial specimens, and found a strikingly higher CD63-integrinβ1 interaction in the DCM membrane protein fraction (but not cytosolic fraction) compared with the non-failing control hearts **(Figure 5.4.5 Bi)**, along with greater TIMP1 protein levels in this group **(Figure 5.4.5 Biii)**.

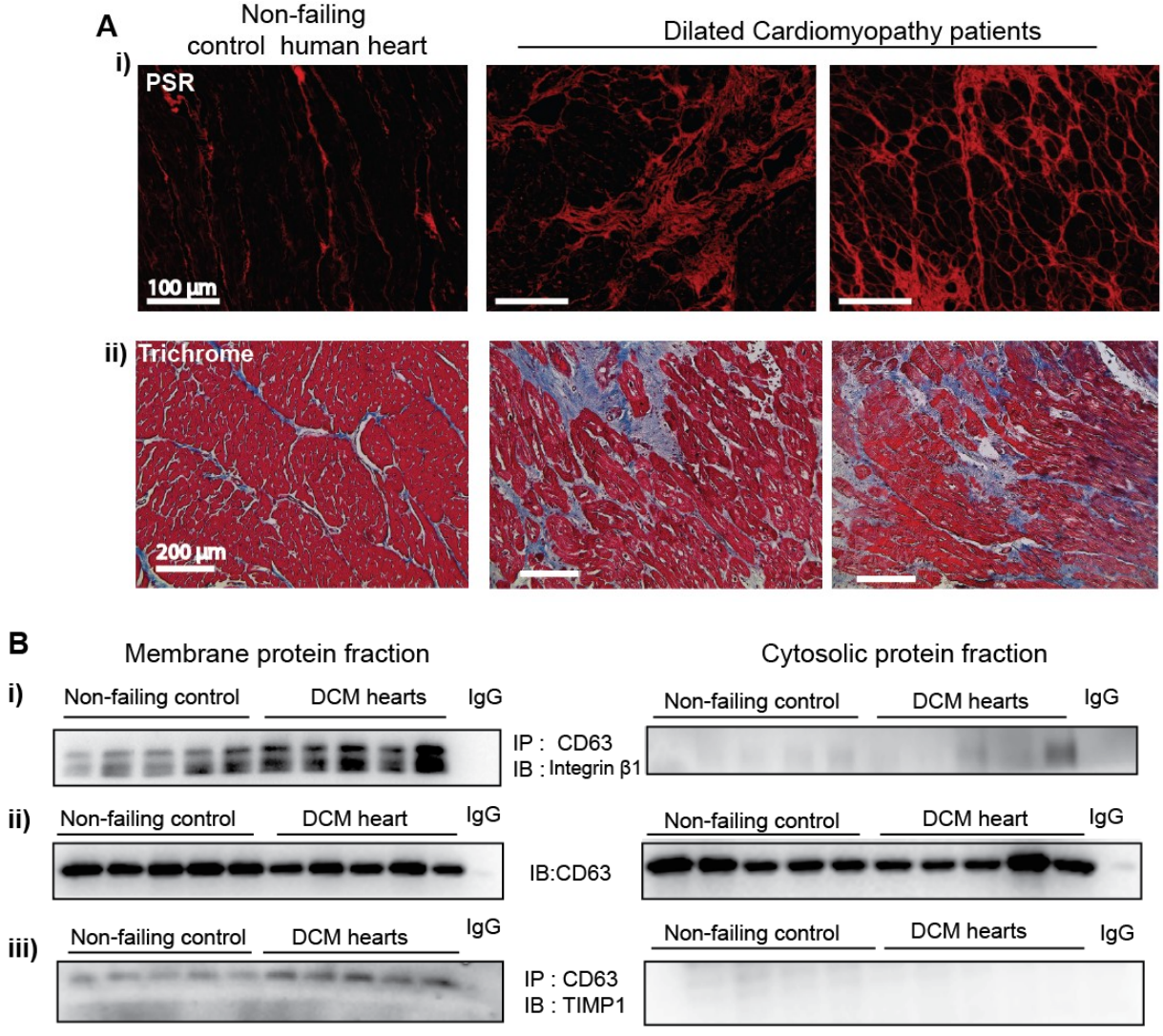

Figure 5.4.5: Myocardial fibrosis in patients with dilated cardiomyopathy correlates with TIMP1-mediated interaction between CD63 and integrinβ1. (A) Representative images of Trichrome-stained **(i)**, and PSR-stained **(ii)** sections from non-failing control and fibrotic human hearts. **(B) (i)** Co-immunoprecipitation of CD63 and integrinβ1 in the membrane fraction, but not the cytosolic fraction of the myocardium, **(ii)** Immunoblotting for CD63 confirms even loading for all samples in membrane and cytosolic fractions, **(iii)** TIMP1 immuno-blot showing higher levels in fibrotic hearts. IP=immunoprecipitation; IB=immunoblot; DCM=dilated cardiomyopathy.

5.4.5 TIMP1 activates a signaling pathway that involves activation and nuclear translocation of Smad2/3 and β-catenin.

Next, we investigated the downstream signaling pathway that could lead to induction of mRNA expression of collagen, and subsequently tissue fibrosis. Smad2/3 is a pro-fibrotic transcription factor that is activated in response to various pro-fibrosis stimuli.[79] Consistent with the greater degree of fibrosis in WT-TAC hearts, phospho-to-total Smad 2/3 ratio was significantly higher in WT compared with TIMP1$^{-/-}$ hearts post-TAC **(Figure 5.4.6A)**. It has also been reported that phospho-Smad2/3 can associate with phosphorylated β-catenin (Y654)[365] or scleraxis[366] prior to its nuclear localization. β-catenin is associated with cadherin and other transmembrane proteins that can interact with CD63.[367-368] Immunoblotting for phosphor-β-catenin and phosphor-Smad 2/3 on the nuclear and cytosolic protein fractions from WT and TIMP1$^{-/-}$ hearts showed a markedly greater level of nuclear translocation for phospho-Smad2/3 and phospho-β-catenin following pressure-overload in WT but not in TIMP1$^{-/-}$ mice **(Figure 5.4.6B)**.

Assessment of contribution of scleraxis showed that in myocardial specimens from DCM patients, scleraxis levels were markedly higher compared with non-failing control hearts **(Figure 5.4.10A)**. Following TAC, scleraxis levels increased more in WT compared with TIMP1$^{-/-}$ hearts (**Figure 5.4.10, C**). However, nuclear translocation of scleraxis was not altered with TIMP1-deficiency **(Figure 5.4.10)**, suggesting that scleraxis may not be a key player in TIMP1-mediated collagen synthesis. Purities of the nuclear and non-nuclear protein fractions in these experiments were confirmed by immunoblotting for histone (nuclear) and caspase 3 (cytoplasm) proteins **(Figure. 5.4.11)**.

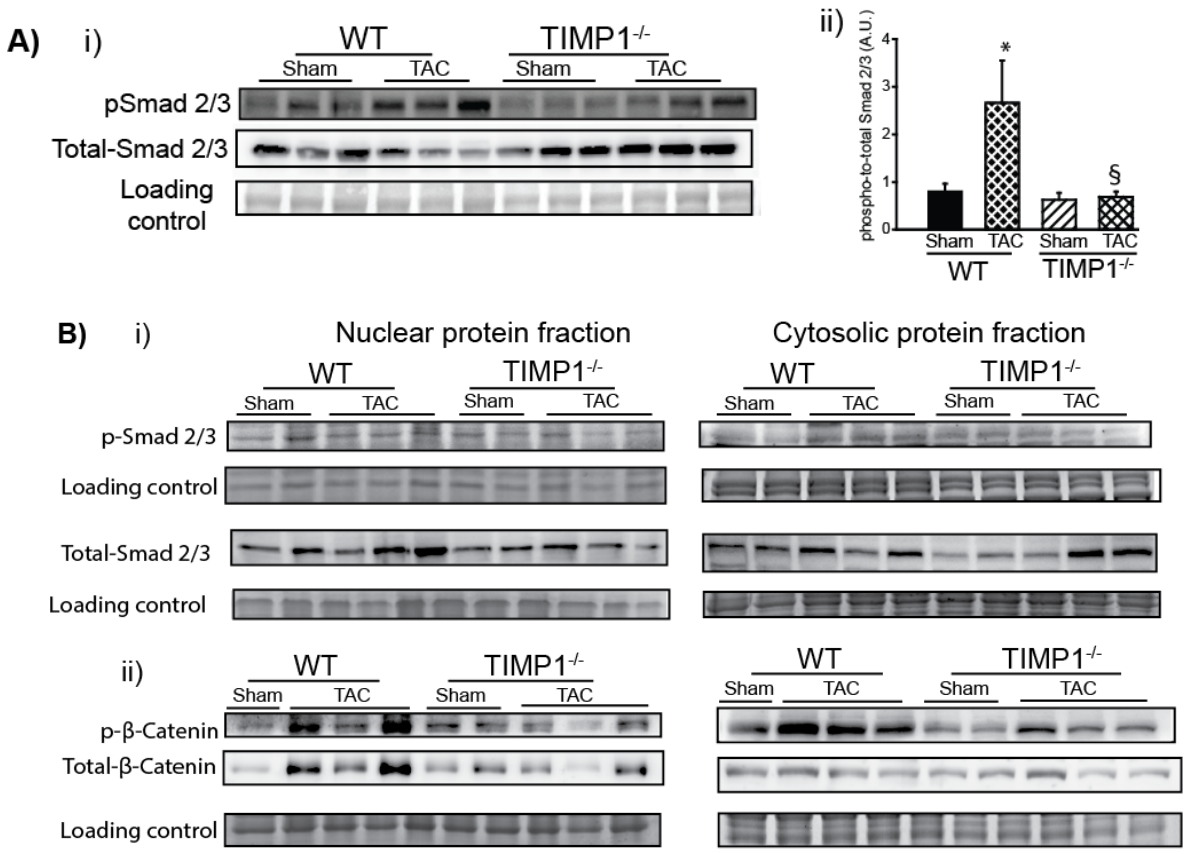

Figure 5.4.6: Absence of TIMP1 suppresses activation of β-catenin, nuclear translocation of p-Smad 2/3 and p-β-catenin. (A) Immunoblot for phospho- and total-Smad 2/3, and averaged phopho-to-total Smad 2/3 ratio in complete heart homogenate (n=5-6/group/genotype). **(B)** Immunoblots on nuclear and cytosolic protein fractions for phospho- and total Smad2/3, phospho- and total β-catenin in indicated groups. Loading control is coomassie blue-stained gel from corresponding blot. A.U.=Arbitrary Units; * $p<0.05$ vs. corresponding sham group; § $p<0.5$ vs. corresponding WT group.

5.4.6. TIMP1-deficiency imposes long term beneficial effects following cardiac pressure-overload

We investigated if the suppressed fibrosis in TIMP1-deficient mice exerts protective (or deleterious) effects over long term following cardiac pressure-overload. The suppressed myocardial fibrosis in TIMP1$^{-/-}$ mice persisted up to 9 weeks post-TAC (**Figure 5.4.7A**), while

these mice also exhibited ameliorated cardiomyopathy compared with WT-TAC mice. Myocardial hypertrophy, measured by heart weight-to-tibial length **(Figure 5.4.7B)**, myocyte cross-sectional area **(Figure 5.4.7C)**, and disease markers (α-skeletal actin, β-myosin heavy chain, and brain natriuretic peptide) **(Figure 5.4.8D)**, and pulmonary edema, a measure of heart failure **(Figure 5.4.8E)**, were significantly lower in TIMP1$^{-/-}$-TAC compared with WT-TAC mice.

Assessment of cardiac structure and function by non-invasive echocardiography showed that biomechanical stress (TAC) led to a significant reduction in LV ejection fraction (i), marked LV dilation (ii, iii), and left atrial enlargement which is a marker of LV diastolic dysfunction and heart failure (iv) in WT mice **(Table 5.1**; **Figure. 5.4.8A**). TIMP1-deficiency, however, ameliorated the decrease in ejection fraction, the LV dilation, and improved the parameters of diastolic dysfunction, E/E' ratio and left atrial enlargement **(Figure 5.4.8Ai-iv)**. Invasive hemodynamic measurements further demonstrated improved cardiac function in TIMP1$^{-/-}$-TAC mice as evident by a left-ward shift in the PV loop compared with WT-TAC mice **(Figure 5.4.8Bi)**, and the lack of elevated LV end-diastolic volume **(Figure 5.4.8C)**. Consistent with the reduced diastolic dysfunction in TIMP1$^{-/-}$ mice, LV stiffness (end diastolic pressure-volume slope) was enhanced in WT-TAC but not in TIMP1$^{-/-}$-TAC mice. These data collectively indicate that absence of TIMP1 prevented decompensation and heart failure following pressure-overload.

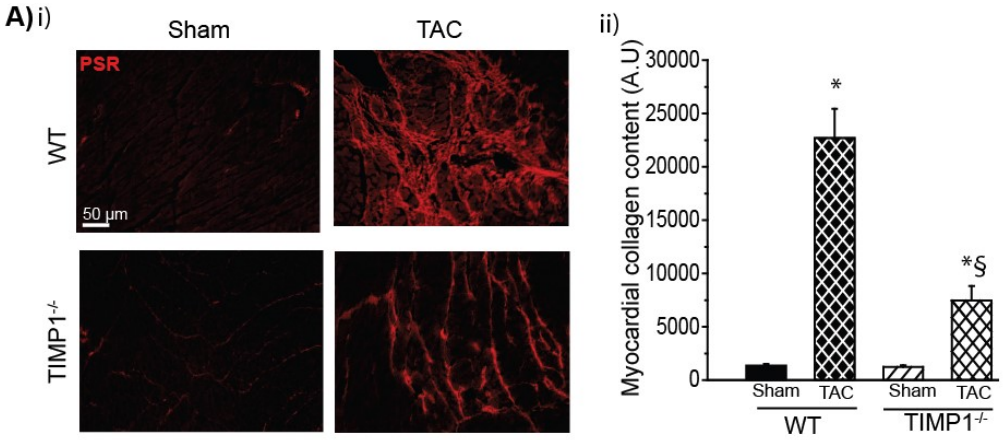

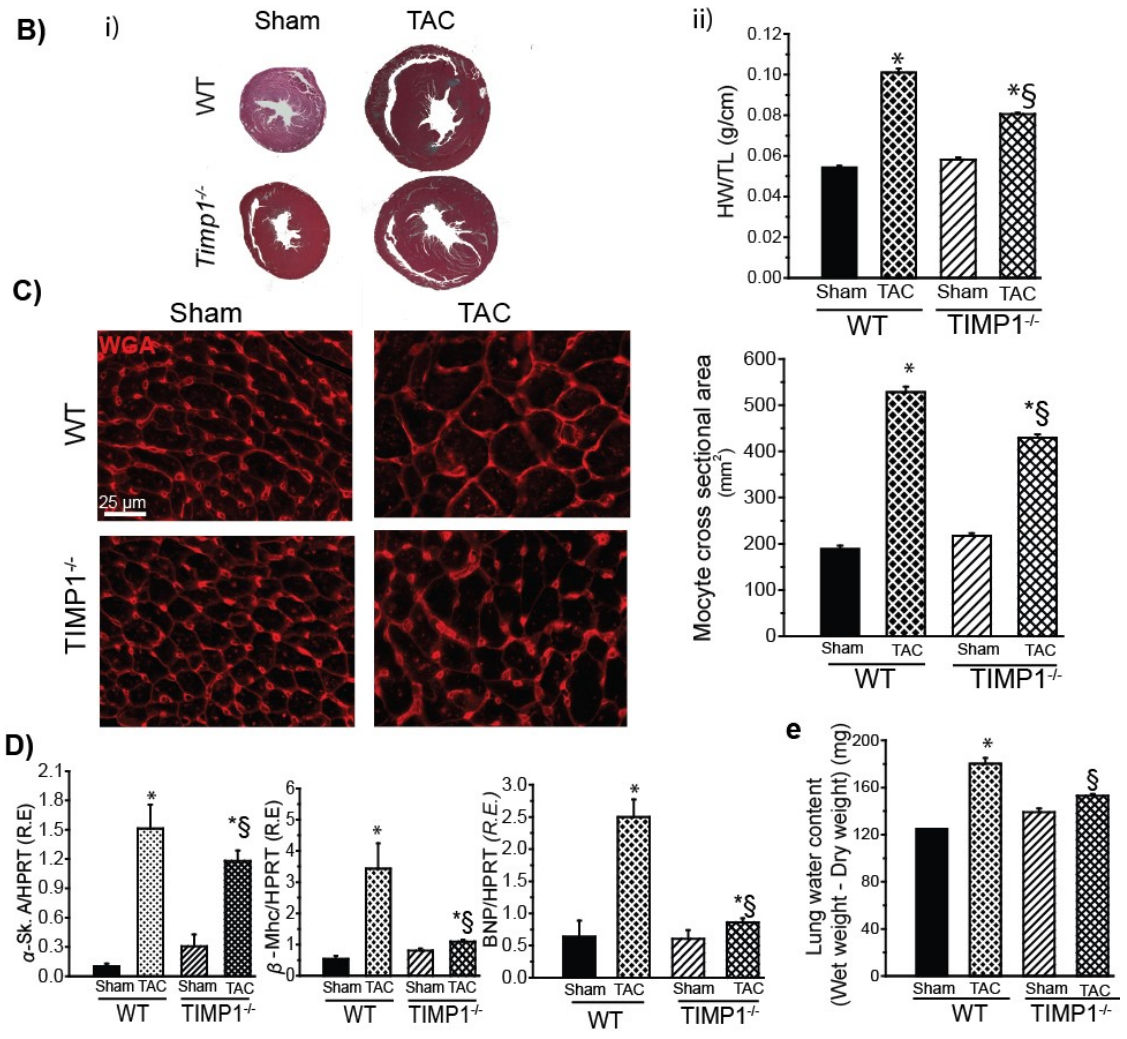

Figure 5.4.7: TIMP1-deficiency ameliorates myocardial fibrosis and hypertrophy long-term post-TAC. (A) Representative PSR stained images (i) and myocardial collagen content (ii) for WT and TIMP1$^{-/-}$ mice at 9 weeks of sham or TAC (n=3-4 hearts/group/genotype). **(B)** Transverse cross sectional images of whole hearts (i), and heart weight-to-tibial length ratio (HW/TL) (ii). **(C)** reprsentative wheat germ aglutinin (WGA)-stained images (i) and averaged myocyte cross-sectional area (ii) in WT and TIMP1$^{-/-}$ mice at 9 weeks post-sham/TAC. **(D)** mRNA expression of markers of heart disease, α-skeletal actin, β-myosin heavy chain, and brain natriuretic peptide. **(E)** Lung water content (edema) in WT and TIMP1$^{-/-}$ mice post-sham/TAC. A.U.=Arbitrary Units. R.E.= Relative Expression *p<0.05 compared with corresponding sham group, § p<0.05 compared with corresponding WT group.

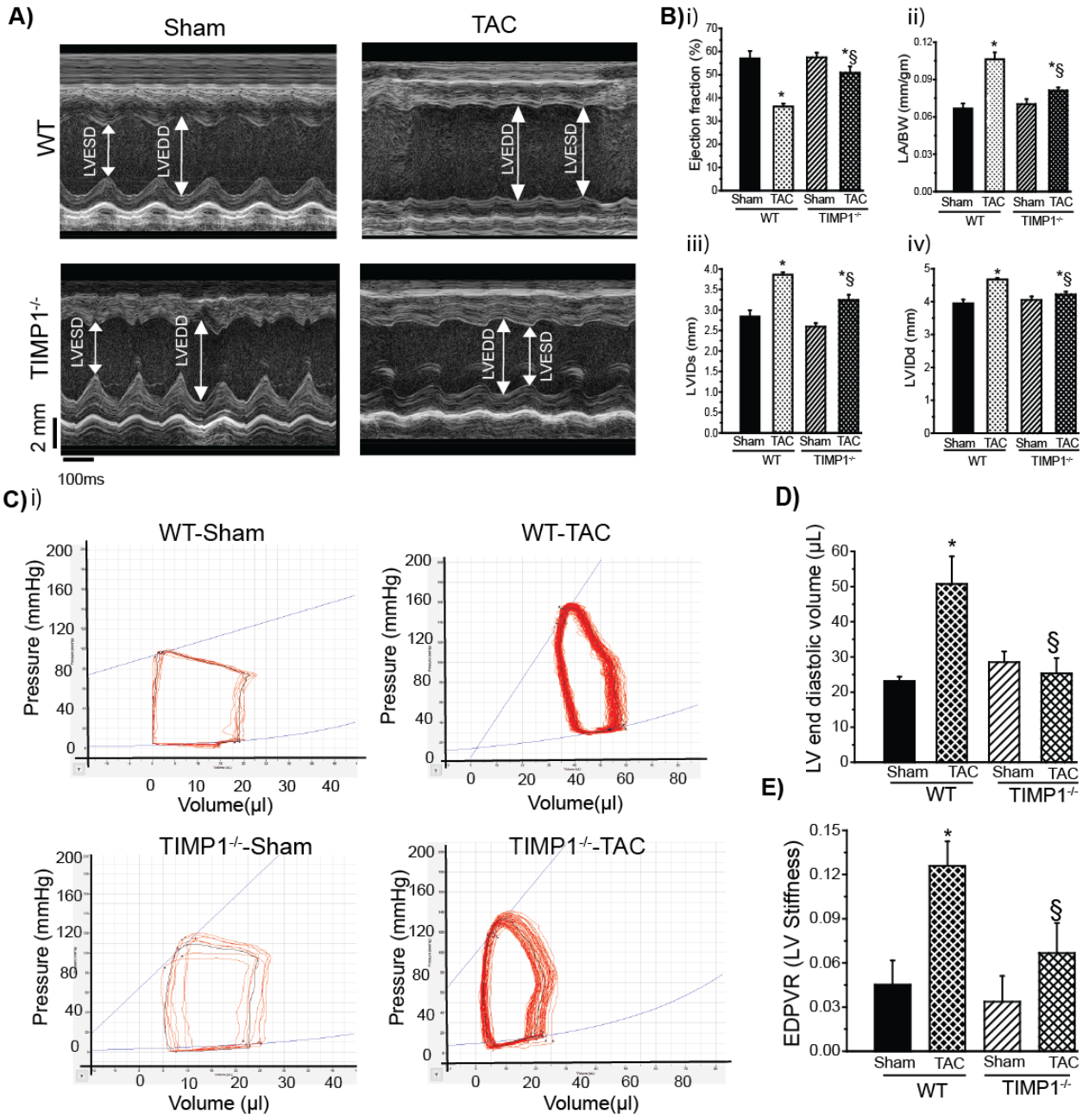

Figure 5.4.8: TIMP1-deficiency lessens cardiac dysfunction and dilation following long-term pressure-overload (9 weeks post-TAC). (A) Representative M-mode images from WT and TIMP1$^{-/-}$ mice for sham and 9 weeks post-TAC. **(B)** Echocardiographic parameters showing ejection fraction, left ventricular end-diastolic (LVIDd) and end-systolic diameter (LVIDs), left atrial, and diameter-to-body weight ratio (LA/BW) in WT and TIMP1$^{-/-}$ mice following sham (n=9) or TAC (n=10-12/group/genotype). Hemodynamic parameters showing the Pressure-

Volume loops **(C)**, left ventricular end diastolic volume (n=5-7/group/genotype) **(D)**, and LV myocardial stiffness as assessed by EDPVR (end-diastolic pressure-volume relationship **(E)** in indicated groups (n=6-10/group/genotype) Averaged data represent mean ± SEM.*p<0.05 compared with corresponding saline group, §p<0.05 compared with corresponding WT group.

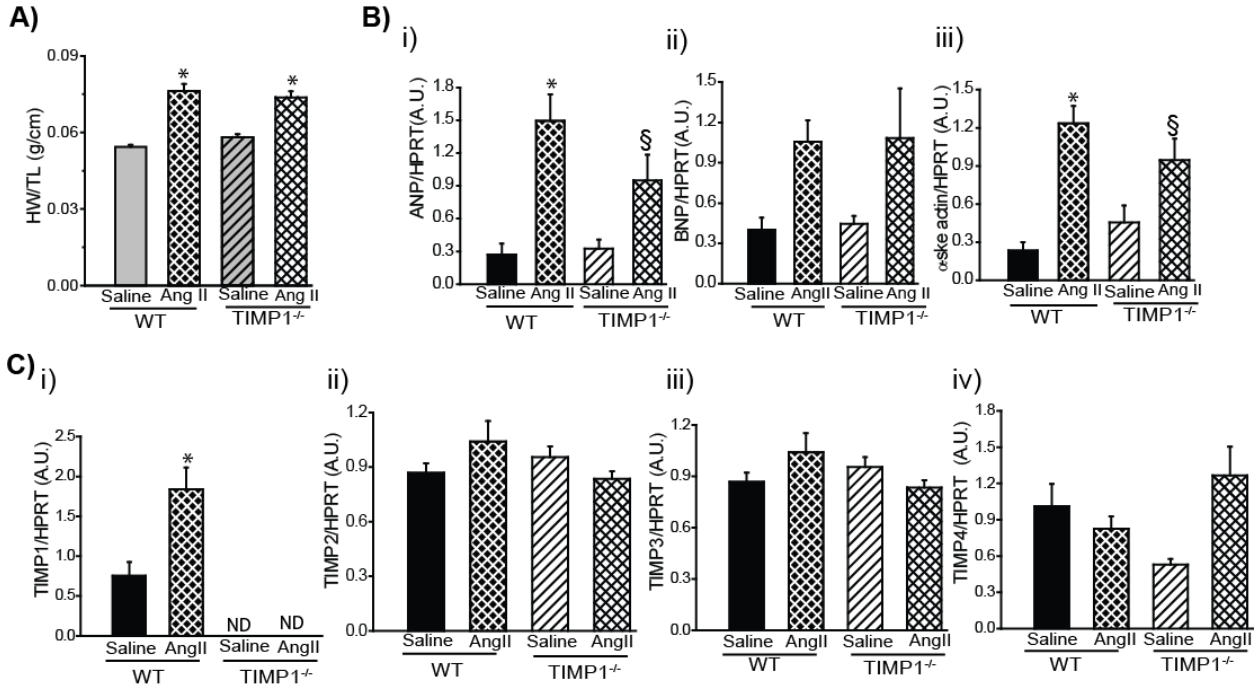

Figure 5.4.9: Hypertrophy and TIMPs expression at 2 weeks post-Ang II (A) Heart weight-to-tibial length ratio (HW/TL) **(B)** mRNA expression of disease markers: ANP **(i)**, BNP**(ii)** and α-ske-actin **(iii)** between WT and TIMP1$^{-/-}$ Sham and post-Ang II infusion (n=6-8/group). **(C)** mRNA expression levels for TIMPs in response to Ang II infusion in WT and TIMP1$^{-/-}$ mice. n=5-6/group/genotype. Data represent Mean±S.E.M. *p<0.05 compared with corresponding saline or sham.

Table 5.1: Echocardiographic parameters from WT and TIMP1 deficient mice at 2, 5 and 9 weeks post-TAC and corresponding sham mice.

	WT Sham	WT TAC			TIMP1$^{-/-}$ Sham	TIMP1$^{-/-}$ TAC		
		2 wks	5 wks	9 wks		2 wks	5 wks	9 wks
n	*10*	*10*	*13*	*12*	*10*	*15*	*13*	*10*
HR (bpm)	466±14	493±18	485±15	470±4	465±16	466±8	472±12	475±18
E wave (mm/s)	753.42±46.25	677.80±65.45	747.54±50.69	561.76±51.07 *	750.28±41.14	720.56±55.93	682.45±34.54	649.69±20.49 §
A wave (mm/s)	457.71±33.75	412.67±59.38	383.46±75.79	265.14±40.31 *	565.65±30.37	348.01±44.08 *	375.23±57.37	410.13±45.91 §
E'(mm/s)	29.71±3.71	24.07±2.11	19.17±1.41*	16.55±1.34*	25.95±1.96	19.60±2.30	18.14±1.88	21.51±1.71§
A' (mm/s)	23.62±2.61	26.99±2.96	25.36±1.98	17.71±1.86*	22.11±1.85	20.68±2.70	19.52±1.84	21.51±2.47§
E'/A' Ratio	1.24±0.04	0.93±0.06	0.78±0.04*	0.99±0.08	1.94±0.04	0.94±0.07	0.95±0.04	1.07 ±0.08
E/E'	25.87±1.98	32.54±4.78	40.19±3.94*	36.12±4.20*	25.86 ± 2.23	34.16±5.99	33.64±5.46	25.06 ± 1.94§
LVEF (%)	57.04±3.21	50.87±3.75	38.58±2.81*	36.29±1.26*	57.53±1.96	54.22±2.21	43.75±3.35	50.86±2.68§
ET (ms)	48.51±1.29	53.95±1.78*	54.06±1.25*	53.99±1.41*	47.66±0.90	49.59±1.63	50.72±1.68	51.17±1.82
LVID-D	3.95±0.11	3.97±0.13	4.54±0.14	4.67±0.04*	4.05±0.10	3.72±0.07	4.37±0.09	4.22±0.04
LVID-S	2.85±0.15	2.95±0.16	3.70±0.17	3.86±0.06*	2.84±0.11	2.59±0.09	3.43±0.15	3.24±0.13
LVPW-S	0.97±0.05	1.21±0.07*	1.12±0.04	1.05±0.02	1.03±0.03	1.06±0.03	1.17±0.05	1.17±0.06
LVPW-D	0.63±0.03	0.95±0.05*	0.90±0.05*	0.83±0.01	0.73±0.03	0.75±0.02	0.93±0.04*	0.90±0.04

Table 5.1: Echocardiographic assessment of systolic and diastolic function in WT and TIMP1$^{-/-}$ mice following sham or 2, 5 and 9 weeks of pressure-overload (TAC). HR-Heart rate; E-wave= early transmitral inflow velocity; A-wave= transmitral inflow velocity due to atrial contraction; E'= Early tissue Doppler velocity; A'= Tissue Doppler velocity due to atrial contraction. E'/A'= Ratio of early Doppler velocity to the tissue Doppler velocity due to atrial contraction; E/E'=Ratio of early transmitral inflow velocity to early tissue doppler velocity, LVEF= Left ventricular ejection fraction; ET=Ejection time, LVID-D= Left ventricular internal diameter at the end of diastole; LVID-S= Left ventricular internal diameter at the end of systole; LVPW-S= Left ventricular posterior wall thickness at the end of systole; LVPW-D= Left ventricular posterior wall thickness at the end of diastole. * $p<0.05$ compared with corresponding sham; § $p<0.05$ compared with the corresponding WT group.

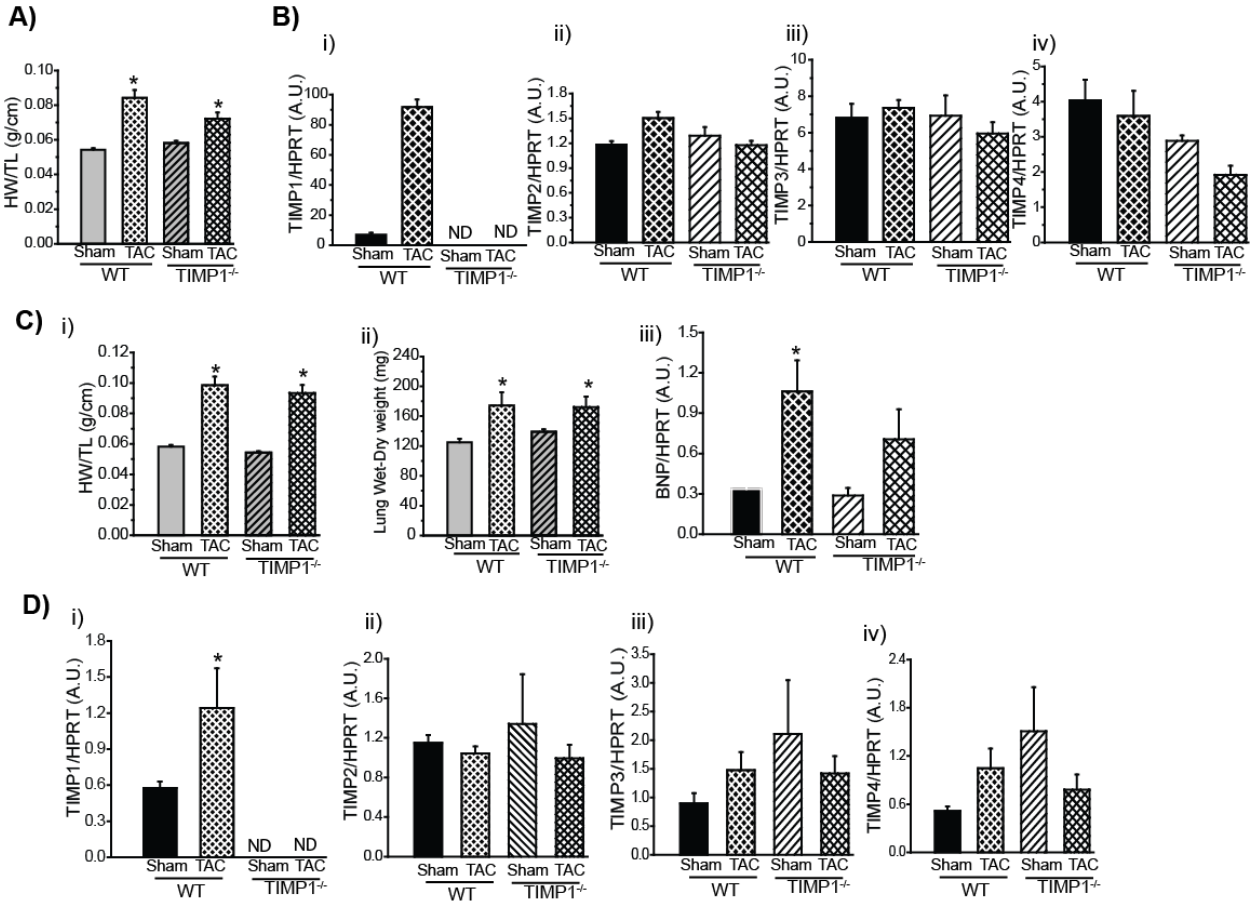

Figure 5.4.10: Hypertrophy and TIMPs expression at 2 weeks post-TAC. (A) Heart weight/Tibial length (HW/TL) (n= 10-12/group/genotype)**. (B)** mRNA expression levels for

TIMPs in WT and TIMP1$^{-/-}$ mice from sham and 2 weeks post-TAC (n= 5-6/group). **(C) (i)** Heart weight/tibial Length (HW/TL) **(ii)** Pulmonary edema (Lung wet-dry weight) (n= 10-12/group) **(iii)** BNP mRNA expression as hypertropic marker from in WT and TIMP1$^{-/-}$ mice from sham and 5 weeks post-TAC (n=5-6/group/genotype). **(D)** mRNA expression levels for TIMPs in WT and TIMP1$^{-/-}$ mice from sham and 5 weeks post-TAC (n=5-6/group/genotype). Data represent mean ± S.E.M. *p<0.05 compared with corresponding saline or sham.

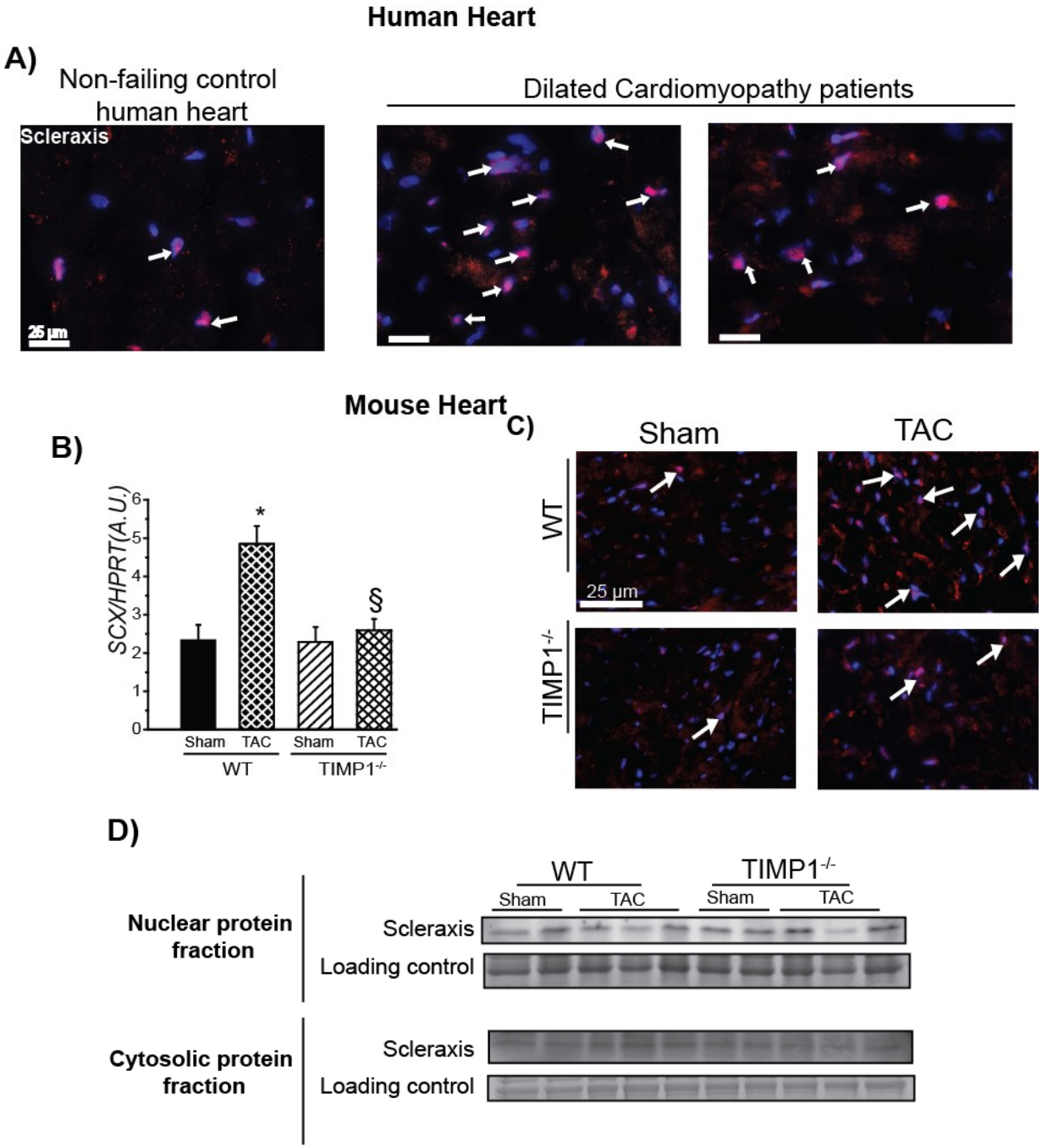

Figure 5.4.11: Scleraxis immunostaining for Scleraxis from myocardial specimens from patients with dilated cardiomyopathy and non-failing **control hearts. (A)** mRNA expression and post-TAC mRNA as well as proteins levels from WT and TIMP1$^{-/-}$ mice (2 weeks post-TAC) **(B)** Representative images of immunostaining for scleraxis in myocardial specimens from patients with dilated cardiomyopathy and non-failing control hearts. mRNA expression, immunostaining for scleraxis (SCX). **(C)** Scleraxis protein levels in the nuclear and cytosolic protein fractions from WT and TIMP1$^{-/-}$ mice post-sham/TAC. Loading control is coomassie blue-stained gel of the corresponding immunoblot. A.U.= Arbitrary units. * $p<0.05$ vs. corresponding sham group; § $p<0.5$ vs. corresponding WT group.

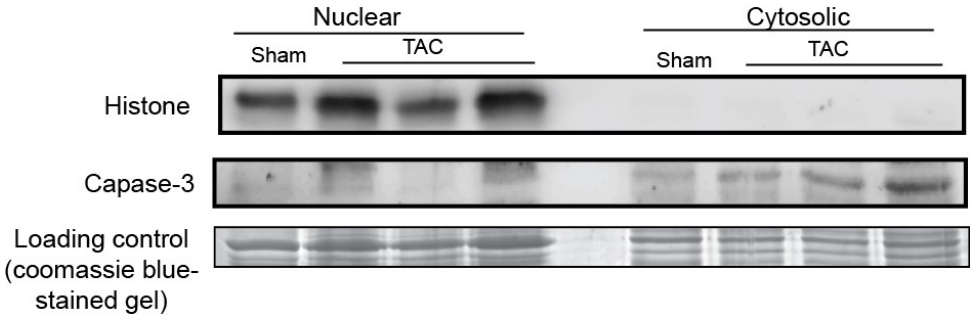

Figure 5.4.12: Assessment of purity of nuclear and non-nuclear protein fractionations. WBs for nuclear specific proteins (Histones) and cytosol specific proteins (Caspase-3).

5.5. Discussion

TIMP1 has been reported as disease biomarker for tissue fibrosis. Lack of TIMP1 resulted significant decrease in myocardial collagen content with Ang-II infusion and post-TAC while WT mice showed consistent increase in cardiac fibrosis indicating TIMP1 is critical in mediating cardiac fibrosis. TIMP1 deficiency further regulated *de novo* collagen transcription post-Ang-II or TAC as TIMP1 deficiency caused a significant reduction of collagen I and collagen II mRNA levels. TIMP1 inhibits MMPs such as MMP2, MMP9 but does not inhibit MT1-MMP[12]. MMP-dependent function of TIMP1 has been reported in a MI model where TIMP1 deficiency with MMP inhibitor treatment improved heart function.[203]

Interestingly, we observed TIMP1 mediated cardiac fibrosis in a MMP-independent manner as gelatinase activity was altered similarly between WT and TIMP1$^{-/-}$ mice with Ang-II

infusion or post-TAC. Also, broad spectrum MMP inhibitor treatment resulted in similar cardiac fibrosis at 2-weeks post-Ang-II.

TIMP1 has been reported to as a receptor for CD63[369-370] and it is important for mediating interaction between integrinβ1 and CD63 in hepatic stellate cells thereby acts as a pro-fibrotic in liver fibrosis model[371]. In cardiac fibroblasts, post-TAC and dilated cardiomyopathy patient's samples, we observed that TIMP1 mediates interaction between integrinβ1 and CD63. Moreover, TIMP1 deficiency resulted in significant reduction of nuclear translocation of p-β-catenin and p-SMAD2/3 thereby less collagen transcription. This suggests that TIMP1-mediated interaction between integrinβ1 and CD63 further activates nuclear translocation of p-β-catenin and p-SMAD2/3 thereby regulating de novo collagen transcription.

TIMP1 deficiency at 9 weeks post-TAC resulted in significantly less cardiac hypertrophy and fibrosis. Also, TIMP1-deficient mice post-TAC showed improved heart function with higher ejection fraction, reduced LA size, and less LV dilation as compared with WT mice measured with echocardiography and less LV dilation as end diastolic volume significantly less at 9 weeks post-TAC. These observations indicate- that absence of TIMP1 prevents LV decompensation thereby improves heart function.

5.6. Conclusions

Findings in this study demonstrate that the rise in TIMP1 levels observed with myocardial fibrosis is not a compensatory mechansism to reduce MMP activities, but rather TIMP1 is involved in directly inducing collagen synthesis by fibroblasts. TIMP1 is a well-known MMP inhibitor, but here we report that its MMP-independent function is key to induce *de novo* collagen synthesis and in triggering reactive fibrosis in the heart, through mediating an interaction between integrinβ1 and CD63 in cardiac fibroblasts. Therefore, TIMP1 is unique among TIMPs since it is the only TIMP whose loss reduced myocardial (reparative) fibrosis, and as such, anti-TIMP1 therapy could be beneficial in limiting cardiac fibrosis and progression to heart failure in patients with non-ischemic cardiomyopathies.

CHAPTER 6
DISCUSSION

6.1. Important findings

6.1.1. TIMP4 is essential for post-I/R myocardial recovery: *In vivo* I/R (20min ischemia, 1week reperfusion) in TIMP4$^{-/-}$ mice resulted in more severe systolic and diastolic dysfunction with enhanced inflammation, oxidative stress (1d post-I/R), hypertrophy and interstitial fibrosis (1wk). Following an initial increase in TIMP4 (1d post-I/R), TIMP4 mRNA and protein decreased in the ischemic myocardium from WT mice by 1 week post-I/R, and in tissue samples from patients with myocardial infarction, which positively correlated with enhanced activity of membrane-bound MMP, MT1-MMP. By 4weeks post-I/R, TIMP4-deficient mice, however, showed exacerbated diastolic dysfunction, sustained elevation of MT1-MMP activity and worsened myocardial hypertrophy and fibrosis, whereas WT mice showed no cardiac dysfunction, elevated TIMP4 levels (to baseline) and normalized MT1-MMP activity.

6.1.2. Intramyocardial injection of hTIMP3 post-MI promotes angiogenesis in a dose-dependent manner: Intramyocardial delivery of hTIMP3 but not hTIMP4 using adenovirus delivery improved heart function, preserved infarct area and resulted in more viable myocytes as compared with the Ad-null control group at 1-week post-MI. Interestingly, hTIMP3 delivery showed increased coronary density and promoted endothelial proliferation as compared with the Ad-null group, which was contrary to the traditional belief of the anti-angiogenic role of TIMPs. The angiogenic response of recombinant TIMP3 to HCEAC and HUVEC was concentration dependent, as higher concentrations of rTIMP3 antagonized VEGFR2, thereby preventing angiogenesis and inhibiting endothelial proliferation. Similar findings were observed with overexpression of hTIMP3 in a myocardial infarction model as hTIMP3 resulted in exacerbation of heart dysfunction and increased infarct size with less viable myocytes as compared with Ad-null mice. These findings suggest that hTIMP3 exerts beneficial effects by promoting angiogenesis at an efficacy dose, while at a higher dose of hTIMP3, these beneficial effects were abolished due to inhibition of angiogenesis.

6.1.3. TIMP1 promotes cardiac fibrosis in an MMP-independent manner: TIMP1 triggers myocardial fibrosis independent of its MMP-inhibitory function, and by mediating an association between CD63 and integrinβ1, initiating activation and nuclear translocation of

Smad2/3 and β-catenin, leading to *de-novo* collagen synthesis. This observation was confirmed using TIMP1-deficient mice subjected to two models of myocardial fibrosis (*in vivo*), adult cardiac fibroblasts (*in vitro*), and fibrotic myocardium from patients with dilated cardiomyopathy. TIMP1-deficiency reduced myocardial fibrosis and ameliorated diastolic dysfunction following long-term pressure-overload. This novel MMP-independent function of TIMP1 in promoting myocardial fibrosis will be valuable in developing anti-fibrosis therapy.

6.2. TIMPs have differential and divergent roles in heart diseases

Adverse ECM remodeling is a heterogeneous process where the loss of the normal ECM structure and function is accompanied by ECM accumulation, which altogether results in impaired LV function [12, 372]. ECM proteins have been shown to have different roles depending on the type of cardiac injury.[61, 204, 373] Interestingly, recent studies have demonstrated that TIMPs have various novel functions beyond the traditional MMP-inhibitory roles.[60] Conclusions from our studies are that TIMP1, TIMP3 and TIMP4 have differential roles in heart failure depending on cardiac injury.

(i) TIMP4 is critical for post-I/R myocardial recovery as its mRNA and protein levels are reduced in patients and mouse myocardium post-I/R. The beneficial effects of TIMP4 post-I/R injury are due to its MT1-MMP inhibitory potential, as TIMP4 deficiency post-I/R caused exacerbation of systolic and diastolic dysfunction, as well as myocardial fibrosis with increased MT1-MMI activity as compared with parallel WT mice. Four weeks after post-I/R, complete recovery in WT mice and normal cardiac function correlated with elevated TIMP4 levels to baseline and normalized MT1-MMP activity. TIMP4 deficiency however, resulted in exacerbated systolic dysfunction, worsened ECM remodeling and sustained MT1-MMP activity that indicated how the MT1-MMP inhibitory potential of TIMP4 is important for its beneficial role in I/R injury. Acute I/R, *ex vivo* (20 minutes or 30 minutes ischemia, 45 minutes reperfusion) resulted in comparable cardiac dysfunction in WT and TIMP4$^{-/-}$ mice. TIMP4-deficiency does not increase susceptibility to acute I/R injury (*ex vivo*), as it resulted in comparable recovery with WT mice post-I/R in an *ex vivo* cardiac injury model.

(ii) TIMP1 promotes cardiac fibrosis in an MMP-independent manner by mediating interaction between integrinβ1 and CD63 in cardiac fibroblasts, dilated cardiomyopathy patients and pressure-overload model. Absence of TIMP1 caused significantly less interaction between

integrinβ1 and CD63 and resulted in improved cardiac function thereby prevented decompensation of heart in response to pressure-overload cardiomyopathy.

(iii) TIMP3 and TIMP4 levels are reduced post-MI during earlier time-points.[204] We observed that TIMP3, but not TIMP4, exerts beneficial effects in a dose dependent manner. Interestingly, adenovirus delivery of hTIMP3 at therapeutic concentrations improved cardiac function, preserved infarct area, resulted in more viable myocytes and promoted angiogenesis, endothelial cell proliferation, while higher concentrations of TIMP3 exacerbated cardiac function and worsened LV remodeling with less viable myocytes as compared to therapeutic TIMP3 concentrations.

6.3 TIMP4 deficiency resulted in advanced myocardial remodeling post-I/R

Cardiac repair after I/R injury consists of a complex series of events with initial inflammation and infiltration of immune cells that serve to digest and clear damaged tissue, followed by a reparative phase with resolution of inflammation, fibroblast proliferation and scar formation that ultimately results in reparative fibrosis. We observed that lack of TIMP4 triggered initial events of I/R injury, such as increased oxidative stress and infiltration of neutrophils with more necrosis of cardiac cells at 1 day-post-I/R, which altogether contributed to exacerbation of I/R injury at 1 week. TIMP4 deficiency regulated collagen transcription at 1 week post-I/R as higher mRNA levels of collagen-I and collagen-III were observed in TIMP4$^{-/-}$compared with WT mice. Similarly, at 1 week post-I/R, TIMP4 deficiency resulted in exacerbated cardiac fibrosis as damaged or necrotic myocytes were replaced by fibrous collagens. By 4 weeks post-I/R, this fibrosis was exacerbated in TIMP4$^{-/-}$ mice but not in WT mice. This decreased fibrosis observed in WT mice at 4 weeks could be due to the presence of TIMP4 as its levels were increased at 1 month post-I/R. These findings suggest that TIMP4 deficiency results in exacerbation of post-I/R events and thereby resulted in advanced myocardial remodeling.

During ischemic cardiomyopathy, activated MMPs are released from infiltrated neutrophils that damage the cardiomyocytes and degrade the ECM proteins leading to LV dilation and heart failure.[197,374-376] TIMPs are physiological inhibitors of MMPs in the tissue compartments and inhibit the activated MMPs. Each TIMP has unique properties and inhibits MMPs with different specificity and affinity. [12,135] Our data from *in vitro* activity assay for rTIMPs against

rMMPs showed that each TIMP inhibits MMP with different specificities, as TIMP2 is the most potent inhibitor of MT1-MMP followed by TIMP4. At 1 week post-I/R, TIMP4$^{-/-}$ mice showed increased MT1-MMP mRNA, protein and activity in the ischemic regions, suggesting MMP dependent function of TIMP4 could offer beneficial effects post-I/R. Similar findings were observed in ischemic cardiomyopathy patients and WT mice where significant reduction of TIMP4 in the ischemic areas post-I/R caused consistent increase in MT1-MMP activity. Therefore, the MT1-MMP inhibitory function of TIMP4 is important for its beneficial role in post-I/R injury. Similarly, it has been reported previously that MT1-MMP can activate the latent TGFβ to trigger cardiac fibrosis and its overexpression post-MI resulted in poor outcomes[326,377-378] and TIMP4 expression was significantly higher in MT1-MMP heterozygous mice post-I/R.[203] These findings suggest that TIMP4 could be beneficial in recovery from I/R injury by reducing advanced myocardial remodeling due to its MT1-MMP inhibitory potential.

6.4. TIMP4 is beneficial for post-I/R recovery of heart function

Post-I/R cardiac dysfunction results in an increase in size of surviving myocytes, myocardial remodeling that suppresses LV systolic and diastolic function, thereby causing heart failure. TIMP4 deficiency results in adverse myocardial remodeling with gross enlargement of the hearts, myocytes and significantly higher LV weight to tibia length ratio as compared with WT mice at week post-I/R. This adverse myocardial remodeling with cardiac hypertrophy causes compromised heart function with exacerbation of systolic dysfunction as determined by reduced ejection fraction and severe diastolic dysfunction with a significantly greater increase in isovolumic relaxation time, deceleration time, E'-to-A' ratio, and LA size as compared with WT mice at 1-week post-I/R. Interestingly, WT mice showed complete recovery of heart function with no cardiac hypertrophy and no fibrosis with increased TIMP4 levels and reduced MT1-MMP activity. However, on the other hand TIMP4$^{-/-}$ mice consistently showed more cardiac fibrosis, hypertrophy and exhibited suppressed systolic function as evident in increased wall thickness and LV dilation, as well as exacerbated LV severe diastolic dysfunction as evident in a marked increase in IVRT, deceleration time [379], LA size, and a decrease in E'-to-A' ratio and consistently higher MT1-MMP activity. The beneficial role of TIMP4 in post-I/R injury could be due to its MT1-MMP inhibitory function as the cytosolic tail of MT1-MMP has been reported to induce

signaling pathways such as ERK,[327] which can contribute to myocardial I/R injury and has been reported to activate TGFβ, thereby promoting cardiac fibrosis.

6.5. TIMP4 is important for post-I/R recovery *in vivo* but not *ex vivo*.

TIMP4 shows a tissue-specific pattern with higher expression in the heart and brain[380]. It has also been reported to be present intracellularly in rat cardiomyocytes[285] that were released from the myocardium during post-ischemic reperfusion, resulting in proteolysis of MMPs leading to myocardial stunning and hibernation.[285] TIMP4, besides inhibiting MMP2, has been suggested to have anti-inflammatory effects in the myocardium.[381] TIMP4-deficient mice showed more infiltration of neutrophils and increased superoxide anion production, which resulted in more cell death at 1 day post-I/R *in vivo* as compared with WT, which acted as stimulus for exacerbation of the heart function at 1 week post-I/R. On the other hand, an *ex vivo* Langendorff's model of I/R injury, which is primarily a model of myocyte cell death, resulted in comparable recovery of heart function between WT and TIMP4$^{-/-}$ mice with I/R injury (20 minutes & 30 minutes ischemia-45 minutes reperfusion) at a constant flow rate. Similarly, creatine kinase levels in perfusate at different time points after reperfusion were similar, indicating that myocyte cell death was altered similarly with *ex vivo* I/R injury and the role of TIMP4 would be beneficial in systemic circulation rather than at myocyte levels only.

6.6. TIMP3 has a novel role of promoting angiogenesis rather than its traditional anti-angiogenic role.

Traditionally, MMPs has been reported to have an anti-angiogenic role by degrading basement membrane proteins, thereby opening up vessels while TIMPs, by inhibiting MMPs, inhibits this angiogenesis process.[382-384] The antiangiogenic role of TIMP3 is reported in a chick embryo model where higher concentrations of TIMP3 (>1μM) antagonized VEGFR2 and inhibited angiogenesis.[350] Interestingly, *in vivo* lectin injections and CD31 staining at 1 week post-MI showed more coronary vessels with Ad-hTIMP3 injection as compared with Ad-null control, indicating hTIMP3 promotes angiogenesis in the infarct and peri-infarct region, and preserving more viable myocytes in the hTIMP3 group as compared with Ad-null. At an earlier phase of post-

MI remodeling, hTIMP3 promoted more endothelial proliferation but did not affect inflammation. Our culture data using venous (HUVEC) and coronary (HCAEC) endothelial cells show biphasic response of rTIMP3 with VEGF treatment. rTIMP3 at lower concentrations promoted more sprouting and increase in sprout number, indicating more endothelial proliferation, whereas a higher concentration of rTIMP3 inhibited endothelial proliferation and angiogenesis. The binding between rTIMP3 and VEGFR2 measured with immunoprecipitation was concentration-dependent as higher concentrations of TIMP3 showed higher binding to VEGFR2. This could explain our finding in HUVEC and HCEAC as biphasic angiogenic response of rTIMP3.

6.7. Intramyocardial Injection of hTIMP3 to physiological level provides therapeutic alternative for post-MI remodeling

Advanced myocardial remodeling post-MI is a complex process involving a number of cellular and extracellular events. Therefore, controlling the progression of myocardial remodeling is critical to develop new therapies and reduce post-MI morbidity and mortality. The gene delivery approach has been tried to develop therapeutic alternatives for post-MI.[385-387] Adenovirus delivery of hTIMP4 did not improve cardiac function, but adenovirus delivery of hTIMP3 significantly lessened LV dilation with reduction of systolic and diastolic volume with improvement in cardiac function as compared with Ad-null control at 1 week post-MI. This improved cardiac function with hTIMP3 post-MI is associated with a significant reduction of LV myocardial remodeling and less infarct area, indicating the preservation of more myocardial muscle. WGA and phalloidin staining showed that hTIMP3 injections to the heart preserved more myocardial muscle mass, as well as more viable myocytes in infarct and per-infarct area as compared with the Ad-Null group. Interestingly, intramyocardial injections of a higher Ad-hTIMP3 dose showed exacerbation of cardiac function. This higher dose of Ad-hTIMP3 caused severe LV dilation and suppressed cardiac function at 1 week and 4 weeks post-MI. Similarly, a high Ad-hTIMP3 resulted in adverse myocardial remodeling and less viable myocytes in infarct and peri-infarct regions, suggesting that a higher dose of hTIMP3 does not provide a beneficial effect, but instead results in exacerbation of cardiac dysfunction and adverse remodeling. This finding is consistent with HUVEC and HCEAC culture data, thereby confirming that Ad-hTIMP3 has a dose-dependent effect for post-MI recovery, as a lower dose of hTIMP3 provides beneficial effects such as improved cardiac

function, angiogenesis, reduced remodeling and more viable myocytes, whereas these effects were abolished at a higher h-TIMP3 dose. Therefore, adenoviral delivery of hTIMP3 post-MI exerts dose-dependent effects as a lower dose promotes angiogenesis, thereby reducing advanced remodeling and improving cardiac function, while higher concentrations of Ad-hTIMP3 abolish these beneficial effects of hTIMP3. Therefore, replenishment of reduced TIMP3 to a normal physiological level with post-MI could provide an effective therapeutic approach rather than overexpressing TIMP3 for post-MI remodeling.

6.8. TIMP1 mediated cardiac fibrosis is MMP-independent

MMP-independent function of TIMP1 and other TIMPs have been reported in different cell types.[305, 388] TIMP1 can promote proliferation of oligodendrocytes.[389] The MMP independent function of TIMP1 have been studied using cancer cell lines. TIMP1 showed growth promoting[390, 391] and anti-apoptic potential[392] in breast and Burkett's lymphoma cell lines, respectively. In a model of MI, TIMP1-deficient mice exhibit a greater rise in MMP activity and exacerbated cardiac dysfunction compared with parallel WT mice, and treatment with an MMP-inhibitor improves the cardiac dysfunction in TIMP1$^{-/-}$-MI mice.[203, 393] Following MI, MMP activity peaks shortly after the onset of MI and drives the remodeling of the infarcted myocardium[206], whereas the rise of MMP activities following pressure-overload occurs gradually so that its impact on tissue remodeling may not be as stark as in post-MI. Therefore, the function of TIMP1 in cardiac response to MI appears to occur primarily through its MMP-inhibitory function. However, following a pressure-overload or Ang II infusion, lack of TIMP1 did not result in an additional rise in MMP activity, and consistently, MMPi-treatment did not reverse the suppressed myocardial fibrosis in TIMP1$^{-/-}$ mice, thus indicating that TIMP1 mediates fibrosis in a MMP independent manner rather than a MMP-dependent as observed in MI model.

6.9. TIMP1 mediates interaction between integrinβ1 and CD63 thereby promoting de novo collagen synthesis

Studies in fibroblasts have shown that TIMP1 can bind to membrane receptor CD63 and activate ERKs [146] [144], protein kinase B (Akt) and related intracellular pathways in an MMP-independent fashion. TIMP1 can regulate cardiac fibroblast proliferation *in vitro*, maintain

immune homeostasis and prevent endothelial cell migration. Integrinβ1 in cardiac fibroblast has been shown to contribute to heart failure,[394] as its levels rise in response to pro-fibrotic factors triggering collagen expression.[395-396] Contribution of fibroblast integrins to fibrosis has also been reported in other organs.[397] CD63 is a membrane protein present on the cell surface of various cell types, and while it is abundant on endosomes and lysosomes[398], it is well-recognized for its lysosome-independent function.[379] CD63 is the only known cell surface receptor for TIMP1.[363] In stellate cells in the liver, binding of TIMP1 to the CD63/integrinβ1 complex promotes cell migration[371], while this interaction inhibits tumor growth through activating the FAK and PI3K signalling pathways[399-400,363], and regulating chemotaxis in neural crest cells[364]. We observed a novel function of TIMP1 in the induction of collagen synthesis and fibrosis in the heart by mediating the interaction between CD63 and integrinβ1 in cardiac fibroblasts, leading to subsequent activation and nuclear translocation of Smad2/3 and β-catenin, and induction of collagen mRNA expression. Scleraxis is another transcription factor that has been reported to work synergistically with Smad2/3 to trigger fibrosis.[366, 401] While scleraxis levels were increased in the fibrotic myocardium, scleraxis was not altered with TIMP1-deficicney, indicating that scleraxis is not a key player in TIMP1-mediated induction of collagen synthesis and fibrosis.

6.10. TIMP1 deficiency prevents decompensation of LV and improves heart function

TIMP1 does not exhibit a beneficial effect in cardiac fibrosis in response to pressure-overload or Ang II infusion. TIMP1 promotes cardiac fibrosis in an MMP-independent manner as a TIMP deficiency resulted in significantly less myocardial remodeling with suppressed cardiac fibrosis and myocyte hypertrophy and reduced heart weight to tibial length ratio as compared with parallel WT mice in a pressure-overload model. TIMP1 deficiency prevented decompensation of LV with less dilation as evidenced by LV systolic and diastolic internal diameters and improved systolic as well as diastolic function with improves ejection fraction and LA size as compared with parallel WT mice in pressure-overload model. Also, TIMP1 deficiency improved dilation as post-TAC PV loop analysis showed significantly less EDV and EDPVR as compared with parallel WT mice. These findings indicate that TIMP1 promotes fibrosis, since its deficiency resulted in improvement in heart function, less myocardial hypertrophy and fibrosis.

6.11. Tissue Inhibitors of Matrix Metalloproteinases (TIMPs) does not necessarily provide beneficial effects.

TIMPs are tissue inhibitors of MMPs that degrade ECM proteins and contribute to myocardial remodeling, hypertrophy in heart failure. The current understanding that TIMPs are MMP inhibitors that could have beneficial effects in the remodeling process, has been proven some of the TIMPs. For example, TIMP1, TIMP2 and TIMP3 deficiency resulted in excessive MMP activities post-MI and results in heart failure and pharmacological inhibition of MMPs by synthetic MMP inhibitors prevents post-MI heart failure in these mice.[203, 204, 206] Interestingly, these beneficial effects of TIMPs in heart disease are not only limited their MMP-dependent role. As well, the MMP-independent role of TIMP2 and TIMP3 has been reported to have beneficial effects in response to Ang-II infusion.[60] The research findings presented in this thesis identify novel roles of TIMPs. We observed that each TIMP is unique in its function depending on cardiac injury and that TIMPs do not have always beneficial effects in heart failure. Furthermore, its function is not necessarily dependent on its MMP inhibitory function.

TIMP4 could be beneficial in patients with ischemic cardiomyopathy with reduced myocardial TIMP4 levels. These beneficial function of TIMP4 are due to its MT-MMP inhibitory potential, which is elevated in post-I/R injury and contribute to myocardial remodeling. Also, during the earlier events of I/R injury, TIMP4 could exert beneficial effects by controlling inflammation and oxidative stress and thereby limiting future myocardial I/R injury.

Injection of hTIMP3 to bring its normal physiological level, but not hTIMP4, could offer beneficial effects, but only at therapeutic concentration at efficacy levels. Our data suggest that the efficacy dose of TIMP3 promotes angiogenesis and improves cardiac function post-MI as well as HUVEC and HCEAC, while a higher dose of TIMP3 results in exacerbation of cardiac function post-MI, antagonizes VEGFR2 and inhibits angiogenesis in HUVEC and HCEAC. This finding suggests that the beneficial role TIMP3 plays for post-MI therapy is dose-dependent, and higher concentrations of TIMP3 could not offer a beneficial role for post-MI therapy.

Inhibition of TIMP1 for anti-fibrotic therapy does not produce beneficial effects, as its levels are consistently elevated in cardiac fibrosis and it is used as a biomarker of cardiac fibrosis. We observed a lack of TIMP1 results in suppressed cardiac fibrosis and prevents decompensation of the LV, thereby improving heart function and suggesting that TIMP1 promotes cardiac fibrosis.

Our findings in animal models and dilated cardiomyopathy patients indicate that this pro-fibrotic function of TIMP1 is MMP independent and it mediates interaction between CD63 and integrinβ1 in fibroblasts and nuclear translocation of SMAD2/3 and β-catenin, thereby regulating collagen transcription. Therefore, novel MMP-independent function of TIMP1 in promoting myocardial fibrosis will be valuable in developing anti-fibrosis therapy.

CHAPTER 7

LIMITATIONS AND FUTURE SCOPE

7.1. Limitations

7.1.1. Disease model for heart failure

Various heart disease models provide a valuable resource for identification of novel therapeutic targets and testing novel approaches for heart failure treatment.[402-403] Mouse models are widely accepted for heart failure studies as these models offer advantages such as the availability of genetically modified mice and greater litter size helps to study underlying mechanisms of heart failure. In our studies, we used well-accepted surgical animal models of heart failure commonly observed in humans, and findings from these studies provide mechanistic insights and add to the literature regarding the role of TIMPs in heart failure. However, severity of diseases produced and degree of injuries produced using mouse models are different from heart failure in humans. Therefore, further studies are needed using larger animal models of heart failure such as pig models which resembles closely human cardiac physiology.

7.1.2. Adenovirus delivery and recognizing human TIMPs in heart

The gene therapy approach involves encapsulation of a therapeutic gene of interest to guide it to the target cell. The target gene is delivered into the body using a viral vector, its internalization and transport of the administered gene to the nucleus and expression of the gene. Adenovirus is a commonly-used vector for gene therapy with demonstrated evidence in a clinical trial.[404] Adenovirus expresses the therapeutic gene and the protein product transiently for up to 2-3 weeks. Also, adenovirus delivers genes efficiently to a wide variety of cells including dividing and quiescent. This offers an advantage for *in vitro* cell-based work, but *in vivo* delivery genes using adenovirus needs the virus to be GFP tagged in order to detect gene delivery. We have used the adenovirus mediated gene delivery approach and recognizing hTIMPs *in vivo* is challenging because there is no specific antibody available to detect hTIMP3 and hTIMP4 and adenovirus transfects to different cell types. Therefore, studies using adeno associated virus using GFP tag can be performed to study long term therapeutic effects of TIMPs

7.2. Future directions

7.2.1. Expression of TIMPs in cardiac diseases

We found that TIMP1, TIMP3 and TIMP4 have differential roles in cardiac diseases. TIMPs have been reported to have a number of MMP-independent and divergent roles in heart diseases. The studies described in this thesis report various differential roles in heart failure. We still have not been able to address the question of what regulates TIMPs expression in response to each cardiac injury. Therefore, further studies using cell culture models and different stimulus are required to answer this question. For example, expression of TIMPs in endothelial cells can be studied using shear stress as the stimulus which can modulate angiogenesis.

7.2.2. Role of TIMPs in macrophage polarization

Monocyte adherence to the ECM initiates its conversion to macrophages and stimulates expression of cytokines (mainly TNFα, M-CSF, TGFα and TGFβ, IL1) which further contribute to macrophage survival, cardiac fibrosis, chemoattractants. Macrophage activation is a heterogeneous process that results in generation of different classes of cells with diverse immunological function. There are two different macrophage activation patterns: Classical (M1) /Pro-inflammatory and alternative (M2)/Anti-inflammatory which show different cell marker expression patterns. M1 macrophages express CCl3, INFγ, IL1β, IL6 and TNF-α and contribute to ECM destruction while M2 macrophages express Arg1, CD163, MRC1, TGFβ, Ym1 thereby contributing to ECM accumulation.[200, 249] TIMP3 deficient mice in response to Ang-II or MI showed significantly higher infiltration of macrophages and further ECM remodeling.[60, 206] Similarly, TIMP2 deficiency resulted in higher macrophage infiltration post-MI or TAC which further caused MT1-MMP activation and ECM remodeling.[61, 204] These studies suggest that TIMPs regulate pro-inflammatory phenotype of macrophages but further investigations are needed for the role of TIMPs in macrophage activation and the shift in macrophage activation to M1 or M2 pathways. [405]

CHAPTER 8

REFERENCES

1.Gadher SJ, Eyre DR, Duance VC, Wotton SF, Heck LW, Schmid TM and Woolley DE. Susceptibility of cartilage collagens type II, IX, X, and XI to human synovial collagenase and neutrophil elastase. *European journal of biochemistry / FEBS*. 1988;175:1-7.
2.Burchfield JS, Xie M and Hill JA. Pathological ventricular remodeling: mechanisms: part 1 of 2. *Circulation*. 2013;128:388-400.
3.Heidenreich PA, Trogdon JG, Khavjou OA, Butler J, Dracup K, Ezekowitz MD, Finkelstein EA, Hong Y, Johnston SC, Khera A, Lloyd-Jones DM, Nelson SA, Nichol G, Orenstein D, Wilson PW and Woo YJ. Forecasting the future of cardiovascular disease in the United States: a policy statement from the American Heart Association. *Circulation*. 2011;123:933-44.
4.Schmitt JP, Kamisago M, Asahi M, Li GH, Ahmad F, Mende U, Kranias EG, MacLennan DH, Seidman JG and Seidman CE. Dilated cardiomyopathy and heart failure caused by a mutation in phospholamban. *Science*. 2003;299:1410-3.
5.Kiss E, Edes I, Sato Y, Luo W, Liggett SB and Kranias EG. beta-Adrenergic regulation of cAMP and protein phosphorylation in phospholamban-knockout mouse hearts. *Am J Physiol*. 1997;272:H785-90.
6.Li L, Chu G, Kranias EG and Bers DM. Cardiac myocyte calcium transport in phospholamban knockout mouse: relaxation and endogenous CaMKII effects. *Am J Physiol*. 1998;274:H1335-47.
7.Kiriazis H, Sato Y, Kadambi VJ, Schmidt AG, Gerst MJ, Hoit BD and Kranias EG. Hypertrophy and functional alterations in hyperdynamic phospholamban-knockout mouse hearts under chronic aortic stenosis. *Cardiovasc Res*. 2002;53:372-81.
8.Souders CA, Bowers SL and Baudino TA. Cardiac fibroblast: the renaissance cell. *Circ Res*. 2009;105:1164-76.
9.Fan D, Takawale A, Lee J and Kassiri Z. Cardiac fibroblasts, fibrosis and extracellular matrix remodeling in heart disease. *Fibrogenesis Tissue Repair*. 2012;5:15.
10.Abrial M, Da Silva CC, Pillot B, Augeul L, Ivanes F, Teixeira G, Cartier R, Angoulvant D, Ovize M and Ferrera R. Cardiac fibroblasts protect cardiomyocytes against lethal ischemia-reperfusion injury. *J Mol Cell Cardiol*. 2014;68:56-65.
11.Giordano FJ, Ping P, McKirnan MD, Nozaki S, DeMaria AN, Dillmann WH, Mathieu-Costello O and Hammond HK. Intracoronary gene transfer of fibroblast growth factor-5 increases blood flow and contractile function in an ischemic region of the heart. *Nat Med*. 1996;2:534-9.
12.Takawale A, Fan D, Basu R, Shen M, Parajuli N, Wang W, Wang X, Oudit GY and Kassiri Z. Myocardial recovery from ischemia-reperfusion is compromised in the absence of tissue inhibitor of metalloproteinase 4. *Circ Heart Fail*. 2014;7:652-62.
13.Takeda N, Manabe I, Uchino Y, Eguchi K, Matsumoto S, Nishimura S, Shindo T, Sano M, Otsu K, Snider P, Conway SJ and Nagai R. Cardiac fibroblasts are essential for the adaptive response of the murine heart to pressure overload. *J Clin Invest*. 2010;120:254-65.
14.Kakkar R and Lee RT. Intramyocardial fibroblast myocyte communication. *Circ Res*. 2010;106:47-57.
15.Ram R, Mickelsen DM, Theodoropoulos C and Blaxall BC. New approaches in small animal echocardiography: imaging the sounds of silence. *Am J Physiol Heart Circ Physiol*. 2011;301:H1765-80.
16.Oh JKS, James B.; Tajik, A. Jamil. *Echo Manual, 3rd Edition*; 2006.
17.Kaddoura S. *Echo Made Easy, 2nd Edition*; 2008.
18.Zhang Y, Takagawa J, Sievers RE, Khan MF, Viswanathan MN, Springer ML, Foster E and Yeghiazarians Y. Validation of the wall motion score and myocardial performance indexes as novel techniques to assess cardiac function in mice after myocardial infarction. *Am J Physiol Heart Circ Physiol*. 2007;292:H1187-92.
19.Moller JE, Hillis GS, Oh JK, Reeder GS, Gersh BJ and Pellikka PA. Wall motion score index and ejection fraction for risk stratification after acute myocardial infarction. *Am Heart J*. 2006;151:419-25.
20.Borlaug BA and Paulus WJ. Heart failure with preserved ejection fraction: pathophysiology, diagnosis, and treatment. *Eur Heart J*. 2011;32:670-9.

21.Little WC and Oh JK. Echocardiographic evaluation of diastolic function can be used to guide clinical care. *Circulation*. 2009;120:802-9.
22.Groban L and Dolinski SY. Transesophageal echocardiographic evaluation of diastolic function. *Chest*. 2005;128:3652-63.
23.Burkhoff D, Mirsky I and Suga H. Assessment of systolic and diastolic ventricular properties via pressure-volume analysis: a guide for clinical, translational, and basic researchers. *Am J Physiol Heart Circ Physiol*. 2005;289:H501-12.
24.Sagawa K. M, W.L; Suga, H. and Sunagawa, K. *Cardiac Contraction and the Pressure-Volume Relationship*; 1988.
25.Pacher P, Nagayama T, Mukhopadhyay P, Batkai S and Kass DA. Measurement of cardiac function using pressure-volume conductance catheter technique in mice and rats. *Nat Protoc*. 2008;3:1422-34.
26.Baan J, van der Velde ET, de Bruin HG, Smeenk GJ, Koops J, van Dijk AD, Temmerman D, Senden J and Buis B. Continuous measurement of left ventricular volume in animals and humans by conductance catheter. *Circulation*. 1984;70:812-23.
27.Heusch G. Molecular basis of cardioprotection: signal transduction in ischemic pre-, post-, and remote conditioning. *Circ Res*. 2015;116:674-99.
28.Yang X, Cohen MV and Downey JM. Mechanism of cardioprotection by early ischemic preconditioning. *Cardiovasc Drugs Ther*. 2010;24:225-34.
29.Hensley K, Robinson KA, Gabbita SP, Salsman S and Floyd RA. Reactive oxygen species, cell signaling, and cell injury. *Free Radic Biol Med*. 2000;28:1456-62.
30.Sivasubramanian N, Coker ML, Kurrelmeyer KM, MacLellan WR, DeMayo FJ, Spinale FG and Mann DL. Left ventricular remodeling in transgenic mice with cardiac restricted overexpression of tumor necrosis factor. *Circulation*. 2001;104:826-31.
31.Frangogiannis NG. Pathophysiology of Myocardial Infarction. *Compr Physiol*. 2015;5:1841-75.
32.Hori M and Nishida K. Oxidative stress and left ventricular remodelling after myocardial infarction. *Cardiovasc Res*. 2009;81:457-64.
33.Takimoto E and Kass DA. Role of oxidative stress in cardiac hypertrophy and remodeling. *Hypertension*. 2007;49:241-8.
34.Maack C, Kartes T, Kilter H, Schafers HJ, Nickenig G, Bohm M and Laufs U. Oxygen free radical release in human failing myocardium is associated with increased activity of rac1-GTPase and represents a target for statin treatment. *Circulation*. 2003;108:1567-74.
35.Giordano FJ. Oxygen, oxidative stress, hypoxia, and heart failure. *J Clin Invest*. 2005;115:500-8.
36.Mani K and Kitsis RN. Myocyte apoptosis: programming ventricular remodeling. *J Am Coll Cardiol*. 2003;41:761-4.
37.Abbate A, Biondi-Zoccai GG, Bussani R, Dobrina A, Camilot D, Feroce F, Rossiello R, Baldi F, Silvestri F, Biasucci LM and Baldi A. Increased myocardial apoptosis in patients with unfavorable left ventricular remodeling and early symptomatic post-infarction heart failure. *J Am Coll Cardiol*. 2003;41:753-60.
38.Prabhu SD and Frangogiannis NG. The Biological Basis for Cardiac Repair After Myocardial Infarction: From Inflammation to Fibrosis. *Circ Res*. 2016;119:91-112.
39.Levine B, Kalman J, Mayer L, Fillit HM and Packer M. Elevated circulating levels of tumor necrosis factor in severe chronic heart failure. *N Engl J Med*. 1990;323:236-41.
40.Torre-Amione G, Kapadia S, Benedict C, Oral H, Young JB and Mann DL. Proinflammatory cytokine levels in patients with depressed left ventricular ejection fraction: a report from the Studies of Left Ventricular Dysfunction (SOLVD). *J Am Coll Cardiol*. 1996;27:1201-6.
41.Tarzami ST, Cheng R, Miao W, Kitsis RN and Berman JW. Chemokine expression in myocardial ischemia: MIP-2 dependent MCP-1 expression protects cardiomyocytes from cell death. *J Mol Cell Cardiol*. 2002;34:209-21.

42.Gwechenberger M, Mendoza LH, Youker KA, Frangogiannis NG, Smith CW, Michael LH and Entman ML. Cardiac myocytes produce interleukin-6 in culture and in viable border zone of reperfused infarctions. *Circulation*. 1999;99:546-51.
43.Zhu M, Goetsch SC, Wang Z, Luo R, Hill JA, Schneider J, Morris SM, Jr. and Liu ZP. FoxO4 promotes early inflammatory response upon myocardial infarction via endothelial Arg1. *Circ Res*. 2015;117:967-77.
44.Kumar AG, Ballantyne CM, Michael LH, Kukielka GL, Youker KA, Lindsey ML, Hawkins HK, Birdsall HH, MacKay CR, LaRosa GJ, Rossen RD, Smith CW and Entman ML. Induction of monocyte chemoattractant protein-1 in the small veins of the ischemic and reperfused canine myocardium. *Circulation*. 1997;95:693-700.
45.Frangogiannis NG, Mendoza LH, Lewallen M, Michael LH, Smith CW and Entman ML. Induction and suppression of interferon-inducible protein 10 in reperfused myocardial infarcts may regulate angiogenesis. *Faseb j*. 2001;15:1428-30.
46.Maroko PR, Carpenter CB, Chiariello M, Fishbein MC, Radvany P, Knostman JD and Hale SL. Reduction by cobra venom factor of myocardial necrosis after coronary artery occlusion. *J Clin Invest*. 1978;61:661-70.
47.Mullane KM, Read N, Salmon JA and Moncada S. Role of leukocytes in acute myocardial infarction in anesthetized dogs: relationship to myocardial salvage by anti-inflammatory drugs. *J Pharmacol Exp Ther*. 1984;228:510-22.
48.Romson JL, Hook BG, Kunkel SL, Abrams GD, Schork MA and Lucchesi BR. Reduction of the extent of ischemic myocardial injury by neutrophil depletion in the dog. *Circulation*. 1983;67:1016-23.
49.Frey N, Katus HA, Olson EN and Hill JA. Hypertrophy of the heart: a new therapeutic target? *Circulation*. 2004;109:1580-9.
50.Norton GR, Woodiwiss AJ, Gaasch WH, Mela T, Chung ES, Aurigemma GP and Meyer TE. Heart failure in pressure overload hypertrophy. The relative roles of ventricular remodeling and myocardial dysfunction. *J Am Coll Cardiol*. 2002;39:664-71.
51.Imamura T, McDermott PJ, Kent RL, Nagatsu M, Cooper Gt and Carabello BA. Acute changes in myosin heavy chain synthesis rate in pressure versus volume overload. *Circ Res*. 1994;75:418-25.
52.Rockman HA, Chien KR, Choi DJ, Iaccarino G, Hunter JJ, Ross J, Jr., Lefkowitz RJ and Koch WJ. Expression of a beta-adrenergic receptor kinase 1 inhibitor prevents the development of myocardial failure in gene-targeted mice. *Proc Natl Acad Sci U S A*. 1998;95:7000-5.
53.Schmidt U, del Monte F, Miyamoto MI, Matsui T, Gwathmey JK, Rosenzweig A and Hajjar RJ. Restoration of diastolic function in senescent rat hearts through adenoviral gene transfer of sarcoplasmic reticulum Ca(2+)-ATPase. *Circulation*. 2000;101:790-6.
54.Chiang CS, Huang CH, Chieng H, Chang YT, Chang D, Chen JJ, Chen YC, Chen YH, Shin HS, Campbell KP and Chen CC. The Ca(v)3.2 T-type Ca(2+) channel is required for pressure overload-induced cardiac hypertrophy in mice. *Circ Res*. 2009;104:522-30.
55.Scamps F, Mayoux E, Charlemagne D and Vassort G. Calcium current in single cells isolated from normal and hypertrophied rat heart. Effects of beta-adrenergic stimulation. *Circ Res*. 1990;67:199-208.
56.Boluyt MO, O'Neill L, Meredith AL, Bing OH, Brooks WW, Conrad CH, Crow MT and Lakatta EG. Alterations in cardiac gene expression during the transition from stable hypertrophy to heart failure. Marked upregulation of genes encoding extracellular matrix components. *Circ Res*. 1994;75:23-32.
57.Weber KT and Brilla CG. Pathological hypertrophy and cardiac interstitium. Fibrosis and renin-angiotensin-aldosterone system. *Circulation*. 1991;83:1849-65.
58.Swynghedauw B. Molecular mechanisms of myocardial remodeling. *Physiol Rev*. 1999;79:215-62.
59.Lorell BH and Carabello BA. Left ventricular hypertrophy: pathogenesis, detection, and prognosis. *Circulation*. 2000;102:470-9.

60.Fan D, Takawale A, Basu R, Patel V, Lee J, Kandalam V, Wang X, Oudit GY and Kassiri Z. Differential role of TIMP2 and TIMP3 in cardiac hypertrophy, fibrosis, and diastolic dysfunction. *Cardiovasc Res*. 2014;103:268-80.
61.Kandalam V, Basu R, Moore L, Fan D, Wang X, Jaworski DM, Oudit GY and Kassiri Z. Lack of Tissue Inhibitor of Metalloproteinases 2 Leads to Exacerbated Left Ventricular Dysfunction and Adverse Extracellular Matrix Remodeling in Response to Biomechanical Stress. *Circulation*. 2011;124:2094-105.
62.Weber KT. Cardiac interstitium in health and disease: the fibrillar collagen network. *J Am Coll Cardiol*. 1989;13:1637-52.
63.Prockop DJ and Kivirikko KI. Collagens: molecular biology, diseases, and potentials for therapy. *Annu Rev Biochem*. 1995;64:403-34.
64.Shamhart PE and Meszaros JG. Non-fibrillar collagens: key mediators of post-infarction cardiac remodeling? *J Mol Cell Cardiol*. 2010;48:530-7.
65.Kadler KE, Baldock C, Bella J and Boot-Handford RP. Collagens at a glance. *J Cell Sci*. 2007;120:1955-8.
66.Vuorio E and de Crombrugghe B. The family of collagen genes. *Annu Rev Biochem*. 1990;59:837-72.
67.Segura AM, Frazier OH and Buja LM. Fibrosis and heart failure. *Heart Fail Rev*. 2012.
68.Jugdutt BI. Remodeling of the myocardium and potential targets in the collagen degradation and synthesis pathways. *Curr Drug Targets Cardiovasc Haematol Disord*. 2003;3:1-30.
69.Lamande SR and Bateman JF. Procollagen folding and assembly: the role of endoplasmic reticulum enzymes and molecular chaperones. *Semin Cell Dev Biol*. 1999;10:455-64.
70.Jin L, Pahuja KB, Wickliffe KE, Gorur A, Baumgartel C, Schekman R and Rape M. Ubiquitin-dependent regulation of COPII coat size and function. *Nature*. 2012;482:495-500.
71.Kobayashi K, Luo M, Zhang Y, Wilkes DC, Ge G, Grieskamp T, Yamada C, Liu TC, Huang G, Basson CT, Kispert A, Greenspan DS and Sato TN. Secreted Frizzled-related protein 2 is a procollagen C proteinase enhancer with a role in fibrosis associated with myocardial infarction. *Nat Cell Biol*. 2009;11:46-55.
72.Baicu CF, Zhang Y, Van Laer AO, Renaud L, Zile MR and Bradshaw AD. Effects of the absence of procollagen C-endopeptidase enhancer-2 on myocardial collagen accumulation in chronic pressure overload. *Am J Physiol Heart Circ Physiol*. 2012;303:H234-40.
73.Steiglitz BM, Keene DR and Greenspan DS. PCOLCE2 encodes a functional procollagen C-proteinase enhancer (PCPE2) that is a collagen-binding protein differing in distribution of expression and post-translational modification from the previously described PCPE1. *J Biol Chem*. 2002;277:49820-30.
74.Vadon-Le Goff S, Kronenberg D, Bourhis JM, Bijakowski C, Raynal N, Ruggiero F, Farndale RW, Stocker W, Hulmes DJ and Moali C. Procollagen C-proteinase enhancer stimulates procollagen processing by binding to the C-propeptide region only. *J Biol Chem*. 2011;286:38932-8.
75.Goldsmith EC, Bradshaw AD and Spinale FG. Cellular mechanisms of tissue fibrosis. 2. Contributory pathways leading to myocardial fibrosis: moving beyond collagen expression. *Am J Physiol Cell Physiol*. 2013;304:C393-402.
76.Broder C, Arnold P, Vadon-Le Goff S, Konerding MA, Bahr K, Muller S, Overall CM, Bond JS, Koudelka T, Tholey A, Hulmes DJ, Moali C and Becker-Pauly C. Metalloproteases meprin alpha and meprin beta are C- and N-procollagen proteinases important for collagen assembly and tensile strength. *Proc Natl Acad Sci U S A*. 2013;110:14219-24.
77.Zuurmond AM, van der Slot-Verhoeven AJ, van Dura EA, De Groot J and Bank RA. Minoxidil exerts different inhibitory effects on gene expression of lysyl hydroxylase 1, 2, and 3: implications for collagen cross-linking and treatment of fibrosis. *Matrix Biol*. 2005;24:261-70.
78.Eyre D, Shao P, Weis MA and Steinmann B. The kyphoscoliotic type of Ehlers-Danlos syndrome (type VI): differential effects on the hydroxylation of lysine in collagens I and II revealed by analysis of cross-linked telopeptides from urine. *Mol Genet Metab*. 2002;76:211-6.
79.Takawale A, Sakamuri SS and Kassiri Z. Extracellular matrix communication and turnover in cardiac physiology and pathology. *Compr Physiol*. 2015;5:687-719.

80.Frangogiannis NG. Matricellular proteins in cardiac adaptation and disease. *Physiol Rev*. 2012;92:635-88.
81.Fitzgerald MC and Schwarzbauer JE. Importance of the basement membrane protein SPARC for viability and fertility in Caenorhabditis elegans. *Curr Biol*. 1998;8:1285-8.
82.Myers DL, Harmon KJ, Lindner V and Liaw L. Alterations of arterial physiology in osteopontin-null mice. *Arterioscler Thromb Vasc Biol*. 2003;23:1021-8.
83.Schellings MW, Vanhoutte D, Swinnen M, Cleutjens JP, Debets J, van Leeuwen RE, d'Hooge J, Van de Werf F, Carmeliet P, Pinto YM, Sage EH and Heymans S. Absence of SPARC results in increased cardiac rupture and dysfunction after acute myocardial infarction. *J Exp Med*. 2009;206:113-23.
84.Murry CE, Giachelli CM, Schwartz SM and Vracko R. Macrophages express osteopontin during repair of myocardial necrosis. *Am J Pathol*. 1994;145:1450-62.
85.Trueblood NA, Xie Z, Communal C, Sam F, Ngoy S, Liaw L, Jenkins AW, Wang J, Sawyer DB, Bing OH, Apstein CS, Colucci WS and Singh K. Exaggerated left ventricular dilation and reduced collagen deposition after myocardial infarction in mice lacking osteopontin. *Circ Res*. 2001;88:1080-7.
86.Ross RS and Borg TK. Integrins and the myocardium. *Circ Res*. 2001;88:1112-9.
87.Manso AM, Elsherif L, Kang SM and Ross RS. Integrins, membrane-type matrix metalloproteinases and ADAMs: potential implications for cardiac remodeling. *Cardiovasc Res*. 2006;69:574-84.
88.Halper J and Kjaer M. Basic components of connective tissues and extracellular matrix: elastin, fibrillin, fibulins, fibrinogen, fibronectin, laminin, tenascins and thrombospondins. *Adv Exp Med Biol*. 2014;802:31-47.
89.Wang J, Hoshijima M, Lam J, Zhou Z, Jokiel A, Dalton ND, Hultenby K, Ruiz-Lozano P, Ross J, Jr., Tryggvason K and Chien KR. Cardiomyopathy associated with microcirculation dysfunction in laminin alpha4 chain-deficient mice. *J Biol Chem*. 2006;281:213-20.
90.Ramirez F, Sakai LY, Dietz HC and Rifkin DB. Fibrillin microfibrils: multipurpose extracellular networks in organismal physiology. *Physiol Genomics*. 2004;19:151-4.
91. Ramirez F and Sakai LY. Biogenesis and function of fibrillin assemblies. *Cell Tissue Res*. 2010;339:71-82.
92.Canadas V, Vilacosta I, Bruna I and Fuster V. Marfan syndrome. Part 1: pathophysiology and diagnosis. *Nat Rev Cardiol*. 2010;7:256-65.
93. Couchman JR, Austria MR and Woods A. Fibronectin-cell interactions. *J Invest Dermatol*. 1990;94:7s-14s.
94.Magnusson MK and Mosher DF. Fibronectin: structure, assembly, and cardiovascular implications. *Arterioscler Thromb Vasc Biol*. 1998;18:1363-70.
95.To WS and Midwood KS. Plasma and cellular fibronectin: distinct and independent functions during tissue repair. *Fibrogenesis Tissue Repair*. 2011;4:21.
96.Allio AE and McKeown-Longo PJ. Extracellular matrix assembly of cell-derived and plasma-derived fibronectins by substrate-attached fibroblasts. *J Cell Physiol*. 1988;135:459-66.
97.Kuhn K. Basement membrane (type IV) collagen. *Matrix Biol*. 1995;14:439-45.
98.Farhadian F, Contard F, Sabri A, Samuel JL and Rappaport L. Fibronectin and basement membrane in cardiovascular organogenesis and disease pathogenesis. *Cardiovasc Res*. 1996;32:433-42.
99.Chapman D, Weber KT and Eghbali M. Regulation of fibrillar collagen types I and III and basement membrane type IV collagen gene expression in pressure overloaded rat myocardium. *Circ Res*. 1990;67:787-94.
100.Ohsato K, Shimizu M, Sugihara N, Ino H, Yoshio H, Takagi Y and Takeda R. Type IV collagen in hypertrophic cardiomyopathy. *Jpn Heart J*. 1994;35:311-21.
101.Fan D, Creemers EE and Kassiri Z. Matrix as an interstitial transport system. *Circ Res*. 2014;114:889-902.

102.Gross J and Lapiere CM. Collagenolytic activity in amphibian tissues: a tissue culture assay. *Proc Natl Acad Sci U S A*. 1962;48:1014-22.
103.Nissinen L and Kahari VM. Matrix metalloproteinases in inflammation. *Biochim Biophys Acta*. 2014.
104.Vincenti MP, Coon CI, Mengshol JA, Yocum S, Mitchell P and Brinckerhoff CE. Cloning of the gene for interstitial collagenase-3 (matrix metalloproteinase-13) from rabbit synovial fibroblasts: differential expression with collagenase-1 (matrix metalloproteinase-1). *Biochem J*. 1998;331 (Pt 1):341-6.
105.Visse R and Nagase H. Matrix metalloproteinases and tissue inhibitors of metalloproteinases: structure, function, and biochemistry. *Circ Res*. 2003;92:827-39.
106.Nuttall RK, Sampieri CL, Pennington CJ, Gill SE, Schultz GA and Edwards DR. Expression analysis of the entire MMP and TIMP gene families during mouse tissue development. *FEBS Lett*. 2004;563:129-34.
107.Aimes RT and Quigley JP. Matrix metalloproteinase-2 is an interstitial collagenase. Inhibitor-free enzyme catalyzes the cleavage of collagen fibrils and soluble native type I collagen generating the specific 3/4- and 1/4-length fragments. *J Biol Chem*. 1995;270:5872-6.
108.Patterson ML, Atkinson SJ, Knauper V and Murphy G. Specific collagenolysis by gelatinase A, MMP-2, is determined by the hemopexin domain and not the fibronectin-like domain. *FEBS Lett*. 2001;503:158-62.
109.Atkinson SJ, Patterson ML, Butler MJ and Murphy G. Membrane type 1 matrix metalloproteinase and gelatinase A synergistically degrade type 1 collagen in a cell model. *FEBS Lett*. 2001;491:222-6.
110.Thompson RW, Holmes DR, Mertens RA, Liao S, Botney MD, Mecham RP, Welgus HG and Parks WC. Production and localization of 92-kilodalton gelatinase in abdominal aortic aneurysms. An elastolytic metalloproteinase expressed by aneurysm-infiltrating macrophages. *J Clin Invest*. 1995;96:318-26.
111.Suzuki K, Enghild JJ, Morodomi T, Salvesen G and Nagase H. Mechanisms of activation of tissue procollagenase by matrix metalloproteinase 3 (stromelysin). *Biochemistry*. 1990;29:10261-70.
112.Murphy G, Segain JP, O'Shea M, Cockett M, Ioannou C, Lefebvre O, Chambon P and Basset P. The 28-kDa N-terminal domain of mouse stromelysin-3 has the general properties of a weak metalloproteinase. *J Biol Chem*. 1993;268:15435-41.
113.Strongin AY, Collier I, Bannikov G, Marmer BL, Grant GA and Goldberg GI. Mechanism of cell surface activation of 72-kDa type IV collagenase. Isolation of the activated form of the membrane metalloprotease. *J Biol Chem*. 1995;270:5331-8.
114.Morrison CJ, Butler GS, Bigg HF, Roberts CR, Soloway PD and Overall CM. Cellular activation of MMP-2 (gelatinase A) by MT2-MMP occurs via a TIMP-2-independent pathway. *J Biol Chem*. 2001;276:47402-10.
115.Barbolina MV and Stack MS. Membrane type 1-matrix metalloproteinase: substrate diversity in pericellular proteolysis. *Semin Cell Dev Biol*. 2008;19:24-33.
116.Takino T, Saeki H, Miyamori H, Kudo T and Sato H. Inhibition of membrane-type 1 matrix metalloproteinase at cell-matrix adhesions. *Cancer Res*. 2007;67:11621-9.
117.Shen XM, Wu YP, Feng YB, Luo ML, Du XL, Zhang Y, Cai Y, Xu X, Han YL, Zhang X, Zhan QM and Wang MR. Interaction of MT1-MMP and laminin-5gamma2 chain correlates with metastasis and invasiveness in human esophageal squamous cell carcinoma. *Clin Exp Metastasis*. 2007;24:541-50.
118.Shapiro SD, Kobayashi DK and Ley TJ. Cloning and characterization of a unique elastolytic metalloproteinase produced by human alveolar macrophages. *J Biol Chem*. 1993;268:23824-9.
119.Shipley JM, Wesselschmidt RL, Kobayashi DK, Ley TJ and Shapiro SD. Metalloelastase is required for macrophage-mediated proteolysis and matrix invasion in mice. *Proc Natl Acad Sci U S A*. 1996;93:3942-6.
120.Kolb C, Mauch S, Peter HH, Krawinkel U and Sedlacek R. The matrix metalloproteinase RASI-1 is expressed in synovial blood vessels of a rheumatoid arthritis patient. *Immunol Lett*. 1997;57:83-8.

121.Yang M and Kurkinen M. Cloning and characterization of a novel matrix metalloproteinase (MMP), CMMP, from chicken embryo fibroblasts. CMMP, Xenopus XMMP, and human MMP19 have a conserved unique cysteine in the catalytic domain. *J Biol Chem*. 1998;273:17893-900.
122.Pei D, Kang T and Qi H. Cysteine array matrix metalloproteinase (CA-MMP)/MMP-23 is a type II transmembrane matrix metalloproteinase regulated by a single cleavage for both secretion and activation. *J Biol Chem*. 2000;275:33988-97.
123.Velasco G, Pendas AM, Fueyo A, Knauper V, Murphy G and Lopez-Otin C. Cloning and characterization of human MMP-23, a new matrix metalloproteinase predominantly expressed in reproductive tissues and lacking conserved domains in other family members. *J Biol Chem*. 1999;274:4570-6.
124.Nagase H, Enghild JJ, Suzuki K and Salvesen G. Stepwise activation mechanisms of the precursor of matrix metalloproteinase 3 (stromelysin) by proteinases and (4-aminophenyl)mercuric acetate. *Biochemistry*. 1990;29:5783-9.
125.Van Wart HE and Birkedal-Hansen H. The cysteine switch: a principle of regulation of metalloproteinase activity with potential applicability to the entire matrix metalloproteinase gene family. *Proc Natl Acad Sci U S A*. 1990;87:5578-82.
126.Lijnen HR. Plasmin and matrix metalloproteinases in vascular remodeling. *Thromb Haemost*. 2001;86:324-33.
127.Ali MA, Cho WJ, Hudson B, Kassiri Z, Granzier H and Schulz R. Titin is a target of matrix metalloproteinase-2: implications in myocardial ischemia/reperfusion injury. *Circulation*. 2010;122:2039-47.
128.Takino T, Sato H, Shinagawa A and Seiki M. Identification of the second membrane-type matrix metalloproteinase (MT-MMP-2) gene from a human placenta cDNA library. MT-MMPs form a unique membrane-type subclass in the MMP family. *J Biol Chem*. 1995;270:23013-20.
129.Llano E, Pendas AM, Freije JP, Nakano A, Knauper V, Murphy G and Lopez-Otin C. Identification and characterization of human MT5-MMP, a new membrane-bound activator of progelatinase a overexpressed in brain tumors. *Cancer Res*. 1999;59:2570-6.
130.Velasco G, Cal S, Merlos-Suarez A, Ferrando AA, Alvarez S, Nakano A, Arribas J and Lopez-Otin C. Human MT6-matrix metalloproteinase: identification, progelatinase A activation, and expression in brain tumors. *Cancer Res*. 2000;60:877-82.
131.English WR, Puente XS, Freije JM, Knauper V, Amour A, Merryweather A, Lopez-Otin C and Murphy G. Membrane type 4 matrix metalloproteinase (MMP17) has tumor necrosis factor-alpha convertase activity but does not activate pro-MMP2. *J Biol Chem*. 2000;275:14046-55.
132.Atkinson SJ, Crabbe T, Cowell S, Ward RV, Butler MJ, Sato H, Seiki M, Reynolds JJ and Murphy G. Intermolecular autolytic cleavage can contribute to the activation of progelatinase A by cell membranes. *J Biol Chem*. 1995;270:30479-85.
133.Zhao H, Bernardo MM, Osenkowski P, Sohail A, Pei D, Nagase H, Kashiwagi M, Soloway PD, DeClerck YA and Fridman R. Differential inhibition of membrane type 3 (MT3)-matrix metalloproteinase (MMP) and MT1-MMP by tissue inhibitor of metalloproteinase (TIMP)-2 and TIMP-3 rgulates pro-MMP-2 activation. *J Biol Chem*. 2004;279:8592-601.
134.Nie J and Pei D. Direct activation of pro-matrix metalloproteinase-2 by leukolysin/membrane-type 6 matrix metalloproteinase/matrix metalloproteinase 25 at the asn(109)-Tyr bond. *Cancer Res*. 2003;63:6758-62.
135.Moore L, Fan D, Basu R, Kandalam V and Kassiri Z. Tissue inhibitor of metalloproteinases (TIMPs) in heart failure. *Heart Fail Rev*. 2012;17:693-706.
136.Will H, Atkinson SJ, Butler GS, Smith B and Murphy G. The soluble catalytic domain of membrane type 1 matrix metalloproteinase cleaves the propeptide of progelatinase A and initiates autoproteolytic activation. Regulation by TIMP-2 and TIMP-3. *J Biol Chem*. 1996;271:17119-23.

137.Adams JC. Thrombospondins: multifunctional regulators of cell interactions. *Annu Rev Cell Dev Biol*. 2001;17:25-51.
138.Amour A, Knight CG, Webster A, Slocombe PM, Stephens PE, Knauper V, Docherty AJ and Murphy G. The in vitro activity of ADAM-10 is inhibited by TIMP-1 and TIMP-3. *FEBS Lett*. 2000;473:275-9.
139.Loechel F, Fox JW, Murphy G, Albrechtsen R and Wewer UM. ADAM 12-S cleaves IGFBP-3 and IGFBP-5 and is inhibited by TIMP-3. *Biochem Biophys Res Commun*. 2000;278:511-5.
140.Amour A, Slocombe PM, Webster A, Butler M, Knight CG, Smith BJ, Stephens PE, Shelley C, Hutton M, Knauper V, Docherty AJ and Murphy G. TNF-alpha converting enzyme (TACE) is inhibited by TIMP-3. *FEBS Lett*. 1998;435:39-44.
141.Kashiwagi M, Tortorella M, Nagase H and Brew K. TIMP-3 is a potent inhibitor of aggrecanase 1 (ADAM-TS4) and aggrecanase 2 (ADAM-TS5). *J Biol Chem*. 2001;276:12501-4.
142.Moore CS and Crocker SJ. An alternate perspective on the roles of TIMPs and MMPs in pathology. *Am J Pathol*. 2012;180:12-6.
143.Seo DW, Li H, Guedez L, Wingfield PT, Diaz T, Salloum R, Wei BY and Stetler-Stevenson WG. TIMP-2 mediated inhibition of angiogenesis: an MMP-independent mechanism. *Cell*. 2003;114:171-80.
144.Gong Y, Scott E, Lu R, Xu Y, Oh WK and Yu Q. TIMP-1 promotes accumulation of cancer associated fibroblasts and cancer progression. *PLoS One*. 2013;8:e77366.
145.Lu Y, Liu S, Zhang S, Cai G, Jiang H, Su H, Li X, Hong Q, Zhang X and Chen X. Tissue inhibitor of metalloproteinase-1 promotes NIH3T3 fibroblast proliferation by activating p-Akt and cell cycle progression. *Mol Cells*. 2011;31:225-30.
146.Watanabe T, Barker TA and Berk BC. Angiotensin II and the endothelium: diverse signals and effects. *Hypertension*. 2005;45:163-9.
147.Hoegy SE, Oh HR, Corcoran ML and Stetler-Stevenson WG. Tissue inhibitor of metalloproteinases-2 (TIMP-2) suppresses TKR-growth factor signaling independent of metalloproteinase inhibition. *J Biol Chem*. 2001;276:3203-14.
148.Nagase H, Visse R and Murphy G. Structure and function of matrix metalloproteinases and TIMPs. *Cardiovasc Res*. 2006;69:562-73.
149.Worley JR, Thompkins PB, Lee MH, Hutton M, Soloway P, Edwards DR, Murphy G and Knauper V. Sequence motifs of tissue inhibitor of metalloproteinases 2 (TIMP-2) determining progelatinase A (proMMP-2) binding and activation by membrane-type metalloproteinase 1 (MT1-MMP). *Biochem J*. 2003;372:799-809.
150.Wei S, Kashiwagi M, Kota S, Xie Z, Nagase H and Brew K. Reactive site mutations in tissue inhibitor of metalloproteinase-3 disrupt inhibition of matrix metalloproteinases but not tumor necrosis factor-alpha-converting enzyme. *J Biol Chem*. 2005;280:32877-82.
151.Morrison CJ and Overall CM. TIMP independence of matrix metalloproteinase (MMP)-2 activation by membrane type 2 (MT2)-MMP is determined by contributions of both the MT2-MMP catalytic and hemopexin C domains. *J Biol Chem*. 2006;281:26528-39.
152.Lambert E, Dasse E, Haye B and Petitfrere E. TIMPs as multifacial proteins. *Crit Rev Oncol Hematol*. 2004;49:187-98.
153.Kadri Z, Petitfrere E, Boudot C, Freyssinier JM, Fichelson S, Mayeux P, Emonard H, Hornebeck W, Haye B and Billat C. Erythropoietin induction of tissue inhibitors of metalloproteinase-1 expression and secretion is mediated by mitogen-activated protein kinase and phosphatidylinositol 3-kinase pathways. *Cell Growth Differ*. 2000;11:573-80.
154.Zhong ZD, Hammani K, Bae WS and DeClerck YA. NF-Y and Sp1 cooperate for the transcriptional activation and cAMP response of human tissue inhibitor of metalloproteinases-2. *J Biol Chem*. 2000;275:18602-10.

155.Li WQ, Qureshi HY, Liacini A, Dehnade F and Zafarullah M. Transforming growth factor Beta1 induction of tissue inhibitor of metalloproteinases 3 in articular chondrocytes is mediated by reactive oxygen species. *Free Radic Biol Med*. 2004;37:196-207.
156.Hoshino Y, Mio T, Nagai S, Ito I, Shigematsu M and Izumi T. Fibrogenic and inflammatory cytokines modulate mRNA expressions of matrix metalloproteinase-3 and tissue inhibitor of metalloproteinase-3 in type II pneumocytes. *Respiration*. 2001;68:509-16.
157.Clark IM, Swingler TE, Sampieri CL and Edwards DR. The regulation of matrix metalloproteinases and their inhibitors. *Int J Biochem Cell Biol*. 2008;40:1362-78.
158.Tong W, Xiong F, Li Y and Zhang L. Hypoxia inhibits cardiomyocyte proliferation in fetal rat hearts via upregulating TIMP-4. *Am J Physiol Regul Integr Comp Physiol*. 2013;304:R613-20.
159.Li YY, McTiernan CF and Feldman AM. Proinflammatory cytokines regulate tissue inhibitors of metalloproteinases and disintegrin metalloproteinase in cardiac cells. *Cardiovasc Res*. 1999;42:162-72.
160.Melendez-Zajgla J, Del Pozo L, Ceballos G and Maldonado V. Tissue inhibitor of metalloproteinases-4. The road less traveled. *Mol Cancer*. 2008;7:85.
161.Clark IM, Rowan AD, Edwards DR, Bech-Hansen T, Mann DA, Bahr MJ and Cawston TE. Transcriptional activity of the human tissue inhibitor of metalloproteinases 1 (TIMP-1) gene in fibroblasts involves elements in the promoter, exon 1 and intron 1. *Biochem J*. 1997;324 (Pt 2):611-7.
162.Hammani K, Blakis A, Morsette D, Bowcock AM, Schmutte C, Henriet P and DeClerck YA. Structure and characterization of the human tissue inhibitor of metalloproteinases-2 gene. *J Biol Chem*. 1996;271:25498-505.
163.Sun Y, Hegamyer G, Kim H, Sithanandam K, Li H, Watts R and Colburn NH. Molecular cloning of mouse tissue inhibitor of metalloproteinases-3 and its promoter. Specific lack of expression in neoplastic JB6 cells may reflect altered gene methylation. *J Biol Chem*. 1995;270:19312-9.
164.Young DA, Phillips BW, Lundy C, Nuttall RK, Hogan A, Schultz GA, Leco KJ, Clark IM and Edwards DR. Identification of an initiator-like element essential for the expression of the tissue inhibitor of metalloproteinases-4 (Timp-4) gene. *Biochem J*. 2002;364:89-99.
165.Zamore PD and Haley B. Ribo-gnome: the big world of small RNAs. *Science*. 2005;309:1519-24.
166.Ambros V. The functions of animal microRNAs. *Nature*. 2004;431:350-5.
167.Wang Z, Wang B, Shi Y, Xu C, Xiao HL, Ma LN, Xu SL, Yang L, Wang QL, Dang WQ, Cui W, Yu SC, Ping YF, Cui YH, Kung HF, Qian C, Zhang X and Bian XW. Oncogenic miR-20a and miR-106a enhance the invasiveness of human glioma stem cells by directly targeting TIMP-2. *Oncogene*. 2014.
168.Dai Y, Xia W, Song T, Su X, Li J, Li S, Chen Y, Wang W, Ding H, Liu X, Li H, Zhao Q and Shao N. MicroRNA-200b is overexpressed in endometrial adenocarcinomas and enhances MMP2 activity by downregulating TIMP2 in human endometrial cancer cell line HEC-1A cells. *Nucleic Acid Ther*. 2013;23:29-34.
169.Li SH, Guo J, Wu J, Sun Z, Han M, Shan SW, Deng Z, Yang BB, Weisel RD and Li RK. miR-17 targets tissue inhibitor of metalloproteinase 1 and 2 to modulate cardiac matrix remodeling. *FASEB J*. 2013;27:4254-65.
170.Garofalo M, Di Leva G, Romano G, Nuovo G, Suh SS, Ngankeu A, Taccioli C, Pichiorri F, Alder H, Secchiero P, Gasparini P, Gonelli A, Costinean S, Acunzo M, Condorelli G and Croce CM. miR-221&222 regulate TRAIL resistance and enhance tumorigenicity through PTEN and TIMP3 downregulation. *Cancer Cell*. 2009;16:498-509.
171.Song B, Wang C, Liu J, Wang X, Lv L, Wei L, Xie L, Zheng Y and Song X. MicroRNA-21 regulates breast cancer invasion partly by targeting tissue inhibitor of metalloproteinase 3 expression. *J Exp Clin Cancer Res*. 2011;29:29.
172.Liu H, Chen SE, Jin B, Carson JA, Niu A, Durham W, Lai JY and Li YP. TIMP3: a physiological regulator of adult myogenesis. *J Cell Sci*. 2010;123:2914-21.

173.Yang X, Du WW, Li H, Liu F, Khorshidi A, Rutnam ZJ and Yang BB. Both mature miR-17-5p and passenger strand miR-17-3p target TIMP3 and induce prostate tumor growth and invasion. *Nucleic Acids Res*. 2013;41:9688-704.
174.Sottrup-Jensen L and Birkedal-Hansen H. Human fibroblast collagenase-alpha-macroglobulin interactions. Localization of cleavage sites in the bait regions of five mammalian alpha-macroglobulins. *J Biol Chem*. 1989;264:393-401.
175.Barrett AJ. Alpha 2-macroglobulin. *Methods Enzymol*. 1981;80 Pt C:737-54.
176.Wang S, Wei X, Zhou J, Zhang J, Li K, Chen Q, Terek R, Fleming BC, Goldring MB, Ehrlich MG, Zhang G and Wei L. Identification of Alpha 2 Macroglobulin (A2M) as a master inhibitor of cartilage degrading factors that attenuates post-traumatic osteoarthritis progression. *Arthritis Rheumatol*. 2014.
177.He H, McCartney DJ, Wei Q, Esadeg S, Zhang J, Foster RA, Hayes MA, Tayade C, Van Leuven F and Croy BA. Characterization of a murine alpha 2 macroglobulin gene expressed in reproductive and cardiovascular tissue. *Biol Reprod*. 2005;72:266-75.
178.Oh J, Takahashi R, Kondo S, Mizoguchi A, Adachi E, Sasahara RM, Nishimura S, Imamura Y, Kitayama H, Alexander DB, Ide C, Horan TP, Arakawa T, Yoshida H, Nishikawa S, Itoh Y, Seiki M, Itohara S, Takahashi C and Noda M. The membrane-anchored MMP inhibitor RECK is a key regulator of extracellular matrix integrity and angiogenesis. *Cell*. 2001;107:789-800.
179.Oh J, Seo DW, Diaz T, Wei B, Ward Y, Ray JM, Morioka Y, Shi S, Kitayama H, Takahashi C, Noda M and Stetler-Stevenson WG. Tissue inhibitors of metalloproteinase 2 inhibits endothelial cell migration through increased expression of RECK. *Cancer Res*. 2004;64:9062-9.
180.Polyakova V, Miyagawa S, Szalay Z, Risteli J and Kostin S. Atrial extracellular matrix remodelling in patients with atrial fibrillation. *J Cell Mol Med*. 2008;12:189-208.
181.Siddesha JM, Valente AJ, Sakamuri SS, Gardner JD, Delafontaine P, Noda M and Chandrasekar B. Acetylsalicylic acid inhibits IL-18-induced cardiac fibroblast migration through the induction of RECK. *J Cell Physiol*. 2014;229:845-55.
182.Siddesha JM, Valente AJ, Sakamuri SS, Yoshida T, Gardner JD, Somanna N, Takahashi C, Noda M and Chandrasekar B. Angiotensin II stimulates cardiac fibroblast migration via the differential regulation of matrixins and RECK. *J Mol Cell Cardiol*. 2013;65:9-18.
183.Mott JD, Thomas CL, Rosenbach MT, Takahara K, Greenspan DS and Banda MJ. Post-translational proteolytic processing of procollagen C-terminal proteinase enhancer releases a metalloproteinase inhibitor. *J Biol Chem*. 2000;275:1384-90.
184.Miyazaki K, Hasegawa M, Funahashi K and Umeda M. A metalloproteinase inhibitor domain in Alzheimer amyloid protein precursor. *Nature*. 1993;362:839-41.
185.Hayashidani S, Tsutsui H, Ikeuchi M, Shiomi T, Matsusaka H, Kubota T, Imanaka-Yoshida K, Itoh T and Takeshita A. Targeted deletion of MMP-2 attenuates early LV rupture and late remodeling after experimental myocardial infarction. *Am J Physiol Heart Circ Physiol*. 2003;285:H1229-35.
186.Matsumura S, Iwanaga S, Mochizuki S, Okamoto H, Ogawa S and Okada Y. Targeted deletion or pharmacological inhibition of MMP-2 prevents cardiac rupture after myocardial infarction in mice. *J Clin Invest*. 2005;115:599-609.
187.Matsusaka H, Ide T, Matsushima S, Ikeuchi M, Kubota T, Sunagawa K, Kinugawa S and Tsutsui H. Targeted deletion of matrix metalloproteinase 2 ameliorates myocardial remodeling in mice with chronic pressure overload. *Hypertension*. 2006;47:711-7.
188.Bergman MR, Teerlink JR, Mahimkar R, Li L, Zhu BQ, Nguyen A, Dahi S, Karliner JS and Lovett DH. Cardiac matrix metalloproteinase-2 expression independently induces marked ventricular remodeling and systolic dysfunction. *Am J Physiol Heart Circ Physiol*. 2007;292:H1847-60.
189.Wang GY, Bergman MR, Nguyen AP, Turcato S, Swigart PM, Rodrigo MC, Simpson PC, Karliner JS, Lovett DH and Baker AJ. Cardiac transgenic matrix metalloproteinase-2 expression directly induces impaired contractility. *Cardiovasc Res*. 2006;69:688-96.

190.Lovett DH, Mahimkar R, Raffai RL, Cape L, Zhu BQ, Jin ZQ, Baker AJ and Karliner JS. N-terminal truncated intracellular matrix metalloproteinase-2 induces cardiomyocyte hypertrophy, inflammation and systolic heart failure. *PLoS One*. 2013;8:e68154.
191.Vanhoutte D, Schellings MW, Gotte M, Swinnen M, Herias V, Wild MK, Vestweber D, Chorianopoulos E, Cortes V, Rigotti A, Stepp MA, Van de Werf F, Carmeliet P, Pinto YM and Heymans S. Increased expression of syndecan-1 protects against cardiac dilatation and dysfunction after myocardial infarction. *Circulation*. 2007;115:475-82.
192.Fears CY and Woods A. The role of syndecans in disease and wound healing. *Matrix Biol*. 2006;25:443-56.
193.Finsen AV, Woldbaek PR, Li J, Wu J, Lyberg T, Tonnessen T and Christensen G. Increased syndecan expression following myocardial infarction indicates a role in cardiac remodeling. *Physiol Genomics*. 2004;16:301-8.
194.Ducharme A, Frantz S, Aikawa M, Rabkin E, Lindsey M, Rohde LE, Schoen FJ, Kelly RA, Werb Z, Libby P and Lee RT. Targeted deletion of matrix metalloproteinase-9 attenuates left ventricular enlargement and collagen accumulation after experimental myocardial infarction. *The Journal of clin investigation*. 2000;106:55-62.
195.Papageorgiou AP and Heymans S. Interactions between the extracellular matrix and inflammation during viral myocarditis. *Immunobiology*. 2012;217:503-10.
196.Marchant D and McManus BM. Matrix metalloproteinases in the pathogenesis of viral heart disease. *Trends Cardiovasc Med*. 2009;19:21-6.
197.Zavadzkas JA, Mukherjee R, Rivers WT, Patel RK, Meyer EC, Black LE, McKinney RA, Oelsen JM, Stroud RE and Spinale FG. Direct regulation of membrane type 1 matrix metalloproteinase following myocardial infarction causes changes in survival, cardiac function, and remodeling. *American journal of physiology Heart and circulatory physiology*. 2011;301:H1656-66.
198.Spinale FG and Zile MR. Integrating the myocardial matrix into heart failure recognition and management. *Circ Res*. 2013;113:725-38.
199.Spinale FG, Janicki JS and Zile MR. Membrane-associated matrix proteolysis and heart failure. *Circ Res*. 2013;112:195-208.
200.Ma Y, Halade GV, Zhang J, Ramirez TA, Levin D, Voorhees A, Jin YF, Han HC, Manicone AM and Lindsey ML. Matrix metalloproteinase-28 deletion exacerbates cardiac dysfunction and rupture after myocardial infarction in mice by inhibiting M2 macrophage activation. *Circ Res*. 2013;112:675-88.
201.Roten L, Nemoto S, Simsic J, Coker ML, Rao V, Baicu S, Defreyte G, Soloway PJ, Zile MR and Spinale FG. Effects of gene deletion of the tissue inhibitor of the matrix metalloproteinase-type 1 (TIMP-1) on left ventricular geometry and function in mice. *J Mol Cell Cardiol*. 2000;32:109-20.
202.Crocker SJ, Frausto RF, Whitmire JK, Benning N, Milner R and Whitton JL. Amelioration of coxsackievirus B3-mediated myocarditis by inhibition of tissue inhibitors of matrix metalloproteinase-1. *Am J Pathol*. 2007;171:1762-73.
203.Ikonomidis JS, Hendrick JW, Parkhurst AM, Herron AR, Escobar PG, Dowdy KB, Stroud RE, Hapke E, Zile MR and Spinale FG. Accelerated LV remodeling after myocardial infarction in TIMP-1-deficient mice: effects of exogenous MMP inhibition. *American journal of physiology Heart and circulatory physiology*. 2005;288:H149-58.
204.Kandalam V, Basu R, Abraham T, Wang X, Soloway PD, Jaworski DM, Oudit GY and Kassiri Z. TIMP2 deficiency accelerates adverse post-myocardial infarction remodeling because of enhanced MT1-MMP activity despite lack of MMP2 activation. *Circ Res*. 2010;106:796-808.
205.Fedak PW, Smookler DS, Kassiri Z, Ohno N, Leco KJ, Verma S, Mickle DA, Watson KL, Hojilla CV, Cruz W, Weisel RD, Li RK and Khokha R. TIMP-3 deficiency leads to dilated cardiomyopathy. *Circulation*. 2004;110:2401-9.

206.Kandalam V, Basu R, Abraham T, Wang X, Awad A, Wang W, Lopaschuk GD, Maeda N, Oudit GY and Kassiri Z. Early activation of matrix metalloproteinases underlies the exacerbated systolic and diastolic dysfunction in mice lacking TIMP3 following myocardial infarction. *Am J Physiol Heart Circ Physiol*. 2010;299:H1012-23.
207.Kassiri Z, Oudit GY, Sanchez O, Dawood F, Mohammed FF, Nuttall RK, Edwards DR, Liu PP, Backx PH and Khokha R. Combination of tumor necrosis factor-alpha ablation and matrix metalloproteinase inhibition prevents heart failure after pressure overload in tissue inhibitor of metalloproteinase-3 knock-out mice. *Circ Res*. 2005;97:380-90.
208.Kassiri Z, Defamie V, Hariri M, Oudit GY, Anthwal S, Dawood F, Liu P and Khokha R. Simultaneous transforming growth factor beta-tumor necrosis factor activation and cross-talk cause aberrant remodeling response and myocardial fibrosis in Timp3-deficient heart. *J Biol Chem*. 2009;284:29893-904.
209. Koskivirta I, Kassiri Z, Rahkonen O, Kiviranta R, Oudit GY, McKee TD, Kyto V, Saraste A, Jokinen E, Liu PP, Vuorio E and Khokha R. Mice with tissue inhibitor of metalloproteinases 4 (Timp4) deletion succumb to induced myocardial infarction but not to cardiac pressure overload. *J Biol Chem*. 2010;285:24487-93.
210.Zavadzkas JA, Stroud RE, Bouges S, Mukherjee R, Jones JR, Patel RK, McDermott PJ and Spinale FG. Targeted overexpression of tissue inhibitor of matrix metalloproteinase-4 modifies post-myocardial infarction remodeling in mice. *Circ Res*. 2014;114:1435-45.
211.Yarbrough WM, Baicu CF, Mukherjee R, Van Laer AO, Rivers WT, McKinney RA, Prescott CB, Stroud RE, Freels PD, Zellars KN, Zile MR and Spinale FG. Cardiac Restricted Overexpression Or Deletion Of Tissue Inhibitor Of Matrix Metalloproteinase-4. *Am J Physiol Heart Circ Physiol*. 2014.
212.Ornitz DM. FGFs, heparan sulfate and FGFRs: complex interactions essential for development. *Bioessays*. 2000;22:108-12.
213.Lin X. Functions of heparan sulfate proteoglycans in cell signaling during development. *Development*. 2004;131:6009-21.
214. Slavin J. Fibroblast growth factors: at the heart of angiogenesis. *Cell Biol Int*. 1995;19:431-44.
215.Zhao T, Zhao W, Chen Y, Ahokas RA and Sun Y. Acidic and basic fibroblast growth factors involved in cardiac angiogenesis following infarction. *Int J Cardiol*. 2011;152:307-13.
216.Powers CJ, McLeskey SW and Wellstein A. Fibroblast growth factors, their receptors and signaling. *Endocr Relat Cancer*. 2000;7:165-97.
217.Lavine KJ, White AC, Park C, Smith CS, Choi K, Long F, Hui CC and Ornitz DM. Fibroblast growth factor signals regulate a wave of Hedgehog activation that is essential for coronary vascular development. *Genes Dev*. 2006;20:1651-66.
218.Hotta Y, Sasaki S, Konishi M, Kinoshita H, Kuwahara K, Nakao K and Itoh N. Fgf16 is required for cardiomyocyte proliferation in the mouse embryonic heart. *Dev Dyn*. 2008;237:2947-54.
219.Buehler A, Martire A, Strohm C, Wolfram S, Fernandez B, Palmen M, Wehrens XH, Doevendans PA, Franz WM, Schaper W and Zimmermann R. Angiogenesis-independent cardioprotection in FGF-1 transgenic mice. *Cardiovasc Res*. 2002;55:768-77.
220.House SL, Branch K, Newman G, Doetschman T and Schultz Jel J. Cardioprotection induced by cardiac-specific overexpression of fibroblast growth factor-2 is mediated by the MAPK cascade. *Am J Physiol Heart Circ Physiol*. 2005;289:H2167-75.
221.Korf-Klingebiel M, Kempf T, Schluter KD, Willenbockel C, Brod T, Heineke J, Schmidt VJ, Jantzen F, Brandes RP, Sugden PH, Drexler H, Molkentin JD and Wollert KC. Conditional transgenic expression of fibroblast growth factor 9 in the adult mouse heart reduces heart failure mortality after myocardial infarction. *Circulation*. 2011;123:504-14.
222.Matsumoto E, Sasaki S, Kinoshita H, Kito T, Ohta H, Konishi M, Kuwahara K, Nakao K and Itoh N. Angiotensin II-induced cardiac hypertrophy and fibrosis are promoted in mice lacking Fgf16. *Genes Cells*. 2013;18:544-53.

223.Taipale J and Keski-Oja J. Growth factors in the extracellular matrix. *FASEB J*. 1997;11:51-9.
224.Shimokawa K, Kimura-Yoshida C, Nagai N, Mukai K, Matsubara K, Watanabe H, Matsuda Y, Mochida K and Matsuo I. Cell surface heparan sulfate chains regulate local reception of FGF signaling in the mouse embryo. *Dev Cell*. 2011;21:257-72.
225.Matsuo I and Kimura-Yoshida C. Extracellular modulation of Fibroblast Growth Factor signaling through heparan sulfate proteoglycans in mammalian development. *Curr Opin Genet Dev*. 2013.
226.Saksela O, Moscatelli D, Sommer A and Rifkin DB. Endothelial cell-derived heparan sulfate binds basic fibroblast growth factor and protects it from proteolytic degradation. *J Cell Biol*. 1988;107:743-51.
227.Muller P, Rogers KW, Yu SR, Brand M and Schier AF. Morphogen transport. *Development*. 2013;140:1621-38.
228.Dowd CJ, Cooney CL and Nugent MA. Heparan sulfate mediates bFGF transport through basement membrane by diffusion with rapid reversible binding. *J Biol Chem*. 1999;274:5236-44.
229.Strand ME, Herum KM, Rana ZA, Skrbic B, Askevold ET, Dahl CP, Vistnes M, Hasic A, Kvaloy H, Sjaastad I, Carlson CR, Tonnessen T, Gullestad L, Christensen G and Lunde IG. Innate immune signaling induces expression and shedding of the heparan sulfate proteoglycan syndecan-4 in cardiac fibroblasts and myocytes, affecting inflammation in the pressure-overloaded heart. *FEBS J*. 2013;280:2228-47.
230.Todorovic V and Rifkin DB. LTBPs, more than just an escort service. *J Cell Biochem*. 2012;113:410-8.
231.Yu Q and Stamenkovic I. Cell surface-localized matrix metalloproteinase-9 proteolytically activates TGF-beta and promotes tumor invasion and angiogenesis. *Genes Dev*. 2000;14:163-76.
232.Mu D, Cambier S, Fjellbirkeland L, Baron JL, Munger JS, Kawakatsu H, Sheppard D, Broaddus VC and Nishimura SL. The integrin alpha(v)beta8 mediates epithelial homeostasis through MT1-MMP-dependent activation of TGF-beta1. *J Cell Biol*. 2002;157:493-507.
233.Wipff PJ and Hinz B. Integrins and the activation of latent transforming growth factor beta1 - an intimate relationship. *Eur J Cell Biol*. 2008;87:601-15.
234.Ge G and Greenspan DS. BMP1 controls TGFbeta1 activation via cleavage of latent TGFbeta-binding protein. *J Cell Biol*. 2006;175:111-20.
235.Lee MK, Pardoux C, Hall MC, Lee PS, Warburton D, Qing J, Smith SM and Derynck R. TGF-beta activates Erk MAP kinase signalling through direct phosphorylation of ShcA. *EMBO J*. 2007;26:3957-67.
236.Yamashita M, Fatyol K, Jin C, Wang X, Liu Z and Zhang YE. TRAF6 mediates Smad-independent activation of JNK and p38 by TGF-beta. *Mol Cell*. 2008;31:918-24.
237.Kang JS, Liu C and Derynck R. New regulatory mechanisms of TGF-beta receptor function. *Trends Cell Biol*. 2009;19:385-94.
238.Nakao A, Afrakhte M, Moren A, Nakayama T, Christian JL, Heuchel R, Itoh S, Kawabata M, Heldin NE, Heldin CH and ten Dijke P. Identification of Smad7, a TGFbeta-inducible antagonist of TGF-beta signalling. *Nature*. 1997;389:631-5.
239.Diez J, Querejeta R, Lopez B, Gonzalez A, Larman M and Martinez Ubago JL. Losartan-dependent regression of myocardial fibrosis is associated with reduction of left ventricular chamber stiffness in hypertensive patients. *Circulation*. 2002;105:2512-7.
240.Harris BS, Zhang Y, Card L, Rivera LB, Brekken RA and Bradshaw AD. SPARC regulates collagen interaction with cardiac fibroblast cell surfaces. *Am J Physiol Heart Circ Physiol*. 2011;301:H841-7.
241.Leening MJ and Steyerberg EW. Fibrosis and mortality in patients with dilated cardiomyopathy. *Jama*. 2013;309:2547-8.
242.Camelliti P, Borg TK and Kohl P. Structural and functional characterisation of cardiac fibroblasts. *Cardiovasc Res*. 2005;65:40-51.
243.Petrov VV, Fagard RH and Lijnen PJ. Stimulation of collagen production by transforming growth factor-beta1 during differentiation of cardiac fibroblasts to myofibroblasts. *Hypertension*. 2002;39:258-63.

244.Houser SR, Margulies KB, Murphy AM, Spinale FG, Francis GS, Prabhu SD, Rockman HA, Kass DA, Molkentin JD and Sussman MA. Animal Models of Heart Failure A Scientific Statement From the American Heart Association. *Circulation research*. 2012;111:131-150.
245.Roger VL, Go AS, Lloyd-Jones DM, Benjamin EJ, Berry JD, Borden WB, Bravata DM, Dai S, Ford ES and Fox CS. Heart Disease and Stroke Statistics—2012 Update A Report From the American Heart Association. *Circulation*. 2012;125:e2-e220.
246.Wynn TA and Ramalingam TR. Mechanisms of fibrosis: therapeutic translation for fibrotic disease. *Nat Med*. 2012;18:1028-40.
247.Vasan RS and Levy D. Defining diastolic heart failure: a call for standardized diagnostic criteria. *Circulation*. 2000;101:2118-21.
248.Aljaroudi W, Alraies MC, Halley C, Rodriguez L, Grimm RA, Thomas JD and Jaber WA. Impact of progression of diastolic dysfunction on mortality in patients with normal ejection fraction. *Circulation*. 2012;125:782-8.
249.Lambert JM, Lopez EF and Lindsey ML. Macrophage roles following myocardial infarction. *Int J Cardiol*. 2008;130:147-58.
250.Widgerow AD. Cellular/extracellular matrix cross-talk in scar evolution and control. *Wound Repair and Regeneration*. 2011;19:117-133.
251.Weber KT, Sun Y, Bhattacharya SK, Ahokas RA and Gerling IC. Myofibroblast-mediated mechanisms of pathological remodelling of the heart. *Nature reviews Cardiology*. 2013;10:15-26.
252.Robert V, Heymes C, Silvestre JS, Sabri A, Swynghedauw B and Delcayre C. Angiotensin AT1 receptor subtype as a cardiac target of aldosterone: role in aldosterone-salt-induced fibrosis. *Hypertension*. 1999;33:981-6.
253.Schnee JM and Hsueh WA. Angiotensin II, adhesion, and cardiac fibrosis. *Cardiovasc Res*. 2000;46:264-8.
254.Lijnen P and Petrov V. Induction of Cardiac Fibrosis by Aldosterone. *Journal of Molecular and Cellular Cardiology*. 2000;32:865-879.
255.Tsukamoto Y, Mano T, Sakata Y, Ohtani T, Takeda Y, Tamaki S, Omori Y, Ikeya Y, Saito Y, Ishii R, Higashimori M, Kaneko M, Miwa T, Yamamoto K and Komuro I. A novel heart failure mice model of hypertensive heart disease by angiotensin II infusion, nephrectomy, and salt loading. *Am J Physiol Heart Circ Physiol*. 2013;305:H1658-67.
256.Sharpe N, Smith H, Murphy J, Greaves S, Hart H and Gamble G. Early prevention of left ventricular dysfunction after myocardial infarction with angiotensin-converting-enzyme inhibition. *Lancet*. 1991;337:872-6.
257.Granger CB, McMurray JJ, Yusuf S, Held P, Michelson EL, Olofsson B, Ostergren J, Pfeffer MA and Swedberg K. Effects of candesartan in patients with chronic heart failure and reduced left-ventricular systolic function intolerant to angiotensin-converting-enzyme inhibitors: the CHARM-Alternative trial. *Lancet*. 2003;362:772-6.
258.Bishop J and Laurent G. Collagen turnover and its regulation in the normal and hypertrophying heart. *European heart journal*. 1995;16:38-44.
259.Felker GM, Thompson RE, Hare JM, Hruban RH, Clemetson DE, Howard DL, Baughman KL and Kasper EK. Underlying causes and long-term survival in patients with initially unexplained cardiomyopathy. *N Engl J Med*. 2000;342:1077-84.
260.Kania G, Blyszczuk P, Stein S, Valaperti A, Germano D, Dirnhofer S, Hunziker L, Matter CM and Eriksson U. Heart-infiltrating prominin-1+/CD133+ progenitor cells represent the cellular source of transforming growth factor beta-mediated cardiac fibrosis in experimental autoimmune myocarditis. *Circ Res*. 2009;105:462-70.
261.Phan SH. The myofibroblast in pulmonary fibrosis. *Chest*. 2002;122:286s-289s.

262.Blyszczuk P, Kania G, Dieterle T, Marty RR, Valaperti A, Berthonneche C, Pedrazzini T, Berger CT, Dirnhofer S, Matter CM, Penninger JM, Luscher TF and Eriksson U. Myeloid differentiation factor-88/interleukin-1 signaling controls cardiac fibrosis and heart failure progression in inflammatory dilated cardiomyopathy. *Circ Res*. 2009;105:912-20.
263.Porter KE and Turner NA. Cardiac fibroblasts: at the heart of myocardial remodeling. *Pharmacol Ther*. 2009;123:255-78.
264.Rutschow S, Leschka S, Westermann D, Puhl K, Weitz A, Ladyszenskij L, Jaeger S, Zeichhardt H, Noutsias M, Schultheiss HP, Tschope C and Pauschinger M. Left ventricular enlargement in coxsackievirus-B3 induced chronic myocarditis--ongoing inflammation and an imbalance of the matrix degrading system. *Eur J Pharmacol*. 2010;630:145-51.
265.Cheung C, Luo H, Yanagawa B, Leong HS, Samarasekera D, Lai JC, Suarez A, Zhang J and McManus BM. Matrix metalloproteinases and tissue inhibitors of metalloproteinases in coxsackievirus-induced myocarditis. *Cardiovasc Pathol*. 2006;15:63-74.
266.Heymans S, Pauschinger M, De Palma A, Kallwellis-Opara A, Rutschow S, Swinnen M, Vanhoutte D, Gao F, Torpai R, Baker AH, Padalko E, Neyts J, Schultheiss HP, Van de Werf F, Carmeliet P and Pinto YM. Inhibition of urokinase-type plasminogen activator or matrix metalloproteinases prevents cardiac injury and dysfunction during viral myocarditis. *Circulation*. 2006;114:565-73.
267.Westermann D, Savvatis K, Schultheiss HP and Tschope C. Immunomodulation and matrix metalloproteinases in viral myocarditis. *J Mol Cell Cardiol*. 2010;48:468-73.
268.Cheung C, Marchant D, Walker EK, Luo Z, Zhang J, Yanagawa B, Rahmani M, Cox J, Overall C, Senior RM, Luo H and McManus BM. Ablation of matrix metalloproteinase-9 increases severity of viral myocarditis in mice. *Circulation*. 2008;117:1574-82.
269.Vanhoutte D, van Almen GC, Van Aelst LN, Van Cleemput J, Droogne W, Jin Y, Van de Werf F, Carmeliet P, Vanhaecke J, Papageorgiou AP and Heymans S. Matricellular proteins and matrix metalloproteinases mark the inflammatory and fibrotic response in human cardiac allograft rejection. *Eur Heart J*. 2013;34:1930-41.
270.Papageorgiou AP, Swinnen M, Vanhoutte D, VandenDriessche T, Chuah M, Lindner D, Verhesen W, de Vries B, D'Hooge J, Lutgens E, Westermann D, Carmeliet P and Heymans S. Thrombospondin-2 prevents cardiac injury and dysfunction in viral myocarditis through the activation of regulatory T-cells. *Cardiovasc Res*. 2012;94:115-24.
271.Szalay G, Sauter M, Haberland M, Zuegel U, Steinmeyer A, Kandolf R and Klingel K. Osteopontin: a fibrosis-related marker molecule in cardiac remodeling of enterovirus myocarditis in the susceptible host. *Circ Res*. 2009;104:851-9.
272.Bradshaw AD, Baicu CF, Rentz TJ, Van Laer AO, Boggs J, Lacy JM and Zile MR. Pressure overload-induced alterations in fibrillar collagen content and myocardial diastolic function: role of secreted protein acidic and rich in cysteine (SPARC) in post-synthetic procollagen processing. *Circulation*. 2009;119:269-80.
273.Xie Z, Singh M and Singh K. Osteopontin modulates myocardial hypertrophy in response to chronic pressure overload in mice. *Hypertension*. 2004;44:826-31.
274.Iyer RP, de Castro Bras LE, Jin YF and Lindsey ML. Translating Koch's postulates to identify matrix metalloproteinase roles in postmyocardial infarction remodeling: cardiac metalloproteinase actions (CarMA) postulates. *Circ Res*. 2014;114:860-71.
275.Peterson JT. The importance of estimating the therapeutic index in the development of matrix metalloproteinase inhibitors. *Cardiovasc Res*. 2006;69:677-87.
276.Brown DL, Desai KK, Vakili BA, Nouneh C, Lee HM and Golub LM. Clinical and biochemical results of the metalloproteinase inhibition with subantimicrobial doses of doxycycline to prevent acute coronary syndromes (MIDAS) pilot trial. *Arterioscler Thromb Vasc Biol*. 2004;24:733-8.

277.Liu G and Chevalier Glatt F. Batimastat (BB94) Anti-Restenosis Trial Utilising the Biodivysio Local Drug Delivery PCstent (BRILLIANT-EU-Trial) - The Final Results. . *Circulation*. 2003;108:(Abstract).
278.Hudson MP, Armstrong PW, Ruzyllo W, Brum J, Cusmano L, Krzeski P, Lyon R, Quinones M, Theroux P, Sydlowski D, Kim HE, Garcia MJ, Jaber WA and Weaver WD. Effects of selective matrix metalloproteinase inhibitor (PG-116800) to prevent ventricular remodeling after myocardial infarction: results of the PREMIER (Prevention of Myocardial Infarction Early Remodeling) trial. *J Am Coll Cardiol*. 2006;48:15-20.
279.Tous E, Purcell B, Ifkovits JL and Burdick JA. Injectable acellular hydrogels for cardiac repair. *J Cardiovasc Transl Res*. 2011;4:528-42.
280.Kofidis T, Lebl DR, Martinez EC, Hoyt G, Tanaka M and Robbins RC. Novel injectable bioartificial tissue facilitates targeted, less invasive, large-scale tissue restoration on the beating heart after myocardial injury. *Circulation*. 2005;112:I173-7.
281.Kofidis T, de Bruin JL, Hoyt G, Lebl DR, Tanaka M, Yamane T, Chang CP and Robbins RC. Injectable bioartificial myocardial tissue for large-scale intramural cell transfer and functional recovery of injured heart muscle. *J Thorac Cardiovasc Surg*. 2004;128:571-8.
282.Huang NF, Yu J, Sievers R, Li S and Lee RJ. Injectable biopolymers enhance angiogenesis after myocardial infarction. *Tissue Eng*. 2005;11:1860-6.
283.Vanhoutte D and Heymans S. TIMPs and cardiac remodeling: 'Embracing the MMP-independent-side of the family'. *J Mol Cell Cardiol*. 2010;48:445-53.
284.Li YY, Feldman AM, Sun Y and McTiernan CF. Differential expression of tissue inhibitors of metalloproteinases in the failing human heart. *Circulation*. 1998;98:1728-34.
285.Schulze CJ, Wang W, Suarez-Pinzon WL, Sawicka J, Sawicki G and Schulz R. Imbalance between tissue inhibitor of metalloproteinase-4 and matrix metalloproteinases during acute myocardial [correction of myoctardial] ischemia-reperfusion injury. *Circulation*. 2003;107:2487-92.
286.Lindsay MM, Maxwell P and Dunn FG. TIMP-1: a marker of left ventricular diastolic dysfunction and fibrosis in hypertension. *Hypertension*. 2002;40:136-41.
287.Heymans S, Schroen B, Vermeersch P, Milting H, Gao F, Kassner A, Gillijns H, Herijgers P, Flameng W, Carmeliet P, Van de Werf F, Pinto YM and Janssens S. Increased cardiac expression of tissue inhibitor of metalloproteinase-1 and tissue inhibitor of metalloproteinase-2 is related to cardiac fibrosis and dysfunction in the chronic pressure-overloaded human heart. *Circulation*. 2005;112:1136-44.
288.Timms PM, Wright A, Maxwell P, Campbell S, Dawnay AB and Srikanthan V. Plasma tissue inhibitor of metalloproteinase-1 levels are elevated in essential hypertension and related to left ventricular hypertrophy. *Am J Hypertens*. 2002;15:269-72.
289.Gonzalez A, Lopez B, Querejeta R, Zubillaga E, Echeverria T and Diez J. Filling pressures and collagen metabolism in hypertensive patients with heart failure and normal ejection fraction. *Hypertension*. 2010;55:1418-24.
290.Parenica J, Nemec P, Tomandl J, Ondrasek J, Pavkova-Goldbergova M, Tretina M, Jarkovsky J, Littnerova S, Poloczek M, Pokorny P, Spinar J, Cermakova Z, Miklik R, Malik P, Pes O, Lipkova J, Tomandlova M and Kala P. Prognostic utility of biomarkers in predicting of one-year outcomes in patients with aortic stenosis treated with transcatheter or surgical aortic valve implantation. *PLoS One*. 2012;7:e48851.
291.Sutton MG and Sharpe N. Left ventricular remodeling after myocardial infarction: pathophysiology and therapy. *Circulation*. 2000;101:2981-8.
292.Quinones MA, Greenberg BH, Kopelen HA, Koilpillai C, Limacher MC, Shindler DM, Shelton BJ and Weiner DH. Echocardiographic predictors of clinical outcome in patients with left ventricular dysfunction enrolled in the SOLVD registry and trials: significance of left ventricular hypertrophy. Studies of Left Ventricular Dysfunction. *J Am Coll Cardiol*. 2000;35:1237-44.

293.Fomovsky GM, Thomopoulos S and Holmes JW. Contribution of extracellular matrix to the mechanical properties of the heart. *J Mol Cell Cardiol*. 2010;48:490-6.
294.Shai SY, Harpf AE, Babbitt CJ, Jordan MC, Fishbein MC, Chen J, Omura M, Leil TA, Becker KD, Jiang M, Smith DJ, Cherry SR, Loftus JC and Ross RS. Cardiac myocyte-specific excision of the beta1 integrin gene results in myocardial fibrosis and cardiac failure. *Circ Res*. 2002;90:458-64.
295.Chen K, Mehta JL, Li D, Joseph L and Joseph J. Transforming growth factor beta receptor endoglin is expressed in cardiac fibroblasts and modulates profibrogenic actions of angiotensin II. *Circ Res*. 2004;95:1167-73.
296.Rodriguez-Vita J, Ruiz-Ortega M, Ruperez M, Esteban V, Sanchez-Lopez E, Plaza JJ and Egido J. Endothelin-1, via ETA receptor and independently of transforming growth factor-beta, increases the connective tissue growth factor in vascular smooth muscle cells. *Circ Res*. 2005;97:125-34.
297.Basu R, Lee J, Morton JS, Takawale A, Fan D, Kandalam V, Wang X, Davidge ST and Kassiri Z. TIMP3 is the primary TIMP to regulate agonist-induced vascular remodelling and hypertension. *Cardiovascular research*. 2013;98:360-71.
298.Ma Y, Halade GV and Lindsey ML. Extracellular matrix and fibroblast communication following myocardial infarction. *J Cardiovasc Transl Res*. 2012;5:848-57.
299.Wang W, McKinnie SM, Patel VB, Haddad G, Wang Z, Zhabyeyev P, Das SK, Basu R, McLean B, Kandalam V, Penninger JM, Kassiri Z, Vederas JC, Murray AG and Oudit GY. Loss of Apelin Exacerbates Myocardial Infarction Adverse Remodeling and Ischemia-reperfusion Injury: Therapeutic Potential of Synthetic Apelin Analogues. *Journal of the American Heart Association*. 2013;2:e000249.
300.Sasaki T, Shishido T, Kadowaki S, Kitahara T, Suzuki S, Katoh S, Funayama A, Netsu S, Watanabe T, Goto K, Takeishi Y and Kubota I. Diacylglycerol kinase alpha exacerbates cardiac injury after ischemia/reperfusion. *Heart and vessels*. 2013.
301.Patel VB, Wang Z, Fan D, Zhabyeyev P, Basu R, Das SK, Wang W, Desaulniers J, Holland SM, Kassiri Z and Oudit GY. Loss of p47phox subunit enhances susceptibility to biomechanical stress and heart failure because of dysregulation of cortactin and actin filaments. *Circ Res*. 2013;112:1542-56.
302.deAlmeida AC, van Oort RJ and Wehrens XH. Transverse aortic constriction in mice. *Journal of visualized experiments : JoVE*. 2010.
303.Fan D, Takawale A, Shen M, Wang W, Wang X, Basu R, Oudit GY and Kassiri Z. Cardiomyocyte A Disintegrin And Metalloproteinase 17 (ADAM17) Is Essential in Post-Myocardial Infarction Repair by Regulating Angiogenesis. *Circ Heart Fail*. 2015;8:970-9.
304.Fan D, Takawale A, Shen M, Samokhvalov V, Basu R, Patel V, Wang X, Fernandez-Patron C, Seubert JM, Oudit GY and Kassiri Z. A Disintegrin and Metalloprotease-17 Regulates Pressure Overload-Induced Myocardial Hypertrophy and Dysfunction Through Proteolytic Processing of Integrin beta1. *Hypertension*. 2016;68:937-48.
305.Lovelock JD, Baker AH, Gao F, Dong JF, Bergeron AL, McPheat W, Sivasubramanian N and Mann DL. Heterogeneous effects of tissue inhibitors of matrix metalloproteinases on cardiac fibroblasts. *Am J Physiol Heart Circ Physiol*. 2005;288:H461-8.
306.Das SK, Wang W, Zhabyeyev P, Basu R, McLean B, Fan D, Parajuli N, DesAulniers J, Patel VB, Hajjar RJ, Dyck JR, Kassiri Z and Oudit GY. Iron-overload injury and cardiomyopathy in acquired and genetic models is attenuated by resveratrol therapy. *Sci Rep*. 2015;5:18132.
307.O'Connell DJ, Molinar AJ, Tavares AL, Mathine DL, Runyan RB and Bahl JJ. Transfection of cells attached to selected cell based biosensor surfaces. *Life Sci*. 2007;80:1395-402.
308.Guo D, Kassiri Z, Basu R, Chow FL, Kandalam V, Damilano F, Liang W, Izumo S, Hirsch E, Penninger JM, Backx PH and Oudit GY. Loss of PI3Kgamma enhances cAMP-dependent MMP remodeling of the myocardial N-cadherin adhesion complexes and extracellular matrix in response to early biomechanical stress. *Circulation research*. 2010;107:1275-89.

309.O'Connell TD, Rodrigo MC and Simpson PC. Isolation and culture of adult mouse cardiac myocytes. *Methods in molecular biology (Clifton, NJ)*. 2007;357:271-96.
310.Melendez GC, McLarty JL, Levick SP, Du Y, Janicki JS and Brower GL. Interleukin 6 mediates myocardial fibrosis, concentric hypertrophy, and diastolic dysfunction in rats. *Hypertension*. 2010;56:225-31.
311.Morimoto H, Hirose M, Takahashi M, Kawaguchi M, Ise H, Kolattukudy PE, Yamada M and Ikeda U. MCP-1 induces cardioprotection against ischaemia/reperfusion injury: role of reactive oxygen species. *Cardiovasc Res*. 2008;78:554-62.
312.Haddad G, Zhabyeyev P, Farhan M, Zhu LF, Kassiri Z, Rayner DC, Vanhaesebroeck B, Oudit GY and Murray AG. Phosphoinositide 3-kinase beta mediates microvascular endothelial repair of thrombotic microangiopathy. *Blood*. 2014;124:2142-9.
313.Farhan MA, Carmine-Simmen K, Lewis JD, Moore RB and Murray AG. Endothelial Cell mTOR Complex-2 Regulates Sprouting Angiogenesis. *PloS one*. 2015;10:e0135245.
314.Zhang QX, Nakhaei-Nejad M, Haddad G, Wang X, Loutzenhiser R and Murray AG. Glomerular endothelial PI3 kinase-alpha couples to VEGFR2, but is not required for eNOS activation. *American journal of physiology Renal physiology*. 2011;301:F1242-50.
315.Basu R, Fan D, Kandalam V, Lee J, Das SK, Wang X, Baldwin TA, Oudit GY and Kassiri Z. Loss of Timp3 gene leads to abdominal aortic aneurysm formation in response to angiotensin II. *J Biol Chem*. 2012;287:44083-96.
316.Patel VB, Bodiga S, Basu R, Das SK, Wang W, Wang Z, Lo J, Grant MB, Zhong J, Kassiri Z and Oudit GY. Loss of angiotensin-converting enzyme-2 exacerbates diabetic cardiovascular complications and leads to systolic and vascular dysfunction: a critical role of the angiotensin II/AT1 receptor axis. *Circ Res*. 2012;110:1322-35.
317.Zile MR, Baicu CF, Stroud RE, Van Laer A, Arroyo J, Mukherjee R, Jones JA and Spinale FG. Pressure overload-dependent membrane type 1-matrix metalloproteinase induction: relationship to LV remodeling and fibrosis. *Am J Physiol Heart Circ Physiol*. 2012;302:H1429-37.
318.Jones JA, Ruddy JM, Bouges S, Zavadzkas JA, Brinsa TA, Stroud RE, Mukherjee R, Spinale FG and Ikonomidis JS. Alterations in membrane type-1 matrix metalloproteinase abundance after the induction of thoracic aortic aneurysm in a murine model. *Am J Physiol Heart Circ Physiol*. 2010;299:H114-24.
319.Hausenloy DJ and Yellon DM. Time to take myocardial reperfusion injury seriously. *N Engl J Med*. 2008;359:518-20.
320.Spinale FG. Myocardial matrix remodeling and the matrix metalloproteinases: influence on cardiac form and function. *Physiol Rev*. 2007;87:1285-342.
321.Deschamps AM, Yarbrough WM, Squires CE, Allen RA, McClister DM, Dowdy KB, McLean JE, Mingoia JT, Sample JA, Mukherjee R and Spinale FG. Trafficking of the membrane type-1 matrix metalloproteinase in ischemia and reperfusion: relation to interstitial membrane type-1 matrix metalloproteinase activity. *Circulation*. 2005;111:1166-74.
322.Kassiri Z, Defamie V, Hariri M, Oudit GY, Anthwal S, Dawood F, Liu P and Khokha R. Simultaneous TGFbeta-TNF activation and cross-talk cause aberrant remodeling response and myocardial fibrosis in tissue inhibitor of metalloproteinase 3 deficient heart. *J Biol Chem*. 2009.
323.Mukherjee R, Akar JG, Wharton JM, Adams DK, McClure CD, Stroud RE, Rice AD, Desantis SM, Spinale FG and Gold MR. Plasma Profiles of Matrix Metalloproteinases and Tissue Inhibitors of the Metalloproteinases Predict Recurrence of Atrial Fibrillation Following Cardioversion. *J Cardiovasc Transl Res*. 2013.
324.Vanhoutte D, Schellings M, Pinto Y and Heymans S. Relevance of matrix metalloproteinases and their inhibitors after myocardial infarction: a temporal and spatial window. *Cardiovasc Res*. 2006;69:604-13.

325.Zile MR, Desantis SM, Baicu CF, Stroud RE, Thompson SB, McClure CD, Mehurg SM and Spinale FG. Plasma biomarkers that reflect determinants of matrix composition identify the presence of left ventricular hypertrophy and diastolic heart failure. *Circ Heart Fail*. 2011;4:246-56.
326.Dixon JA, Gaillard WF, 2nd, Rivers WT, Koval CN, Stroud RE, Mukherjee R and Spinale FG. Heterogeneity in MT1-MMP activity with ischemia-reperfusion and previous myocardial infarction: relation to regional myocardial function. *American journal of physiology Heart and circulatory physiology*. 2010;299:H1947-58.
327.Gingras D and Beliveau R. Emerging concepts in the regulation of membrane-type 1 matrix metalloproteinase activity. *Biochim Biophys Acta*. 2010;1803:142-50.
328.Spinale FG, Escobar GP, Mukherjee R, Zavadzkas JA, Saunders SM, Jeffords LB, Leone AM, Beck C, Bouges S and Stroud RE. Cardiac-restricted overexpression of membrane type-1 matrix metalloproteinase in mice: effects on myocardial remodeling with aging. *Circ Heart Fail*. 2009;2:351-60.
329.Zile MR, Baicu CF, Stroud RE, Van Laer AO, Jones JA, Patel R, Mukherjee R and Spinale FG. Mechanistic Relationship Between MT1-MMP and the Myocardial Response to Pressure-Overload. *Circ Heart Fail*. 2014.
330.Knauper V, Will H, Lopez-Otin C, Smith B, Atkinson SJ, Stanton H, Hembry RM and Murphy G. Cellular mechanisms for human procollagenase-3 (MMP-13) activation. Evidence that MT1-MMP (MMP-14) and gelatinase a (MMP-2) are able to generate active enzyme. *J Biol Chem*. 1996;271:17124-31.
331. Wang M, Zhang J, Walker SJ, Dworakowski R, Lakatta EG and Shah AM. Involvement of NADPH oxidase in age-associated cardiac remodeling. *J Mol Cell Cardiol*. 2010;48:765-72.
332.Nguyen HL, Zucker S, Zarrabi K, Kadam P, Schmidt C and Cao J. Oxidative stress and prostate cancer progression are elicited by membrane-type 1 matrix metalloproteinase. *Mol Cancer Res*. 2011;9:1305-18.
333.Wang K, Lin B, Brems JJ and Gamelli RL. Hepatic apoptosis can modulate liver fibrosis through TIMP1 pathway. *Apoptosis : an international journal on programmed cell death*. 2013;18:566-77.
334.Kassiri Z, Oudit GY, Kandalam V, Awad A, Wang X, Ziou X, Maeda N, Herzenberg AM and Scholey JW. Loss of TIMP3 enhances interstitial nephritis and fibrosis. *J Am Soc Nephrol*. 2009;20:1223-35.
335.Tayebjee MH, Lim HS, Nadar S, MacFadyen RJ and Lip GY. Tissue inhibitor of metalloproteinse-1 is a marker of diastolic dysfunction using tissue doppler in patients with type 2 diabetes and hypertension. *Eur J Clin Invest*. 2005;35:8-12.
336.Tayebjee MH, Karalis I, Nadar SK, Beevers DG, MacFadyen RJ and Lip GY. Circulating matrix metalloproteinase-9 and tissue inhibitors of metalloproteinases-1 and -2 levels in gestational hypertension. *Am J Hypertens*. 2005;18:325-9.
337.Lee MH, Rapti M and Murphy G. Unveiling the surface epitopes that render tissue inhibitor of metalloproteinase-1 inactive against membrane type 1-matrix metalloproteinase. *J Biol Chem*. 2003;278:40224-30.
338.Zile MR and Brutsaert DL. New concepts in diastolic dysfunction and diastolic heart failure: Part II: causal mechanisms and treatment. *Circulation*. 2002;105:1503-8.
339. Sharp WW, Fang YH, Han M, Zhang HJ, Hong Z, Banathy A, Morrow E, Ryan JJ and Archer SL. Dynamin-related protein 1 (Drp1)-mediated diastolic dysfunction in myocardial ischemia-reperfusion injury: therapeutic benefits of Drp1 inhibition to reduce mitochondrial fission. *Faseb j*. 2014;28:316-26.
340.Mozaffarian D, Benjamin EJ, Go AS, Arnett DK, Blaha MJ, Cushman M, de Ferranti S, Despres JP, Fullerton HJ, Howard VJ, Huffman MD, Judd SE, Kissela BM, Lackland DT, Lichtman JH, Lisabeth LD, Liu S, Mackey RH, Matchar DB, McGuire DK, Mohler ER, 3rd, Moy CS, Muntner P, Mussolino ME, Nasir K, Neumar RW, Nichol G, Palaniappan L, Pandey DK, Reeves MJ, Rodriguez CJ, Sorlie PD, Stein J, Towfighi A, Turan TN, Virani SS, Willey JZ, Woo D, Yeh RW, Turner MB, American Heart Association Statistics C and Stroke Statistics S. Heart disease and stroke statistics--2015 update: a report from the American Heart Association. *Circulation*. 2015;131:e29-322.

341.Roger VL. Epidemiology of heart failure. *Circ Res*. 2013;113:646-59.
342.Webb CS, Bonnema DD, Ahmed SH, Leonardi AH, McClure CD, Clark LL, Stroud RE, Corn WC, Finklea L, Zile MR and Spinale FG. Specific temporal profile of matrix metalloproteinase release occurs in patients after myocardial infarction: relation to left ventricular remodeling. *Circulation*. 2006;114:1020-7.
343.Kameda K, Matsunaga T, Abe N, Fujiwara T, Hanada H, Fukui K, Fukuda I, Osanai T and Okumura K. Increased pericardial fluid level of matrix metalloproteinase-9 activity in patients with acute myocardial infarction: possible role in the development of cardiac rupture. *Circulation journal : official journal of the Japanese Circulation Society*. 2006;70:673-8.
344.Spinale FG and Villarreal F. Targeting matrix metalloproteinases in heart disease: lessons from endogenous inhibitors. *Biochem Pharmacol*. 2014;90:7-15.
345.Tian H, Cimini M, Fedak PW, Altamentova S, Fazel S, Huang ML, Weisel RD and Li RK. TIMP-3 deficiency accelerates cardiac remodeling after myocardial infarction. *J Mol Cell Cardiol*. 2007;43:733-43.
346.Eckhouse SR, Purcell BP, McGarvey JR, Lobb D, Logdon CB, Doviak H, O'Neill JW, Shuman JA, Novack CP, Zellars KN, Pettaway S, Black RA, Khakoo A, Lee T, Mukherjee R, Gorman JH, Gorman RC, Burdick JA and Spinale FG. Local Hydrogel Release of Recombinant TIMP-3 Attenuates Adverse Left Ventricular Remodeling After Experimental Myocardial Infarction. *Sci Transl Med*. 2014;6:223ra21.
347.Johnson TD and Christman KL. Injectable hydrogel therapies and their delivery strategies for treating myocardial infarction. *Expert Opinion on Drug Delivery*. 2013;10:59-72.
348.Suwaidi JA, Hamasaki S, Higano ST, Nishimura RA, Holmes DR, Jr. and Lerman A. Long-term follow-up of patients with mild coronary artery disease and endothelial dysfunction. *Circulation*. 2000;101:948-54.
349.Heitzer T, Schlinzig T, Krohn K, Meinertz T and Munzel T. Endothelial dysfunction, oxidative stress, and risk of cardiovascular events in patients with coronary artery disease. *Circulation*. 2001;104:2673-8.
350.Qi JH, Ebrahem Q, Moore N, Murphy G, Claesson-Welsh L, Bond M, Baker A and Anand-Apte B. A novel function for tissue inhibitor of metalloproteinases-3 (TIMP3): inhibition of angiogenesis by blockage of VEGF binding to VEGF receptor-2. *Nat Med*. 2003;9:407-15.
351.Guedez L, Jensen-Taubman S, Bourboulia D, Kwityn CJ, Wei B, Caterina J and Stetler-Stevenson WG. TIMP-2 targets tumor-associated myeloid suppressor cells with effects in cancer immune dysfunction and angiogenesis. *J Immunother*. 2012;35:502-12.
352.Starr AE, Dufour A, Maier J and Overall CM. Biochemical analysis of matrix metalloproteinase activation of chemokines CCL15 and CCL23 and increased glycosaminoglycan binding of CCL16. *J Biol Chem*. 2012;287:5848-60.
353.Lucitti JL, Mackey JK, Morrison JC, Haigh JJ, Adams RH and Faber JE. Formation of the collateral circulation is regulated by vascular endothelial growth factor-A and a disintegrin and metalloprotease family members 10 and 17. *Circ Res*. 2012;111:1539-50.
354.Lavine KJ, Kovacs A, Weinheimer C and Mann DL. Repetitive myocardial ischemia promotes coronary growth in the adult mammalian heart. *Journal of the American Heart Association*. 2013;2:e000343.
355.Frangogiannis NG. Emerging roles for macrophages in cardiac injury: cytoprotection, repair, and regeneration. *J Clin Invest*. 2015;125:2927-30.
356.Kanisicak O, Khalil H, Ivey MJ, Karch J, Maliken BD, Correll RN, Brody MJ, SC JL, Aronow BJ, Tallquist MD and Molkentin JD. Genetic lineage tracing defines myofibroblast origin and function in the injured heart. *Nature communications*. 2016;7:12260.
357.Rienks M, Papageorgiou AP, Frangogiannis NG and Heymans S. Myocardial extracellular matrix: an ever-changing and diverse entity. *Circ Res*. 2014;114:872-88.

358.Spinale FG, Frangogiannis NG, Hinz B, Holmes JW, Kassiri Z and Lindsey ML. Crossing Into the Next Frontier of Cardiac Extracellular Matrix Research. *Circ Res*. 2016;119:1040-1045.
359.Yarbrough WM, Baicu C, Mukherjee R, Van Laer A, Rivers WT, McKinney RA, Prescott CB, Stroud RE, Freels PD, Zellars KN, Zile MR and Spinale FG. Cardiac-restricted overexpression or deletion of tissue inhibitor of matrix metalloproteinase-4: differential effects on left ventricular structure and function following pressure overload-induced hypertrophy. *Am J Physiol Heart Circ Physiol*. 2014;307:H752-61.
360.Sundstrom J, Evans JC, Benjamin EJ, Levy D, Larson MG, Sawyer DB, Siwik DA, Colucci WS, Wilson PW and Vasan RS. Relations of plasma total TIMP-1 levels to cardiovascular risk factors and echocardiographic measures: the Framingham heart study. *Eur Heart J*. 2004;25:1509-16.
361.Lopez B, Gonzalez A and Diez J. Circulating biomarkers of collagen metabolism in cardiac diseases. *Circulation*. 2010;121:1645-54.
362.Essa EM, Zile MR, Stroud RE, Rice A, Gumina RJ, Leier CV and Spinale FG. Changes in plasma profiles of matrix metalloproteinases (MMPs) and tissue inhibitors of MMPs in stress-induced cardiomyopathy. *J Card Fail*. 2012;18:487-92.
363.Stetler-Stevenson WG. Tissue inhibitors of metalloproteinases in cell signaling: metalloproteinase-independent biological activities. *Sci Signal*. 2008;1:re6.
364.Lee SY, Kim JM, Cho SY, Kim HS, Shin HS, Jeon JY, Kausar R, Jeong SY, Lee YS and Lee MA. TIMP-1 modulates chemotaxis of human neural stem cells through CD63 and integrin signalling. *Biochem J*. 2014;459:565-76.
365.Kim KK, Wei Y, Szekeres C, Kugler MC, Wolters PJ, Hill ML, Frank JA, Brumwell AN, Wheeler SE, Kreidberg JA and Chapman HA. Epithelial cell alpha3beta1 integrin links beta-catenin and Smad signaling to promote myofibroblast formation and pulmonary fibrosis. *J Clin Invest*. 2009;119:213-24.
366.Bagchi RA and Czubryt MP. Synergistic roles of scleraxis and Smads in the regulation of collagen 1alpha2 gene expression. *Biochim Biophys Acta*. 2012;1823:1936-44.
367Weber GF, Bjerke MA and DeSimone DW. Integrins and cadherins join forces to form adhesive networks. *J Cell Sci*. 2011;124:1183-93.
368.Lupia A, Peppicelli S, Witort E, Bianchini F, Carloni V, Pimpinelli N, Urso C, Borgognoni L, Capaccioli S, Calorini L and Lulli M. CD63 tetraspanin is a negative driver of epithelial-to-mesenchymal transition in human melanoma cells. *J Invest Dermatol*. 2014;134:2947-56.
369.Toricelli M, Melo FH, Peres GB, Silva DC and Jasiulionis MG. Erratum: Timp1 interacts with beta-1 integrin and CD63 along melanoma genesis and confers anoikis resistance by activating PI3-K signaling pathway independently of Akt phosphorylation. *Mol Cancer*. 2015;14:161.
370.Rossi L, Forte D, Migliardi G, Salvestrini V, Buzzi M, Ricciardi MR, Licchetta R, Tafuri A, Bicciato S, Cavo M, Catani L, Lemoli RM and Curti A. The tissue inhibitor of metalloproteinases 1 increases the clonogenic efficiency of human hematopoietic progenitor cells through CD63/PI3K/Akt signaling. *Exp Hematol*. 2015;43:974-985.e1.
371.Ramezani-Moghadam M, Wang J, Ho V, Iseli TJ, Alzahrani B, Xu A, Van der Poorten D, Qiao L, George J and Hebbard L. Adiponectin reduces hepatic stellate cell migration by promoting tissue inhibitor of metalloproteinase-1 (TIMP-1) secretion. *J Biol Chem*. 2015;290:5533-42.
372.Wang X, Berry E, Hernandez-Anzaldo S, Takawale A, Kassiri Z and Fernandez-Patron C. Matrix metalloproteinase-2 mediates a mechanism of metabolic cardioprotection consisting of negative regulation of the sterol regulatory element-binding protein-2/3-hydroxy-3-methylglutaryl-CoA reductase pathway in the heart. *Hypertension (Dallas, Tex : 1979)*. 2015;65:882-8.
373.Shen M, Lee J, Basu R, Sakamuri SS, Wang X, Fan D and Kassiri Z. Divergent roles of matrix metalloproteinase 2 in pathogenesis of thoracic aortic aneurysm. *Arterioscler Thromb Vasc Biol*. 2015;35:888-98.
374.Iyer RP, de Castro Bras LE, Patterson NL, Bhowmick M, Flynn ER, Asher M, Cannon PL, Deleon-Pennell KY, Fields GB and Lindsey ML. Early matrix metalloproteinase-9 inhibition post-myocardial

infarction worsens cardiac dysfunction by delaying inflammation resolution. *J Mol Cell Cardiol*. 2016;100:109-117.
375.Iyer RP, Jung M and Lindsey ML. MMP-9 signaling in the left ventricle following myocardial infarction. *American journal of physiology Heart and circulatory physiology*. 2016;311:H190-8.
376.Lindsey ML, Iyer RP, Jung M, DeLeon-Pennell KY and Ma Y. Matrix metalloproteinases as input and output signals for post-myocardial infarction remodeling. *J Mol Cell Cardiol*. 2016;91:134-40.
377.Eckhouse SR, Akerman AW, Logdon CB, Oelsen JM, O'Quinn EC, Nadeau EK, Stroud RE, Mukherjee R, Jones JA and Spinale FG. Differential membrane type 1 matrix metalloproteinase substrate processing with ischemia-reperfusion: relationship to interstitial microRNA dynamics and myocardial function. *The Journal of thoracic and cardiovascular surgery*. 2013;145:267-275, 277.e1-4; discussion 275-7.
378.Spinale FG, Mukherjee R, Zavadzkas JA, Koval CN, Bouges S, Stroud RE, Dobrucki LW and Sinusas AJ. Cardiac restricted overexpression of membrane type-1 matrix metalloproteinase causes adverse myocardial remodeling following myocardial infarction. *The Journal of biological chemistry*. 2010;285:30316-27.
379.Schroder J, Lullmann-Rauch R, Himmerkus N, Pleines I, Nieswandt B, Orinska Z, Koch-Nolte F, Schroder B, Bleich M and Saftig P. Deficiency of the tetraspanin CD63 associated with kidney pathology but normal lysosomal function. *Mol Cell Biol*. 2009;29:1083-94.
380.Mann DL and Spinale FG. *Activation of matrix metalloproteinases in the failing human heart: breaking the tie that binds*: Circulation. 1998 Oct 27;98(17):1699-702.
381.Guo Y, Li Q, Chen G, Tang J and Gao W. [Adenovirus-mediated transfer of TIMP-4 gene inhibits neointimal formation after balloon injury]. *Beijing da xue xue bao Yi xue ban = Journal of Peking University Health sciences*. 2003;35:434-7.
382.Bhoopathi P, Chetty C, Gujrati M, Dinh DH, Rao JS and Lakka SS. The role of MMP-9 in the anti-angiogenic effect of secreted protein acidic and rich in cysteine. *British Journal of Cancer*. 2010;102:530-40.
383.Sang QX. Complex role of matrix metalloproteinases in angiogenesis. *Cell research*. 1998;8:171-7.
384.van Hinsbergh VW and Koolwijk P. Endothelial sprouting and angiogenesis: matrix metalloproteinases in the lead. *Cardiovascular Research*. 2008;78:203-12.
385.Greenberg B, Yaroshinsky A, Zsebo KM, Butler J, Felker GM, Voors AA, Rudy JJ, Wagner K and Hajjar RJ. Design of a phase 2b trial of intracoronary administration of AAV1/SERCA2a in patients with advanced heart failure: the CUPID 2 trial (calcium up-regulation by percutaneous administration of gene therapy in cardiac disease phase 2b). *JACC Heart failure*. 2014;2:84-92.
386.Jessup M, Greenberg B, Mancini D, Cappola T, Pauly DF, Jaski B, Yaroshinsky A, Zsebo KM, Dittrich H and Hajjar RJ. Calcium Upregulation by Percutaneous Administration of Gene Therapy in Cardiac Disease (CUPID): a phase 2 trial of intracoronary gene therapy of sarcoplasmic reticulum Ca2+-ATPase in patients with advanced heart failure. *Circulation*. 2011;124:304-13.
387.Bajgelman MC, dos Santos L, Silva GJ, Nakamuta J, Sirvente RA, Chaves M, Krieger JE and Strauss BE. Preservation of cardiac function in left ventricle cardiac hypertrophy using an AAV vector which provides VEGF-A expression in response to p53. *Virology*. 2015;476:106-14.
388.Akahane T, Akahane M, Shah A, Connor CM and Thorgeirsson UP. TIMP-1 inhibits microvascular endothelial cell migration by MMP-dependent and MMP-independent mechanisms. *Experimental Cell Research*. 2004;301:158-67.
389.Moore CS, Milner R, Nishiyama A, Frausto RF, Serwanski DR, Pagarigan RR, Whitton JL, Miller RH and Crocker SJ. Astrocytic tissue inhibitor of metalloproteinase-1 (TIMP-1) promotes oligodendrocyte differentiation and enhances CNS myelination. *J Neurosci*. 2011;31:6247-54.
390.Bertaux B, Hornebeck W, Eisen AZ and Dubertret L. Growth stimulation of human keratinocytes by tissue inhibitor of metalloproteinases. *J Invest Dermatol*. 1991;97:679-85.

391.Saika S, Kawashima Y, Okada Y, Tanaka SI, Yamanaka O, Ohnishi Y and Ooshima A. Recombinant TIMP-1 and -2 enhance the proliferation of rabbit corneal epithelial cells in vitro and the spreading of rabbit corneal epithelium in situ. *Curr Eye Res*. 1998;17:47-52.
392.Guedez L, Stetler-Stevenson WG, Wolff L, Wang J, Fukushima P, Mansoor A and Stetler-Stevenson M. In vitro suppression of programmed cell death of B cells by tissue inhibitor of metalloproteinases-1. *The Journal of clinical investigation*. 1998;102:2002-10.
393.Creemers EE, Davis JN, Parkhurst AM, Leenders P, Dowdy KB, Hapke E, Hauet AM, Escobar PG, Cleutjens JP, Smits JF, Daemen MJ, Zile MR and Spinale FG. Deficiency of TIMP-1 exacerbates LV remodeling after myocardial infarction in mice. *Am J Physiol Heart Circ Physiol*. 2003;284:H364-71.
394.Manso AM, Kang SM and Ross RS. Integrins, focal adhesions, and cardiac fibroblasts. *J Investig Med*. 2009;57:856-60.
395.Thibault G, Lacombe MJ, Schnapp LM, Lacasse A, Bouzeghrane F and Lapalme G. Upregulation of alpha(8)beta(1)-integrin in cardiac fibroblast by angiotensin II and transforming growth factor-beta1. *Am J Physiol Cell Physiol*. 2001;281:C1457-67.
396.Burgess ML, Carver WE, Terracio L, Wilson SP, Wilson MA and Borg TK. Integrin-mediated collagen gel contraction by cardiac fibroblasts. Effects of angiotensin II. *Circ Res*. 1994;74:291-8.
397.Chen H, Qu J, Huang X, Kurundkar A, Zhu L, Yang N, Venado A, Ding Q, Liu G, Antony VB, Thannickal VJ and Zhou Y. Mechanosensing by the alpha6-integrin confers an invasive fibroblast phenotype and mediates lung fibrosis. *Nature Communications*. 2016;7:12564.
398.Pols MS and Klumperman J. Trafficking and function of the tetraspanin CD63. *Exp Cell Res*. 2009;315:1584-92.
399.Xia Y, Yeddula N, Leblanc M, Ke E, Zhang Y, Oldfield E, Shaw RJ and Verma IM. Reduced cell proliferation by IKK2 depletion in a mouse lung-cancer model. *Nature Cell Biology*. 2012;14:257-65.
400.Toricelli M, Melo FH, Peres GB, Silva DC and Jasiulionis MG. Timp1 interacts with beta-1 integrin and CD63 along melanoma genesis and confers anoikis resistance by activating PI3-K signaling pathway independently of Akt phosphorylation. *Mol Cancer*. 2013;12:22.
401.Bagchi RA, Roche P, Aroutiounova N, Espira L, Abrenica B, Schweitzer R and Czubryt MP. The transcription factor scleraxis is a critical regulator of cardiac fibroblast phenotype. *BMC Biol*. 2016;14:21.
402.Houser SR, Margulies KB, Murphy AM, Spinale FG, Francis GS, Prabhu SD, Rockman HA, Kass DA, Molkentin JD, Sussman MA and Koch WJ. Animal models of heart failure: a scientific statement from the American Heart Association. *Circ Res*. 2012;111:131-50.
403.Patten RD and Hall-Porter MR. Small animal models of heart failure: development of novel therapies, past and present. *Circ Heart Fail*. 2009;2:138-44.
404.John Wiley & Sons Inc; Hoboken N, USA. *Gene Therapy Clinical Trials Workdwide*; 2009.
405.Porcheray F, Viaud S, Rimaniol AC, Leone C, Samah B, Dereuddre-Bosquet N, Dormont D and Gras G. Macrophage activation switching: an asset for the resolution of inflammation. *Clin Exp Immunol*. 2005;142:481-9.